

3356

NATIONAL LIBRARY

OTTAWA



BIBLIOTHÈQUE NATIONALE

OTTAWA

NAME OF AUTHOR.....K. L. BHANOT.....
 TITLE OF THESIS...BEHAVIOUR OF SCALED AND
 FULL-LENGTH CAST-IN-PLACE
 CONCRETE PILES.....
 UNIVERSITY.....OF ALBERTA (EDMONTON).....
 DEGREE.....Ph.D.....YEAR GRANTED.....1968.....

Permission is hereby granted to THE NATIONAL
 LIBRARY OF CANADA to microfilm this thesis and to
 lend or sell copies of the film.

The author reserves other publication rights,
 and neither the thesis nor extensive extracts from
 it may be printed or otherwise reproduced without
 the author's written permission.

(Signed).....

(K. L. BHANOT)

PERMANENT ADDRESS:

Associate Professor
 of Civil Engineering
 PUNJAB ENGINEERING
 COLLEGE,
 CHANDIGARH,
 INDIA.

DATED...Dec...30.....1968.

THE UNIVERSITY OF ALBERTA

BEHAVIOUR OF
SCALED AND FULL-LENGTH CAST-IN-PLACE
CONCRETE PILES

by



KANWAL LAL BHANOT

A THESIS
SUBMITTED TO THE FACULTY OF GRADUATE STUDIES
IN PARTIAL FULFILMENT OF THE REQUIREMENTS FOR THE DEGREE OF
DOCTOR OF PHILOSOPHY

DEPARTMENT OF CIVIL ENGINEERING

EDMONTON, ALBERTA

OCTOBER, 1968

UNIVERSITY OF ALBERTA
FACULTY OF GRADUATE STUDIES

The undersigned certify that they have read, and recommend
to the Faculty of Graduate Studies for acceptance, a thesis entitled,
BEHAVIOUR OF SCALED AND FULL-LENGTH CAST-IN-PLACE CONCRETE PILES,
submitted by Kanwal Lal Bhanot in partial fulfilment of the requirements
for the degree of Doctor of Philosophy.

Edmund W. Brooker
.....
Dr. E. W. Brooker
Supervisor

Wm. J. Bruce
.....
Dr. W. Bruce

J. J. Warwayuk
.....
Dr. J. J. Warwayuk

T. Blench
.....
Professor T. Blench

S. R. Sinclair
.....
Professor S. R. Sinclair

W. G. Watt
.....
Professor W. G. Watt
External Examiner

Date *Nov. 6/68*
.....

ABSTRACT

The work under report includes a study of the behaviour of scaled piles in uniformly graded plastic silt and the performance and analysis of full-length field piles in Edmonton soil. All the eight piles tested were of Concrete Bored-in Type. Piles in silt were scaled down to a nominal diameter of 5 inches and overall length of about 60 inches. The belled pile and one of the straight-shaft piles were instrumented close to the bottom for measuring the load transferred to the tip. The ends of two full-length piles terminated in the lake deposit whereas the other two were embedded solely in dense till below, passing clear through the overlying lake deposit. All the four field piles were provided with load-cells for measuring the load transferred to soil at the lower ends of the piles.

Too much emphasis has not been placed on summarising the details of published theories of bearing capacity, settlement and other related topics. A brief review and a large number of references pertaining in particular to the pile load tests have, however, been included.

Availability of free water from fresh concrete or from any other source, was found to have a major influence on the shear strength of the shaft soil as also on the ultimate bearing capacity of a pile in silt. Effect of variation in the embedded length was quite conspicuous for piles in till, in which the shafts developed a high degree of adhesion and the ultimate resistance corresponded nearly to the residual shear strength of

soil. Dominant in the behaviour of piles in Lake Edmonton soil was the effect of remolding of the sandy-silty-clayey shaft soil offering a comparatively small resistance which would correspond roughly to the remolded strength of the soil. Behaviour of various types of soils under different physical and environmental conditions being different, it was concluded that the method of describing the shaft capacity of a pile by making use of a reduction coefficient such as α which would absorb all the variations in the shear strength of soil due to various causes, was the best.

For the type of soil encountered locally, it was established that correlations for computing shaft and tip capacities of a pile if based on field penetration N-values, would give more dependable results than if evaluated from laboratory test results. Recommendations for further study in this connection have been suggested.

ACKNOWLEDGMENTS

The author wishes to express his sincere thanks to Professor S.R. Sinclair, Professor E. W. Brooker and Professor S. Thomson of the Civil Engineering Department for their continued guidance, advice and encouragement at all stages of the work, and to Professor J. Warwaruk also of the Civil Engineering Department, who assisted in the design of load cells for field piles.

The help extended by Messrs. Heinz Panse of the Structural Engineering Laboratory, Mr. George Edward of the Central Machine Shop, Jim McLean and O. Wood of the Civil Engineering Department in fabricating the load-cells is gratefully appreciated. Thanks are also due to Mr. P. Ali, formerly of the Civil Engineering Department, for his assistance in the calibration of load-cells and field installation of piles.

The author is obligated to the Canadian Commonwealth Scholarship and Fellowship Committee for providing him with an opportunity to pursue the present course of studies. Assistance in various forms during installation and testing of field piles made available by Western Caissons Foundations Limited, Bernard and Hogan Engineering and Testing Limited and the Department of Public Works is gratefully acknowledged.

Finally, thanks are extended to my wife who helped in summarising the huge field data and applying arithmetical checks thereto.

TABLE OF CONTENTS

	<u>Page</u>
Title Page	i
Approval Sheet	ii
Abstract	iii
Acknowledgments	v
Table of Contents	vi
List of Tables	viii
List of Figures	ix
CHAPTER I INTRODUCTION	1
CHAPTER II BACKGROUND OF PILE LOAD TESTS	8
CHAPTER III BEHAVIOUR OF CAST-IN-PLACE CONCRETE SCALED PILES IN SILT	31
CHAPTER IV FULL-LENGTH FIELD PILES--DEVELOPMENT OF TESTING PROGRAMME	72
CHAPTER V TEST SITE SOIL CHARACTERISTICS, LABORATORY TEST RESULTS AND DISCUSSION	101
CHAPTER VI PRESENTATION OF FIELD PILE LOADING TEST RESULTS	117
CHAPTER VII ANALYSES OF TEST DATA AND DISCUSSION	138
CHAPTER VIII SUMMARY STATEMENT OF THE FINDINGS	175
CHAPTER IX RECOMMENDED PROCEDURE FOR DESIGN	187
CHAPTER X CONCLUSIONS AND RECOMMENDATIONS	200

	<u>Page</u>
List of References	211
APPENDIX A Design of the Load-Cell, Properties of Cell Material, Gage Connections and Calibration Curves (Scaled Piles in Silt)	219
APPENDIX B Concrete Materials, Mix Design and Cylinder Strength (Piles in Silt)	230
APPENDIX C Engineering Properties of Pit Soil and Typical Strength Plots	237
APPENDIX D Calibration Curves and Data for 25-Ton Hydraulic Jack (Scaled Piles in Silt)	242
APPENDIX E Load Test Data (Scaled Piles in Silt)	245
APPENDIX F Design and Fabrication Details of Load-Cells for Field Piles	256
APPENDIX G Calibration Curves and Data for Load-Cells (Full-Length Piles)	261
APPENDIX H Calibration Curves and Data for Hydraulic Jacks and Details of Load Maintenance Scheme Used for Field Piles	270
APPENDIX I Schematic Arrangement of Set-Up Used for Piles in Till	276
APPENDIX J Resultant Side-Sway at Top of 28-in. Diameter Pile under a Load of 1200 Kips	278
APPENDIX K Laboratory Data for Shear Strength of Field Soil	280
APPENDIX L Summaries of Load Test Data and Computations (Full-Length Field Piles)	297
APPENDIX M Data for Time vs. Settlement and Base Resistance Plots under Sustained Loads (Full-Length Piles)	318
APPENDIX N Determination of Critical Load Q_c on the Pile Top When Its Effect Just Reaches the Pile Tip, and Computation of Shaft Compression from Known Average Value of Elastic Modulus and Measured Dimensions of Piles	326
APPENDIX O List of Symbols used in the text	331

LIST OF TABLES

		<u>Page</u>
TABLE II-1	PILE LOADING TEST DATA	30
TABLE III-1	RESULTS OF STRENGTH TESTS ON PIT SOIL	40
TABLE III-2	SHEAR STRENGTH OF SOIL BEFORE (a) AND AFTER (b) CONCRETING	45
TABLE III-3	DATA FOR SOIL MOISTURE CONTENT, SOIL SHEAR STRENGTH AND SLUMP OF CONCRETE	46
TABLE III-4	COEFFICIENT OF LOAD-TRANSFER AS RELATED TO INCREASE IN MOISTURE CONTENT OF SOIL AROUND THE SHAFT	62
TABLE V-1	RESULTS OF UNDRAINED TRIAXIAL COMPRESSION TESTS ON UNDISTURBED AND REMOLDED RECOMPACTED SAMPLES OF CLAY AND TILL	113
TABLE VII-1	ESSENTIAL PILE DATA FOR COMPUTATIONS	144
TABLE VIII-1	SUMMARY OF PILE-LOADING TEST RESULTS (FULL-LENGTH PILES)	188
TABLE VIII-2	SUMMARY OF CORRELATIONS DEVELOPED FOR COMPUTING BASE CAPACITY AND SHAFT RESISTANCE OF FULL-LENGTH PILES	194

LIST OF FIGURES

<u>Figures</u>	<u>Page</u>
1.1* A View of the Test Site Showing the Average Prevailing Conditions During the Period of Testing Full-Length Field Piles	5
3.1* Lay-Out of Piles in the Test Pit	32
3.2* Belling Tool	32
3.3* Suspension Arrangement Used for Piles A and E (Unsupported at Bottom)	34
3.4* Pile with Air-Vent Pipes Communicating with Air-Gap Below the Pile (Seen Projecting Out of Left Face of Pile)	34
3.5* & 3.6* Parts and Assembly of 5-in. Diameter Load-Cells with Strain Recording Indicator and Switch Box	34
3.7 Lengths of Installation of Various Piles in Silt	37
3.8 Particle-Size Curve for Pit Soil	39
3.9 Soil Classification Charts Showing the Positions Occupied by Pit Soil	39
3.10* Load Test Set-Up for Pile B	42
3.11* Load Test Set-Up for Pile E	42
3.12* & 3.13* Load Test Set-Up for Pile D	42
3.14* Lower Portions of Piles B, C and E Photographed after Removing Top Soil from One Side of Vertical Diametral Plane	44
3.15* Piles as Recovered after Excavation of Pit Soil	44
3.16 Moisture Content and Shear Strength Variation of Pit Soil With Depth	47
3.17 Decrease in Soil Shear Strength vs. Increase in Moisture Content	49

* Photographic Illustrations.

<u>Figures</u>		<u>Page</u>
3.18	Decrease in Soil Shear Strength vs. Increase in Slump of Concrete	49
3.19	Load-Settlement Curves for Piles in Silt	51
3.20	Load-Time-Settlement Curves for Piles in Silt	52
3.21	Relative Proportion of Tip Load and Shaft Load (Pile B in Silt)	53
3.22	Relative Proportion of Tip Load and Shaft Load (Pile C in Silt)	53
3.23	Relation Between Settlement and Tip Load (as Percentage of Failure Load)	55
3.24	Relation Between Settlement and Tip Load (as Percentage of Tip Load at Failure)	55
3.25	Mobilization of Base Resistance vs. Settlement	55
3.26	Variation of Load Transferred Through Cell During Half-Hour Interval	59
3.27	Shaft Load vs. Settlement for Piles in Silt	60
3.28	Skin Friction Developed (as Percentage of Skin Friction at Failure Load) vs. Settlement, for Piles in Silt	60
3.29	Relation Between Coefficient of Skin Friction and Increase in Moisture Content (%) of Shaft Soil	64
3.30	Load Settlement Curves for Base, Shaft and Total Capacity for Piles in Silt (Summary)	69
4.1	Site Plan: Full-Length Pile Tests (U. of A.)	74
4.2	Lay-Out Plan: Full-Length Pile Tests (U. of A.)	77
4.3*	Drilling Equipment at Work	78
4.4*	Penetration N-values Being Taken	78
4.5	Test Hole Logs: Full-Length Pile Tests (U. of A.)	79
4.6*	28-in. Diameter Load-Cell as Received from the Fabrication Shop	81

<u>Figures</u>		<u>Page</u>
4.7*	Load-Cell after the Application of Strain Gages and Wiring Connections	81
4.8*	Calibration of the Load-Cell with 1-in. to 2-in. Thick Steel Plates Placed One above the Other	82
4.9*	Calibration of the Load-Cell with Concrete Blocks Placed below and above	82
4.10*	Drilling Process in Progress for 20-in. Diameter Pile	85
4.11*	Load-Cell Being Lowered into the Hole	85
4.12*	A View of the Pile Immediately after Installation	87
4.13*	16-in. Diameter Pipe Being Lowered into the 28-in. Diameter Hole	87
4.14	Installation Dimensions of Test Piles: Full-Length Pile Tests (U. of A.)	88
4.15*	A View of the Anchor Piles with the Reinforcing Rods Projecting Out	90
4.16*	A View of the Loading Beam as Supported by Anchor Piles	90
4.17*	Preparation of the Pile Top for Testing	92
4.18*	Heating the Soil near Surface to Avoid Possible Freezing	92
4.19*	Showing the Arrangement of the Loading Head to Provide Space for the Projecting Shaft Compression Measurement Rod	93
4.20*	Showing the Hydraulic Jack Centered on the Pile Top	93
4.21*	Load-Maintainer Used for Pressures up to 2,000 psi.	95
4.22*	Load Maintainer Used for Pressures up to 10,000 psi.	95
4.23*	System of Measurements Used for 20-in. Pile in Clay	97
4.24*	System of Measurements Used for 20-in. Pile in Till	97
4.25*	Two-Jack Set-Up and System of Measurements Used for 28-in. Pile in Till	98

<u>Figures</u>		<u>Page</u>
5.1	Plots for Soil Composition (Per Cent Clay, Silt, and Sand; Natural Moisture Content; Liquid Limit, Plastic Limit; Degree of Saturation and Bulk Density of Soil)	104
5.2	Classification of Field Soil at Various Depths on Casagrande's Plasticity Chart	105
5.3	Strength Characteristics of Field Soil: (a) Moisture Content vs. Depth Plot (b) N-Values vs. Depth Plot (c) Shear Strength vs. Depth Plot	108
5.4	Plots for Residual and Softened Shear Strength of Soil	115
6.1	Load vs. Settlement at Top (16-in. Pile in Clay)	118
6.2	Load vs. Settlement at Top (20-in. Pile in Clay)	119
6.3	Load vs. Settlement at Top (20-in. Pile in Till)	120
6.4	Load vs. Settlement at Top (28-in. Pile in Till)	121
6.5	Plots for Base Resistance Q_b , Shaft Resistance Q_s and Total Load Q vs. Top Settlement: 16-in. Pile in Clay	126
6.6	Plots for Base Resistance Q_b , Shaft Resistance Q_s and Total Load Q vs. Top Settlement: 20-in. Pile in Till	127
6.7	Plots for Base Resistance Q_b , Shaft Resistance Q_s and Total Load Q vs. Top Settlement: 28-in. Pile in Till	128
6.8	Time-Load-Settlement Curve (16-in. and 20-in. Diameter Piles in Clay)	131
6.9	Time-Load-Settlement Curve (20-in. and 28-in. Diameter Piles in Till)	132
6.10	Typical Time Settlement Curves under Sustained Loads	133
6.11	Typical Plots Showing Variation of Base Resistance with Time under Sustained Loads	135

<u>Figures</u>	<u>Page</u>
7.1 Plots for Measured Shaft Compression vs. Applied Total Load and Measured Tip Resistance for 16-in. Pile (I) in Clay	141
7.2 Plots for Measured Shaft Compression vs. Applied Total Load and Top Settlement vs. Computed Base Resistance for 20-in. Pile (III) in Clay	143
7.3 Load vs. Tip Settlement Curves, Adjusted for Shaft Compression and the Contribution of Concrete Plug below Load-Cells: 16-in. Pile (I) in Clay	144
7.4 Load vs. Tip Settlement Curves, Adjusted for Shaft Compression and the Contribution of Concrete Plug below Load-Cells: 20-in. Pile (III) in Clay	145
7.5 Developed Skin Friction and Coefficient of Load-Transfer Plotted Against Tip Settlement: 16-in. and 20-in. Piles in Clay	151
7.6 Load vs. Tip Settlement Curves Adjusted for Shaft Compression and the Contribution of Concrete Plug below Load-Cell: 20-in. Pile (IV) in Till	155
7.7 Load vs. Tip Settlement Curves Adjusted for Shaft Compression and the Contribution of Concrete Plug below Load-Cell: 28-in. Pile (II) in Till	161
7.8 Plots for Evaluating Constant of Compressibility of Soil	169
7.9 Typical Stress-Strain Curves for an Undisturbed Soil Specimen with Superimposed Pile Length at Various Stages of Failure	172
9.1 Curves Representing Tip Bearing Capacity by Various Equations at Various Depths	190
9.2 (a) Plots for Net Settlement Curves for Piles in Clay; (b) Idealized Plots for Q_B , Q_S and Q for 16-in. Pile (I) in Clay	196
9.3 Relation Between Overall Factor of Safety F and Derived Factors of Safety F_s and F_b on Shaft and Base Capacities	198

<u>Figures</u>		<u>Page</u>
A-3	Load-Cell Assembly Details	223
A-4	Gage Connections Within the Cell (Piles in Pit Soil)	224
A-8	Calibration Curve: 5-in. Diameter Load-Cell No. I	228
A-9	Calibration Curve: 5-in. Diameter Load-Cell No. II	229
B-3	Gradation Curves for Coarse and Fine Aggregate (Concrete Mix)	233
C-2	Typical Results on the British Portable Compression Testing Machine	239
C-3	Typical Stress-Strain Curves for Pit Silt	240
C-4	Mohr's Envelopes for Total Stresses--Results of Undrained Triaxial Tests on Lab-Compacted Samples	241
D-2	Hydraulic Jack Calibration Curve (Piles in Silt)	244
F-1	Design Details of Load-Cells for Field Piles	257
F-3	Wiring Details for Full Bridge Circuit	259
F-4	Half-Section Through Assembled Load-Cell	260
G-5 to G-8	Calibration Curves for 16-in., 20-in., 20-in., 28-in. Cells	266 to 269
H-3 & H-4	Calibration Curves for Hydraulic Jacks 1, 2	273 & 274
H-5	Load Maintenance System--Schematic Diagram	275
I-1	Schematic Arrangement of Set-Up Used for Measurements (20-in., 28-in. Diameter Piles in Till)	277
J-1	Resultant Side-Sway at Top of 28-in. Diameter Pile under a Load of 1200 Kips	279
K-1	Typical Stress-Strain Curve for Unconfined Compression Test on Till	281
K-2 to K-12	Mohr's Envelopes for Total Stresses	282 to 292
K-13	Stress Deformation Plots for Box Shear Tests	293

<u>Figures</u>		<u>Page</u>
K-14	Stress Deformation Plots for Box Shear Tests	294
K-15	Stress Deformation Plot for Box Shear Tests	295
K-16	Undisturbed and Residual Strength Parameters from Box Shear Tests	296

CHAPTER I

INTRODUCTION

1.1 General

As a result of the rapid all-round tempo of development during the recent past, the metropolitan areas have become centres of industrial, educational and recreational activities, resulting in the ever-increasing demand for covered accommodation. Want of adequate space has made the large industrial complexes and apartment buildings rise more vertically than spread horizontally. This is true of all the major cities the world over and Edmonton is no exception. Requirement of stronger and deeper foundations has been the result. Foundation engineers have been answering it by providing support on piles taken down into the soil deep enough to develop adequate bearing capacity warranted by the structure. The problem of determining the number, the spacing and the economical depth of the piles together with the proportion of load shared by skin and the tip of individual piles driven or cast into non-homogeneous soil possessing inconsistent characteristics has baffled many a soils engineer.

With these and many other related problems in mind, the Department of Civil Engineering, University of Alberta, embarked upon the programme of testing individual piles, aimed at separating the magnitudes of the two components, viz., skin friction and tip resistance, for the local soil conditions, and making recommendations for the design of the

piles in and around Edmonton. The pioneer work in this direction was done by HARRIS (1964) who studied the behaviour of axially-loaded single piles embedded in cohesive soil by making use of one-inch diameter, fifteen-inch long brass tubing piles instrumented along the shaft and a little above the interchangeable base (one-inch or two-inch diameter). The next series included the test-loading of bored, cast-in-place, scaled piles in uniformly-graded compacted silt. Five-inch diameter, sixty-inch long piles (one supported by soil both along the shaft and at base with a load-cell near the bottom, the other similar one without any instrumentation, the third one also without instrumentation but with a clear gap at bottom, i.e., supported by skin-friction alone and a fourth one with a bell at the bottom and provided with a load-cell immediately above the bell) were test-loaded during summer 1966, and a report on the findings was submitted by the present author to the Department of Civil Engineering. A condensed version of the same appears in Chapter III of this thesis.

Full-length field testing of bored cast-in-situ piles was next taken in hand by the University, in collaboration with Western Caisson Foundations Ltd., Bernard Hogan Engineering Ltd. and the Department of Public Works. A site with supposedly representative soil conditions was selected in the University Farm and four piles (two in dense clay-till and two in the upper lake clay overlying till) were installed during summer 1967, and were test-loaded to failure. The detailed programme of investigation has been outlined in Chapter IV of this report and the analysis of the test-results given thereafter.

1.2 Statement of the Problem

The number of pile-supported structures is steadily increasing and the cost of conducting a full-scale pile-loading test is not justified for each one of these separately. Pile-load tests already performed by various foundation engineering firms give some information on the ultimate bearing capacity of the pile only for specific locations. No attempt has been made either to determine the proportions of shaft and base capacities of the piles or to generalize the design procedure for the area so as to economise on the cost of site investigations in the future. An acceptable design method should consider both the settlement as well as the end-bearing and shaft capacity of the pile during various stages of loading. The purpose of this investigation, therefore, is to attempt to evaluate these factors and to correlate these with the soil characteristics in general for cast-in-place concrete piles in uniform silty pit-soil, as also in the soil type generally encountered in the Edmonton area, by making use of load-tests on individual instrumented piles.

1.3 Scope of Investigation and Limitations

This thesis summarises the present state of knowledge about load tests in general, and reviews the work done in this University on scaled piles in silt, during summer 1966. Details of field investigation for full-length tests, fabrication, calibration and installation of heavy-duty load-cells have been given and the results of the loading tests and their possible correlations with the soil properties discussed. An attempt has been made to evolve a rational design procedure for bored cast-in-place

piles in the Edmonton area taking into consideration all the pertinent factors.

The scope of the investigation has, however, been limited by a number of factors, the most important affecting the results, interpretations and recommendations being the available time at the disposal of the present author. Design, fabrication, calibration and installation of the load-cells for use in the scaled-piles testing programme, test-loading the piles and laboratory testing of soil together with the preparation of the report, were all completed in a matter of about four months. Field piles, on the other hand, were installed during July/August 1967, but the loading frame was not available for about five months thereafter. This dragged the actual testing programme into the midst of winter, with freezing temperatures reigning all around the site. Erection of a temporary roofing gave no relief. Gas heating inside was not effective beyond two to three feet from the source of the heat. Loading tests on piles in clay were performed when the temperature inside the shed ranged from -5 to +5 degrees centigrade. The heating, however, did ensure that the top soil around the piles did not freeze. Thermal lining of the shed from inside improved matters considerably and the remaining two tests were conducted comfortably thereafter, concluding the series on April 16, 1968. FIGURE 1.1 gives a view of the test site representing the average conditions prevailing during the entire period of testing.

There was a gap of about 6 to 10 months reckoned from the date the strain gauges were applied to the pillars of a particular load-cell to the date when the corresponding pile was tested. This, together with possibly some other unknown factors, presumably made the strain gauges



**FIGURE 1.1 A VIEW OF THE TEST SITE SHOWING THE AVERAGE
PREVAILING CONDITIONS DURING THE PERIOD OF
TESTING FULL LENGTH FIELD PILES.**

strip off the pillars at least in one of the four load-cells, making it impossible to evaluate the base resistance directly. Indirect methods have therefore been attempted for analysis in that case. After installation and prior to testing, there were periods of rain and snow; and though the pile tops were kept covered, water did find its way at least into the surrounding soil, thereby changing its strength characteristics to a certain extent. Two additional test holes were therefore bored close to the site and samples obtained for laboratory testing.

Load-cells placed near the tips of the two piles in dense till indicated, during the process of testing, values of maximum base resistance much in excess of the design capacity of the cells. Actual values, in these cases, have been obtained from the calibration curves by linear extrapolation. It has been presumed that there was no plastic yield of the material of the cell for loads up to about 1.5 times the design capacity. A built-in factor of safety of 1.5 was, however, available for the cells, having been originally designed on that basis.

The correlations developed and the recommendations made are further limited by the extent of time-consuming laboratory testing. The number of strength tests performed in till are relatively few compared to those in clay for which samples from four test holes were available. A large number of till samples crumbled during preparation or extraction from the sampling tubes due to the frequent presence of pockets of loose silt and fine sand. The average value of strength parameters had therefore to be obtained from just a few results. Continuously non-homogeneous profile, however, perhaps did merit further laboratory investigations, but the available time has once again been a limiting factor.

1.4 Symbols and Definitions

Symbols used in the text have been defined in APPENDIX O of this thesis. In general, the terms used hereafter are those recommended by the American Society of Civil Engineers (ASCE, 1958) or by the American Society for Testing and Materials (ASTM: D 653-64). All symbols used have however been defined wherever they occur first in the text.

CHAPTER II

BACKGROUND OF PILE LOAD TESTS

2.1 Introduction

Use of piles to support structures has been in vogue for hundreds of years. Their design, however, was purely empirical or based on past experience. For all these years there has been a continuous though slow progress both in design and in the construction methods. There have, however, been periods of gloom and uncertainty when during the early 20th century, engineers discovered that the empirical rules for design of piles were far from correct. The opening remarks by GRANDALL (1936) in the discussion on the Bearing Capacity of Piles are quoted below in this connection:

The use of pile foundations used to be a simple problem and one to which engineers would always resort when in doubt or difficulty. Pile driving was then a pleasant and profitable pastime. Today the problem is becoming so complex and involved that the use of piles may soon have to be abandoned. In the past it was so easy to drive piles to some resistance by some formula, multiply the number of piles by this resistance and thus obtain a foundation. Today we know that our formulae were faulty, that the resistance of one pile is not indicative of the resistance of the entire group and that the entire group with its surrounding soil mass may be constantly settling. Such is progress.

In spite of this, improved methods, both theoretical and those based on actual loading tests, kept on being developed during the last thirty years with the result that "the design procedure is now on its way to becoming a method that can be judged, designed and controlled by scientifically sound theories (KEZDI, 1965)."

Having designed a pile-foundation on the basis of theory, or the available semi-empirical formulae, it is necessary, at least in the case of certain major or important structures, to verify the assumptions made in the theoretical design and thus to ensure that a certain minimum factor of safety against failure is definitely available. This, precisely, is the purpose of conducting a pile load test. And since it is not possible to predict the behaviour of a group of piles from that of a single pile, and since it is almost impracticable to perform field tests on groups, laboratory load tests on groups of model piles have become popular in recent years (WHITAKER, 1957; COOKE and WHITAKER, 1961; SOWERS and FAUSOLD, 1961; KISHIDA and MEYERHOF, 1965).

Computations of the Ultimate Bearing Capacity of piles have been based both on the plastic and on the elastic behaviour of soil under loads. Validity of the simplifying assumptions made in the two cases has often been questioned. The assumption that a soil behaves elastically is probably far from true under static loads but is considered valid under dynamic stress conditions. Many investigators have based their analyses of the stress conditions for the ultimate plastic failure of the soil by assuming various possible mechanisms of failure. The accuracy of the expressions derived by them therefore depends upon the extent to which the assumed shapes of surfaces of failure approach reality. Most of the clayey soils in nature are saturated or nearly saturated and behave as frictionless materials under applied total stresses, provided no change takes place in the moisture content. The general expression for ultimate bearing capacity q_u for such soils, based on the assumption that $\phi = 0$,

assumes the form:

$$q_u = c N_c \quad (2.1)$$

where c is the unit cohesion and N_c the bearing capacity factor. PRANDTL (1920, 1921), HENCKY (1923), and MEYERHOF (1951) conducted investigations using circular or strip foundations (smooth and rough bases) and obtained values of N_c in the above expression, ranging generally from 5 to 6 for surface loadings. Further contributions in this respect have been made by TERZAGHI (1943), MEYERHOF (1951) and SKEMPTON (1951) and solutions for deep foundations ($D/B > 2$) have been presented. The failure mechanism assumed in each case has been discussed by HARRIS (1964). Additional effect of depth and unit weight of soil has been considered separately. Assuming plastic failure, following semi-empirical expressions for bearing capacity of circular foundations at any depth have been obtained by these investigators:

$$\text{TERZAGHI (1943): } q_u = 1.3 c N_c + \gamma_1 D_f N_q + 0.6 \gamma r N_\gamma \quad \dots (2.2)$$

$$\text{MEYERHOF (1951): } q_u = c N_c + \gamma D_f N_q + r \gamma N_\gamma \quad \dots (2.3)$$

$$\text{SKEMPTON (1951): } q_a = \frac{1}{F} [c N_c + p_o (N_q - 1) + \frac{\gamma \cdot B}{2} N_\gamma] + p \quad \dots (2.4)$$

where:

q_u = ultimate unit bearing capacity,

q_a = allowable unit bearing capacity,

c = unit cohesion of the soil,

γ = moist unit weight of soil above water table
or buoyant weight if below water table,

D_f = depth of foundation to the bottom of the footing,

r = radius of the circular footing,

F = desired factor of safety,

p_o = effective overburden pressure at foundation level,

B = breadth of the foundation,

N_c , N_q , and N_γ = dimensionless bearing capacity factors dependent upon the angle of shearing resistance of the soil for use in equation (2.2); dependent upon the shape factor λ for various D/B ratios and the roughness of base for use in equation (2.3) and dependent upon ϕ the angle of shearing resistance and the ratios L/B and D/B of the foundation for use in equation (2.4). Here L and D represent the length and depth of the foundation respectively,

γ_1 = increased unit weight of the soil produced to counteract the shear stress developed over the surface of Terzaghi's outer failure cylinder and the skin friction developed over the pile shaft (TERZAGHI, 1943, p. 135).

The general equations for bearing capacity given by Terzaghi and Meyerhof are similar but the values of the bearing capacity factors differ. Both Terzaghi and Meyerhof have added up the additional component equal to $2f_s D/r$ (where f_s is the unit skin friction developed over the shaft) to the values obtained from equation (2.2) or (2.3) above, so as to obtain the ultimate bearing capacity of a pile. From his general equation (2.4) above, and for the condition: $\phi = 0$ (saturated clays) in which case the bearing capacity factors N_q and N_γ equal unity and zero respectively, SKEMPTON (1951) obtained the expression:

$$q_u = cN_c + p \quad \dots (2.5)$$

$$\text{or } q_n = cN_c \quad \dots (2.5a)$$

wherein q_n = net ultimate bearing capacity,

and $N_c = 6.2, 7.1, 7.7, 8.1, 8.4, 8.6$ and 9.0 for D/B ratios of the pile equal to $0, 0.5, 1.0, 1.5, 2.0, 2.5, 3.0, 4.0$ and over respectively. Maximum value of $N_c = 9$ corresponding to D/B ratio of 4 or more, according to Skempton, is satisfactory both on the basis of theoretical and on the basis of experimental results. WHITAKER and COOKE (1966), however, have introduced another factor ω to be determined from field tests and have re-written Skempton's equation (2.5a) as:

$$q_n = \omega \cdot cN_c \quad \dots (2.6)$$

Herein the value of $N_c = 9$ has been retained so that the factor ω accounts for the variation in the values of the shear strength due to the physical and environmental characteristics of the clay. For diameters of piles between about 1.5 and 3 feet, a value of $\omega = 0.75$ has been suggested for fissured London Clay on the basis of results obtained by the authors.

For the safety of structures, it is essential to ensure that settlement does not exceed a certain maximum value. Some theoretical and semi-empirical approaches have been made to predict the total expected settlement under a loaded area. In general, it would include the immediate settlement Δ_i due to the plastic deformation of the soil and the long-time settlement Δ_c due to the consolidation of the strata below the loaded area. Based on the Theory of Elasticity, the immediate settlement of a foundation on the surface of a semi-infinite solid is usually computed from the following equation (TERZAGHI, 1943; SKEMPTON, 1951):

$$\Delta_1 = q_n \cdot B I \frac{1 - \mu^2}{E} \quad \dots (2.7)$$

wherein:

q_n is the net foundation pressure,

B is the breadth of the foundation,

I is the influence factor, the value of which depends on shape and rigidity of the foundation,

μ is the Poisson's ratio of the material, and

E is the modulus of elasticity of the material.

For use in the above equation, the value of E is taken from the laboratory stress-strain curve corresponding to the existing overburden pressure (being the secant modulus) and μ for clay is assumed to be 0.5. Values of I which depend on L/B ratio of the foundation and the thickness of the compressible layer are obtained from Steinbrenner's curves (TOMLINSON, 1963) or from Terzaghi's approximation of the curves (TERZAGHI, 1943, p. 425).

The above expression has been simplified by SKEMPTON (1951) according to whom the immediate settlement for fully-saturated clay undergoing no volume change under applied stresses ($\phi = 0$ condition) is given by:

$$\Delta_1 = 2B \cdot \epsilon \quad \dots (2.8)$$

where ϵ is the axial strain in a triaxial undrained test under a deviator stress $(\sigma_1 - \sigma_3)$ and is obtained from the relation:

$\epsilon = \frac{1}{E} (\sigma_1 - \sigma_3)$, E being the secant modulus at the stress $(\sigma_1 - \sigma_3)$. The above expression assumes a rigid circular footing and the value of $N_c = 6.8$.

Long-time settlement of foundations on clayey soils is obtained from laboratory consolidation tests run on undisturbed samples. At any depth z below the foundation, consolidation settlement based on these laboratory tests may be computed from the following expression given by SKEMPTON (1951):

$$\Delta_{lab} = \int_0^{H_c} m_v \cdot \sigma_z \cdot dz \quad \dots (2.9)$$

The term $(m_v \cdot \sigma_z)$ in the above expression represents the product of compressibility and the corresponding pressure determined for the range of depth 0 to H_c for the pressures varying from p_o to $(p_o + \sigma_z)$, where p_o is the original effective overburden pressure at depth z , and σ_z is the increment of vertical pressure set up at this depth by the net foundation pressure. H_c represents the maximum depth of the compressible layer below the foundation or some depth such as $4B$ or $2B$ beneath which the settlement is negligible. For obtaining an approximate average value, the above equation can be written as:

$$\Delta_{lab} = m_v \cdot \sigma_z \cdot H_c \quad \dots (2.9a)$$

where σ_z is the increment of vertical stress at mid-depth of layer resulting from the effective overburden pressure and m_v is the average coefficient of compressibility for the layer under consideration.

Actual settlement due to consolidation may generally be less than the value indicated by the laboratory tests (SKEMPTON and BJERRUM, 1957). The value of the reduction coefficient μ_c according to the authors varies from 0.2 for heavily overconsolidated clays to 1.0 (or even 1.2) for

very sensitive clays. The value of settlement so computed shall be satisfactory for a foundation at the surface. A correction f_D for depth factor depending upon the depth-to-area ratio and the length-to-breadth ratio of the foundation may further be applied to obtain the consolidation settlement Δ_c at any depth and for any flexible rectangular foundation. Thus:

$$\Delta_c = \mu_c \cdot f_D \cdot \Delta_{lab} \quad \dots (2.10)$$

The values of f_D in the above expression may be obtained from the correction curves presented by FOX (1948).

Having computed both the immediate and the long-time settlements, the total net settlement for foundations on clay is obtained by adding up the two. Thus:

$$\Delta = \Delta_i + \Delta_c \quad \dots (2.11)$$

It is generally not possible to obtain undisturbed samples of cohesionless soils. Correlations on the basis of laboratory test results are therefore not possible. Settlement of foundations on sand is generally estimated from the field test results. TERZAGHI and PECK (1967) have given an empirical relationship both in the form of a curve and as an approximate empirical formula obtained on the basis of experimental results, as well as field observations, for obtaining the settlement of any foundation on sand by extrapolating the results of plate loading tests. The following empirical relationship due to DE BEER and MARTENS (1957) which makes use of Terzaghi's formula for obtaining consolidation settlement and is based on

static cone penetration tests in the field, is claimed by the authors to give satisfactory results for foundations on sand:

$$\Delta = \frac{H_c}{C} \log_e \frac{P_o + \sigma_z}{P_o} \quad \dots (2.12)$$

where $C = 1.5 \frac{C_{kd}}{P_o}$ and other symbols used have the same meaning as before. C_{kd} here represents the static cone resistance in kg/cm^2 or tons/ft^2 .

Capacities of piles computed by static formulae discussed earlier in this chapter make use of a certain reduced value of the shear strength of clay as determined by undrained compression tests, for the computation of load-transfer from shaft to the surrounding soil mass, the coefficient of reduction not having a unique value. Dynamic formulae which employ the driving energy of the falling hammer can give values as much in error as 100 per cent (MANSUR and FOCHT, 1956) when compared with the field test results. None of these formulae yields the load-settlement data. Methods of ascertaining settlement are too approximate in nature. Load-settlement data obtained from full-length pile tests would generally apply only to a single site and to one pile length. Moreover, the tests are expensive. Such considerations have made the present-day research workers think of developing analytical methods for predicting load-carrying capacity and load-settlement data for loaded piles.

HOBBS (1963) presented an analysis on the basis of the theory of elasticity for obtaining load-settlement curves for a pile. He derived an expression for base load in terms of modulus of elasticity of the soil, Poisson's ratio, settlement at surface and the bearing capacity factor the

value of which depends upon the rigidity and shape of the base. The expression accounts for elastic compression of the shaft, load-transfer from shaft to the soil around and deformation of the soil at base under the balance load. The expression gives only the immediate settlement leaving out the deep-seated settlement and the contribution due to consolidation with time. The analysis given by REESE (1964) and COYLE and REESE (1966) has been based on the correlations of the ratio of load-transfer to soil shear strength as a function of pile movement and presented in the form of curves. Field and laboratory verification indicates the suitability of the method for general use in the case of axially-loaded piles in clay. Theoretical solutions to the problem have also been presented by THURMAN and D'APPOLONIA (1965) for single piles making use of theory of elasticity and by SALAS and BELZUNCE (1965) based on Mindlin's solution (MINDLIN, 1936) for stress due to a point load in the interior of a semi-infinite half space.

Based on the results of plate-bearing tests and the general equation from the theory of elasticity (equation 2.7), BURLAND et al. have recently (1966) presented the following relationship for computing the load-settlement data suitable for plotting the initial one-third portion of the curve, assuming it to be a straight line:

$$\Delta_i = K \cdot B \cdot \frac{q}{q_{ult}} \quad \dots (2.13)$$

wherein Δ_i is the immediate elastic settlement,
 B is the diameter of the pile,
 q and q_{ult} pertain to the loading pressure
on the plate

and K is a dimensionless number related to both the stress-strain properties and the strength characteristics of the soil;

its value is given by:

$$K = (N_c + \frac{\bar{\gamma}D}{c_u} \cdot I \cdot \frac{1 - \mu^2}{E/c_u} \quad \dots (2.14)$$

where $\bar{\gamma}$ is the average density of the soil within the total depth D of the pile,

c_u is the undrained shear strength, and

other symbols have the same meaning as before.

The expressions given in the paragraphs above and many others have been employed in the past to arrive at the allowable bearing capacity and settlement of a pile with considerable amount of success but many a conservative engineer still feels that there is no substitute for an actual load-test at least for specific locations. Various types of tests and test procedures that have been used in the past, as also the methods available for separating the magnitudes of skin friction and end-bearing as well as the design criteria based on such tests have been discussed in the paragraphs that follow.

2.2 Types of Load-Tests and Test Procedures

Until recently the procedure of testing known as the Maintained Load Test (M.L. Test) Method according to which increments of loads are applied and maintained at the pile top while its settlement is continuously measured, was commonly employed. The increments of load as also the duration of its maintenance on the pile were quite arbitrary, in some cases dependent upon a certain minimum rate of penetration or a certain specified period of time after which the next increment would be applied. The load would be removed completely after each increment and applied again (Cyclic

Loading) or would be increased continuously (Continuous Loading) and the pile rebounded only at end, measurements of the settlement being taken in each case and at each stage. The repeated unloading and re-loading cycles enable the measurement of net settlement after each unloading phase. Cyclic loading, however, is not permitted by many of the standard building codes (FLETCHER, 1962). The ASTM method of testing (D 1143-57 T) makes use of the continuous loading procedure. Total test load to be applied is twice the anticipated working load, the successive increments of loading being 25, 50, 75, 100, 125, 150, 175 and 200 per cent of the anticipated load. Settlement readings made to an accuracy of 0.001 ft. are taken before and after the application of each increment. A new increment is applied after the rate of settlement under the previous settlement is less than 0.001 ft. in 1 hour or until 2 hours have elapsed, whichever occurs first. Full test load is required to remain on the pile for 24 hours. An alternative method according to which load increments are added at constant time intervals (minimum, 30 minutes) is also available. After the completion of loading, the pile is rebounded with the remaining loads amounting to 75, 50, 25, 10, 0 per cent of full test load. Final rebound is recorded 24 hours after the entire test load has been removed.

WHITAKER and COOKE (1961), for their tests on model piles, used a method called the Constant Rate of Penetration (C.R.P.) Test, which requires the pile to penetrate at a constant speed, the force applied at the top of the pile to maintain the rate and penetration being continuously measured. Though the method does not give an indication of the settlement at loads other than the ultimate load, the major attraction is the rapidity

by which it can be performed. The other advantage is that the rate of penetration can be matched with the laboratory rate of testing. For obtaining the settlements at loads other than the ultimate, the authors recommend that the C.R.P. test be followed by the determination of settlement under a maintained load equal to the design load.

Another method, claimed by the authors (MOHAN et al., 1967) to be simpler than the two described above, involves the application of each increment of load about five to ten per cent in excess of the actual and maintained constant for about five minutes and then allowed to reduce by itself due to the yielding of the ground. A state of equilibrium is reached between load and subsequent settlement and the ultimate load is obtained with fair accuracy from the load-settlement curve. The method eliminates the need for a load maintainer and is claimed to be quicker, providing a better indication of the load-settlement behaviour of the pile. It has been called the Method of Equilibrium by the authors.

Each of the three methods outlined above has its own advantages and disadvantages. In general, however, load-tests give reliable results for piles in granular soils and in such other soils where the bearing capacity cannot be established otherwise. In fine-grained soils they give the ultimate bearing capacity but the results do not indicate true load-settlement relationship due to the subsequent long-time effects of consolidation. Initially the results would indicate relatively large bearing capacity for a small settlement. With the passage of time, a large proportion of load carried by skin friction may get transferred to the pile point and the settlement may suddenly increase. In such cases it is extremely useful to have a knowledge of the ultimate value of skin friction.

2.3 Loading Methods

The method of applying load at the top of the pile depends on its expected magnitude and the equipment available. Where loads are not too great, reaction can be applied by loaded trucks or by reaction against the structural members of a building. Direct loading, by supporting a heavily-loaded platform at the pile top may be suitable if higher magnitudes are required. Application of the reaction obtained by jacking against the loaded platform or by making use of two or more anchor piles installed around the test pile permits an easy control and is useful for cyclic type of loading where it is required to load, unload and reload the pile many times during a test. Another method suggested by CHELLIS (1961) consists in the application of the load by means of a cantilever arm loaded at the free end with the pile top situated closer to the hinged end.

2.4 Separation of Skin Friction and End Bearing

Total bearing capacity of a pile is made up of point bearing capacity and shaft capacity (or mobilized skin friction). Many a time it is necessary to separate the two components. For instance, in the case of friction piles in clay, silt or a combination of the two, there is a gradual transfer of load from the shaft to the tip of the pile. The pile then starts sinking rapidly. It is thus necessary, not only to determine the maximum magnitudes of the two components separately, but also to estimate their variability as a function of time, together with the corresponding settlements. And, since long-time tests are impracticable to carry, it would be

at least worth while knowing the magnitude of load on the shaft, part of which shall eventually be transferred to the pile base. With that aim in view, sophisticated instrumentation for measurements at the base as well as along the shaft has been developed and semi-empirical relationships based on the results of laboratory and field testing of piles have been presented. Purely theoretical solutions have also been offered.

Based upon the value of the bearing capacity factor $N_c = 9$ for deep foundations on saturated clay, SKEMPTON (1959) developed from the field tests on bored piles, the following expression between average adhesion c_a (between clay and pile shaft) and the mean undisturbed shear strength \bar{c} of clay within the depth of penetration of the pile:

$$c_a = \alpha \cdot \bar{c} \quad \dots (2.15)$$

Here α is the coefficient of adhesion the value of which varies from 0.3 to 0.6 for London Clay. Lower value of 0.3 has been recommended for relatively short piles installed in heavily fissured clay and corresponds to the fully softened shear strength of the soil whereas the higher value of 0.6 (with the maximum value of $\alpha \cdot \bar{c}$ limited to 2000 psf) has been recommended for heavy foundations supported on long piles. In general, an average value of $\alpha = 0.45$ could be adopted for shear strength of the order of 4500 psi or less. The values of α given by Skempton were obtained by him from the test results in fissured London Clay only. Other investigators (COOKE and WHITAKER, 1961; WHITAKER, 1962; LO and STERMAC, 1964; HARRIS, 1964; WHITAKER and COOKE, 1965) experimenting with either model or full-length piles obtained values of α ranging from as low as 0.248 (HARRIS, 1964) to as high as 1.0 (LO and STERMAC, 1964) for remoulded

Lake Edmonton Clay and for stiff clay respectively.

Instrumentation of the test pile along the shaft and the base for obtaining shaft capacity and tip resistance or for checking and re-calculating the values of N_c and α is relatively a recent development. Other methods employed for the same purpose include plate-bearing tests performed at the bottom of the hole (GOLDER and LEONARD, 1954) for evaluating the tip resistance; use of cone penetrometers passing through a casing tube for finding out end bearing and friction values by pushing the two alternately (DELF SOIL MECHANICS LABORATORY, 1936) and provision of an air-gap at the bottom of the pile for evaluating the skin friction (MOHAN and CHANDRA, 1961). Stress distribution along the shaft for a displacement pile was determined by REESE and SEED (1955) by installing total pressure and pore-water pressure gages at a number of places along the shaft. Use of electrical extensometers installed at various elevations along the depth of the pile as well as at the bottom was probably first made by VAN WEEL (1957). A calibrated miniature load-cell with electric resistance strain gages mounted on it was placed at the bottom of the model pile for the measurement of tip resistance by COOKE and WHITAKER (1961). Installation of resistance strain gages along the shaft and at the bottom of the pile have now become normal features of many pile-testing programmes. WHITAKER and COOKE (1966) and COYLE and REESE (1966), making use of instrumented piles, have produced comprehensive and valuable test/research reports for the design of piles.

2.5 Pile Settlement Data from Load Tests

Useful settlement data on full-scale field testing concerning, in

particular, the shaft and base resistance, is scanty and the information available cannot be extended to other sites without considerable deliberation. According to a suggestion offered by TERZAGHI (1942), the ultimate load on a pile is reached when the net settlement is equal to $1/10$ of the tip diameter of the pile. SKEMPTON (1959) and WHITAKER and COOKE (1965) have now come up with some information for bored cast-in-place concrete piles. For piles between 12 in. and 24 in. diameter, the settlement at ultimate capacity of the pile, according to Skempton, is of the order of $0.085 B$, where B is the diameter of the pile base. At 90% of the ultimate load, the settlement averages to about $0.04 B$. Whitaker and Cooke, working in the same type of soil (fissured London Clay) found the maximum resistance to have been offered at a settlement of about 10 per cent of the shaft diameter (i.e., $0.1 B$). Taking separately, the maximum shaft resistance mobilized at just one per cent of shaft diameter ($0.01 B$) and maximum base resistance corresponding to 10 per cent settlement (i.e., $0.1 B$).

2.6 Tests on Model Piles

Simplicity and ease of test performance under laboratory conditions and the impracticability of full-length field-testing of groups of piles have brought in the use of small model piles for predicting the general pile performance. Model piles so far used, have generally been instrumented. WHITAKER (1957) performed experiments on groups of $1/8$ inch diameter solid brass piles measuring the loads by making use of probing rings calibrated by electrical resistance strain gages. Tests on piles with enlarged bases, using hollow brass piles of various lengths, were performed by COOKE and WHITAKER (1961). The piles were provided with miniature load cells near the

base, thus enabling the authors to separate the magnitudes of base resistance and skin friction. Experiments on groups of piles of diameter 0.5 in. and 1.25 in. were performed by SOWERS (1961) who evaluated the effect of various spacings on the bearing capacity of the group, as also the load-distribution among various piles within the group. HARRIS (1964) used 1-in. diameter 15-in. long brass piles (straight shaft and enlarged base) instrumented along the shaft with strain gages and provided with a small load-cell near the base and studied the load-settlement relationships both for the shaft and base resistances. KISHIDA and MEYERHOF (1965) derived a theoretical equation for the bearing capacity in sand including lateral forces on the sides of the model pile groups.

2.7 Presentation of Test Results

Results of a pile-loading test are presented in the form of the following curves:

1. Load vs. Settlement of Pile Head,
2. Load vs. Time,
3. Time vs. Settlement.

If the pile has been instrumented to measure the base resistance, the following two curves may also be plotted:

4. Base Resistance vs. Settlement of Pile Head,
5. Shaft Resistance vs. Settlement of Pile Head.

Making use of the rebound part of the load settlement curve, Net Settlement, which is the difference between the top settlement under any load and the total elastic recovery on the removal of the load, is obtained. A curve representing the relationship between the load and net settlement

is then plotted. For purposes of analysis and comparison of results from any two or more tests, it is convenient to plot the above-mentioned curves, using dimensionless parameters Q/Q_T , Q_S/Q_T , Q_B/Q_T and Δ/B , where Q is the applied load at any stage, Q_T the maximum test load and Q_S , Q_B the shaft and base components of load Q . The design criteria are then developed on the basis of these curves as described in the paragraph below.

2.8 Evaluation of Test Results, Design Criteria and Safety Factors

For evolving a satisfactory design, the bearing capacity must be so selected that a certain minimum factor of safety (2 to 3) is ensured and that the resulting settlement is not objectionable from the point of view of structural or architectural damage. The first requirement therefore is the selection of the point on the load settlement curve indicating failure. Many criteria based on the steepness of the last portion of the curve, based on arbitrarily chosen increased rate of settlement beyond a certain stage or based on some geometrical construction have been suggested by CHELLIS (1961) and FLETCHER (1962). A novel method of determining the ultimate load capacity of the pile, taking into consideration the effect of cyclic loading, the time duration for which each load is maintained and the settlement, has been described by VAN DER VEEN (1953). The one method commonly adopted, as also used in this thesis, is to assume the yield load corresponding to the point of intersection of the two tangent lines drawn to the general slopes of the upper and the lower portions of the curve. The determination of safe load is based both on the ultimate load capacity and on gross or net settlement. Most building codes suggest a factor of safety of 2 on the ultimate load capacity and a maximum net settlement of 0.01 in.

per ton of total load. Different limits either on the basis of net or gross settlement have been specified by some other codes (TENG, 1962; FLETCHER, 1962).

The criteria of evaluating safe load on a pile discussed above applies to the load tests on non-instrumented piles where data are available only for the total load. A similar determination, when the base and shaft resistances have been separated out, is complicated by the fact that the two peak values occur at widely different settlements. Further, in terms of stability of the structure, which can sustain only a limited amount of settlement, failure load may be much lower than the ultimate load capacity of the pile. The working load therefore may not necessarily be based on the ultimate bearing resistance of the pile. TOMLINSON (1963) has suggested a factor of safety of 2 to 3 on the sum of full base resistance and the ultimate shaft load calculated on the basis of average adhesion. With a view to evolving an economic design procedure by making maximum use of the ultimate load capacity of the pile, WHITAKER and COOKE (1965, 1966) have suggested the choice of two load factors, one for shaft resistance (F_s) and the other for base resistance (F_b), and calculation of the working load by making use of the following expression:

$$\text{Working Load } W = \frac{Q_{SU}}{F_s} + \frac{Q_{BU}}{F_b} \quad \dots (2.16)$$

where Q_{SU} = Ultimate Shaft Resistance, and
 Q_{BU} = Ultimate Base Resistance.

Knowing the allowable settlement, the value of F_s (which is more significant since the shaft resistance is mobilized more quickly than the

base resistance) is scaled from a curve between load factor and settlement ratio Δ/B for pile top, drawn by making use of the plot between shaft-resistance and settlement ratio Δ/B . From a similar plot for base resistance, the corresponding load factor F_b for base is read off. Working values for shaft friction and base load are then determined, shaft compression calculated and used for determining the revised value F_b now for the settlement of the pile base. After a few approximations the working load is finally determined.

Summing up his comments after the conclusion of the Symposium on Large Bored Piles, SKEMPTON (1966) has suggested the following rules for arriving at the safe working loads of piles:

- i. For straight-shaft piles--

$$W. L. = \frac{Q_T}{2} \quad \dots (2.17)$$

- ii. For belled piles--

$$W. L. = \frac{Q_T}{2.5}$$

or

for $B < 6$ feet.

... (2.18
a,b)

$$W. L. = \frac{Q_S}{1.5} + \frac{Q_B}{3}$$

For $B > 6$ feet, working load is required to be evaluated from settlement calculations.

In the case of straight-shaft piles, friction is fully mobilized at movements of the order of 1 in. or less in which case a major portion of the load is taken by the shaft and therefore, according to Skempton, settlement considerations are not critical. For belled piles, however, settlement

considerations would generally govern the design.

2.9 Pile Loading Test Data

For piles loaded to failure or sufficiently near failure, driven wholly within clay or terminating in clay, TOMLINSON (1957) has compiled complete data for loading tests made on 56 piles. It includes information about the soil type, its average shear strength (along shaft and at base); the embedded length, diameter and material of the pile; ultimate load capacity, estimated cohesion and theoretical adhesion magnitudes as also the period that elapsed between driving and loading of the piles. A very large number of load-settlement curves for load tests on Friction Piles together with the relevant soil data for piles of different materials installed in various types of soils, has been presented by PECK (1961). Table II-1, included in this report, summarizes data on some load tests on model as well as full length field piles (both straight-shaft and belled) giving, in particular, information about the Base Bearing Capacity Factor N_c , the coefficient of load-transfer α and the corresponding values of the settlement ratio Δ/B obtained in those cases.

TABLE 11-1
FILE LOADING TEST DATA

S. No.	Investigator, Year	Type of Soil	Pile Depth, D	Pile Shaft Diam., s _s	Pile Base Diam., s _b	Average Soil Shear Strength		Settlement Ratio ($\frac{\Delta}{s}$)		Coef. of Load- Transfer: α		Base Bearing Cap. Factor: N_c		Remarks
						below base: c_b (lbs/ft ²)	around shaft: \bar{c} (lbs/ft ²)	Corr. to ultimate pile capacity	Corr. to q_{max}	Corr. to ultimate pile capacity	q_{max}	Corr. to ultimate pile capacity	Corr. to q_{max}	
1.	Meyerhof & Murdoch, 1953	London Clay	20 to 40 ft.	12 - 14 in.	12 - 14 in.	4000 to 6000	2000 to 6000	0.1 - 0.2						Bored cast-in- situ concrete piles
2.	Golder & Leonard, 1954	London Clay	13 to 35 ft.	18 - 24 in.	18 - 24 in.	Av. 1 1800	Av. 1 2200			0.64 - 0.74		9 to 13		Bored cast-in- situ concrete piles.
3.	Tomlinson, 1957									0.93 av. for soft clay with conc. 0.71 av. for firm clay with conc. 0.49 av. for stiff clay with conc.				Based on test- results by a large no. of investigators.
4.	Skempton, 1959	London Clay	Variable up to 90 ft.	10 - 30 in.	10 - 30 in.	2310 - 6600	1420 - 4900	0.085 (for 12 - 24 in. diam.)		0.3 - 0.6		8.4 - 10		Bored cast-in- situ conc. piles - no influence of length observed.
5.	Cooke & Whitaker, 1961	London Clay (Rem.)	Variable	0.75 in.	Variable	1435 - 2870	1435 - 2870	0.10 - 0.15	0.005	0.42 - 0.62	0.51 - 0.69	6.4 - 9.6 for $\frac{\Delta}{s} = 101$ 7.1 - 10.3 " " = 151 8.5 - 10.5 " " = 202		Brass Model Piles
6.	Sowers, 1961	Commer- cial Ben- tonite (Rem.)	29 in.	1.21 in.	1.21 in.	1640	1640					5 apply.		Aluminum model piles.
7.	Whitaker, 1962	London Clay	27 ft.	15 in.	15 in.	2670	2460			0.38		9.2		Bored cast-in- situ concrete piles.
8.	Fetschman, 1962	London Clay	70 ft.	36 in.	73 in.	5840	3790			Variable		9.0		Bored cast-in- situ concrete piles.
9.	Lo, 1964	Silty Clay	26 ft.	22 in.	36 in.		890 - 2000			1.0				Displacement conc. caisson.
10.	Harris, 1964	Compacted L. Exp. Clay	11 - 12.4 in.	1 in.	1 and 2 in.	2230 - 5470	2230 - 4300	0.062 - 0.157	0.0047 - 0.0093	0.135 - 0.309	0.248 - 0.419	7.53 - 9.92	0.34 - 2.37	Brass model piles.
11.	Whitaker & Cooke, 1965	London Clay	30 - 50 ft.	24 - 36 in.	48 - 72 in.			0.1	0.01 or less	0.3 - 0.6		6 to 9		Full scale bored concrete piles

NOTE 1. Ultimate Bearing Capacity of a Single Pile, $Q_u = \alpha \bar{c} \cdot A_s + c_b N_c \cdot A_b$
where

A_s = shaft area in contact with the soil = $s_s \cdot D$

A_b = base area of the pile tip = $\frac{1}{4} \cdot (\pi s_b)^2$

2. In the table above,

Δ = settlement of the pile measured at the head,

α = the ratio of the average adhesion between clay and soil to the average undisturbed shear strength of clay within the depth of penetration of the pile,

N_c = computed value of the base bearing capacity factor = $Q_b/c_b \cdot A_b$, where Q is equal to the measured base capacity.

CHAPTER III

BEHAVIOUR OF CAST IN PLACE CONCRETE SCALED PILES IN SILT

3.1 Introduction

The next stage, after the performance of tests on small model piles by HARRIS (1964) was to obtain information on the load-carrying capacity of piles in uniformly graded silt. Pile load tests were carried out in the existing 15' x 12' x 8' test pit filled to a depth of about 6½ feet with medium plasticity silt compacted in layers of 6 inches. Diameter and the depth of the piles were determined so as to utilize the entire pit soil for performing the four proposed tests. For the unobstructed development of slip-line fields, under the loaded piles, the maximum diameter of the shaft worked out to 5 inches and depth to 50 inches, diameter of the centrally located belled pile being 9 inches. The available clearance below the pile tip and around were checked using Mindlin-Ruderman Stress Diagrams (BURMISTER, 1940). Lay-out of piles in the pit and the specially designed bellling tool for the centrally located pile are shown in FIGURES 3.1 and 3.2 respectively. The programme of testing, characteristics of the silty soil and the results of the pile loading tests have been discussed in the paragraphs that follow.

3.2 Testing Programme

Testing programme included the installation of three straight-shaft piles designated A, B and D, each having a uniform diameter of

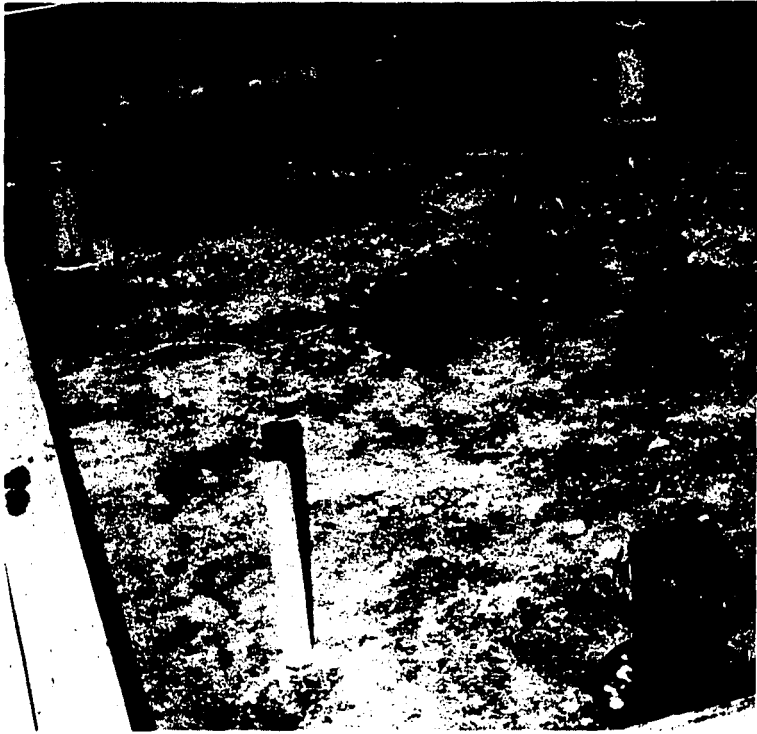
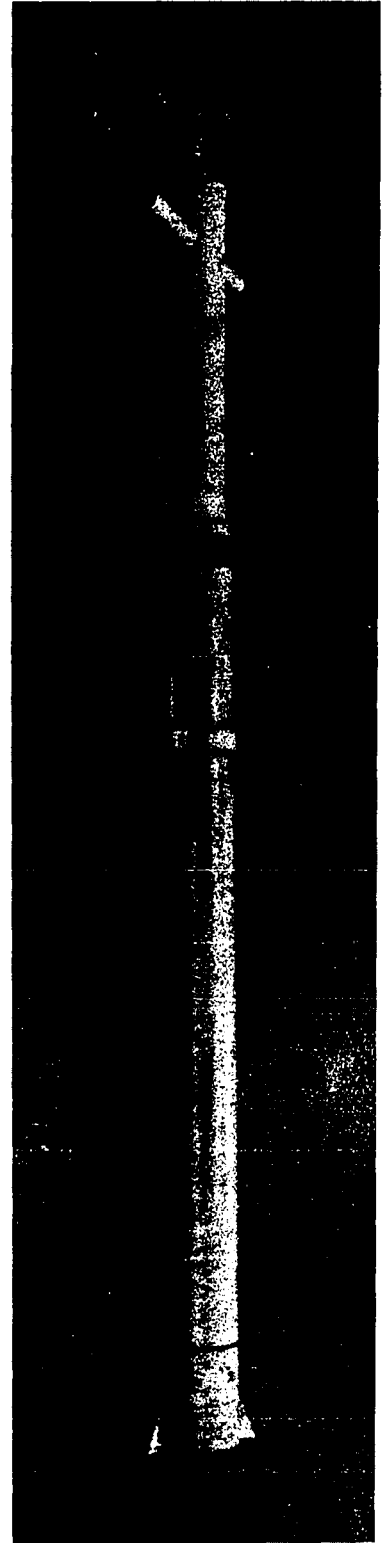


FIGURE: 3.1 LAY-OUT OF PILES IN THE TEST PIT.



**FIGURE: 3.2
BELLING TOOL**

5 inches and one pile designated C, having the base belled out to 9 inch diameter. All holes were bored to the required depths by using an auger. The bottom of the central hole was subsequently enlarged with the bellling tool.

For the elimination of tip resistance, a small air-gap at the bottom of the hole A was proposed to be retained so as to hold the pile in position by skin friction alone. Suspension arrangement used for the purpose has been shown in FIGURE 3.3. Data obtained from the load test on pile A had, however, to be discarded since it was discovered that the effect of the compression of the air-gap below resulted in an unexpectedly high failure-load. Another pile designated E, was therefore installed with air-vent pipes communicating between the gap below and the outside atmosphere (FIGURE 3.4). But for this, all other features of Pile E were similar to those of Pile A.

Pile B with base diameter equal to the shaft diameter, was designed to measure the base resistance by means of a load-cell installed near the bottom of the pile. A three inch long plug of concrete was, however, introduced below the cell, i.e., at the bottom of the hole so as to provide a rough surface at base.

Pile C was similar to Pile B except that its base diameter was enlarged to 9 inches. Load cell was placed a little above the bell.

Pile in position D was a simple straight shaft without any instrumentation and installed by concreting the hole so as to be supported by soil both at base and along the periphery.

Concreting of the holes was done immediately after boring was complete, by using concrete mix designed to have a slump of the order of

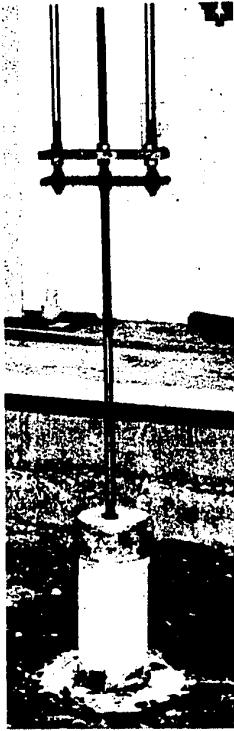


FIGURE: 3.3 SUSPENSION ARRANGEMENT USED FOR PILES A & E (UNSUPPORTED AT BOTTOM).

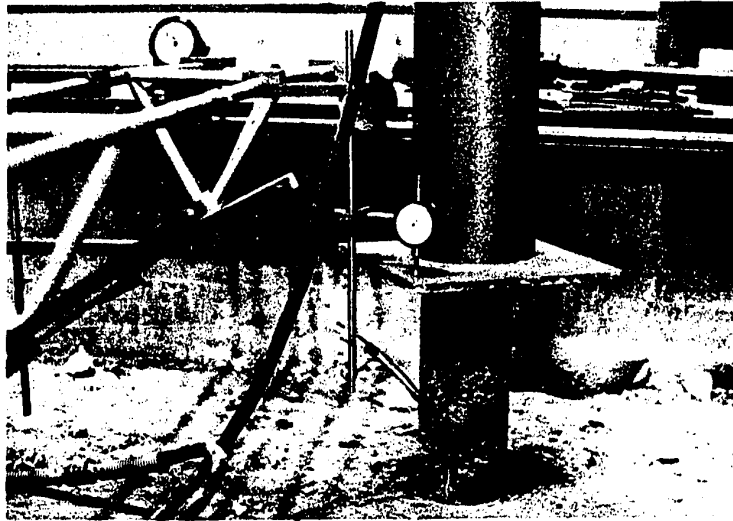
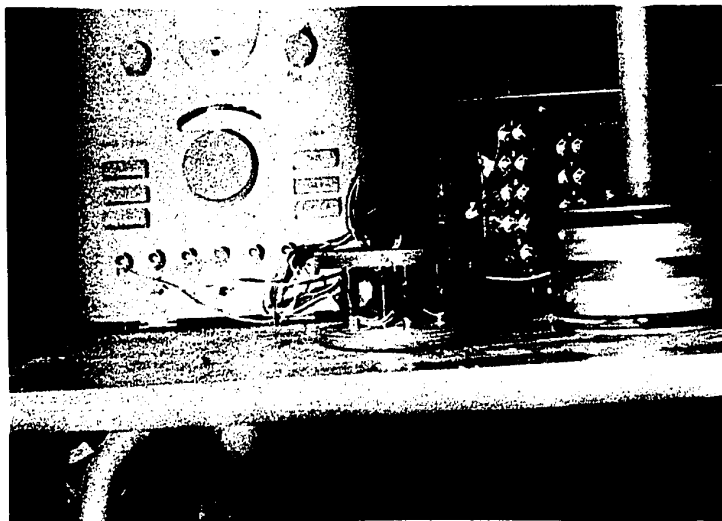


FIGURE: 3.4 PILE E WITH AIR-VENT PIPES COMMUNICATING WITH AIR-GAP BELOW THE PILE (SEEN PROJECTING OUT OF LEFT FACE OF PILE).

FIGURES: 3.5 and 3.6 PARTS & ASSEMBLY OF 5-in. DIAMETER LOAD-CELLS WITH STRAIN-RECORDING INDICATOR & SWITCH-BOX.



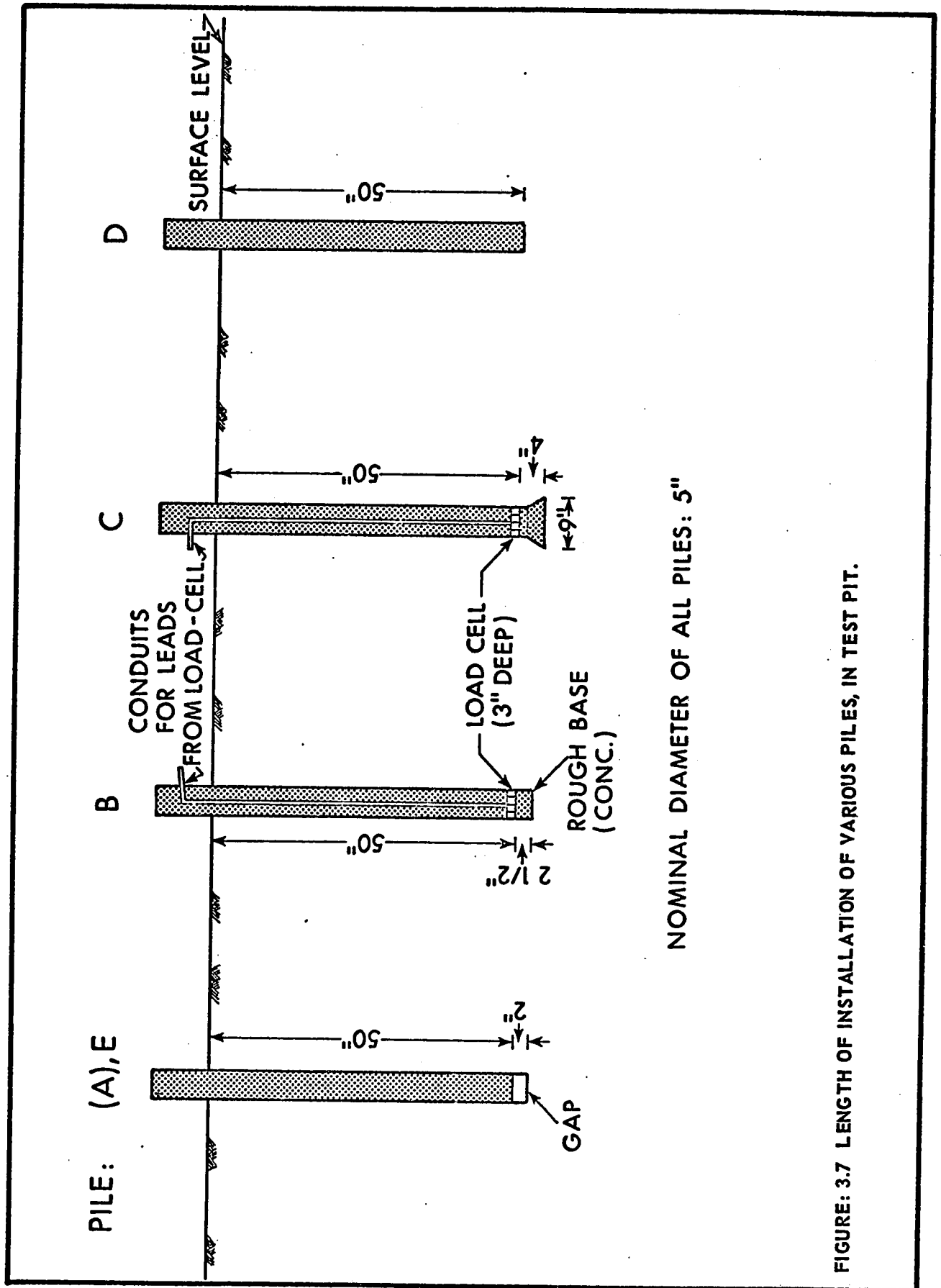
3 to 4 inches. All piles were made to project 12 inches above the surface of the soil.

The two load cells used for measuring base resistance were fabricated in the central Machine Shop, University of Alberta, from Aluminum 65 S-T6. Each cell had four vertical pillars 0.30 in. diameter, 1.50 in. high, snug-fitted into holes in the two plates $\frac{3}{8}$ in. thick, one each at top and bottom. Four SR-4 resistance strain gages (resistance: 120.5 ± 0.3 ohms; gage factor: $1.94 \pm 2\%$) were mounted, one on each pillar, with their axes of length parallel to the centre line of the pillars. A temperature compensation gage was used to counter the effects of heat of hydration from the freshly laid concrete coming in contact with the cell after the concreting operation. There was one common lead connecting one end of each of the gages and four individual leads connected to the other ends. The strain produced as a result of loading could therefore be read separately for each of the pillars, the four added together indicating the load on the cell. FIGURES 3.5 and 3.6 show the two cells, one with the top and the bottom caps removed and the other properly waterproofed and connected to the aluminum shaft ready to be lowered into the hole. Switch box and the strain indicator used to record the strain also appear in the figures. Overall depth of the cell when screwed fully into the top and bottom plates was 3 inches. Both the cells were calibrated for known loads in the Baldwin Compression Machine. Sensitivities of 0.608 micro-inches for cell No. I and 0.83 micro-inches for cell No. II were recorded, each for one pound of load applied at the top. Design details of the load-cells, gage connections, assembly details, calibration curves and data appear in APPENDIX A. With a view to recording the zero-shift, calibration checks were

made immediately before installation of the cells in the holes as well as after their recovery at the end of the testing programme. Before lowering into the holes, the cells were thoroughly waterproofed by pulling a thin membrane (double layer) kept in position by plastic thread, as shown in FIGURE 3.5. All other joints were also leakproofed and the leads taken out through the aluminum conduit (also used as the suspender) up to the middle of the 12-in. high concrete mould from where they were led out through a flexible tubing passing through a hole in the side of the mould.

Concrete mix used for casting the piles was designed by the standard method of mix design (MURDOCK, 1948; LONDE and JONES, 1961; CANADA CEMENT, 1966) to give a slump of the order of 3 to 4 inches. Maximum size of the coarse aggregate chosen was $3/4$ in. Fineness modulus of sand available in the laboratory was 2.53. Since the quantities involved were small, mixing had to be done manually. Actual slump as measured after mixing, ranged from $2\ 3/4$ in. to 4 in. Crushing strength tests were performed on 6 in. diameter 12 in. high cylinders after 7 days. Grain size characteristics of the coarse and the fine aggregates as also the details of mix design and the results of crushing strength tests on concrete cylinders have been recorded in APPENDIX B.

Only one hole was bored and concreted in one day. The depths up to which the holes were excavated by the hand-operated auger have been shown in FIGURE 3.7. Pouring was done in a single operation in small quantities carefully, to avoid segregation, tamping the concrete continuously with a $5/8$ in. diameter steel rod. Hole E was concreted after suspending the five-inch diameter close fitting disc and keeping its level two inches above the bottom of the hole. Rough base, as shown in the figure, was provided



for Pile B by installing a 2½ in. deep concrete plug below the load cell. Belled out hole for Pile C was concreted to a depth of about 4 inches before placing the load-cell thereon. Pile D was constructed in the ordinary way by filling concrete from bottom to top.

A period of seven days was allowed to elapse for the development of adequate strength by self-curing before the piles were test-loaded.

3.3 Physical and Strength Characteristics of Pit Soil

Distribution Curve for particle-size analysis (FIGURE 3.8) shows a uniform gradation of silt size particles. The proportion of silt is as high as 86% with equal amounts of clay and sand-size particles. In spite of the predominance of silt-size particles, the soil plots within the region of clay of medium plasticity above the Casagrande A-Line as shown in FIGURE 3.9(a). The position occupied by it on the Textural Classification chart is indicated in FIGURE 3.9(b).

A majority of laboratory tests were run in the British Portable Testing Apparatus (COOLING and GOLDER, 1940) on samples 1½ in. diameter, 3 3/8 in. overall length removed by sampling inside the pit, yielding the stress deformation curves directly. Some more unconfined compressive strength tests were carried out on specimens compacted in the laboratory at an average moisture-content corresponding to that in the pit and compactive effort comparable to standard Proctor Test. Finally, a series of undrained triaxial tests were run on similar samples compacted in the laboratory. The results of the strength tests are summarized in TABLE III-1 below. Engineering properties of the pit soil have been reported in APPENDIX C.

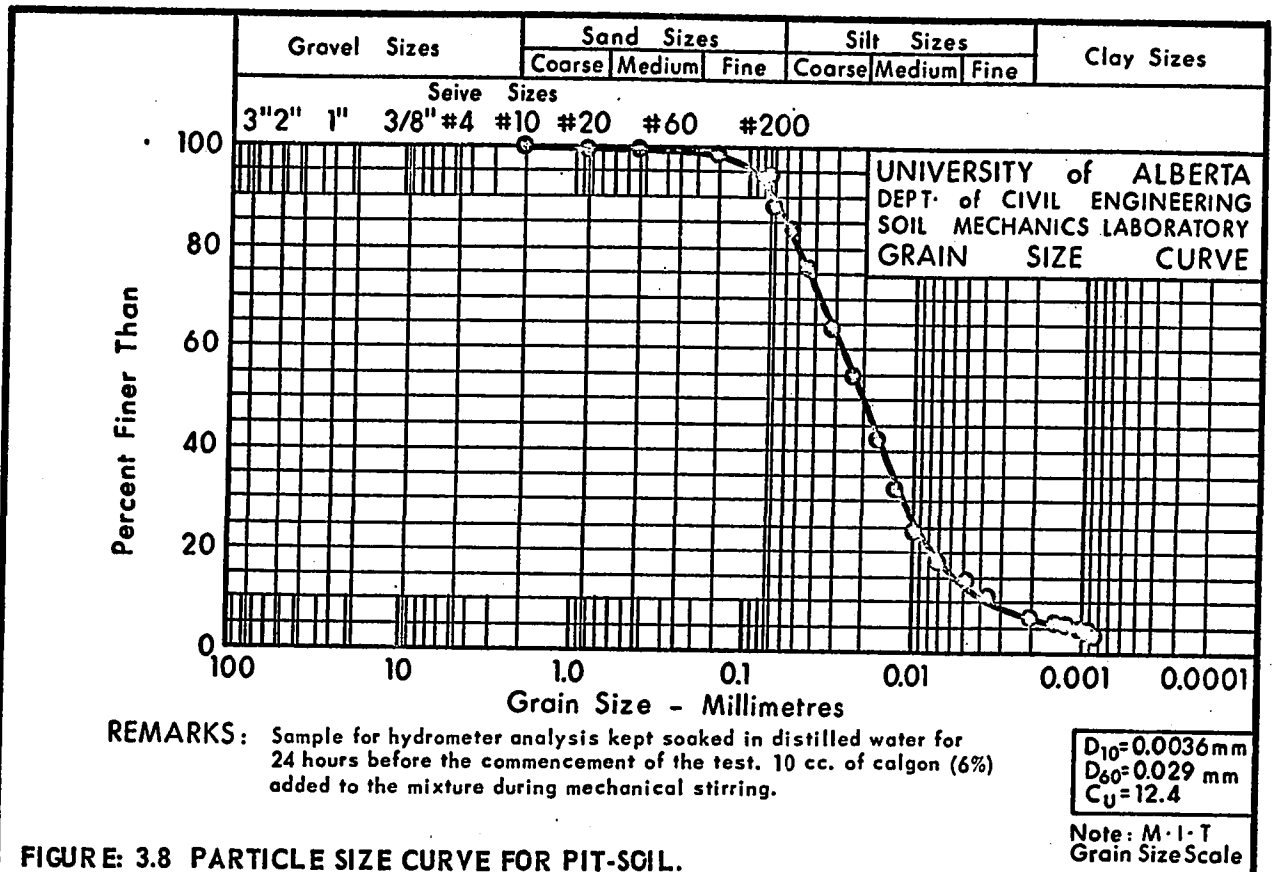
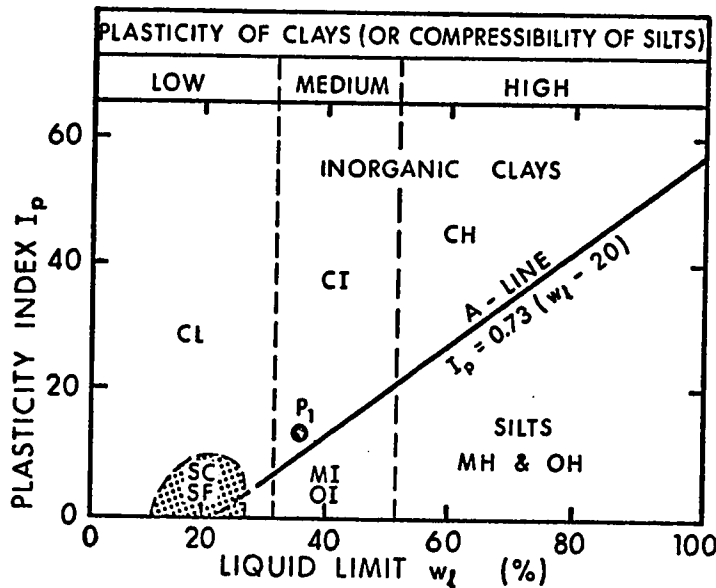
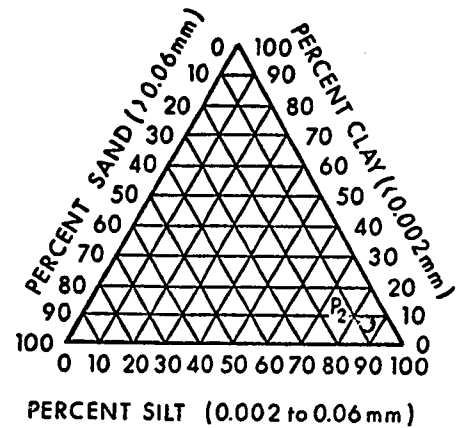


FIGURE: 3.8 PARTICLE SIZE CURVE FOR PIT-SOIL.



(a) Casagrande's Plasticity chart.



(b) Textural classification chart (based on M.I.T. System).

FIGURE: 3.9 SOIL CLASSIFICATION CHARTS SHOWING THE POSITIONS OCCUPIED BY PIT SOIL. (The soil plots as P_1 and P_2 on the two charts.)

TABLE III-1
RESULTS OF STRENGTH TESTS ON PIT SOIL

NATURE OF TEST	ORIGINAL MOISTURE CONTENT (%)	SHEAR STRENGTH (psi)	REMARKS
1. Unconfined compression Tests (British Portable Apparatus)	23.3 (avg.)	8.04	Undisturbed samples as removed from the pit, earlier compacted at standard proctor specifications at o.m.c.
2. Unconfined compression Tests (Chicago Compression Testing Apparatus)	23.7 (avg.)	6.4	Laboratory-compacted samples (Proctor specifications)
3. Undrained Triaxial Tests (Farnell Motorised Machine)	20.0 24.0	9.5 6.5	Laboratory-compacted samples (Proctor specifications)

3.4 Loading Procedure

The procedure of loading the piles conformed, in general, to ASTM Designation D 1143-57 T. It was proposed to load all the piles to failure, i.e., to continue loading till rapid progressive settlement occurred or till the total settlement was of the order of one inch. Piles with bearing areas equal to the sectional area of the pile were expected to sustain an ultimate load of about 6400 lbs. each. The one with the base belled out to 9 in. diameter was estimated to take up to 9000 lbs. and the fourth pile supported by skin friction alone would withstand a load of about 4500 lbs. at top. These loads were estimated on the basis of average shear strength of the soil along the shaft and at base. The loading increments were based on these

values, the increment of loading having been reduced to half as the piles approached failure. Settlement readings were taken immediately after the application of each load increment, before the application of the next increment and thrice in between. The corresponding strain indicator readings indicating the load transferred through the base were recorded for Piles B and C. At the end of the test, unloading was done in three increments and the corresponding dial readings were recorded. Each increment of the load during loading or unloading was maintained for a period of half an hour.

Loading was done with a 25-ton hydraulic jack calibrated for known loads in Baldwin-Compression Machine. Calibration curve and data appear in APPENDIX D.

Jacking reaction was obtained by moving and fixing in position, the overhead steel beam covering a range of about half the pit area. Test loading set-up used for Piles B, C and E, making use of the said beam has been shown in FIGURES 3.10 and 3.11. Since the range of movement of the overhead beam did not cover the position for Pile D, a different arrangement had to be used for obtaining the reaction. A one-ton welded plate-girder was placed across the pit longitudinally and the contact between the top of this girder and bottom of the overhead beam rolled over to the middle of the pit, was established by inserting steel plates in between the gap. Reaction due to jacking was then applied at the free end of the plate girder acting as a cantilever for half of its length. This arrangement has been shown in FIGURE 3.12 and 3.13. Data for pile load tests and the record for strain indicator readings (for Piles B and C) appear in APPENDIX E.

FIGURES: 3-10 LOAD TEST SET-UP FOR PILE B.

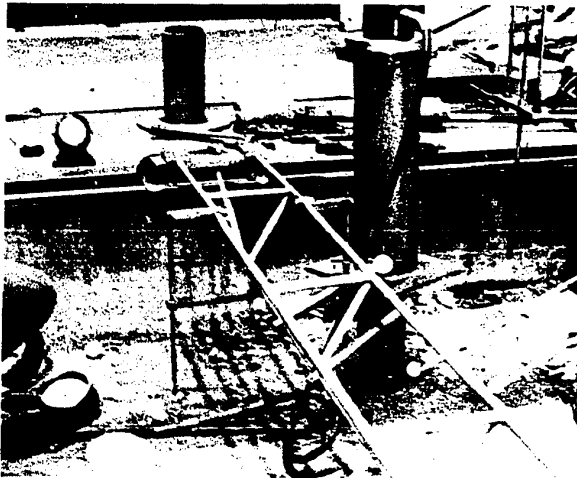
HYDRAULIC JACK

STRAIN INDICATOR
AND SWITCH BOX

OVERHEAD BEAM



FIGURE: 3.11 LOAD TEST SET-UP FOR PILE E.



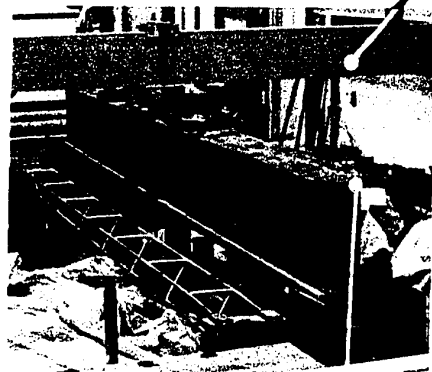
TEST PILE

MOVABLE FRAME
FOR HOLDING
DIAL GAGE.

FIGURES: 3.12, 3.13 LOAD TEST SET-UP FOR PILE D.



OVERHEAD BEAM



1-TON PLATE GIRDER

3.5 Recovery of Piles

The pit soil was partly excavated out to expose all the piles on one side up to a depth ranging between 6 and 10 inches below the tip of the piles with a view to studying the failure patterns developed if any. The same, however, were not noticeable. FIGURES 3.14 and 3.15 show the exposed views of the piles after the conclusion of the testing programme.

The actual length and diameter of each pile was measured after their removal. Whereas the effective lengths and shaft diameters of all piles were almost the same as desired, the diameter of the bell (Pile C) was measured to be about 8 in. This was probably due to the caving in of the sides and the roof of the bell during the time that elapsed after the removal of the belling tool and the concreting of the hole.

3.6 Analysis of Laboratory Test Results on Pit Soil

Moisture-content in the pit varied from about 20 per cent at the surface to about 29 per cent at a depth of 54 inches with the degree of saturation reaching about 85 per cent. A study of the moisture-content, shear strength and density data vis-a-vis consistency of cement concrete mix used for concreting reveals interesting relationships. Slump of concrete (as measured after mixing) and strength characteristics of the soil have been given in TABLES III-2 and III-3. Values of shear strength before and after concreting are represented graphically in FIGURE 3.16. Initial moisture-content profile is also drawn alongside. The drop in shearing strength of soil after concreting the hole, was found to have a close relationship both with the value of slump (in inches) measured after mixing

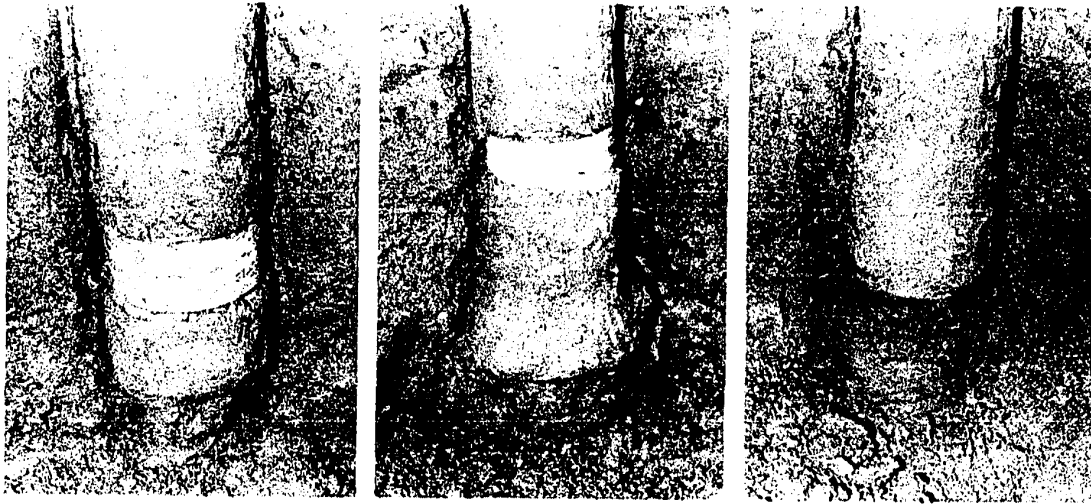


FIGURE: 3.14 LOWER PORTIONS OF PILES B, C & E PHOTOGRAPHED AFTER REMOVING TOP SOIL FROM ONE SIDE OF VERTICAL DIAMETRAL PLANE.



FIGURE: 3.15 PILES AS RECOVERED AFTER EXCAVATION OF PIT SOIL.

TABLE III-2
SHEAR STRENGTH OF SOIL BEFORE (a) AND AFTER (b) CONCRETING

Sampling Depth (in.)	Shear Strength (lbs./in. ²)							
	B		C		D		E	
	Before	After	Before	After	Before	After	Before	After
0 - 9	8.0	5.2	9.0	7.9	9.2	7.6	8.2	6.4
9 - 18	9.2	7.7	9.8	9.5	9.8	7.9	9.5	7.5
18 - 27	8.1	7.2	8.7	8.0	7.6	7.7	7.6	5.5
27 - 36	7.4	6.0	7.3	7.7	7.0	6.5	6.7	5.4
36 - 45	7.2	4.0	7.0	7.0	7.0	6.3	6.8	5.2
45 - 54	2.7	2.8	2.7	2.0(c)	2.7	2.5(c)	2.7	2.8(c)

Explanation:

- (a) For shear strength values before concreting, samples were removed along the centre-lines of the holes.
- (b) For shear strength values after concreting, samples were removed from within one inch of pile face.
- (c) These values represent the average shear strength of soil samples taken around the piles at levels below the pile tip up to maximum depth of 59 in. below surface.

Note: The values reported in the table above are those obtained from unconfined compression tests carried out with the British Portable Machine.

TABLE III-3
DATA FOR SOIL MOISTURE CONTENT, SOIL SHEAR STRENGTH
AND SLUMP OF CONCRETE

Description	PILE			
	B	C	D	E
1. Soil moisture content (avg.) before concreting the hole (%).	23.7	23.2	22.2	24.1
2. Soil moisture content (avg.) after concreting the hole (%).	25.6	23.9	23.5	26.5
3. Increase in M.C. (shaft soil) as a percentage of original m.c.	8.05	3.02	5.85	9.12
4. Soil Shear Strength (avg.) before concreting the hole (lbs./in. ²).	7.98	8.30	8.12	7.76
5. Soil Shear Strength (avg.) after concreting the hole (lbs./in. ²).	6.02	8.02	7.10	6.00
6. Percentage decrease in shear strengths (shaft soil).	24.6	3.4	12.5	22.6
7. Slump of concrete (in.)	4	2 3/4	3 1/2	4

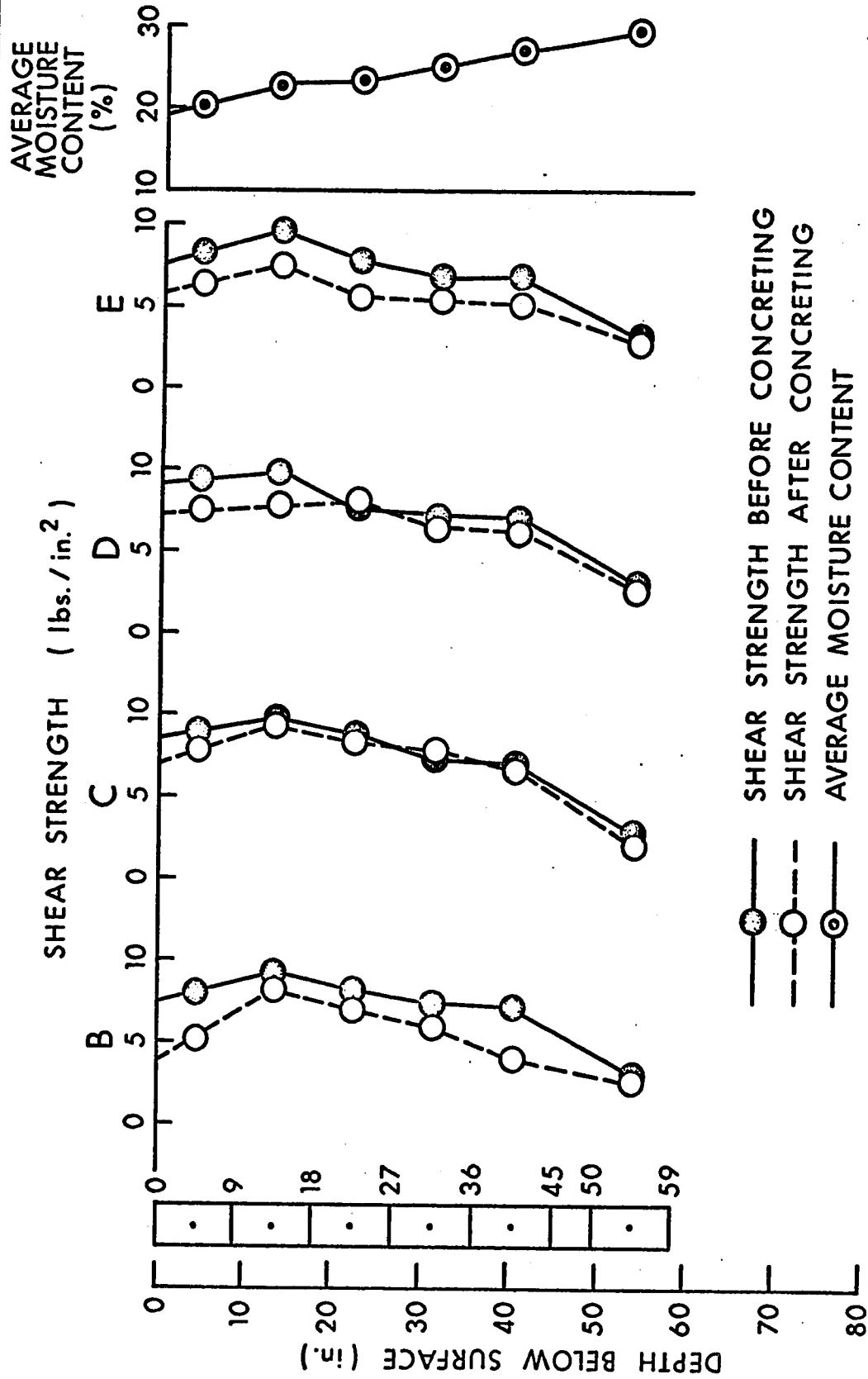


FIGURE: 3.16 MOISTURE CONTENT AND SHEAR STRENGTH VARIATION OF PIT SOIL WITH DEPTH.

the concrete and with the increase in moisture content of the soil after concreting. As seen from FIGURES 3.17 and 3.18, both these relationships are found to be linear.

Methods of concrete mix design are usually based on the value of the water-cement ratio so as to ensure adequate supply of water for complete ultimate hydration. The quantity of water, therefore, more often than not, is in excess of the actual requirement. Further, since the process of hydration continues for a long time, all the water in the mix is not immediately needed for chemical action. Initially surplus water especially along the interface between concrete and soil may have greater affinity for soil than for the saturated aggregate cement mixture, depending upon the vapour-pressure gradient set up between concrete and soil, which in turn would be further dependent upon the initial degree of saturation of the soil. A reverse gradient might be set up after equilibrium conditions are established and water, if available, might then be sucked towards the pile for the process of hydration to continue. Moisture content of the soil immediately surrounding the pile and hence its shear strength thus appear to be very much a function of water-cement ratio (or slump) for cast-in-place uncased concrete piles in silt. This aspect becomes all the more important for short term loading tests wherein adequate time is not available for equilibrium conditions to establish. The pertinent factors which appear to be important in this respect thus are the average size of the soil particles, initial degree of saturation, quantity of surplus water from fresh concrete immediately available and the diameter of the pile.

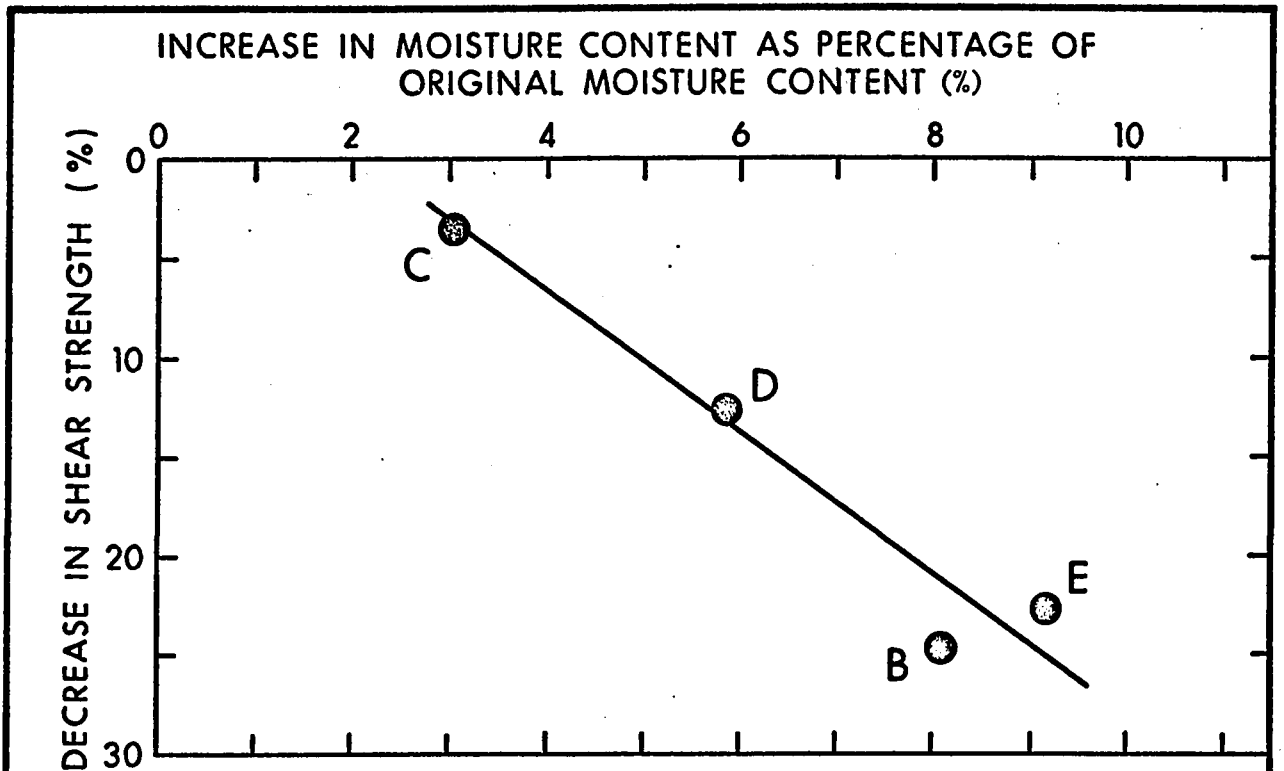


FIGURE: 3.17 DECREASE IN SOIL SHEAR STRENGTH vs. INCREASE IN MOISTURE CONTENT.

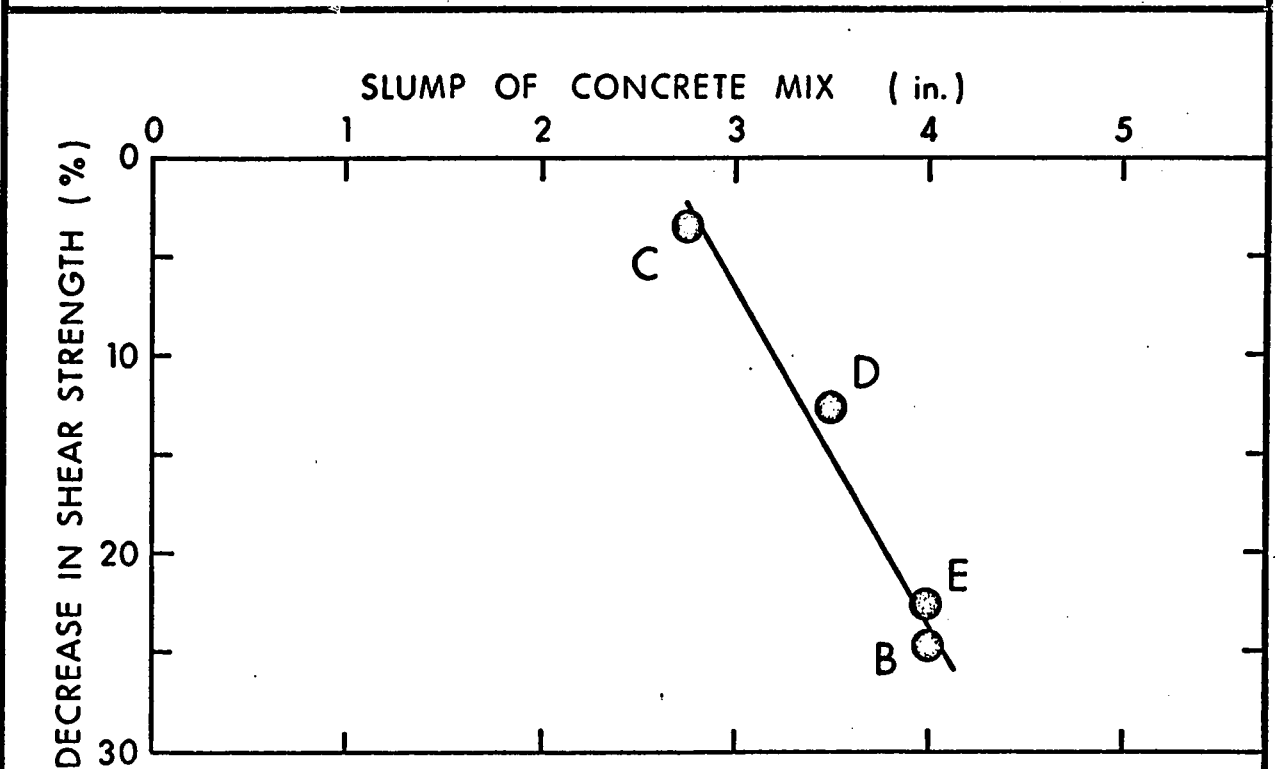


FIGURE: 3.18 DECREASE IN SOIL SHEAR STRENGTH vs. INCREASE IN SLUMP OF CONCRETE.

3.7 Pile Loading Test Results

Load tests on piles were performed in accordance with the procedure described earlier in paragraph 3.4. Load Settlement Curves between total load at any stage and the corresponding ultimate settlement after a half-hour interval are shown in FIGURE 3.19. Settlement curves as related to the duration of loading have been shown in FIGURE 3.20. All the curves indicate quick building up of resistance, with the maximum loads corresponding to settlement ratios (i.e., $\frac{\text{top settlement}}{\text{pile diameter}}$) designated Δ/B , of the order of 2.8 to 4.2%. Settlements beyond the point of ultimate load are relatively large and show a small linear increase in the sustaining capacity of the pile. Total rebound after the removal of the load in increments, was of the order of 12 to 20% of the total settlement for all piles except for the one unsupported at the bottom in which case it was about half as much. Assuming modulus of elasticity for concrete to be 5×10^6 lbs./in.², the elastic compression of the concrete shaft would amount to 0.0002 to 0.0003 in., which being negligible has been ignored. The rebound was thus either due to the elastic expansion of the soil below the tip or due to release of stresses along the shaft. Net settlement at the failure load averages out to be about 85% of total settlement at that load.

3.8 Analysis of Tip Resistance

FIGURES 3.21 and 3.22 indicate the Tip Load or Base Load Q_B transferred to soil through the lower end of Piles B and C, as recorded by the load-cells installed near the tips. The rate of building up of tip resistance for relatively small values of settlement is large compared to

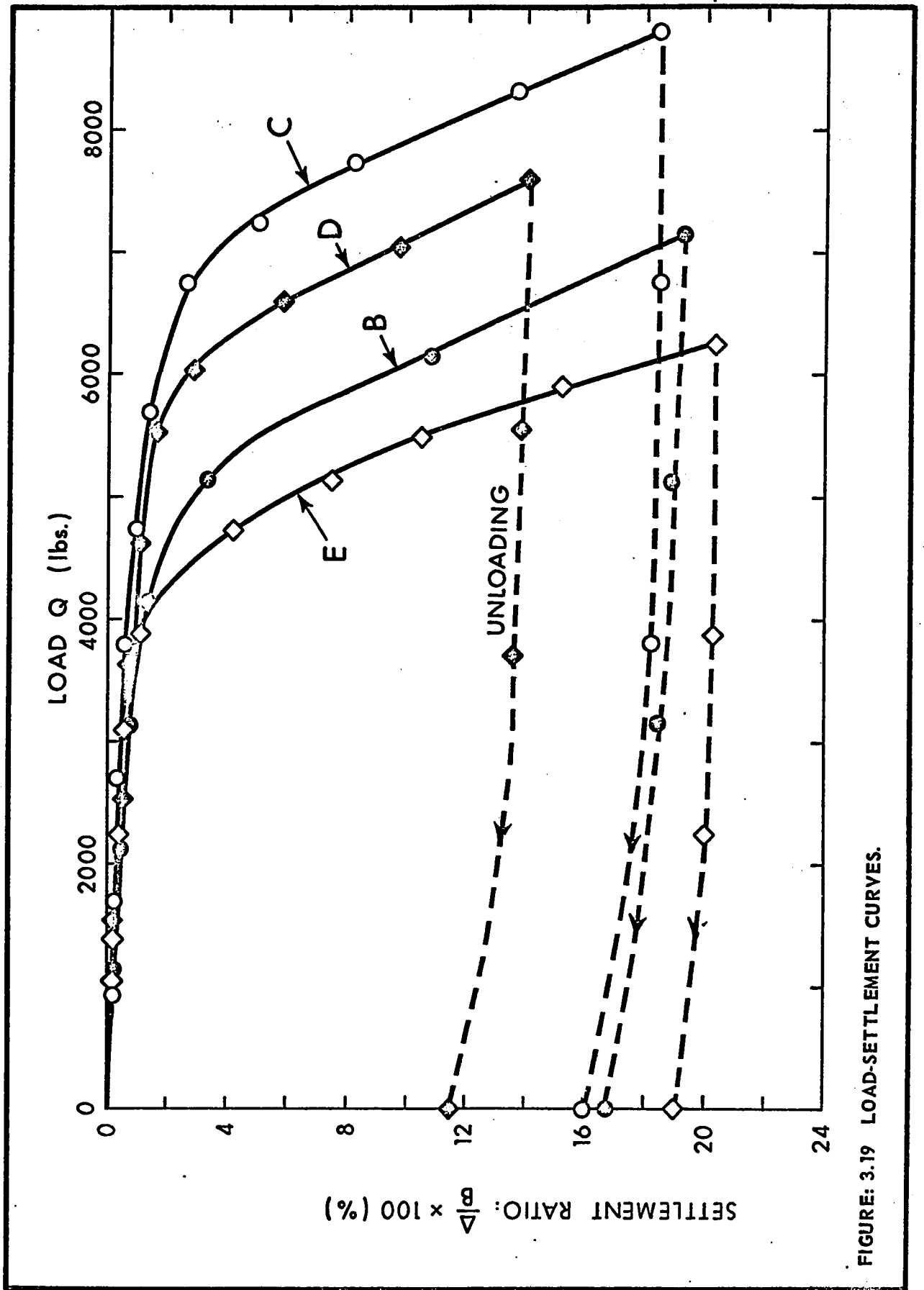


FIGURE: 3.19 LOAD-SETTLEMENT CURVES.

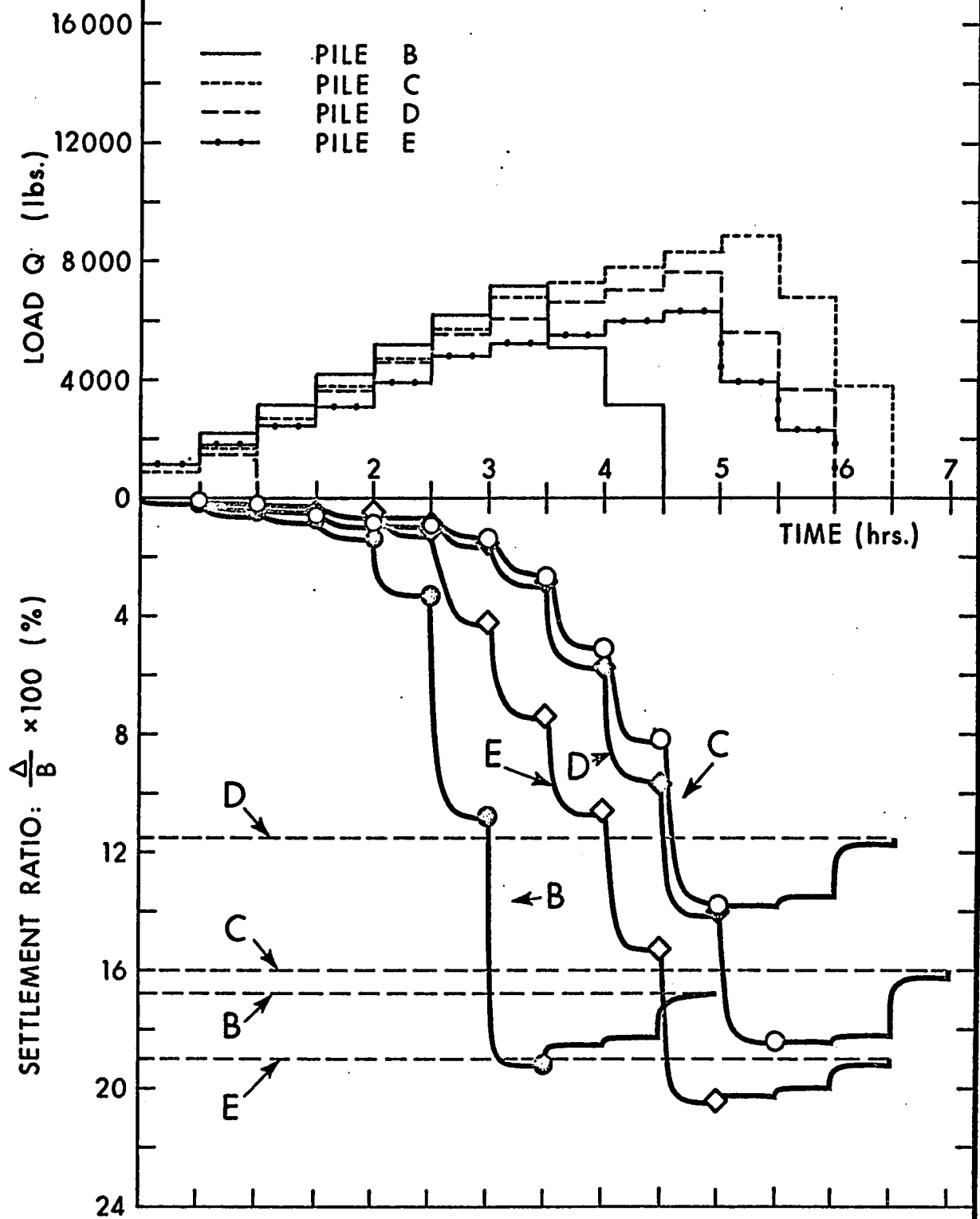


FIGURE: 3.20 LOAD-TIME-SETTLEMENT CURVES.

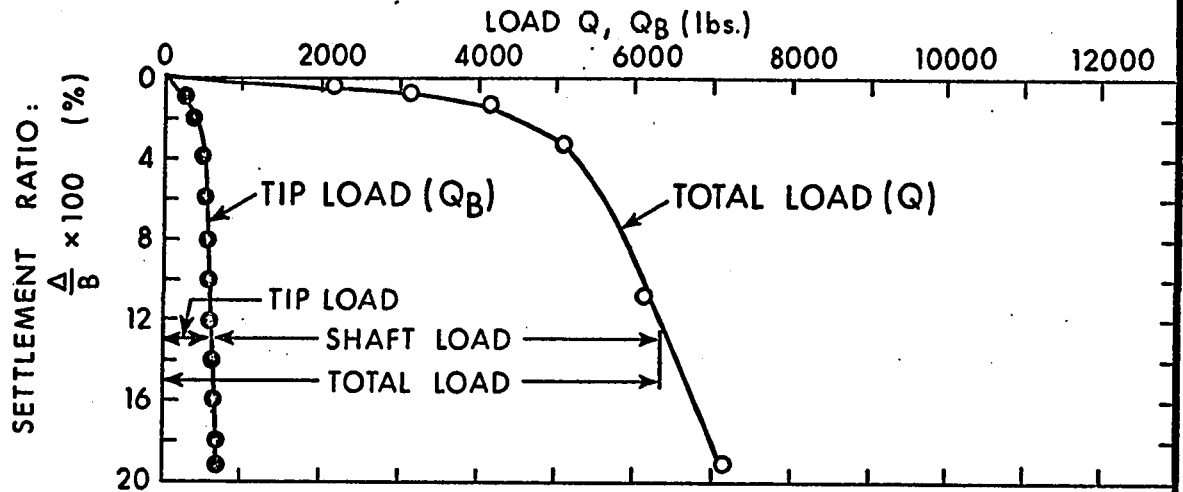


FIGURE: 3.21 RELATIVE PROPORTIONS OF TIP LOAD AND SHAFT LOAD (PILE B IN SILT).

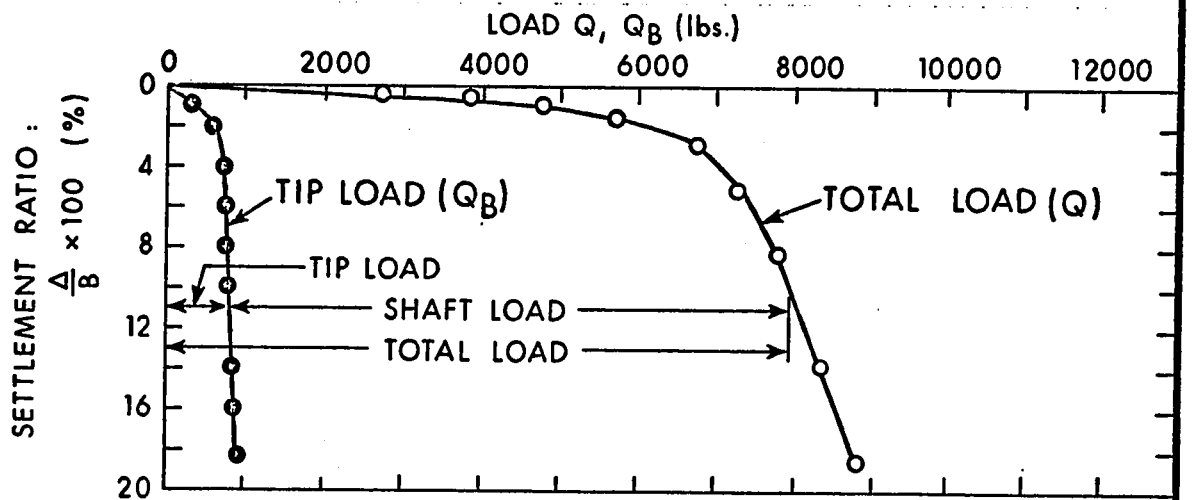


FIGURE: 3.22 RELATIVE PROPORTIONS OF TIP LOAD AND SHAFT LOAD (PILE C IN SILT).

that for settlements exceeding about 4% of the base diameter. The effective bearing area of the belled-out pile C is approximately two-and-a-half times that of Pile B but the indicated maximum base resistance is only slightly higher.

FIGURE 3.23 reveals that only a small percentage of the total load at failure (6.5 per cent for Pile B and 8.5 per cent for Pile C) is transferred to the base, the rest all having been taken by skin friction. The percentage load transmitted through the base increases more or less uniformly with settlement up to about 50% of the settlement at failure load but the rate of increase falls gradually thereafter. The mean curve in FIGURE 3.24 represents the manner in which the base-resistance is mobilized. A major portion of the base-resistance is built up when the settlement ratio reaches a value of about 1.5 per cent while the rest is built up when the settlement further increases to about 3.7 per cent of the base diameter. Depending upon the magnitude of base resistance so built up, the Bearing Capacity Factor N_c (= base load/base area x undrained shear strength of the soil below tip) varies as indicated by the mean curve in FIGURE 3.25. Its values corresponding to the ultimate load are: 6.0 approximately for Pile B and 6.25 for Pile C. Variation of the bearing capacity factor N_c as percentage of N_c at failure for the mean of the values for Piles B and C has been shown plotted against settlement in the same figure. Steady increase in the values of N_c reflects the mode of mobilization of base resistance with increase in the penetration of the pile.

With over 90 per cent load transferred to soil through skin friction, the piles can be termed Friction Piles. Compared to a natural soil

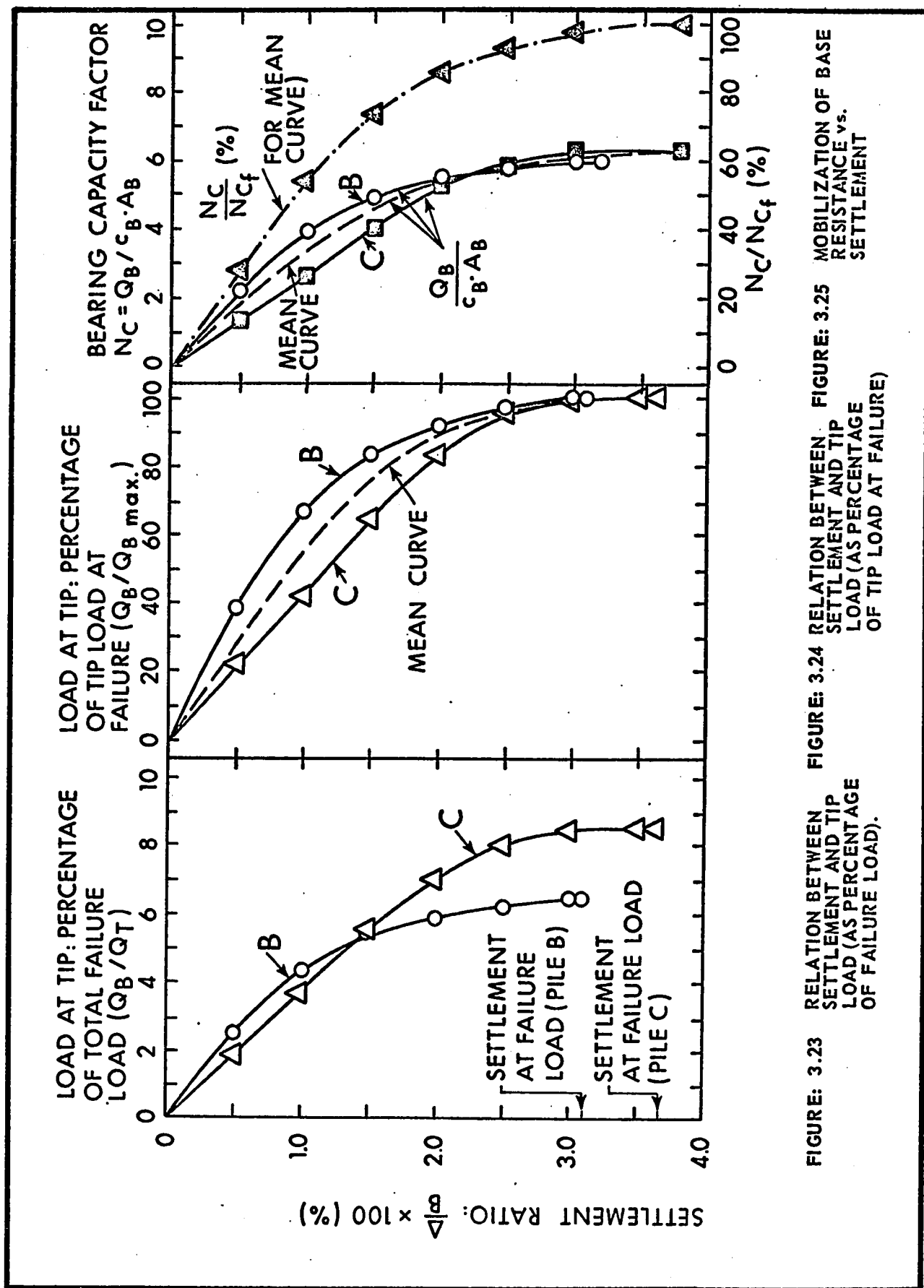


FIGURE: 3.23 RELATION BETWEEN SETTLEMENT AND TIP LOAD (AS PERCENTAGE OF FAILURE LOAD).

FIGURE: 3.24 RELATION BETWEEN SETTLEMENT AND TIP LOAD (AS PERCENTAGE OF TIP LOAD AT FAILURE)

FIGURE: 3.25 MOBILIZATION OF BASE RESISTANCE vs. SETTLEMENT

stratum where the shear strength, in general increases gradually with depth, the conditions pertaining in the test pit showed an opposite trend. The average value of shear strength near the pile tip is less than 25 per cent of that near the surface so that contribution of tip resistance to the total load capacity of the pile is not significant. Pile action, i.e., the mechanism of load transfer from pile shaft to surrounding soil and at base, is a function of deformation of the soil. The stress vs. strain curves (APPENDIX C) for soil samples at moisture contents of 22% and 26% respectively representing average conditions for shaft soil and those close to the pile tip, indicate moduli of deformation of 1650 lbs./in.² and 380 lbs./in.² respectively corresponding to about 2 per cent strain. Fall in the value of deformation modulus with depth is indicative of the reduction in shear strength and hence in the rate of load transfer. This is in conformity with the observed behaviour of piles.

Compared to N_c values of 6.0 and 6.25 in the present series of tests on pit silt having a degree of saturation of about 90% observed 7 days after concreting the holes), significantly different values for deep foundations on saturated clay were obtained by other investigators (9.0: Skempton; 10 to 13: Golder and Leonard; 9.3: Meyerhof and Murdock). The assumption that $\phi = 0$ and often found appropriate for saturated or nearly saturated clay soils, forms the basis for all normal calculations of ultimate bearing capacity in clays but the same for silty clay is, according to SKEMPTON (1951), sufficiently far from the truth. In order to verify this point in relation to soil conditions in the test pit, a series of undrained triaxial tests was run. Typical stress-strain curves and Mohr's total stress diagrams have been

shown in APPENDIX C. The convex-up shapes of plots are indicative of the presence of air or the degree of saturation being less than 100 per cent. The two typical moisture contents, viz. 22 per cent and 26 per cent, chosen for tests represent approximately the average conditions along the shaft and below the tip of the pile. As normal stress on the sample increases, the soil rapidly approaches saturation. Thus when the stress corresponds to the ultimate load on the pile, the angle of shearing resistance falls down from an average of 25 degrees to 8 degrees along the shaft and from 13 degrees to nearly zero below the pile tip. Pore-water pressures would build up thereafter. The " $\phi = 0$ " failure condition can there be assumed under the pile tip at the ultimate failure load of the pile. It can therefore be concluded that saturated plastic silt shows up ultimate unit bearing values considerably less than saturated clay under similar conditions. Values of N_c generally attainable in saturated clays therefore do not apply for silts. SCHMITTER (1961) has reported a value of N_c equal to 7. Very low bearing values for saturated silts have also been hinted at by BOLOGNESI (1961). The conclusion is in general agreement with the earlier observation by MEYERHOF (1950).

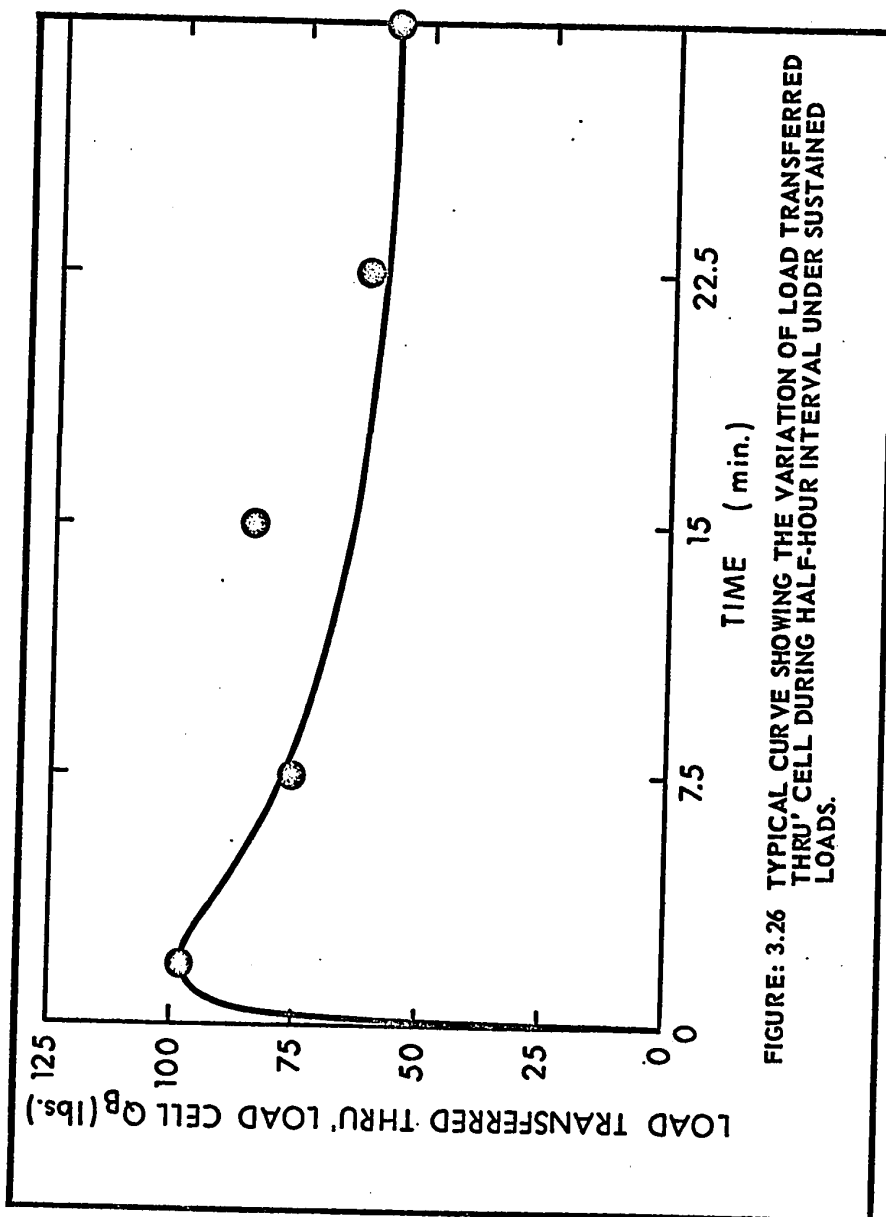
Major contribution to the settlement of piles in the present case, unlike that in saturated clays, appears to have been made by the compressibility of the soil because the soil was not completely saturated and the soil skeleton being relatively less rigid, particles could shift positions by sliding and rolling thus pushing out air from the voids during the process.

Computations for the values of N_c reported in the above paragraphs have been made on the basis of horizontal portions of the curve between the load transferred through the cell and time under sustained loads.

A typical Q_p vs. time curve for 30 minutes during which a constant load of 2700 lbs. was maintained on Pile C has been shown in FIGURE 3.26. Each increment, during the process of loading, was built up within 1 to 2 minutes and was maintained for half an hour. Maximum transfer of load through the load cell was recorded in the beginning and the same fell thereafter to about 80 per cent of the peak value after about $7\frac{1}{2}$ minutes. The rate of decrease was gradual after that and a constant value of the order of 60 to 65 per cent of the peak value was maintained after about 20 minutes.

3.9 Analysis of the Shaft Capacity

All the physical features of Piles B and D (FIGURE 3.7) being similar except that B was provided with a load cell at bottom whereas D was not, the ultimate load capacity should have been approximately the same. The actual values, however, were 6050 lbs. and 5100 lbs. respectively. Subtracting the tip resistance equal to 330 lbs. as recorded by the load cell, the shaft capacity of pile B, at failure load, works out to 4770 lbs. On the other hand, the shaft capacity of Pile D after allowing an approximate value of base resistance of 305 lbs. (base area x shear strength of soil below tip x assumed average value of 6.15 for N_c), works out to 5745 lbs. The difference is accounted for by the variation in the average value of soil shear strength after concreting, being 5.95 lbs./in.² in the former and 7.05 lbs./in.² in the latter case, as recorded in TABLE III-3. Shaft resistance of Piles B, C and E have been shown plotted in FIGURE 3.27 against settlement. Curve for Pile E (unsupported at bottom) has been plotted from load test data directly, whereas those for B and C



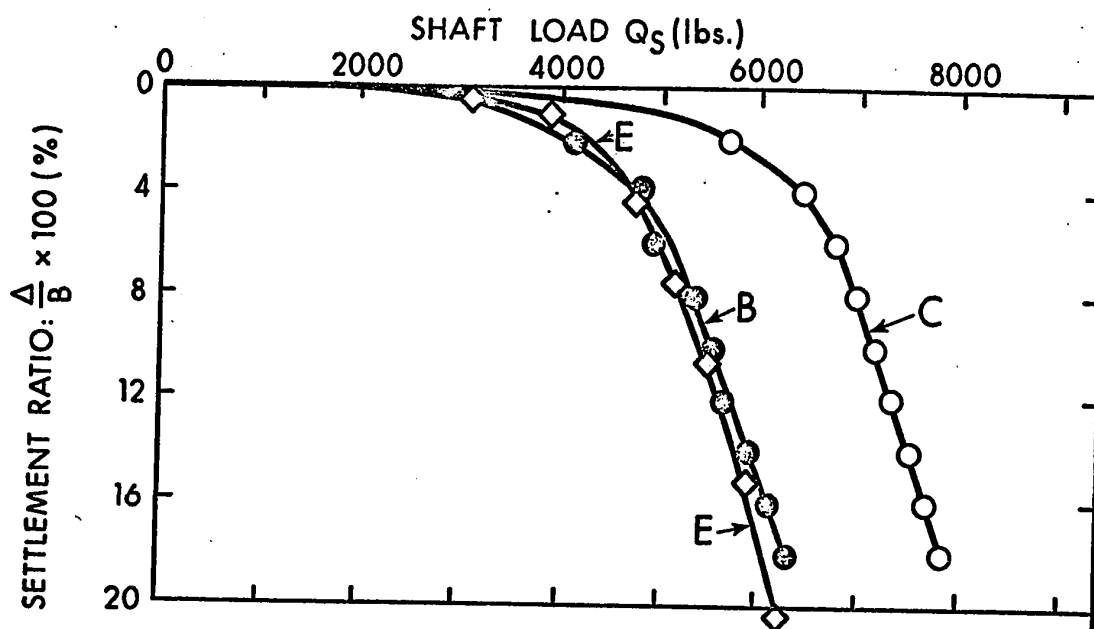


FIGURE: 3.27 SHAFT LOAD vs. SETTLEMENT.

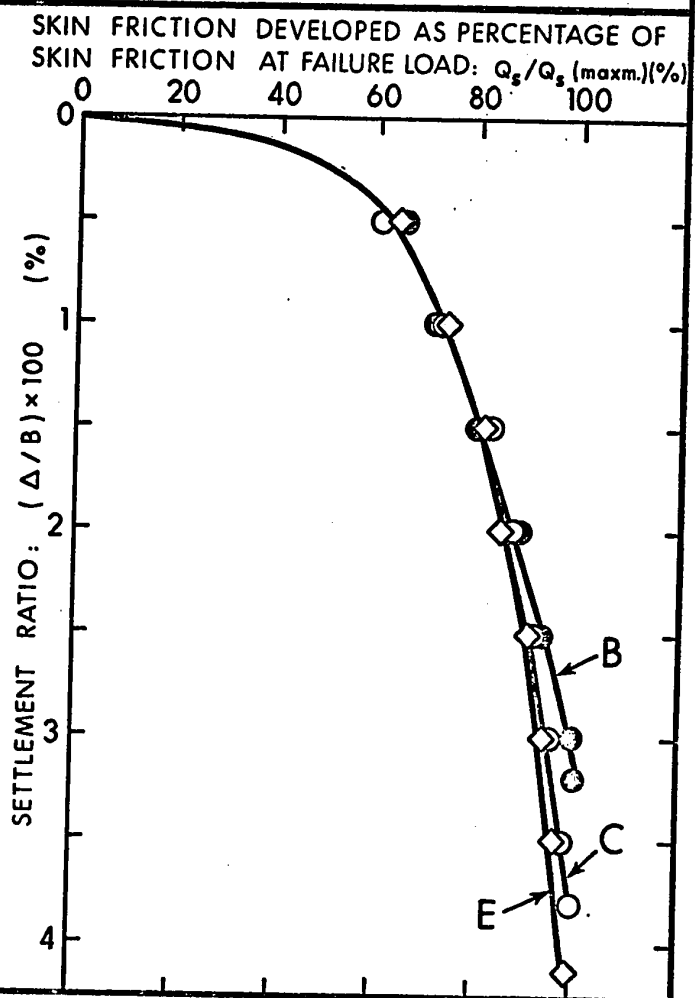


FIGURE: 3.28 SKIN FRICTION DEVELOPED (AS PERCENTAGE OF SKIN FRICTION AT FAILURE LOAD) vs. SETTLEMENT.

have been plotted after deducting the values for tip resistance as recorded by load cells. This method of analysis, however, ignores the effect of interaction, since actually the load at top is shared simultaneously by shaft and base. There is theoretical evidence to show (MEYERHOF, 1951) that the value of end bearing is only about 4 per cent higher for friction acting along the shaft than for none. Plots for Piles B and E fall on each other almost completely whereas the one for Pile C does not, the difference as stated earlier being due to the enlarged area of the bell and higher average value of shearing strength of the soil around the shaft. The nature of variation exhibited by all the curves is the same, being indicative of quick build-up of shaft resistance for small values of pile penetration and an abrupt fall in the rate-increase thereafter. The maximum shaft resistance built up is over 90 per cent of the total load capacity of the pile and corresponds to approximately the same value of settlement. Unlike piles in clay, curves for shaft resistance did not show any pronounced peak. The manner in which the average skin friction (being the ratio of the load transferred through the shaft at any instant to the contact area of the shaft) is mobilized as the pile penetration increases, is shown in FIGURE 3.28. All the curves are coincident to a large extent and so are indicative of similar behaviour. The development of skin friction is rapid in the beginning but drops off gradually as the settlement increases.

3.10 Coefficient of Skin Friction

Soil lost part of its shear strength as a result of increase in moisture content after concreting. Strength decrease has been expressed in terms of the Coefficient of Softened Shear Strength α_1 (TABLE III-4)

TABLE III-4
COEFFICIENT OF LOAD-TRANSFER AS RELATED TO INCREASE IN MOISTURE CONTENT
OF SOIL AROUND THE SHAFT

Pile	Unit Adhesion Developed at Failure Load, c_a (lbs./in. ²)	Shear Strength of Shaft Soil		Coefficients:			Increase in Moisture Con- tent Due to Concreting (%)
		Before correcting: \bar{c} (lbs./in. ²)	After correcting: \bar{c}_1 (lbs./in. ²)	$\alpha_1 = \frac{\bar{c}_1}{\bar{c}}$	$\alpha_2 = \frac{c_a}{\bar{c}_1}$	$\alpha = \alpha_1 \cdot \alpha_2$ $= c_a / \bar{c}$	
B	5.95	7.98	6.02	0.755	0.987	0.745	8.05
C	8.00	8.30	8.02	0.966	0.996	0.962	3.02
D	7.05	8.12	7.10	0.875	0.994	0.860	5.85
E	5.82	7.76	6.00	0.772	0.960	0.750	9.12

Explanation:

1. In the above table, c_a , \bar{c} and \bar{c}_1 , all represent the average soil strength values along the shaft.
2. α_1 represents the coefficient of Softened Shear Strength;
 α_2 represents the Coefficient of Reduction; and
 α represents the overall Coefficient of Load Transfer.

where:

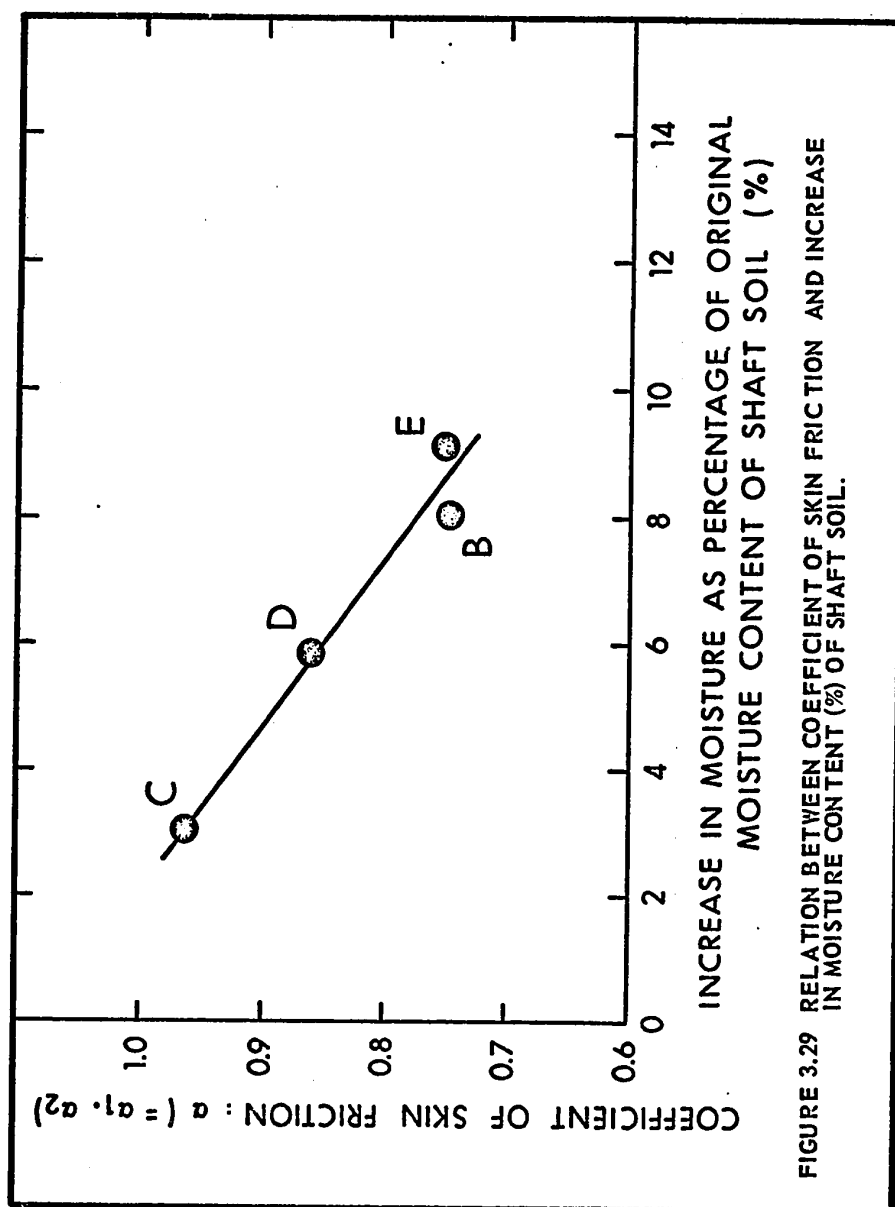
$$\alpha_1 = \frac{\text{shear strength of soil after concreting}}{\text{shear strength of soil before concreting}} \quad \dots (3.1)$$

Further, the value of unit adhesion or skin friction actually responsible for the load transfer was found to be further less than the softened shear strength of soil and has been expressed in terms of Coefficient of Reduction α_2 , where:

$$\alpha_2 = \frac{\text{unit adhesion or skin friction developed along shaft.}}{\text{shear strength of shaft soil after concreting}} \quad \dots (3.2)$$

The net Coefficient of Load Transfer relating the value of unit adhesion to the original shear strength of soil (before concreting) represented by SKEMPTON (1959) by the letter α is thus equal to $(\alpha_1 \cdot \alpha_2)$. The value of α_1 , as seen from TABLE III-4, ranges between 0.755 and 0.966 but that of α_2 is close to unity in all cases. It appears, therefore, that the value of α is more dependent upon the decrease in shear strength of soil as a result of increase in moisture content than due to any other cause. This, therefore, has been related to the proportion of water used in the concrete mix or to the increase in moisture content of the soil as a result thereof. The relationship in the present case works out to be linear, and has been shown in FIGURE 3.29.

A very wide range of the values of α , varying from as low as 0.3 (SKEMPTON, 1959) to as high as 1.0 (MEYERHOF and MURDOCK, 1953), have been reported for bored piles in saturated clays. Under approximately similar soil conditions, this perhaps cannot be considered accidental. It is known that the upper section of a pile shaft near the ground surface



remains relatively ineffective due to the influence of weathering. According to COYLE and REESE (1966), rate of load-transfer increases with the depth of the pile. Embedded length of the pile therefore may be considered to be one factor affecting the value of α . Shaft capacity of a circular pile of diameter d , may accordingly be represented by the equation:

$$Q_s = \pi d (\alpha' \cdot c_1 \cdot h_1 + \alpha'' \cdot c_2 \cdot h_2 + \alpha''' \cdot c_3 \cdot h_3 + \dots) \dots (3.3)$$

where α' , α'' , α''' are the coefficients of load transfer for the elemental depths h_1 , h_2 , $h_3 \dots$ of the shaft for which the corresponding shear strengths of the shaft soil c_1 , c_2 , $c_3 \dots$ could be considered constant. Evaluation on this basis is possible only if the pile is instrumented along the entire depth to record the load transferred to the soil at various sections. The equation $Q_s = A_s \cdot \alpha \cdot \bar{c}$, where A_s is the peripheral area of the shaft in contact with soil, thus becomes a special case of the above general equation. Water flowing out of clay itself during the process of boring, as pointed out by SKEMPTON (1959), may be another cause responsible for the reduction in the value of α , due to soil softening. In the opinion of the author, the most important factor affecting the soil shear strength after the concreting operation, is the relative abundance of water used in the concrete mix. This would result in the development of increased pore-water pressure in saturated clays and relatively quick softening of soil in silts. Other factors remaining the same, the reduction in soil shear strength of silt, it appears, is directly related to the water-cement ratio or the slump of concrete measured immediately after mixing. Another factor which may be of significance in this respect is the period between concreting the hole and load-testing the pile; or in other words, the value of α is

also time-dependent.

3.11 General Softening of the Soil

Piles B and C provided with load cells near their tips recorded loads of 79 lbs. and 54 lbs. transferred through the base, immediately after fresh concrete was poured into the holes, the weight of concrete poured in each case being about 100 lbs. After a lapse of seven days when concrete had completely hardened, the load indicated by the cell at B was 625 lbs. and that at C was 405 lbs. What appears to have happened is that initially excess water immediately available from fresh concrete found its way into the surrounding soil, softened it within a certain radius and caused the soil to lose cohesion to a considerable extent. Possible migration of water towards the wall of the hole from adjacent mass of soil during the process of augering, as could be expected in silts, would be another cause responsible for the increase in moisture content of soil around the shaft. Horizontal pressure exerted by fluid concrete would initially make the surrounding soil mobilize considerable passive resistance. After the setting and subsequent hardening of concrete, when shrinkage takes place, lower values of coefficient of earth pressure would be called into play. A portion of soil would then perhaps be adhering to the shaft. Additional load (i.e., load in addition to the pile weight assumed having been transferred in full) that came to be borne by the cell as a result of soil softening works out to be about 15 psi of the bearing area for the straight shaft pile and 10 psi for belled pile.

3.12 Summary

Summary of Chapter III, being the results of laboratory tests on pit soil and the behaviour of loaded piles in silt, is given below:

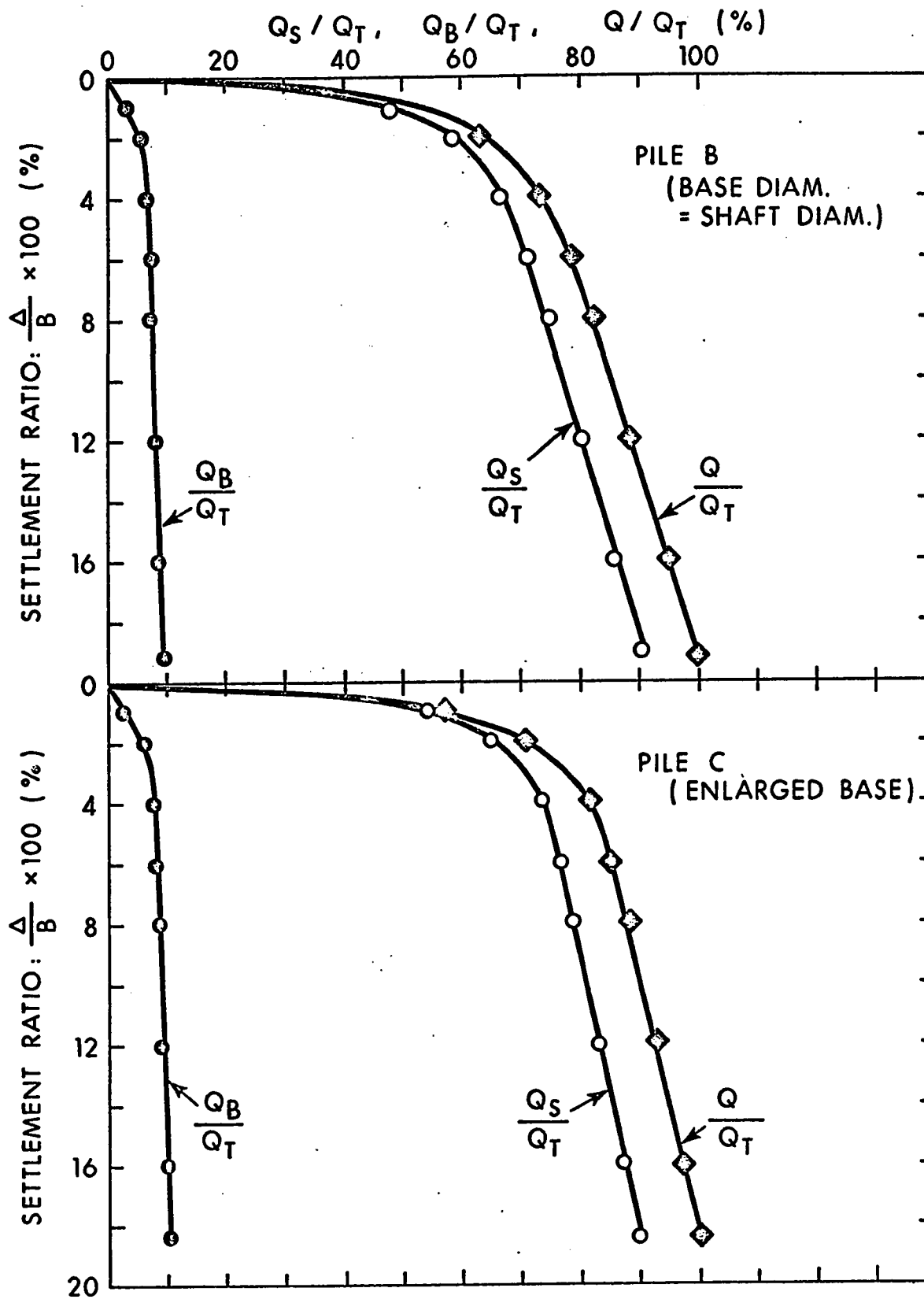
1. The test pit soil had initially a moisture content varying from about 20 per cent at top surface to nearly 29 per cent with a degree of saturation of 85 per cent at a depth of 54 in. Nearly 86 per cent particles of soil, it was found, were lying within the silt-size range and 7 per cent each within sand and clay-size ranges.
2. After the concreting of holes, moisture content of soil along the shaft increased by 3 to 9.1 per cent of the original moisture content, and the corresponding shear strength dropped by 3.4 to 24.6 per cent. Decrease in strength was found to bear a close relationship (linear) with the value of slump measured immediately after mixing and with increase in moisture content (FIGURES 3.17 and 3.18).
3. All the water in the concrete mix is not immediately needed for hydration. Initially surplus water after concreting flows radially away from the pile towards the soil. A reverse gradient may be set up after equilibrium conditions are once established.
4. Load settlement curves indicate a quick building up of resistance to penetration. Maximum loads correspond to settlement ratio: Δ/B of 2.8 per cent to 4.2 per cent. The rebound after the removal of load, is of the order of

15 per cent of total settlement.

5. The maximum tip resistance is mobilized at a settlement nearly of the same order as that for total capacity. Base resistance being very small, a major portion of the load on the pile (over 90 per cent) is taken by the shaft, so that all the piles may be said to have behaved as Friction Piles.

Load-Settlement characteristics of Piles B and C have been summarized in FIGURE 3.30 showing the plots of settlement ratio Δ/B against shaft load Q_s , base load Q_b and total load Q as proportions of maximum test load Q_T .

6. Values of Base Bearing Capacity Factor N_c , corresponding to ultimate load work to 6.0 and 6.25 for the two instrumented piles. This being significantly lower than the usual average of 9 for saturated clays, it has been concluded that under " $\phi = 0$ " condition, saturated or near-saturated silt does not behave like saturated clay and gives smaller values of base bearing capacity.
7. Curves for Shaft Capacities of the two piles having the same base diameter and nearly the same soil shearing strength are almost identical. Higher capacity for the third pile could be accounted for by higher shear strength of soil along the shaft. Shaft resistance is mobilized quickly for small values of penetration--approximately the same as that for total capacity.



FIGURES: 3.30 LOAD SETTLEMENT CURVES FOR BASE, SHAFT, AND TOTAL PILE CAPACITY (PILES B, C IN SILT)

8. A study of moisture content of the shaft soil before and after concreting, the corresponding shear strength and load transfer, indicated that the value of the coefficient of load-transfer α depends upon the decrease in shear strength as a result of increase in moisture content. Increase in moisture content bears a linear relationship with the decreases in the value of α (FIGURE 3.29).

9. In order to account for the variation in the value of α as a result of change in the value of shear strength along the depth of the shaft, the shaft capacity may be represented by the equation:

$$Q_S = \pi d (\alpha' \cdot c_1 \cdot h_1 + \alpha'' \cdot c_2 \cdot h_2 + \alpha''' \cdot c_3 \cdot h_3 \dots)$$

Average value of α on the basis of present series of tests in silt works out to 0.83.

10. Of the various factors responsible for the reduction in the value of soil shear strength for a bored cast-in-place concrete pile in silt, the most significant is perhaps the relative abundance of water used in the concrete mix.

11. The effect of water from fresh concrete soaking into soil around the shaft during the seven-day period permitted for curing was observed in the form of general softening of the soil and its possible adhesion to the shaft resulting in a considerable increase in the value of load transferred to pile tip through the load-cells. The softening resulted in

transfer to the base an additional pressure of the order of 15 psi of the bearing area for straight-shaft pile and 10 psi for belled pile.

CHAPTER IV

FULL-LENGTH FIELD PILES: DEVELOPMENT OF TESTING PROGRAMME

4.1 Introduction

The aims and objectives of carrying out the present series of Full-Length Pile Loading Tests in the representative Edmonton Soil, are best expressed in the words of Dr. E. W. Brooker. The following lines are quoted from his letter, dated December 7, 1966, copies of which were sent to all the interested parties:

...A properly instrumented pile with a load cell near the base of the pile would provide information with respect to amount of load carried by the shaft and by the base during various stages of the loading test. Such information would permit a rational analysis of the load test data and would permit a design procedure to be evolved from the information. A rational design procedure is needed by the engineering profession in Alberta. Because the stratigraphy at the University Farm site is typical of many areas in which one would like to instal a bored-in type of pile foundation, the Dept. of Civil Engineering believes that tests in this area would be of a more general value to the profession....We are naturally less interested in the result of any specific pile loading test than we are in discovering general design principles...

The decision about the selection of a suitable site inside the University Farm was earlier taken primarily because of the following obvious advantages:

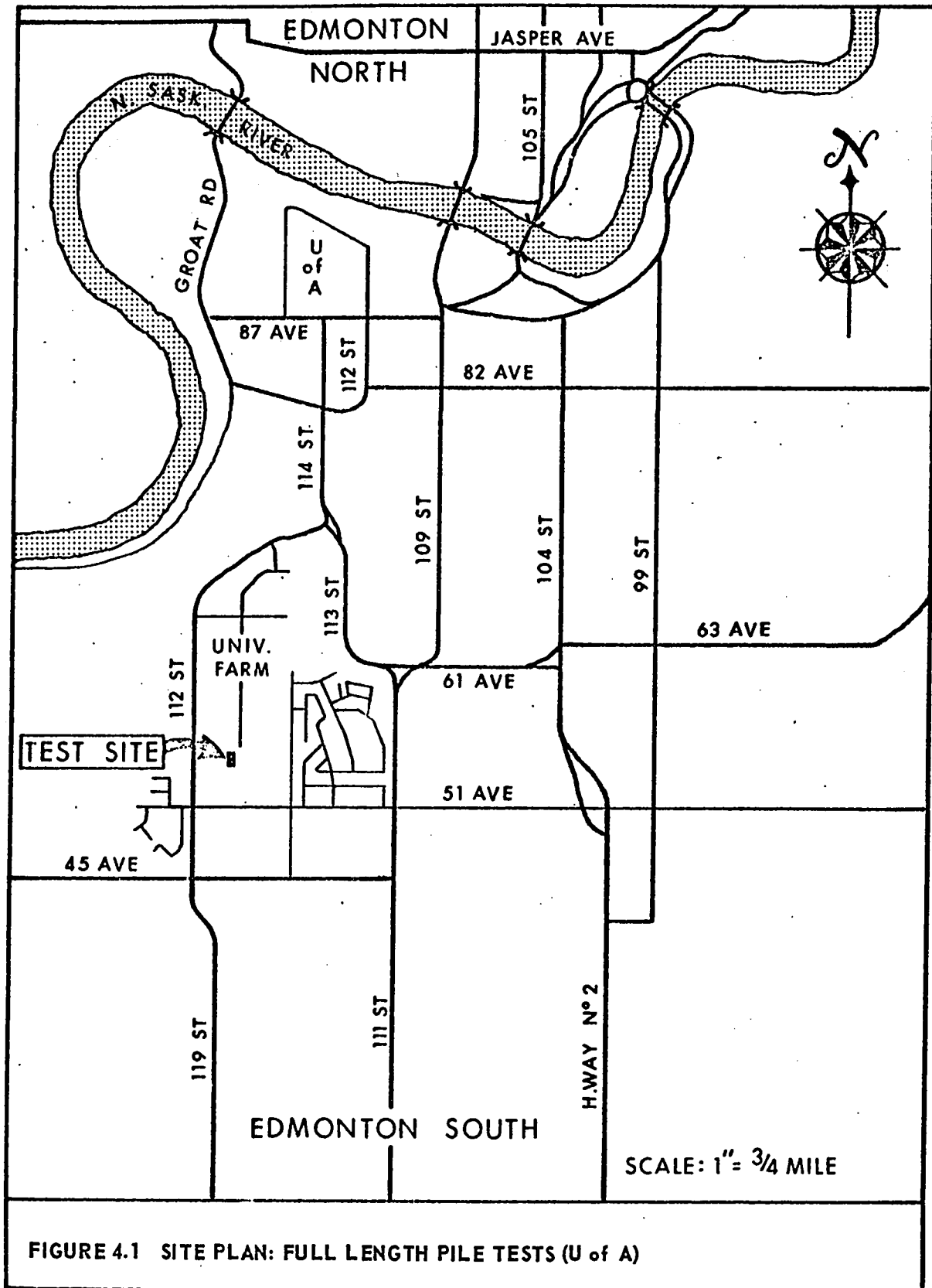
1. The characteristics of the soil and the soil profile up to a considerable depth, as determined tentatively on the basis of preliminary study of the available existing information in the vicinity of the Farm as also elsewhere in the rest of the city, were considered to be quite representative for the entire area.

2. Unlike other sites, any suitable site within the Farm, being under the administrative jurisdiction of the University authorities, would not pose any problem involving temporary acquisition of land for an extended period of time.

After considerable deliberation, the site marked in FIGURE 4.1 was finally selected. Four test holes were drilled, two up to about 30 feet depth in the overlying clay, silty-clay deposit and two further deep up to about 50 feet below the surface, into dense till. Four bored-in type of piles, two with their tips resting in clay and the other two solely in till (being unsupported on sides in the upper 27 feet clay deposit) were then installed and test-loaded to failure. General geological characteristics of the area, details about the log data, development of the testing programme, instrumentation and the testing procedure followed, have been discussed in the paragraphs below.

4.2 General Geology of the Area

The Edmonton Formation consisting of interbedded bentonitic shales and sand-stones with numerous coal seams, the sediments being poorly consolidated and dipping southwestward at about 20 feet per mile, were deposited near the end of the Cretaceous time (BAYROCK and BERG, 1966). The Alberta plains were then subjected to a series of erosion cycles during Tertiary and early Pleistocene times. The last of these cycles led to the establishment of a drainage system, now largely buried by glacial deposit. The preglacial North Saskatchewan River formed part of the drainage system. Saskatchewan Sands and Gravels were deposited during the Pleistocene Epoch (GRAVENOR and BAYROCK, 1968). The deposition of Sands and Gravels ceased



as they were overridden by Continental Ice Sheet advancing from Northeast during Wisconsin time, some 20,000 years ago. Deglaciation took place about 10,000 years ago. The retreat was largely by stagnation. As the natural drainage of Central Alberta is Northeasterly and as the glacier retreated in the same direction, melt-waters were impounded in front of the glacier producing large, relatively short-lived lakes many hundreds of square miles in area. The rapid recession of the stagnating glacier allowed these proglacial lakes to find constantly new and lower outlets. Lake Edmonton at one time covering most of the Edmonton district, was one such lake. It was finally drained by North Saskatchewan River in post-glacial times (BAYROCK and HUGHES, 1962).

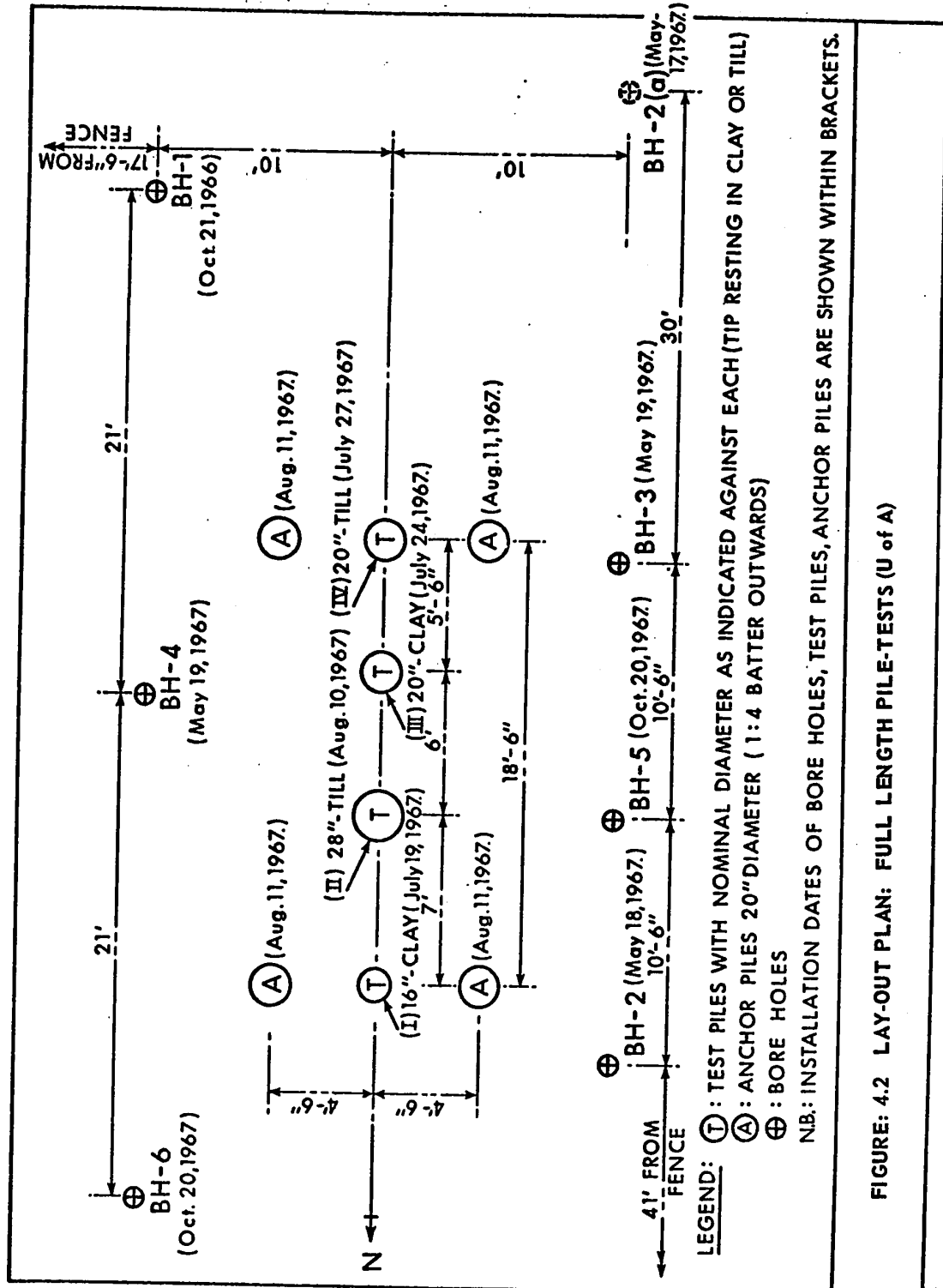
The city of Edmonton is built upon surficial deposits of variable thickness made up of well sorted pre-glacial sands and gravels, glacial till and proglacial lake sediments in ascending order. Sands and gravels are in general sandwiched between the bed rock below and the till deposit above, but do outcrop at some places. Percentage of silt and clay present is of the order of 3 and 6 respectively (BAYROCK and BERG, 1966). Till, which constitutes unsorted unstratified sediment deposited by the glacier, makes up most of the ground moraine and the hummocky dead-ice moraine and underlies most of the other glacial deposits in Edmonton area. Lake Edmonton deposits overlying till are either the normal deposits consisting of bedded fine sands, silts and clays, not altered by later action or the modified deposits having been redeposited with or without additional materials, after being partly or wholly eroded. The lake basin has the shape of trough and the thickness of the deposit varies from about 34 feet near the centre of the basin to less than a foot

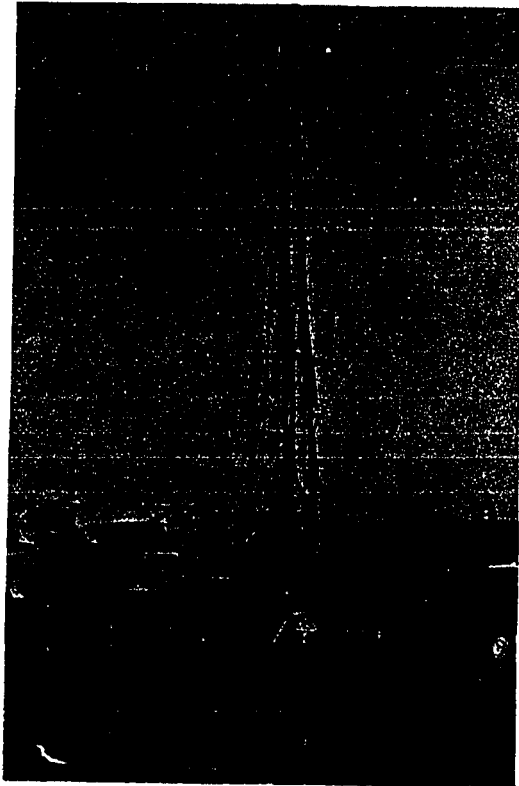
at boundaries (BAYROCK and HUGHES, 1962). In general, the sediments consist of varved silts and clays with scattered pebbles. They are more clayey in the uppermost few feet than in the lower portions. The lowermost portions may consist of fine sand. Till-like lenses of clay with pebbles may be encountered in a few places (BAYROCK and BERG, 1966).

4.3 Field Exploration

Five test-holes, designated BH-1, BH-2(a), BH-2, BH-3 and BH-4, arranged three in one row and two in a parallel row 20 feet away, were bored in the beginning, both lines having been oriented in North-South direction. It was decided to install the four piles at suitable spacings in a third row parallel to the alignment of the two rows mentioned above, being exactly in between them. The relative positions of the bore-holes vis-a-vis the ultimate locations of the piles are shown in the lay-out plan (FIGURE 4.2). Two more holes, viz., BH-5 and BH-6, were bored subsequently (after the installation of piles) for obtaining undisturbed samples in till, their locations having been selected so as to fit in the whole scheme in an appropriate manner.

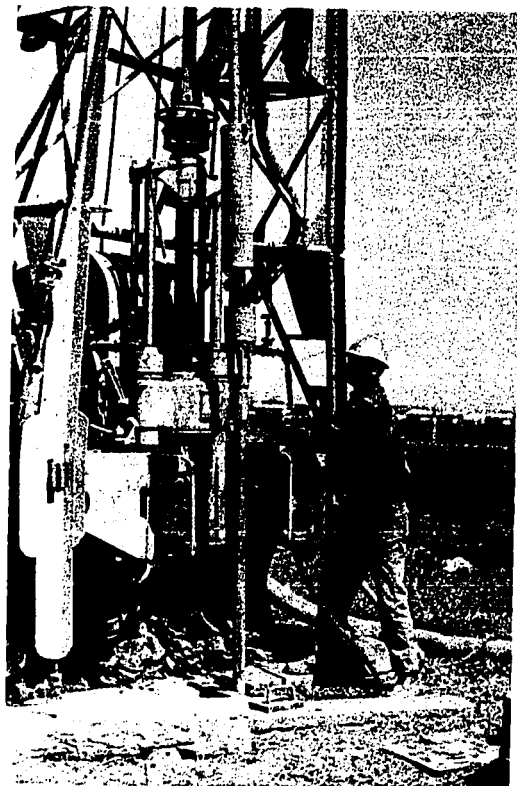
Drilling and sampling were done by making use of helical hollow centre-core auger. Samples were removed both for moisture content determination and strength tests. Standard penetrometer N-values were taken for 12-in. penetration every 2 to 5 feet. FIGURES 4.3 and 4.4 indicate the drilling equipment at work in the field. Log data have been summarised and plotted in FIGURE 4.5. The dates of drilling of various test holes have been recorded under the respective logs in the figure.

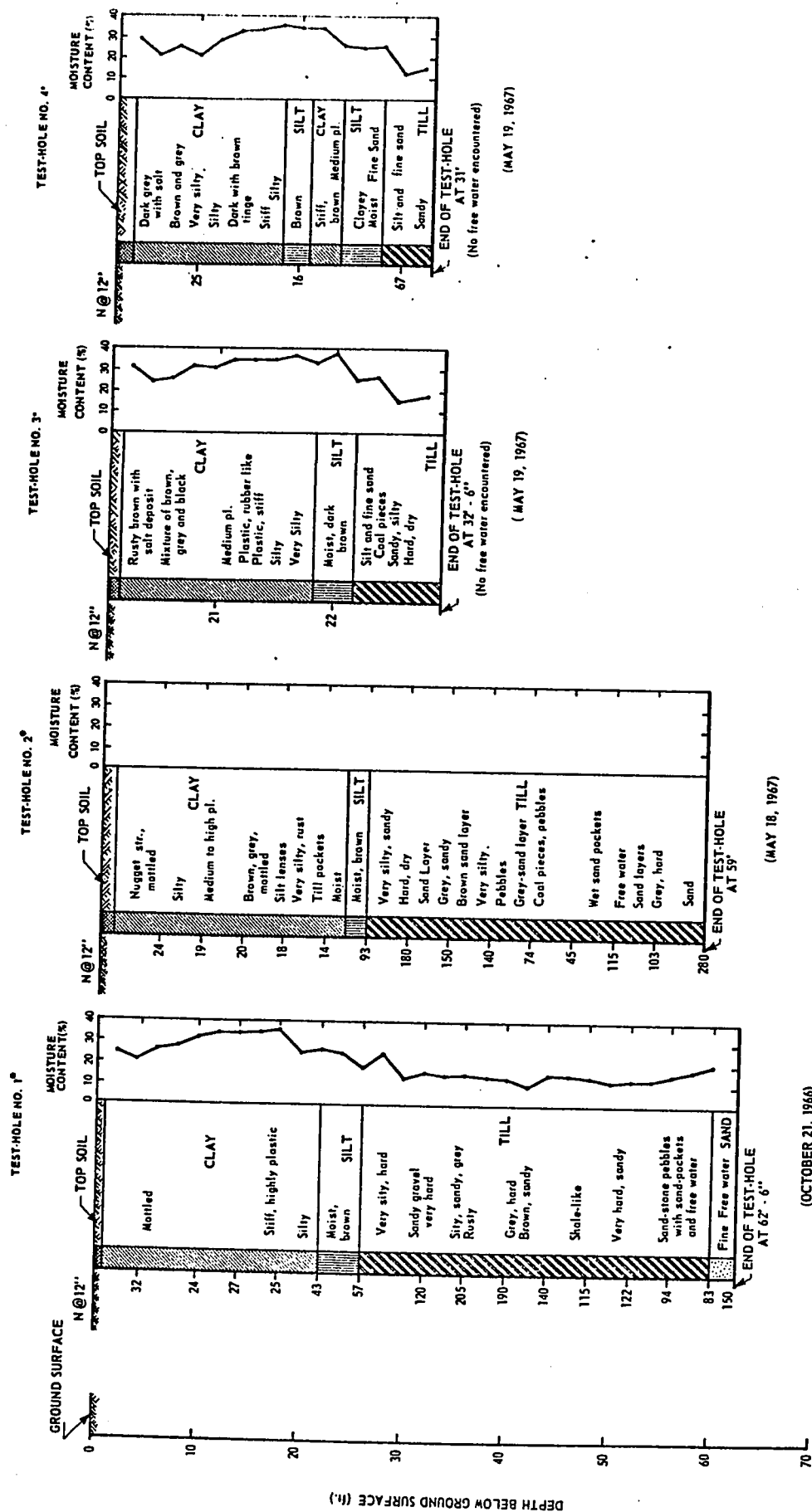




**FIGURE: 4.3 DRILLING EQUIPMENT
AT WORK.**

**FIGURE: 4.4 PENETRATION N-
VALUES BEING TAKEN.**





- LOG DATA BY COURTESY OF BERNARD HOGGAN ENG. & TESTING LTD.
- LOG DATA OBTAINED BY THE UNIVERSITY OF ALBERTA

FIGURE: 4.5 TEST-HOLE LOGS: FULL LENGTH PILE TESTS (U. of A.)

4.4 Design, Fabrication and Calibration of Load Cells

Four load cells were to be installed one near the bottom of each pile. They were fabricated from cold rolled steel. Total sectional area of the pillars was so provided as to make the stress due to maximum estimated working load on it fall well within the elastic range of the stress-strain curve for the material and at the same time be reasonably sensitive for smaller increments of loading. FIGURE 4.6 shows the 28 in. diameter load cell as received from the fabrication shop. Instrumentation consisted of installing two BUDD type strain gages, one aligned vertically and the other along the circumference of each of the eight pillars (FIGURE 4.7). The design details and the finished dimensions together with the wiring details and bridge connections appear in APPENDIX F. These were similar to those used by WHITAKER (1962).

Calibration of the load cells was first done by using steel plates 1 to 2 inches thick, placed one above the other with decreasing diameters (FIGURE 4.8). The indicated strains on the recorder were found to be significantly different from those computed by theory of elasticity. Consequently, the concrete blocks (FIGURE 4.9) placed one below and the other above the cell were employed for calibration. The data so recorded were found satisfactory and were used to plot the calibration curves (APPENDIX G). At the time of calibration, the 16 in. diameter cell and one of the two 20 in. diameter cells had all the four quadrants working satisfactorily. The other 20 in. diameter cell and the 28 in. diameter cell had only three quadrants working properly, in which case it was decided to go ahead with the calibration by using only two opposite working quadrants. The curves for calibration

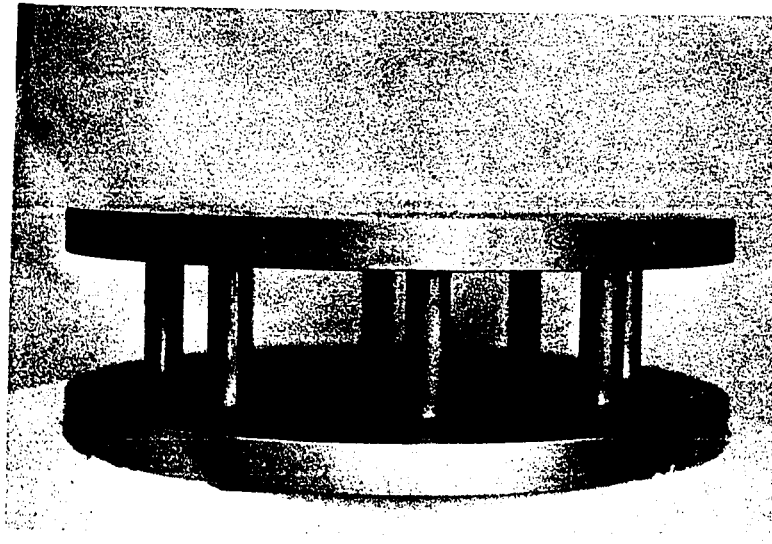


FIGURE: 4.6 28-in. DIAMETER CELL AS RECEIVED FROM THE FABRICATION SHOP.

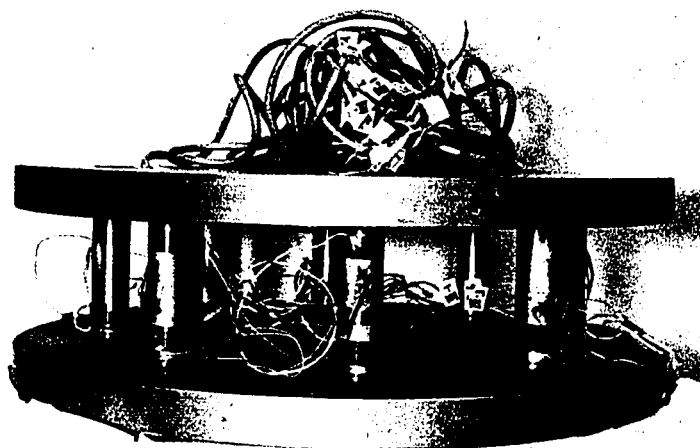


FIGURE: 4.7 LOAD CELL AFTER THE APPLICATION OF STRAIN GAGES AND WIRING CONNECTIONS.

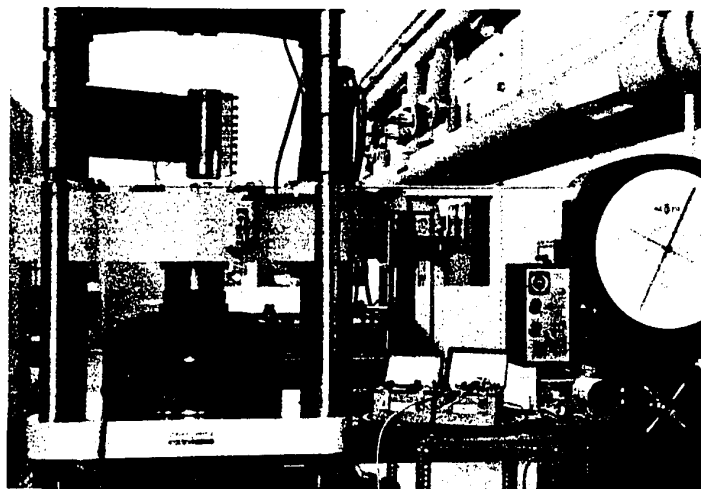


FIGURE: 4.8 CALIBRATION OF THE LOAD CELL WITH 1-in. TO 2-in. THICK STEEL PLATES PLACED ONE ABOVE THE OTHER.

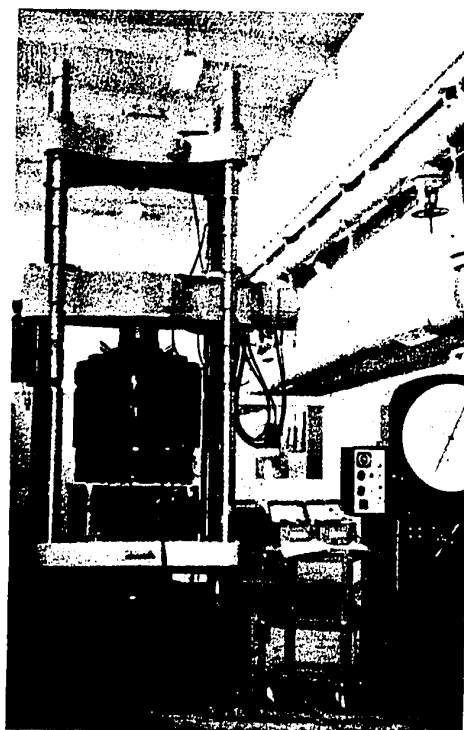


FIGURE: 4.9 CALIBRATION OF THE LOAD CELL WITH CONCRETE BLOCKS PLACED BELOW AND ABOVE.

were therefore plotted for the first two cells mentioned above on the basis of strain indicator readings from all the four quadrants added together, whereas those for the remaining two cells were plotted for the sum of the strain indicator readings for the two opposite working quadrants only.

4.5. Installation of Test Piles

Lay-out plan for the four piles has already been shown in FIGURE 4.2. The distance, 18 ft. 6 in., between the centres of northernmost and southernmost piles corresponds to the effective length of the available loading beam. The other two piles were located in between to ensure that the stressed zone of one did not seriously overlap that of the adjacent pile. Piles in clay being 16 feet and 20 feet long, and those in till passing clear through the upper 27 feet of clay deposit and held by side friction and end-bearing entirely in till, being 38 feet and 49 feet 6 inches long, were placed alternately within the available distance. The short piles stressing only the upper strata (clay) were thus located with their centres 13 feet apart and the long piles stressing only the lower strata (till) were located with their centres 11 feet 6 inches apart. This gives an average spacing of $4.3B$ in the former and $2.9 B$ in the latter case, compared to $4.35 B$ adopted by WHITAKER and COOKE (1966). KEZDI (1957) on the basis of work on groups of model piles, found out a minimum spacing of $6 B$ for the two adjacent piles to act independently and so did recommend MEYERHOF (1959). In the present series of tests, with a view to avoiding a double set-up for the loading beam and thus effecting

an appreciable saving, it was decided to go ahead with the above-mentioned arrangement. Location of pile tips at variable depths with respect to each other was, however, a relieving factor.

Holes were drilled by means of helical augers (FIGURE 4.10) to the appropriate depths, the diameter being about $\frac{1}{2}$ -in. to 1-in. larger than the nominal diameter of the pile. After cleaning the hole thoroughly, a concrete plug was placed at bottom and the cell lowered into it carefully, so as to make it rest level at the top of the concrete plug (FIGURE 4.11). The suspender shaft was then unscrewed and removed. A closed-end aluminum pipe 1 $\frac{3}{8}$ inch diameter, built up in lengths of 20 feet and holding inside it a free-standing $\frac{5}{8}$ inch diameter rod welded at its lower end to the plate closing the end of the pipe, was then lowered into the hole. The closed end was centred and made to rest in the housing at the top of the cell. This arrangement was used to measure the compression of the shaft and the actual settlement at the level of the load cell.

The operation of concreting performed within one to two hours after drilling, was slightly different for piles in clay than for those in till. In the former case, a reinforcement cage was lowered into the hole, making the rubber hose and the aluminum pipe emerge from within the cage. Its lower end was kept about 3 inches above the top of the cell and the upper end about a foot below the ground surface. The peripheral rubber sleeve on the cell was then inflated to a pressure of about 15 psi. by supplying air from the compressed air cylinders filled in the laboratory. Pressure in the sleeve was maintained during the concreting operation which was completed in lifts of about 5 feet, vibrating and compacting the mix after each lift. The inflated sleeve which was supposed to be pressing hard

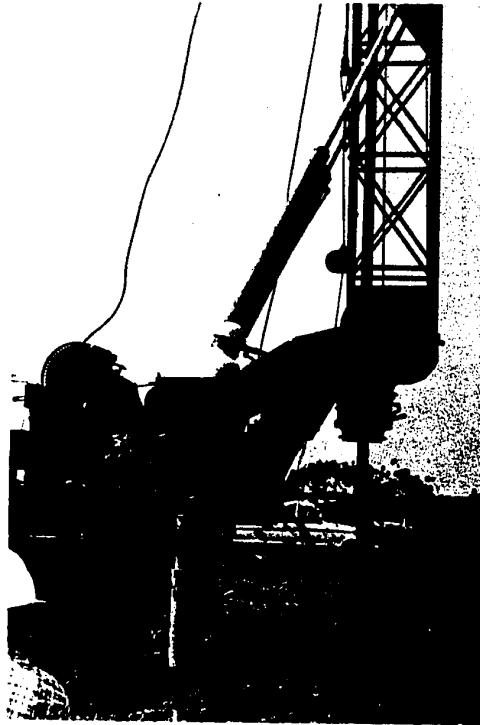


**FIGURE: 4.10 DRILLING PROCESS IN
PROGRESS FOR 20-in.
DIAMETER PILE.**

**FIGURE: 4.11 LOAD CELL BEING
LOWERED INTO THE
HOLE.**



against the wall of the hole, was thus helpful in avoiding direct contact between top and bottom concrete which would have perhaps otherwise occurred due to the downward flow of cement-sand slurry from fresh concrete all around the edge of the cell. The top three-and-one-half feet length of the pile was provided with a steel casing made to project 1 to 2 feet above the ground surface. Concrete was poured up to the top of this casing and struck level leaving the aluminum pipe projecting out in the centre and the rubber hose coming out elsewhere, as seen in FIGURE 4.12.

Reinforcing cage was not used for the two piles 20-in. and 28-in. diameter installed in till. A 16-in. diameter steel pipe (wall thickness: 0.28 in.) lowered to within a foot from the top of the cell and made to project above the ground surface, was used for each of these two piles (FIGURE 4.13). After pulling out the rubber hose from within, holding the pipe centrally around the aluminum pipe and inflating the rubber membrane, the inside of the pipes were concreted up to top. The level of concrete outside the 16 in. diameter pipe was kept about two feet below the interface between clay and till, leaving the rest of the height, about 27 feet, unconcreted. The installed dimensions of the test piles are shown in FIGURE 4.14.

4.6 Installation of the Loading Beam

It was decided to use a single set-up of the loading beam for test-loading all the piles, by employing four bored-in anchor piles to support it. The layout plan (FIGURE 4.2) shows the locations of the anchor piles relative to the test piles. The minimum centre-to-centre distance between any anchor pile and the nearest test pile works out to

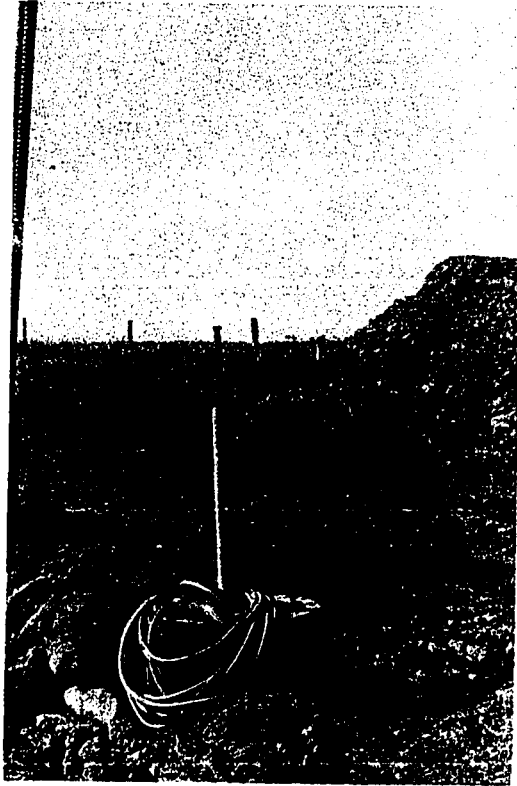
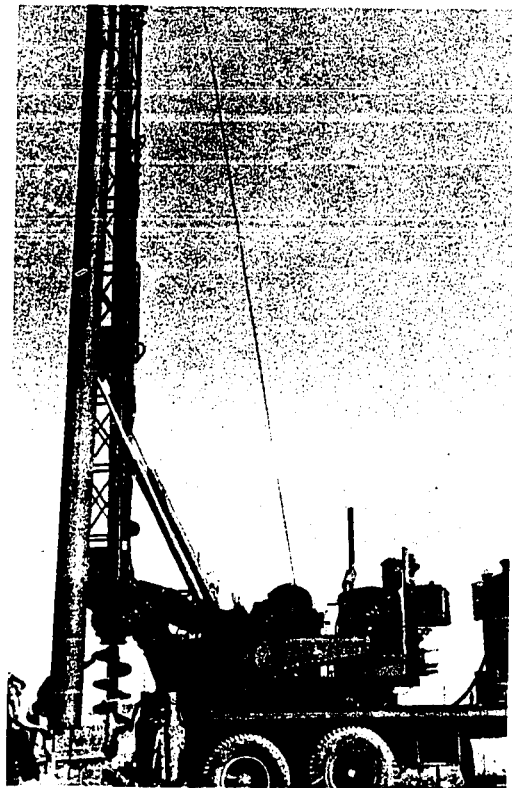


FIGURE: 4.12 A VIEW OF THE PILE IMMEDIATELY AFTER INSTALLATION.

FIGURE: 4.13 16-inch DIAMETER PIPE BEING LOWERED INTO THE 28-inch DIAMETER HOLE.



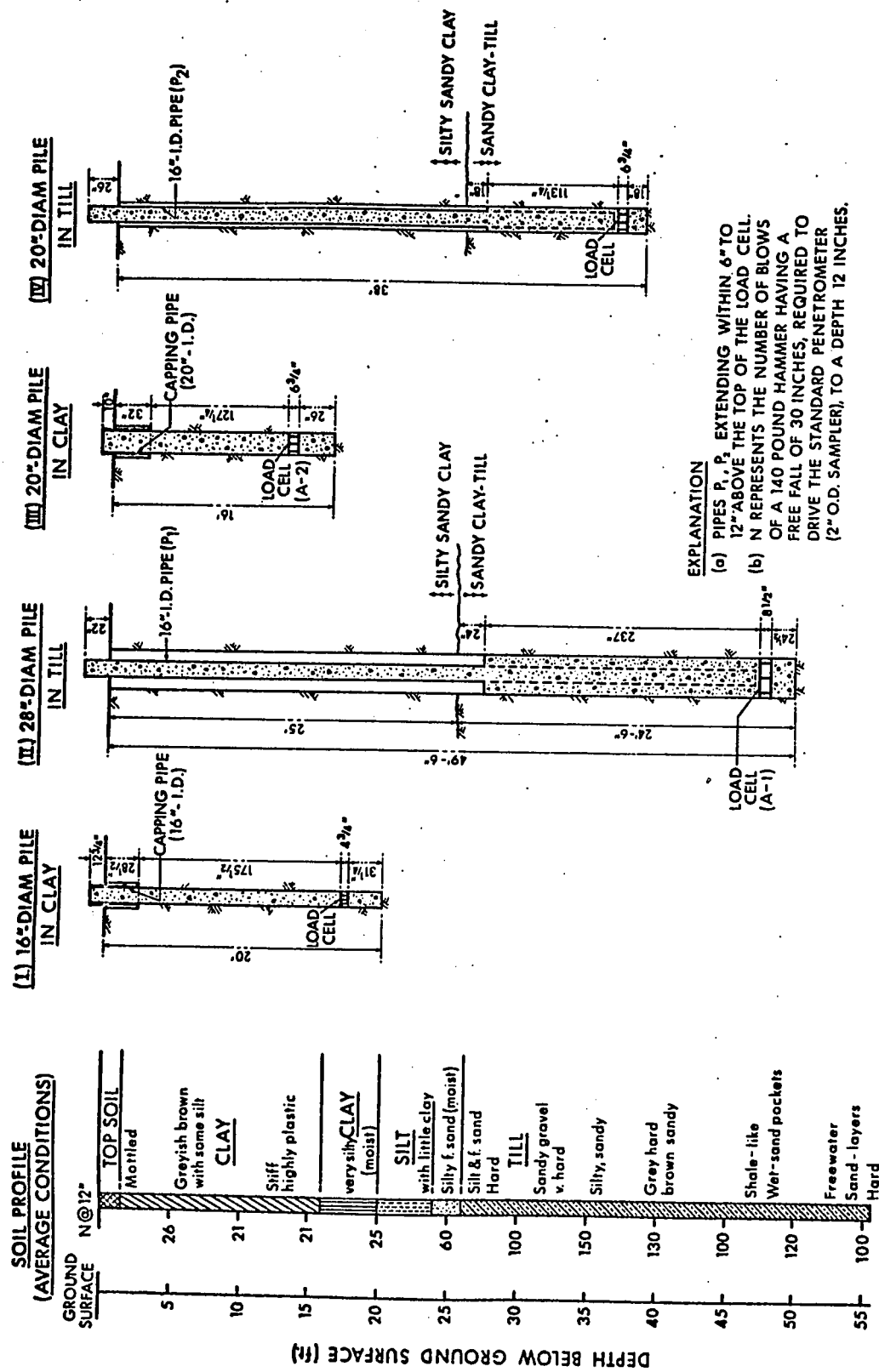


FIGURE: 4.14 INSTALLATION DIMENSIONS OF TEST-PILES: FULL LENGTH PILE TESTS (U of A)

about $3B$ where B is the average diameter of the two piles in question. This, though not adequate for avoiding the overlapping of the stressed zones, had to be adopted due to the limited size of the available loading frame. The anchor piles, 24-in. diameter 40 feet deep, were reinforced with 4 #10 and 2 #8 mild steel rods and were concreted with 4000-lb. ready mix concrete. The maximum reaction of 1200 kips provided by the beam for loading the 28-in. diameter pile would require a skin friction of the order of 14.5 psi. against the approximate estimated weighted average value of 22.5 psi. of the undisturbed peak shear strength of the soil. Actually, however, the unit frictional resistance required to be mobilized by two anchor piles on one side would be more than 14.5 psi. since the 28-in. diameter pile was located 2 feet 3 inches away from the centre of the beam and secondly, the available value of unit adhesion acting in the opposite direction would be considerably less than 22.5 psi. due to the softening of the soil after concreting.

These factors, combined perhaps with the effect of possible heaving of soil due to the loading of the adjacent pile, resulted in relatively large upward movements of two anchor piles when reaction of 1200 kips was applied by the loading beam. This pile therefore could not be tested to ultimate failure. FIGURE 4.15 shows a view of the anchor piles concreted up to the ground surface with the reinforcing rods projecting above.

The loading beam constituted a welded plate girder 22 feet overall length supporting two cross beams 18 ft. 6 in. apart welded to the plate girder along the surface of contact and stiffened at the ends by means of short length pipes and plates as is seen in FIGURE 4.16. This beam had reportedly withstood satisfactorily loads up to about 1000 kips prior to

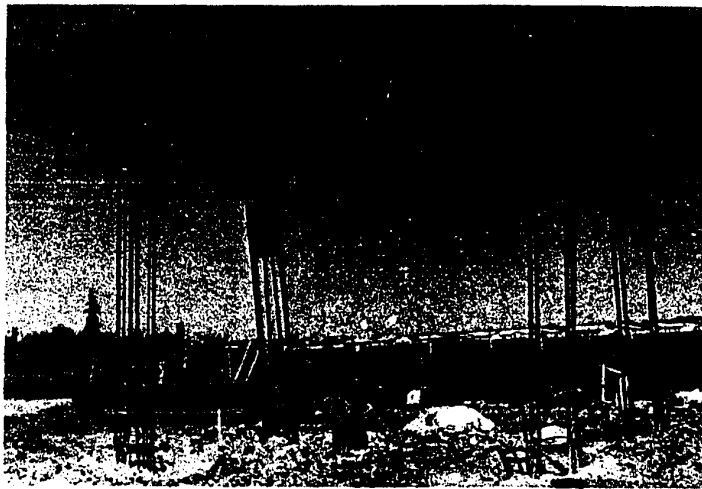


FIGURE: 4.15 A VIEW OF THE ANCHOR PILES WITH THE REINFORCING RODS PROJECTING OUT.



FIGURE: 4.16 A VIEW OF THE LOADING BEAM AS SUPPORTED BY ANCHOR PILES.

this test.

4.7 Preparation for Load-Testing of Piles

The entire testing programme was carried out inside the temporary wooden shack erected to house the piles and the loading beam. Preparation for testing included clearing the area around the pile up to a depth of 18 inches or more, cutting off the aluminum pipe flush with the top surface of the pile as shown in FIGURE 4.17, keeping it heated when necessary to ensure that the top soil did not freeze (FIGURE 4.18) and providing a suitably designed loading head under the hydraulic jack as shown in FIGURES 4.19 and 4.20. For the two piles in till, the annular space between the outside of the casing pipe and the wall of the hole had to be cleared of any debris or soil that had dropped in due to caving. The site, after being cleared, is seen in FIGURE 4.18. The 20-in. diameter pile in till estimated to withstand over 500 kips of load to failure, was located far away from the centre of the loading beam. To avoid possible slipping out of the jack due to the anticipated curvature of the beam under such heavy reaction loads, contact between the beam and the jack was established through a specially-machined spherical head and a cap placed at the top of ram of the hydraulic jack, as seen in FIGURE 4.20 (cap not shown).

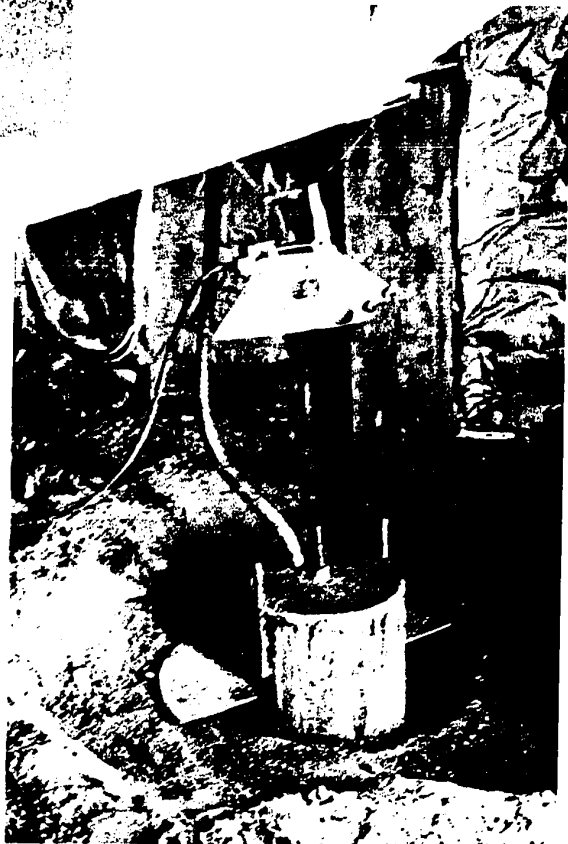
4.8 System of Load Application and Maintenance

Two hydraulic jacks each having a loading capacity of 1600 kips were used for testing. One jack was made use of for loading the 16-in. or the 20-in. diameter piles and both of these for the 28-in. pile. Calibration was done in the 200-ton TINUS OLSON Machine. No hysteresis loss was



**FIGURE: 4.17 PREPARATION OF THE
PILE TOP FOR TESTING.**

**FIGURE: 4.18 HEATING THE SOIL NEAR
SURFACE TO AVOID
POSSIBLE FREEZING.**



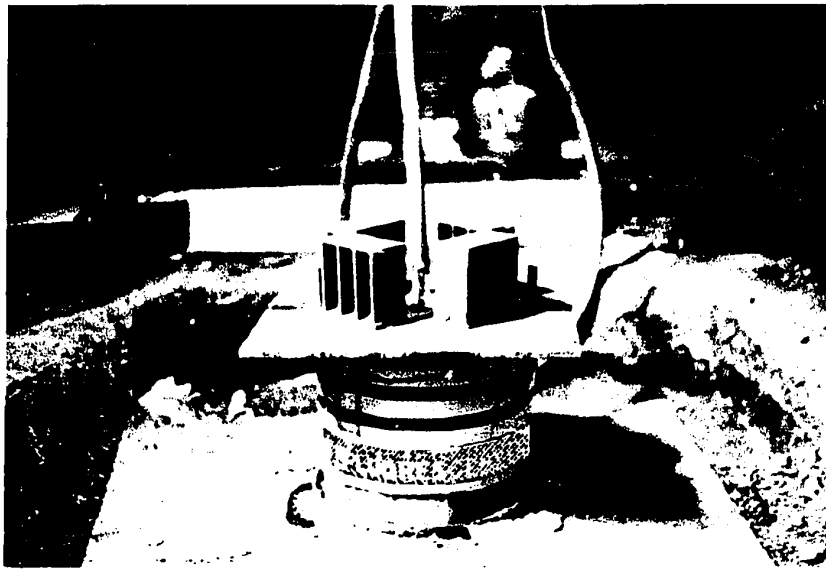


FIGURE: 4.19 SHOWING THE ARRANGEMENT OF THE LOADING HEAD TO PROVIDE SPACE FOR THE PROJECTING SHAFT-COMPRESSION MEASUREMENT ROD.



FIGURE: 4.20 SHOWING THE HYDRAULIC JACK CENTERED ON THE PILE TOP.

indicated. Data and the calibration curves appear in APPENDIX H.

The required pressures were initially built up by pumping and subsequently maintained overnight by the load maintainer. The apparatus shown in FIGURE 4.21 could maintain a load of the order of 250 kips corresponding to a gage pressure of 2000 psi. For the application of higher loads needed for the two piles in till, the maintainer shown in FIGURE 4.22, good for use up to a pressure of 10,000 psi., was employed. The valve connecting the pump and jack would be closed after building up the pressure by hand-pumping and transferring it thereafter to the oil phase in the one-gallon capacity hydraulic accumulator wherein the pressure in upper phase (air or nitrogen) could be maintained at any desired value by admitting a controlled supply of air or nitrogen from the supply cylinders seen in FIGURE 4.21 (the accumulator attached at the back of the panel board is not seen in the figure). The capacity of this accumulator would be exhausted when the movement of the piston of the jack was of the order of two inches. It required refilling by pumping in oil from reservoir under the hand pump. For higher loads and larger anticipated settlements, the other apparatus (FIGURE 4.22), capable of supplying oil deficiency in the jack directly from the oil tank under the hand pump, was made use of. A schematic diagram illustrating the method of load application and maintenance has been included in APPENDIX H.

4.9 System of Measurement

In addition to the settlement at pile top and strain indicator readings for base resistance at the level of the load-cells, measurements were recorded for the compression of the shaft, settlement of the cell

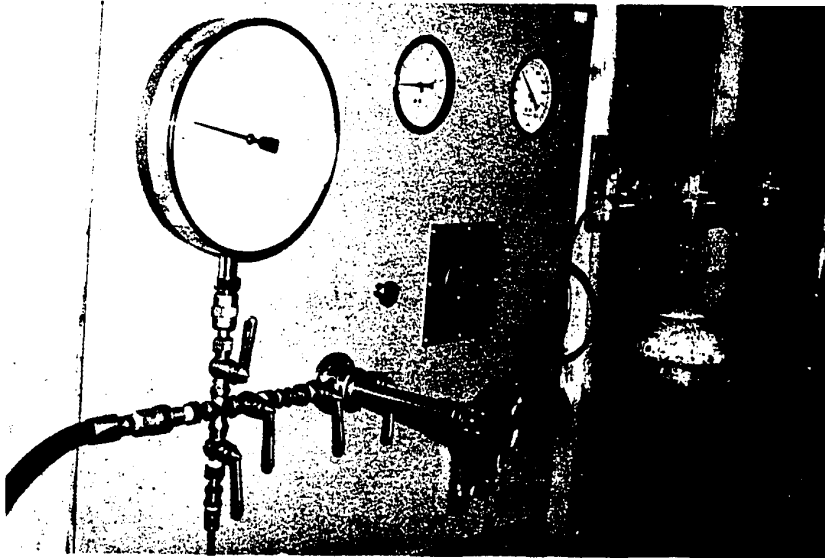


FIGURE: 4.21 LOAD MAINTAINER USED FOR PRESSURES UP TO 2,000 psi.

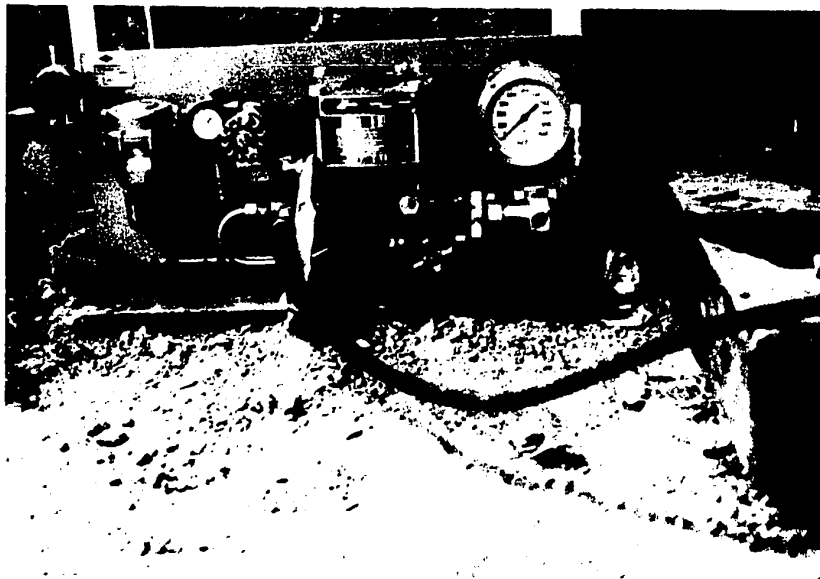


FIGURE: 4.22 LOAD MAINTAINER USED FOR PRESSURES UP TO 10,000 psi.

(being approximately equal to the tip settlement) and the upward movement of the anchor piles. Two 0.001-in. dial gages placed diagonally opposite across the pile top were used for settlement measurements. Actual compression of the shaft was recorded by a 0.0001-in. dial gage firmly attached to the free-standing 5/8-in. rod projecting out of the pile top at centre, measurements being made relative to the movement of the pile top. These arrangements are clearly seen in FIGURE 4.23, showing the set-up used for 20-in. diameter pile in clay. The set-up used for piles in till was a little more elaborate. Additional 0.001-in. gages, one on either side of the pile, were attached to the shaft-compression rod and measurements made relative to a fixed surface so as to record the actual settlement at the level of the cell. Four gages, one each attached to the steel rods projecting from the anchor piles, were employed to record their uplift at various stages of loading. FIGURES 4.24 and 4.25 illustrate the set-ups used for 20-in. and 28-in. piles in till. A schematic arrangement has been shown in APPENDIX I.

4.10 Pile Loading Test Procedure

All the piles were tested by the "Maintained-Load" Testing Method. For piles in clay, each new increment of load was applied after allowing the pile to settle for 24 hours under the previous increment, till failure occurred. Unloading was thereafter done under loads corresponding to 75%, 50%, 25%, 10%, of the maximum load applied, finally reducing it to zero, the load in each case being maintained for half-an-hour duration. Measurements for settlement at top, for shaft compression and base resistance (indicator readings) were recorded immediately after the application of any

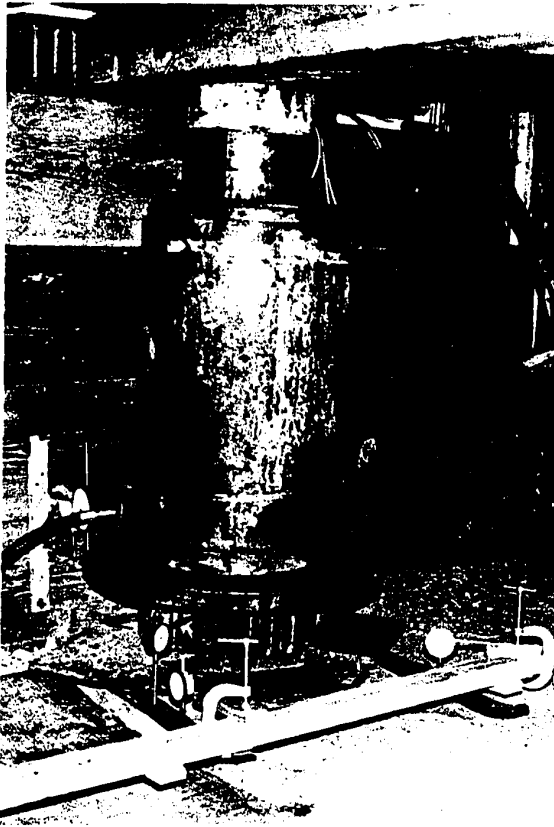
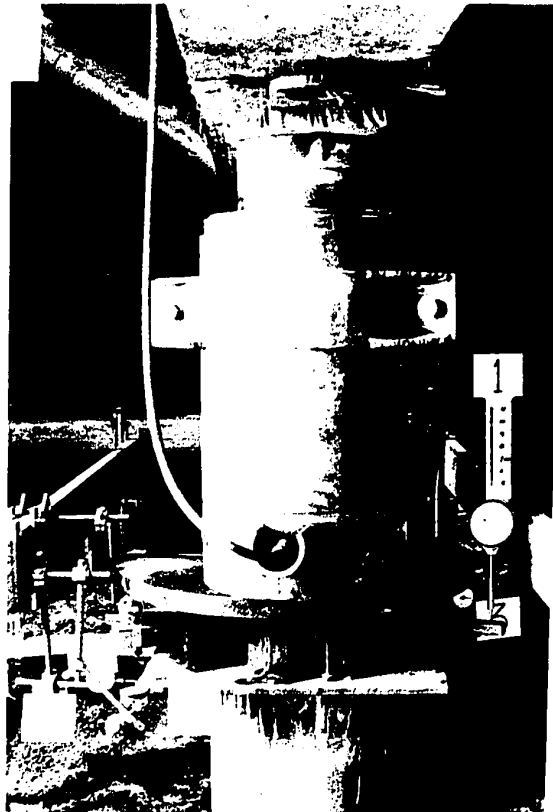


FIGURE: 4.23 SYSTEM OF MEASUREMENTS
USED FOR 20-in. PILE IN
CLAY.

FIGURE: 4.24 SYSTEM OF MEASUREMENTS
USED FOR 20-in. PILE IN
TILL.



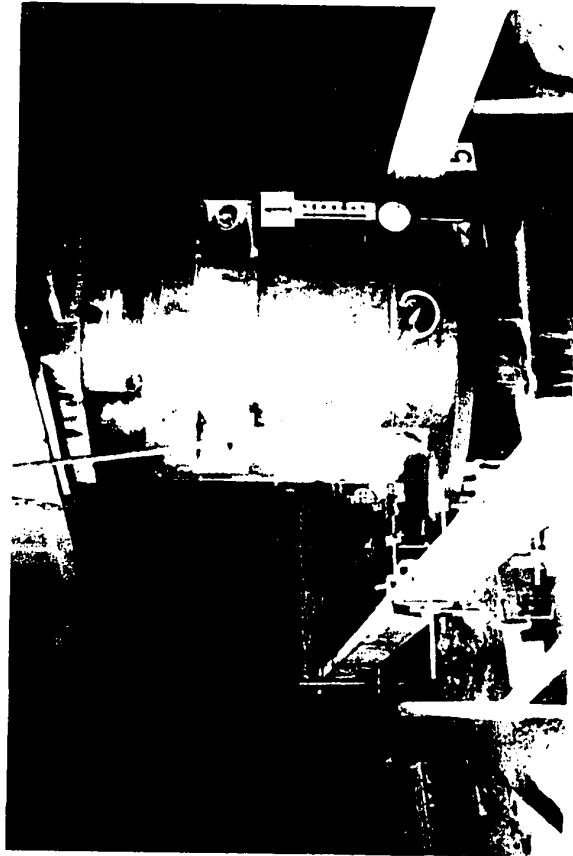


FIGURE: 4.25 TWO JACK SET-UP AND SYSTEM OF MEASUREMENTS USED FOR
28-in. PILE IN TILL.

increment, and after 2 min., 4 min., 8 min., 15 min., 30 min., 1 hr., 2 hrs., 4 hrs., and 24 hrs. Magnitudes of various increments of loads to be applied were approximately estimated on the basis of unconfined shear strength of the soil, value of $\alpha = 0.5$ and $N_c = 9$.

For piles in till, cyclic procedure of loading was adopted. Each increment of load was maintained for half an hour or till such time as the rate of settlement indicated on the dial gage fell below 0.001 ft. in one hour, whichever occurred later. Each time a Design Load was assumed and the pile loaded in increments of 25, 50, 75, 100, 125, 150 and 200 per cent of that and unloaded in increments of 75, 50, 25, 10, 0 per cent of the full test load (i.e., twice the assumed design load), after maintaining the maximum load for 24 hours or more. Final rebound at zero load was also recorded 24 hours after the removal of the entire load. Settlement and other readings during loading and unloading were recorded at the same time intervals as used for piles in clay. Magnitudes of various increments were decided on the basis of embedded length and diameter of pile and the average unconfined compressive strength of till.

Piles in clay were tested first and those in till thereafter. With reference to FIGURE 4.2, the order of testing was: I, III, IV, and II.

4.11 Structural Stability of Piles under Loads

The pile most vulnerable to possible structural failure under the highest load of 1200 kips to which it was subjected, was the 28-in. one. Failure could occur either due to the crushing of concrete or due to disproportionate side-sway at the upper free end of the pile, the bottom

end being assumed fixed. Accounting for the sectional area of the 16-in. diameter 0.28-in. thick steel pipe, the equivalent composite sectional area of concrete works out to 295 in.² and the maximum stress on concrete about 4050 psi. against the design strength 4000 psi. of the mix. A large margin of safety inherent in steel and the redistribution and automatic readjustment of stresses between steel and concrete areas forcing a possible plastic behaviour of the composite section, were probably responsible for the actual value of stress in concrete being below 4050 psi., with the result that no structural failure was noticeable under the highest load.

Fixity at the lower end of the pile and probably a very small value of eccentricity of loading helped to reduce the maximum side-sway under the highest load to about 0.4 in. (APPENDIX J), which was responsible for inducing a moment of the order of 40 k-ft. in the pile at the interface between clay and till. Increase in the vertical pressure on one edge due to this and the corresponding decrease in stress on the opposite edge of the steel pipe encasing concrete, would be negligible. Its effect in the lower part of the pile would be partly dissipated due to larger sectional area of concrete below the clay-till interface. It was assumed that the value of coefficient of load-transfer α would not be adversely affected as a result of development of passive pressures along the shaft due to the above-mentioned cause.

CHAPTER V
TEST SITE SOIL CHARACTERISTICS, LABORATORY TEST RESULTS
AND DISCUSSION

5.1 Introduction

Visual examination of the soil samples as the drilling proceeded, showed a large degree of non-homogeneity indicated by the presence of varves of silt of varying thickness interbedded between clay layers, numerous pockets of fine sand, ice-rafted pebbles and chunks of till inside the upper lake deposit; and relatively loose pockets of silt and sand, pebbles and coal pieces in the lower till deposit. In fact, there was hardly a 15-inch long continuous sample removed from any sampling tube, that showed uniform characteristics even visually. The log data recorded in FIGURE 4.5 reflect these characteristics only crudely. Though the test holes were located in a line barely 10 feet from the centre line of piles, the soil properties could very well be significantly different. The actual difference, whatever it was, particularly in the strength characteristics, could not but be ignored and assumed nil for analysis. The base bearing capacity of the piles, it was obvious, would be considerably affected by the type and the physical condition of the soil immediately below the tip. These factors made the laboratory testing programme quite complicated. Many samples where loose silt and fine sand portions fell apart on removal from the sampling tube, were not strictly "undisturbed." A large number of tests of various types were needed to arrive at any meaningful value of

average shear strength for the purpose of establishing some suitable correlation with field performance. Strength tests carried out included Unconfined Compressive Strength tests, Box Shear tests and Undrained Triaxial tests on whatever undisturbed samples could be carved out. The results so obtained indicated a considerable amount of scatter particularly for till samples. In order to better define the angle of shearing resistance, some Consolidated Undrained tests were run on remolded samples recompacted at original moisture content and density and consolidated at overburden pressure. Softened Shear Strength values were obtained by soaking undisturbed samples in water for 96 hours and shearing them at overburden pressure under undrained conditions. For the same purpose Unconfined Compression tests were run on samples removed from within one to two inches of the pile face immediately after the conclusion of the tests on piles in clay. Many more tests such as Residual Strength tests at large strains on undisturbed samples, Sliding Friction tests on hardened concrete against till surface under varying normal loads and Plate Bearing tests in the field, appeared to be closely related to field performance of piles and so were amply justified. A number of factors, including lack of time were, however, responsible for holding these up.

Results of laboratory tests performed on clay and till are given in the paragraphs that follow. A discussion on the choice of suitable strength parameters for analysis, has also been included at the end of this chapter.

5.2 Index Properties

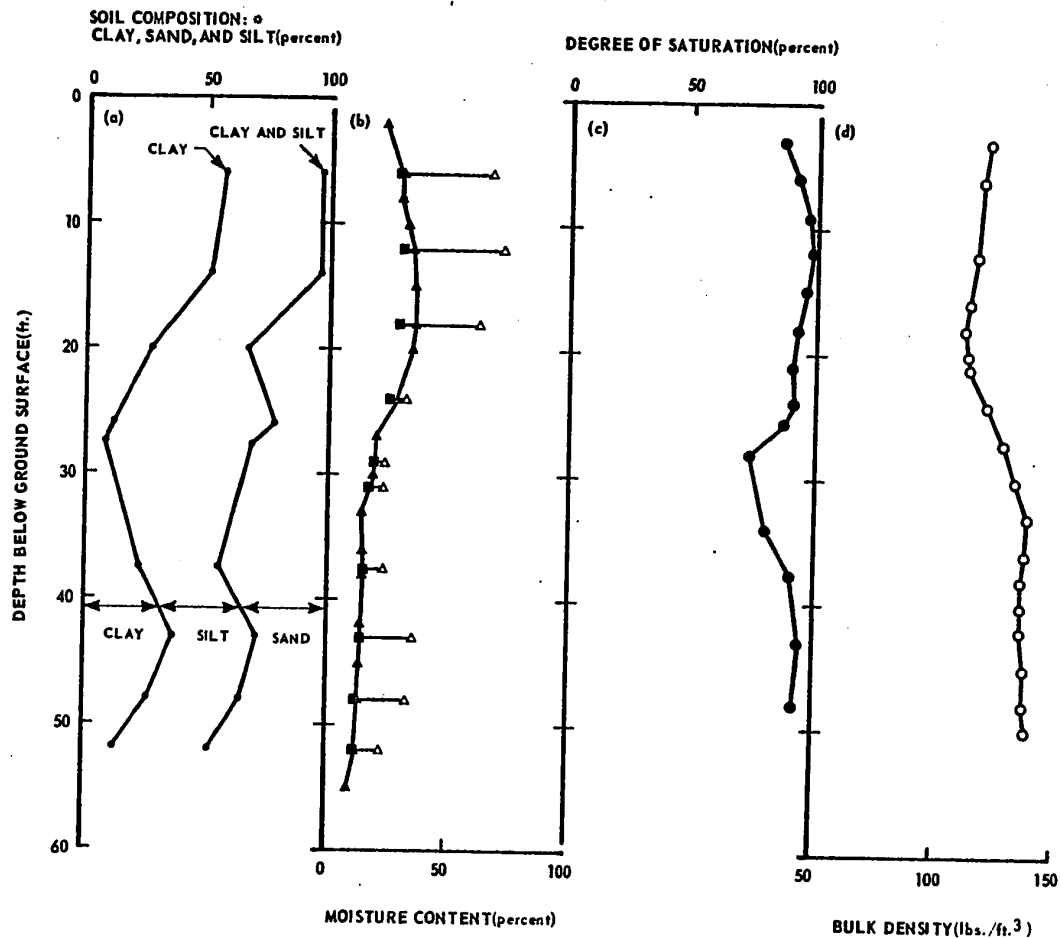
Classification tests were run on a large number of samples removed from various depths below the ground surface. Only those results which are

of immediate interest in the present analysis have been presented here, in the form of plots, in FIGURES 5.1 and 5.2.

Composition of soil, split into percentage proportions of clay, silt and sand-size particles (scaled off from the individual distribution curves drawn on M.I.T. scale for samples at various depths) as seen in FIGURE 5.1(a), is continuously changing along the entire depth. It is predominantly clayey for the upper fourteen feet (percentage of clay being 50 or more) and predominantly sandy-silty for the rest of the depth. Proportion of silt for the entire depth shown is rather high, being not less than 40 per cent anywhere and over 50 per cent in the depth range 22 to 32 feet. Whereas the amount of clay present in certain sections of the profile is negligible (less than 10 per cent), that of sand for the entire depth below 15 feet is of the order of 25 to 45 per cent. A major portion of sand, as observed from the distribution curves, falls in the fine grade. The average proportions of clay, silt and sand worked out from the plot for upper lake deposits and for till, agree favourably with those for East-Central Alberta in general and with those for Edmonton area in particular (BAYROCK and HUGHES, 1962; BAYROCK and BERG, 1965).

In FIGURE 5.1(b), the plot of average moisture content falls very close to the plastic limit. The overconsolidation in the upper layers is due to desiccation and that in till is due to the weight of the receding glacier. Soil is highly plastic in the upper fifteen feet but shows a rapid decrease in the value of plasticity index below this depth. The soil in the region between 15 and 40 feet depth possesses a low plasticity value.

Degree of saturation (FIGURE 5.1 c) registers a sharp decrease from an average of about 97 per cent in the upper clay region to an average

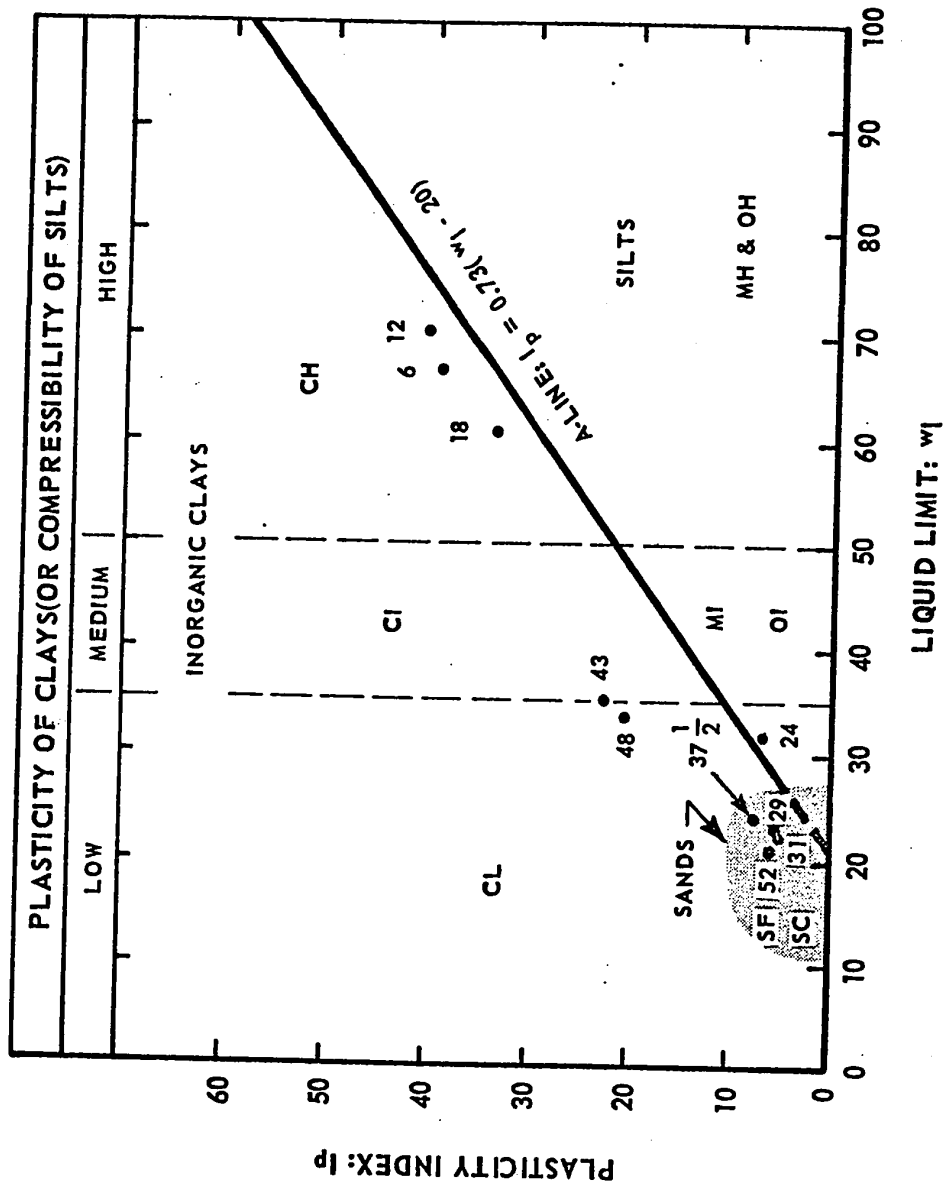


LEGEND:

- M.I.T. CLASSIFICATION
- ▲ NATURAL MOISTURE CONTENT(Average)
- △ LIQUID LIMIT
- PLASTIC LIMIT
- DEGREE OF SATURATION
- BULK DENSITY

NOTE: EACH POINT REPRESENTS AVERAGE OF THREE OR MORE VALUES.

FIGURE: 5.1 PLOTS FOR SOIL COMPOSITION (PERCENT CLAY, SILT AND SAND), NATURAL MOISTURE CONTENT, LIQUID LIMIT, PLASTIC LIMIT, DEGREE OF SATURATION AND BULK DENSITY OF SOIL.



NOTE: THE NUMBERS APPEARING IN THE PLOT INDICATE THE DEPTH AT WHICH THE SAMPLE WAS REMOVED.

FIGURE: 5.2 CLASSIFICATION OF FIELD SOIL AT VARIOUS DEPTHS ON CASAGRANDE'S PLASTICITY CHART.

of 80 per cent in the silty-sandy region. An average of about 90 per cent saturation is maintained below 36 feet depth.

FIGURE 5.1(d) indicates relatively high value of bulk density, being about 137 pounds per cubic foot for dense clay-till compared to about 118 pounds per cubic foot for upper lake deposits.

Both the lake and the till deposits contain a high proportion of montmorillonite in the clay fraction, the exchangeable ion present being calcium (BAYROCK and BERG, 1966).

Plotted on the Casagrande Plasticity Chart, three out of a total of ten samples (depths 6, 12 and 18 feet) fall in the CH region, two in the CI region (depths 43, 48 feet), four in the SF region (depths 29, 31, 37.5 and 52 feet), all above the A-line and one (depth 24 feet) in the MI region below the A-line.

5.3 Compressibility Characteristics

Eight oedometer tests, four for lake soil and four for till, on undisturbed samples removed from the ground at the levels of the pile tips, were performed. Test-runs on clay, silty-clay samples indicated values of Compression Index C_c varying from 0.254 to 0.485 and those of Swelling Index C_s less than 0.11, the higher value of the compression index representing the silty sample. One sample removed from a depth of 22 ft. 6 in. constituting a compact mixture of silt, clay and fine sand showed C_c and C_s values of 0.054 and 0.010 respectively. Maximum value of Swelling Pressure P_s indicated was 0.3 tons ft.⁻². Preconsolidation pressure was of the order of 1 to 2 tons ft.⁻².

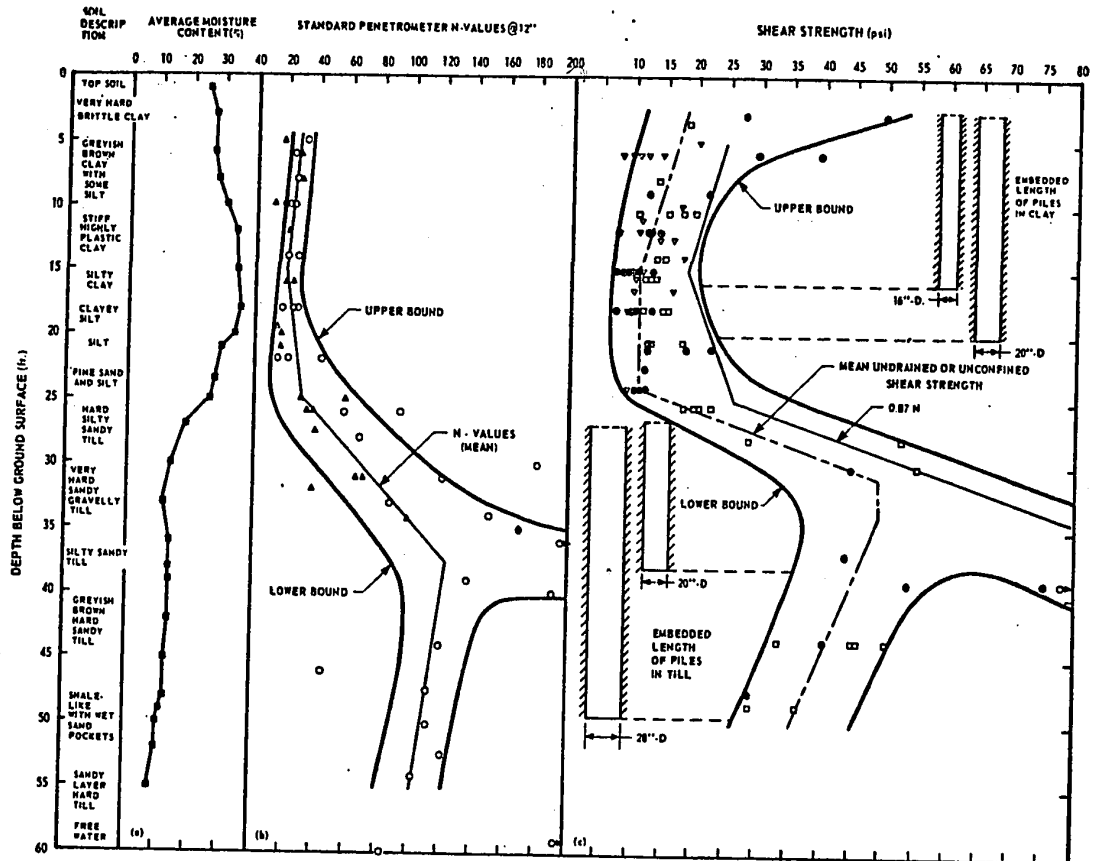
Compression and Swelling Indices for samples in till were

considerably low. Values of C_c ranged from 0.094 to 0.159 and those of C_s from 0.030 to 0.038. Highest value of swelling pressure indicated was 1.5 tons ft.⁻². Preconsolidation pressure was of the order of 7 to 12 tons ft.⁻².

5.4 Undisturbed Laboratory Shear Strength

Results of unconfined compressive strength tests performed on undisturbed samples have been plotted in FIGURE 5.3. The points appearing in the lower region are relatively small in number compared to those in clay. This, as stated in the above paragraph, is due to the difficulty experienced in obtaining intact till samples from the sampling tubes.

Six sets of undrained tests, each on 3 to 4 undisturbed samples removed from the same sampling tube, were performed on clay in the triaxial cell. Four additional sets of triaxial undrained tests were run on clay samples remolded and recompactd at the original moisture content and density. Nine tests were carried out on samples of till compacted as mentioned above and sheared at the overburden pressure under undrained conditions. Values of strength parameters as obtained from triaxial undrained tests appear in TABLE V-1. Due to the complete change in soil structure, as a result of remolding, the strength parameters obtained from tests on the two types of samples cannot be compared as such. The results from remolded samples have, however, been used to interpret those from undisturbed samples in a better way. For the upper nine feet, the soil being very hard and brittle, angles of shearing resistance increasing from 3.5 degrees at nine feet depth to about 26 degrees near the surface are indicated. From 9 to 15 feet, angle of shearing resistance has a value of



- MOISTURE CONTENT
- PENETROMETER N-VALUES (U. of A.)
- ▲ PENETROMETER N-VALUES FROM DATA OBTAINED FROM R. M. HARDY AND ASSOCIATES
- ▲ PENETROMETER N-VALUES FROM DATA OBTAINED FROM BERNARD AND HOGGAN ENGINEERING AND TESTING LTD.
- SHEAR STRENGTH FROM UNCONFINED COMPRESSIVE STRENGTH TESTS ON UNDISTURBED SAMPLES (U. of A.)
- ▼ SHEAR STRENGTH FROM UNCONFINED COMPRESSIVE STRENGTH TESTS ON UNDISTURBED SAMPLES/ DATA OBTAINED FROM R. M. HARDY AND ASSOCIATES.
- ▼ SHEAR STRENGTH FROM UNCONFINED COMPRESSIVE STRENGTH TESTS ON UNDISTURBED SAMPLES/ DATA OBTAINED FROM BERNARD AND HOGGAN ENGINEERING AND TESTING LTD.
- UNDRAINED SHEAR STRENGTH FROM TRIAXIAL COMPRESSION TESTS ON UNDISTURBED SAMPLES (U. of A.)
- UNDRAINED SHEAR STRENGTH FROM BOX SHEAR TESTS ON UNDISTURBED SAMPLES (U. of A.)

FIGURE: 5.3 STRENGTH CHARACTERISTICS OF FIELD SOIL:
(a) MOISTURE CONTENT vs. DEPTH PLOT.
(b) N-VALUE vs. DEPTH PLOT.
(c) SHEAR STRENGTH vs. DEPTH PLOT.

TABLE V-1
RESULTS OF UNDRAINED TRIAXIAL COMPRESSION TESTS
ON UNDISTURBED AND REMOLDED RECOMPACTED
SAMPLES OF CLAY AND TILL

Depth below Ground Surface (ft.)	Soil Description	Undisturbed Samples		Remolded Recompacted Samples	
		Undrained Cohesion: c_u (psi.)	Angle of Shearing Re- sistance: ϕ_u (degrees)	Undrained Cohesion: c_{ru} (psi.)	Angle of Shearing Re- sistance: ϕ_{ru} (degrees)
3	Very hard brittle clay	-	-	13.8	25.4
6	Stiff clay with some silt	26.9	26.0	16.1	14.5
9	Stiff highly plastic clay	-	-	8.5	3.5
12	Stiff highly plastic clay	13.1	4.5		
15	Stiff highly plastic clay	-	-	8.5	3.5
16	Silty-sandy clay	10.1 9.0 13.5	4.5 3.5 8.5		
20	Silty-clay sand	7.8	11.5	-	-
24	Sandy-clayey silt	-	-	3.0	19.5
27-30	Hard silty-sandy- gravelly till	-	-	5.5	25.0
30-45	Sandy-silty clay- till	-	-	4.9 to 5.5	15.5 to 25.0
45-50	Sandy-silty clay- till	-	-	5.5	25.0

the order of 3.5 to 4.5 degrees. In the till region, higher values are indicated for the layers made up predominantly of sand and gravel and relatively low values for those wherein clay is present in relative abundance. Undrained shearing resistance as obtained by using the undrained cohesion c_u and the angle of shearing resistance being the average of ϕ_u and ϕ_{ru} , have been superimposed in the plot for shear strength (FIGURE 5.3). Value of ϕ_{ru} being obviously different from that of ϕ_u , even its partial use as stated above, may be objectionable. This had to be done due to lack of test data on undisturbed samples. And further, as shall be observed from FIGURE 5.3(c), since the number of points so obtained are very few, its ultimate effect on the mean value of shear strength may be considered insignificant.

A large number of box shear tests were carried out on undisturbed samples at varying normal pressures. The samples for the tests were so cut as to ensure that the induced failure surface in the shear box was in vertical natural orientation comparable to field conditions. Values of shear strength corresponding to the overburden pressure based on the strength envelope obtained from box shear tests or by making use of the angle of shearing resistance obtained from TABLE V-1 have been plotted in FIGURE 5.3, together with the results from other tests mentioned earlier.

Laboratory data on shear strength being too voluminous to be presented in full, only a few typical plots have been included in APPENDIX K.

5.5 Shear Strength from Standard Penetrometer N-Values

Penetrometer N-values, being the Number of Blows of a 140 pound

ram having a free fall of 30 inches, required to drive the Standard Spoon Sampler (2-in. O.D.) to a depth of 12 in., were obtained at appropriate depths while drilling the test-holes. The blow-counts for the individual holes have been shown in FIGURE 4.5. They have been plotted alongside the plot for shear strength of the soil, in FIGURE 5.3 and a line representing the mean values has been drawn through these points. An approximate method of estimating the unconfined compressive strength of clay from N-values is given by TERZAGHI and PECK (1967). Table 45.2 (page 347) in this reference results in the relation: $q_u = N/8$, where q_u is the unconfined compressive strength in tons per square foot. Assuming the value of shear strength to be half the unconfined compressive strength, and changing the units of undisturbed shear strength c to pounds per square inch, this relation can be re-written as:

$$c = 0.87 N \quad \dots (5.1)$$

A plot representing this equation has been superimposed on the plot for shear strength in FIGURE 5.3. The relation has been specifically mentioned by the authors to be suitable for application in clay so that its authenticity for soil below about 20 feet depth may be questionable. In any case, however, the general trend indicated is unmistakable and the value of shear strength, if based on N-values which reflect the in-situ conditions at all depths, may perhaps be more appropriate than those obtained from any laboratory test for the type of soil encountered in the present case. Values indicated by this plot are slightly on the higher side compared to those obtained from laboratory tests on undisturbed samples or alternately, the laboratory strengths, due to disturbance of the samples or in some cases

due to their partial collapse, are rather on the low side.

5.6 Strength Data from Other Sources

An attempt was made to collect field and laboratory strength data from local foundation engineering firms. None of those contacted had carried out any plate bearing tests in the vicinity of the site. Laboratory shear strength tests were few and were available for the upper clay deposit only. Blow count and shear strength data for bore holes installed in soil with similar characteristics within about one mile radius of the test site, obtained by courtesy of R. M. Hardy and Associates, and Bernard Hoggan Engineering and Testing Ltd., have been included in the plots in FIGURE 5.3.

5.7 Undrained Shear Strength Values Used in Computations

SKEMPTON (1966) in his summing up address at the conclusion of the Symposium on Large Bored Piles suggested three methods of drawing the true laboratory shear strength vs. depth line, viz., the best line drawn by visual observation showing the mean values, the line indicating the lower limit of strength and the average strength line drawn by using statistical methods. Of these, the last method was considered to be the least satisfying. In the present case, there does not appear to be much justification for adopting the lower bound values shown in the shear strength plot of FIGURE 5.3, since these are mostly indicative of the disturbed test specimens not representing the in-situ strength. The mean strength line drawn as the best fit has been used for computation and analysis of test data. For the very hard sandy gravelly till layer around 30 feet depth, a

uniform value of 49 psi. has been adopted, though the actual indication as seen from the N-value plot is toward much higher strengths.

5.8 Residual Strength Parameters for Clay and Till

Box shear tests on undisturbed specimens could unfortunately not be carried out to large strains by repeated reversals in the direction of the applied shear force. In the apparatus used, the strains were limited to a maximum of about 0.4 in. Further, in many cases it was almost impossible to obtain three truly undisturbed samples at the same depth, and since samples obtained from other depths would not possess similar characteristics, the values of Residual Strength parameters reported in the paragraph below represent only a very rough approximation.

As described in paragraph 5.4 of this chapter, undrained angle of shearing resistance corresponding to peak shear strength decreased from 26 degrees at the surface to about 3.5 degrees at a depth of 9 feet, below which a somewhat constant value between 3.5 and 4.5 degrees is indicated. Only two sets of box shear tests are available for estimating roughly the Residual Strength parameters of undisturbed specimens for the upper nine feet depth. Samples taken at 3 feet depth indicate a residual cohesion value c_r of 9.1 psi. and a residual angle of shearing resistance ϕ_r of 19 degrees. The other set of results for samples at 8 feet depth, shows a c_r value of 7.9 psi. and ϕ_r equal to 4.5 degrees. Residual cohesion values are obviously higher than those expected, since according to SKEMPTON (1964) the cohesion intercept vanishes almost completely while passing from peak to residual. The effect of the applied shearing strains not being too large, is thus clearly reflected. Residual shear strength

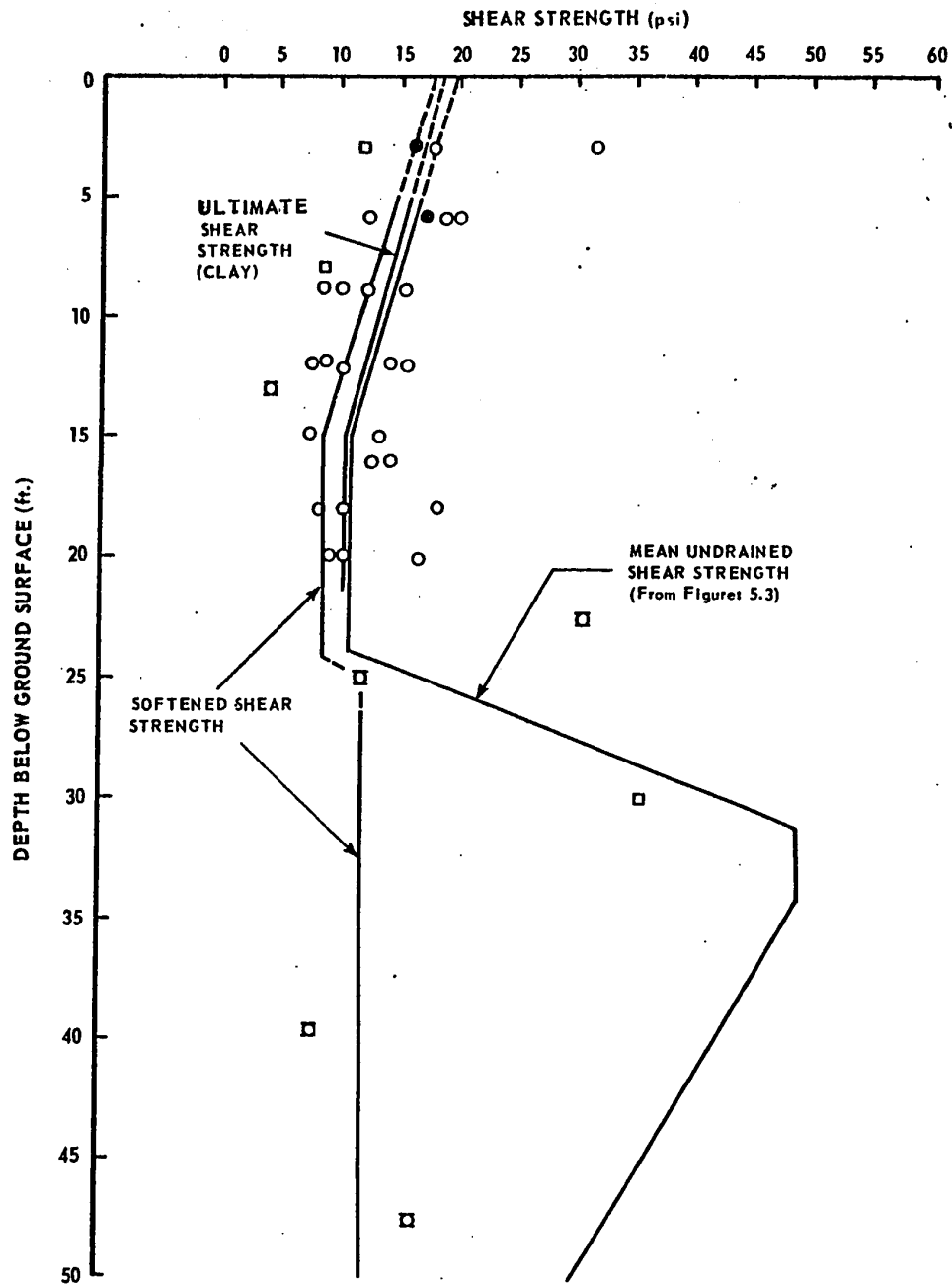
values which in the present context may better be called ultimate strength values computed on the basis of these parameters have, however, been plotted in FIGURE 5.4 alongside the Undrained Undisturbed Shear Strength plot taken from FIGURE 5.3. Relevant data on Residual Strength parameters appear in APPENDIX K.

A majority of samples taken at depths ranging from about 9 feet to 23 feet indicated plastic mode of failure during testing. The elastic moduli were observed to be consistently decreasing until the maximum load was reached. Almost all the stress deformation curves flatten out without showing conspicuous peaks. The soil in this region being a mixture of clay, silt and sand in varying proportions, it does not appear to be unreasonable to adopt residual strength parameters to be slightly less than those corresponding to the peak values. The portion of the Residual Strength plot in FIGURE 5.4 for depths of 9 to 22.5 feet below ground surface has been drawn on this basis.

Soil strata below 25 feet depth abound in coarse particles wherein drainage conditions may be assumed to be slightly better than those above. Undisturbed samples were enough only for a single set of box shear tests carried to strains of the order of 0.4 inch. The value of 35.6 psi. obtained in that case has been shown in FIGURE 5.4. Corresponding data appears in APPENDIX K.

5.9 Softened Shear Strength

Test specimens for obtaining softened shear strength of soil were prepared by first trimming the undisturbed samples to size, then



LEGEND

- RESIDUAL SHEAR STRENGTH FROM BOX SHEAR RESULTS
- RESIDUAL SHEAR STRENGTH BASED ON c -VALUE REMOULDED RECOMPACTED SPECIMENS AND ϕ_r FROM BOXSHEAR RESULTS
- ◻ SOFTENED SHEAR STRENGTH (AFTER 96 HOUR SOAKING) FROM UNDRAINED TRIAXIAL TESTS.
- SOFTENED SHEAR STRENGTH FROM UNCONFINED COMPRESSION TESTS AND UNDRAINED TRIAXIAL TESTS ON SAMPLES REMOVED FROM WITHIN 1 TO 2 INCHES OF FACE OF PILES IN CLAY.

FIGURE: 5.4 PLOTS FOR RESIDUAL AND SOFTENED SHEAR STRENGTH OF SOIL.

wrapping them up in filter paper, the ends having been covered by porous discs held in position by thin elastic bands, and finally soaking them in water for 96 hours. Triaxial undrained tests were run on five samples thus prepared at cell pressures equal to the corresponding overburden pressures. Shear strength values, assumed equal to half the deviator stress at failure (taken at 15% strain for samples yielding plastically) have been plotted in FIGURE 5.4. The lower part of the plot for softened shear strength indicates an average of only three values and is rather on the low side. There appears to be little justification for using this part for analysis since the strata at the corresponding depths abound in sand. Such severe conditions as represented by undrained tests on samples soaked for four days would perhaps never exist since moisture from any source would get dissipated from the soil which in general would provide comparatively better drainage. The sketching of the upper part of this plot has been facilitated by an additional set of points representing the undisturbed shear strength of the soil samples removed from within one to two inches of the faces of the piles of clay. The data include the results of nineteen tests on the unconfined compression machine and four sets of undrained tests in the triaxial apparatus. The plot is offset to the left of the mean undrained shear strength plot for intact soil almost uniformly by horizontal distance representing a loss of about 2 psi. up to a depth of 24 feet.

CHAPTER VI

PRESENTATION OF FIELD PILE LOADING TEST RESULTS

6.1 Introduction

Presented in this chapter are the various curves representing the behaviour of field piles. In addition to the usual plots of settlement at top against total load Q and against time-duration, the settlement behaviour as related to the base-resistance of the pile computed from the indicator readings for the load-cell, has also been shown. The manner in which the settlement and the tip resistance of the pile vary with passage of time under sustained loads has been presented separately.

6.2 Settlement Behaviour of the Loaded Piles

FIGURES 6.1, 6.2, 6.3 and 6.4 representing the settlement behaviour of full length piles under loads, have been plotted directly from the field data and observations summarized in APPENDIX L.

It is not difficult to estimate the Failure Loads for the two piles in clay (FIGURES 6.1 and 6.2) where the point of intersection of the two tangent lines drawn to the general slopes of the upper and lower portions of the curves are easily selected. Yield-point loads of 93 kips and 100 kips are indicated for the 16-in. and 20-in. piles respectively. If the failure criteria be taken as the maximum gross settlement not exceeding 0.03 in. per ton of additional load (CHELLIS, 1961), yield-point loads of 93 and 102 kips are observed. The points on the curves, where a 24-hr. application

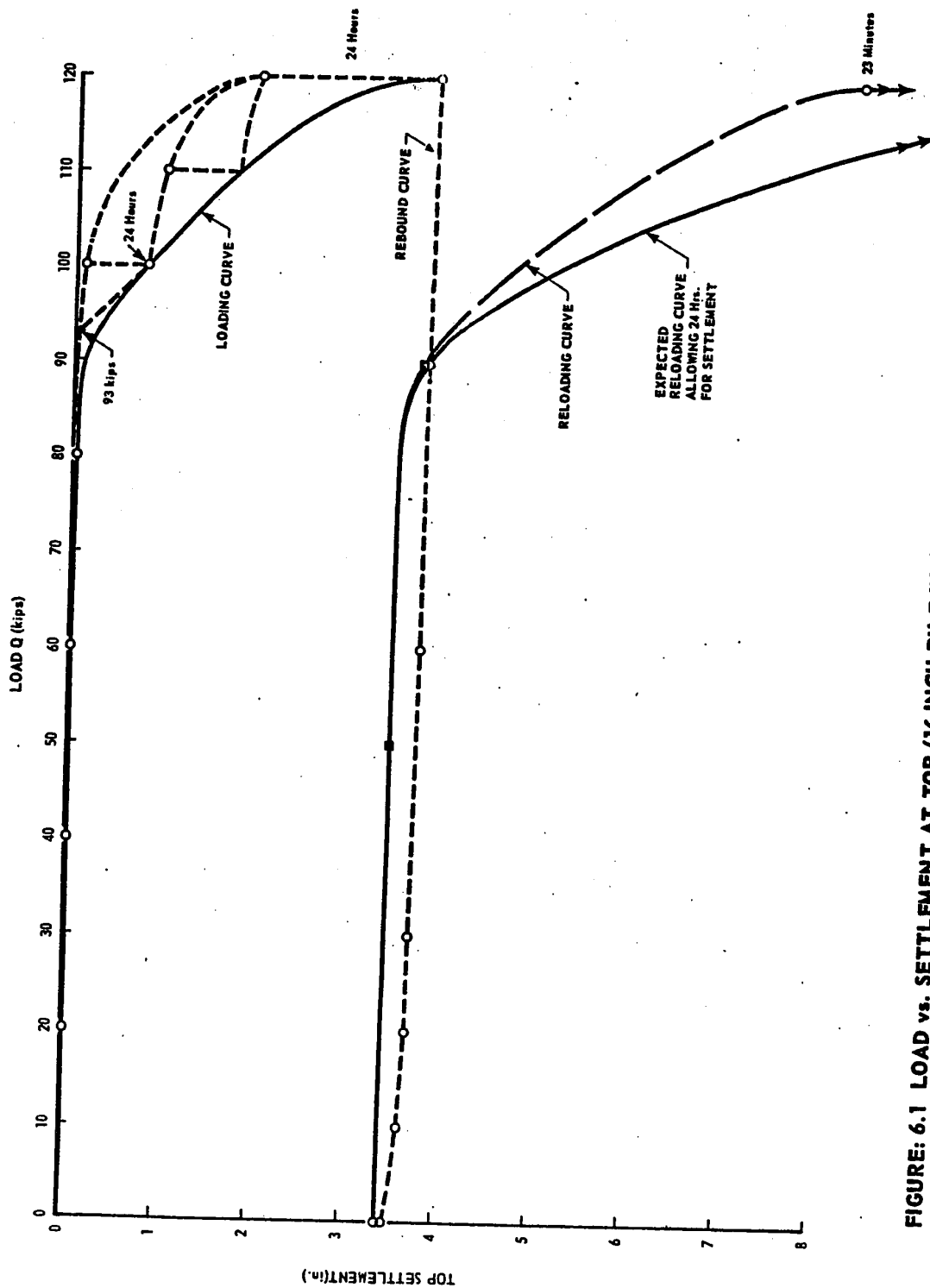


FIGURE: 6.1 LOAD vs. SETTLEMENT AT TOP (16 INCH PILE IN CLAY).

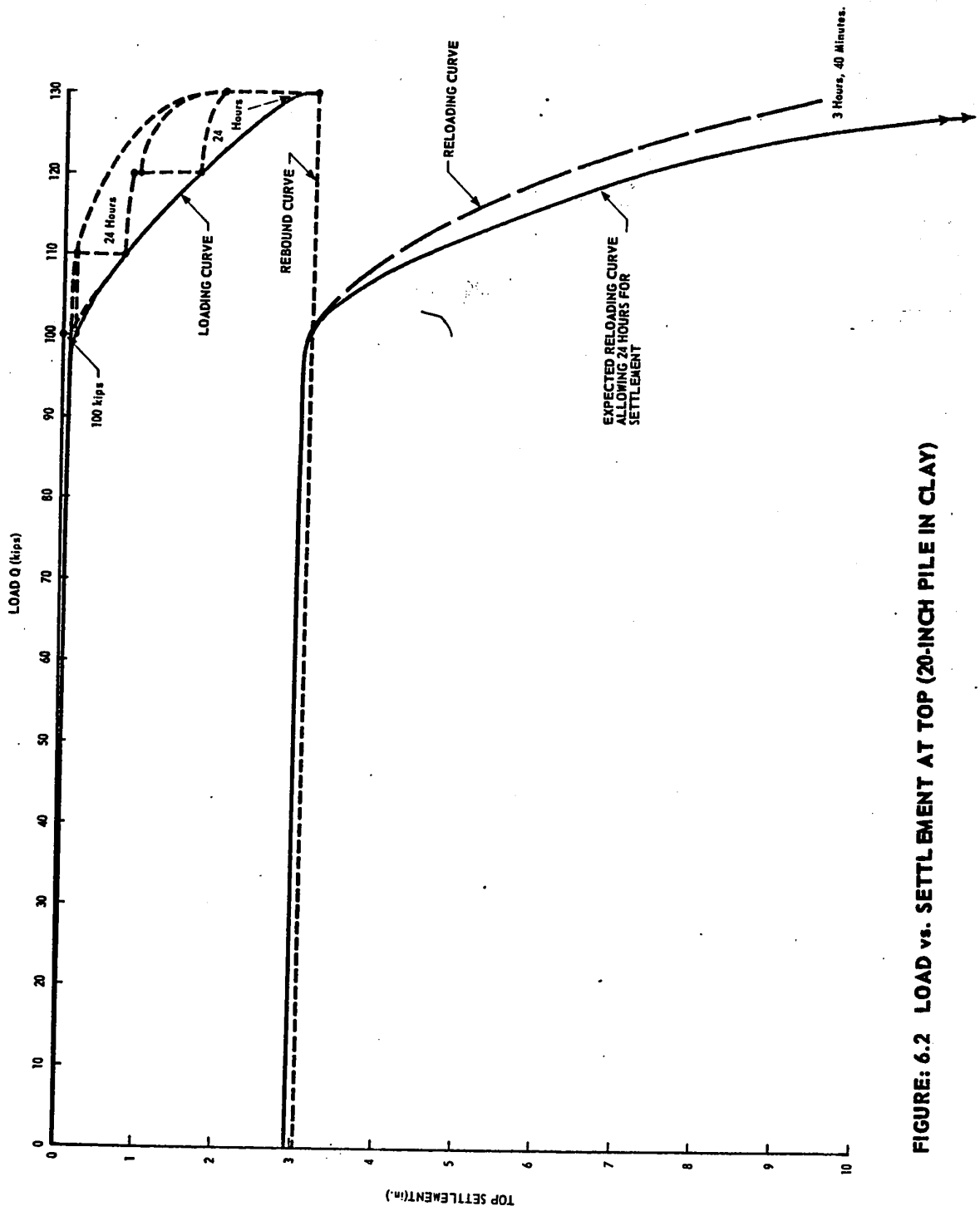


FIGURE: 6.2 LOAD vs. SETTLEMENT AT TOP (20-INCH PILE IN CLAY)

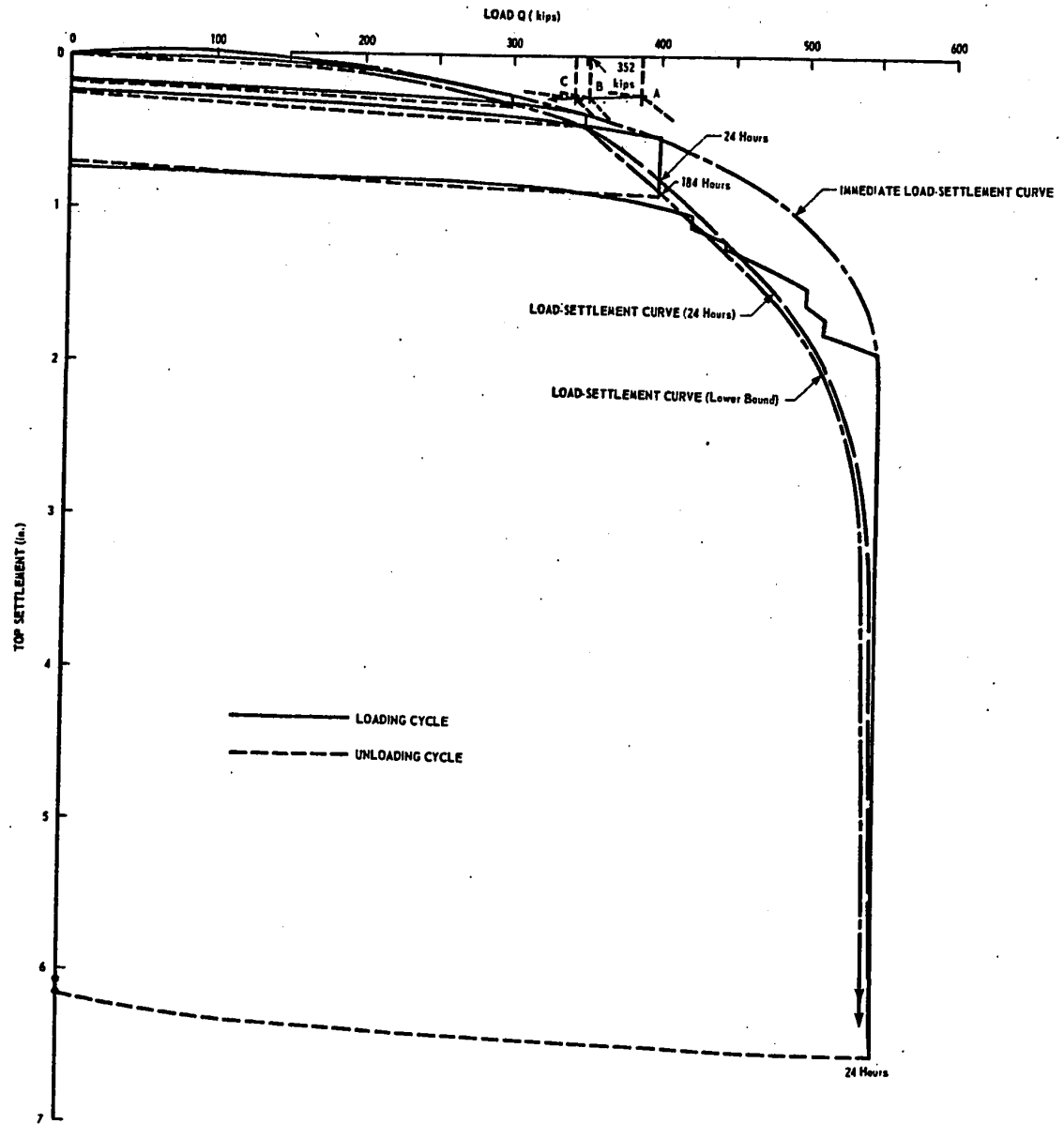


FIGURE: 6.3 LOAD vs. SETTLEMENT AT TOP (20 INCH PILE IN TILL).

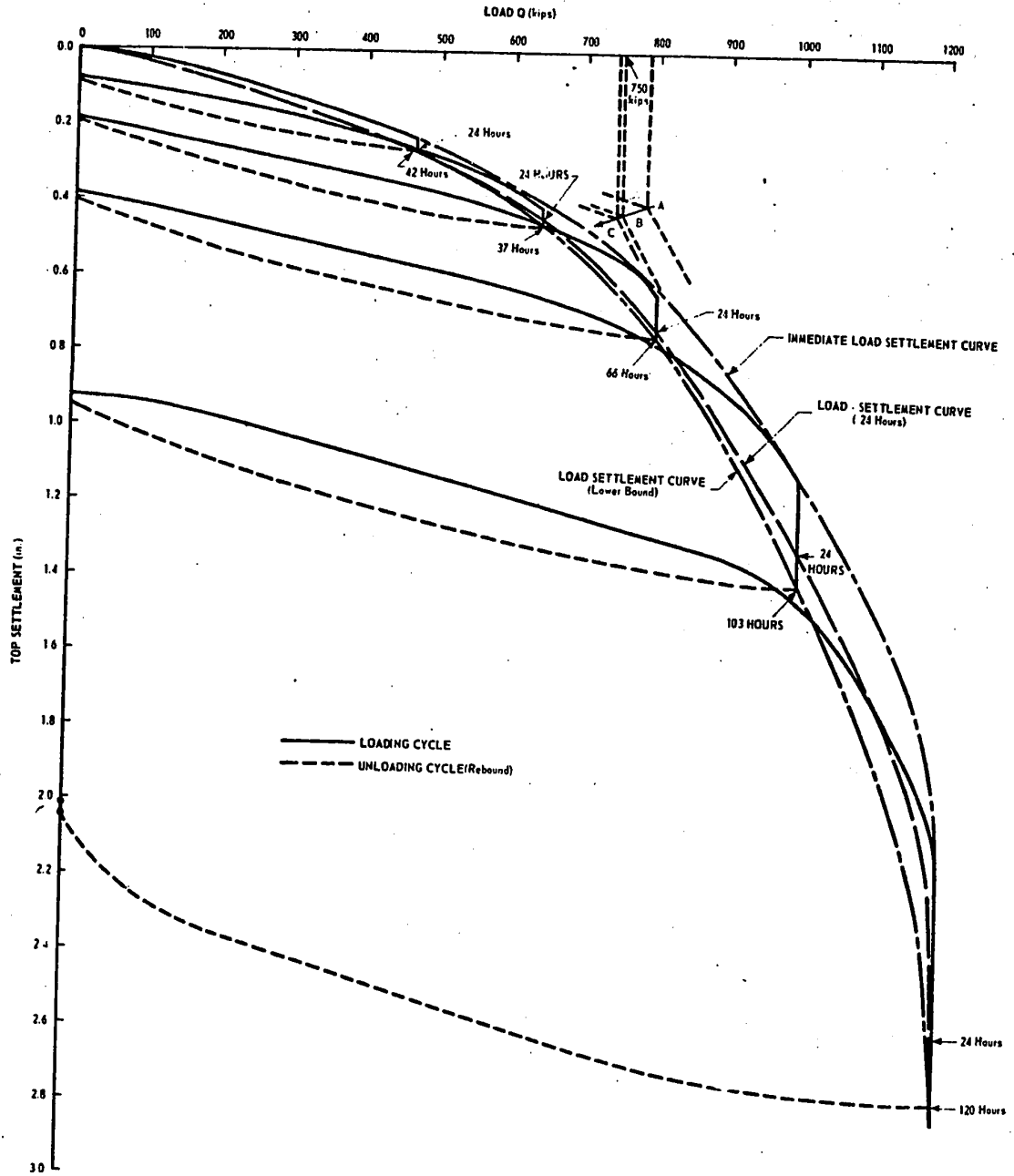


FIGURE 6.4: LOAD vs. SETTLEMENT AT TOP (28-INCH PILE IN TILL)

of load caused a permanent settlement of not more than 0.25 in., correspond roughly to loads of 93 and 104 kips respectively. Ultimate values of 93 kips and 100 kips have therefore been chosen for analysis. The initial portions of the curves are practically straight lines indicating negligible amount of settlement up to about 90 per cent of the failure load. Additional loading in excess of that, causes large settlements in both cases. Recovery of settlement on the removal of the entire load from pile top is insignificant except for last increment (corresponding to about 10 per cent of the maximum load on the pile), the total rebound amounting to 10.7 per cent of gross settlement for 16-in. pile and 6.5 per cent for 20-in. pile. The yield-point, on reloading the pile, fell down from 93 to 88 kips in the former and from 100 to 98 in the latter case, the lower portion of the two curves becoming steeper and the gross settlement increasing from less than 0.1 in. to a little over 0.2 in. in both cases. Reloading at 120 and 130 kips respectively, being about 30 per cent in excess of the failure loads, caused the piles to settle rapidly.

Piles in till were tested by the cyclic method of loading, i.e., by allowing them to rebound after each increment of load was maintained for a certain length of time and reloading it thereafter by applying the next increment. Due to practical difficulties, it was not possible to maintain the loads for the same duration for every increment. Likewise, the periods allowed for rebound were also not the same. For the 20-in. pile in till, load was increased until the pile started settling rapidly. Failure by obtaining a rapid settlement of the 28-in. pile, however, could not be achieved due to excessive upward movement of the anchor piles,

relatively large deflection in the loading beam and due to the stress in concrete having reached the ultimate strength value when the last increment was applied. The maximum load in that case was limited to 1200 kips, producing a top settlement of 2.78 in. compared to 550 kips maximum load and 6.51 in. settlement in the former case.

Due to unequal loading increments and considerable variation in the time duration for which a particular load was maintained at the pile top, the drawing of smooth load-settlement curves for the two piles in till became difficult. Three curves have been shown for each of the two piles (FIGURES 6.3 and 6.4). The upper enveloping curves indicate settlement of the pile head immediately after the application of any load increment. The lower bound curves have been roughly sketched through the points representing ultimate recorded settlements. The intermediate curves are the 24-hour settlement curves drawn on the basis of recorded values of settlement for each of the loading increments maintained for this period. Tangent lines drawn to the general slopes of the upper and lower parts of the curves intersect at points A, B and C as indicated in the figures. Values of the failure loads represented by these points are significantly different, whereas the corresponding settlements are nearly the same. The yield-point load fell down from 387 kips initially to 348 kips after long-time settlement in the case of 20-in. pile and from 785 kips to 742 kips in the case of 28-in. pile. With a view to providing a uniform basis for analysis, 24-hour settlement curves have been adopted for analysis. Failure loads indicated are 352 kips for the 20-in. pile and 750 kips for the 28-in. pile corresponding to settlements of 0.46 in. and 0.61 in. respectively.

All the reloading curves for cyclic loading of piles in till are

straight and parallel to each other, indicating an average settlement rate of 0.05 in. per hundred kips up to the failure load. The rebound curves, also roughly parallel to each other but slightly curving upwards, indicate total average recovery of about 0.04 in. per hundred kips, recovery being relatively high for the portion of the curve representing the removal of the last increment which finally reduces the load on the pile to zero.

The effect of repeated loading and unloading cycles on the total settlement of the pile top, as would be observed from FIGURES 6.3 and 6.4, has not been too significant. For loads up to about 70 per cent of the maximum test load, the settlement on reloading at a load corresponding to the previous increment is approximately the same as the maximum settlement under that increment. A slight increase in settlement is, however, indicated by the reloading curves beyond that stage.

6.3 Base Resistance Developed under the Tip of the Penetrating Pile

Values of base resistance at various stages of loading were scaled off from the calibration curves against the cumulative differences of the indicator readings for all the working quadrants added together. Load cells under the 16-in. diameter pile (in clay) and 20-in. diameter pile (in till) worked satisfactorily. Strain differences in the opposite quadrants added together indicated approximately equal values, showing central loading of cells during testing. One quadrant in each of the remaining two cells was showing erratic values and the same was ignored at the time of calibration. Some doubt was cast on the base resistance values obtained on the basis of readings from quadrants I and III for 28-in. pile in till, since the behaviour indicated was not similar to the other pile in

till. But since there was no malfunctioning indicated, being easily detectable on the strain indicator, and since the behaviour of a pile in this type of glacial till can be very different from that of another one just a few feet away (PARSONS, 1966) and further, since the embedded lengths of the two piles were significantly different, the doubt was dismissed as unfounded. The load-cell under the 20-in. diameter pile in clay was the only one for which the indicator showed little or no response. This appears to have happened due to the possible stripping off of the gages from the pillars with the passage of time (about six months in this case). None of the active quadrants of the cell functioned properly.

The capacity of two out of the three working cells was overtaxed and base resistance values had to be obtained by linear extrapolation of the calibration curves. This has been assumed to be quite in order since the maximum stress so induced in the pillars still falls well within the limit of proportionality for the material.

Values of Base Resistance Q_b , as obtained from the load cell readings, have been shown plotted against top settlement of the pile in FIGURES 6.5, 6.6 and 6.7. An alternative method of approximating the Base Resistance for the fourth pile (20-in. diameter in clay) has been attempted in the next chapter. Corresponding values of Shaft Resistance Q_s , obtained by subtracting the Q_b values from corresponding total load Q have also been plotted in the figures. Both the loading and the rebound portions of the curves (last rebound cycle for piles in till) have been included in each case. Data for the plots appear in APPENDIX L.

After the shear failure of the softened soil around the shaft represented by the pronounced peak in the curve for Shaft Resistance Q_s ,

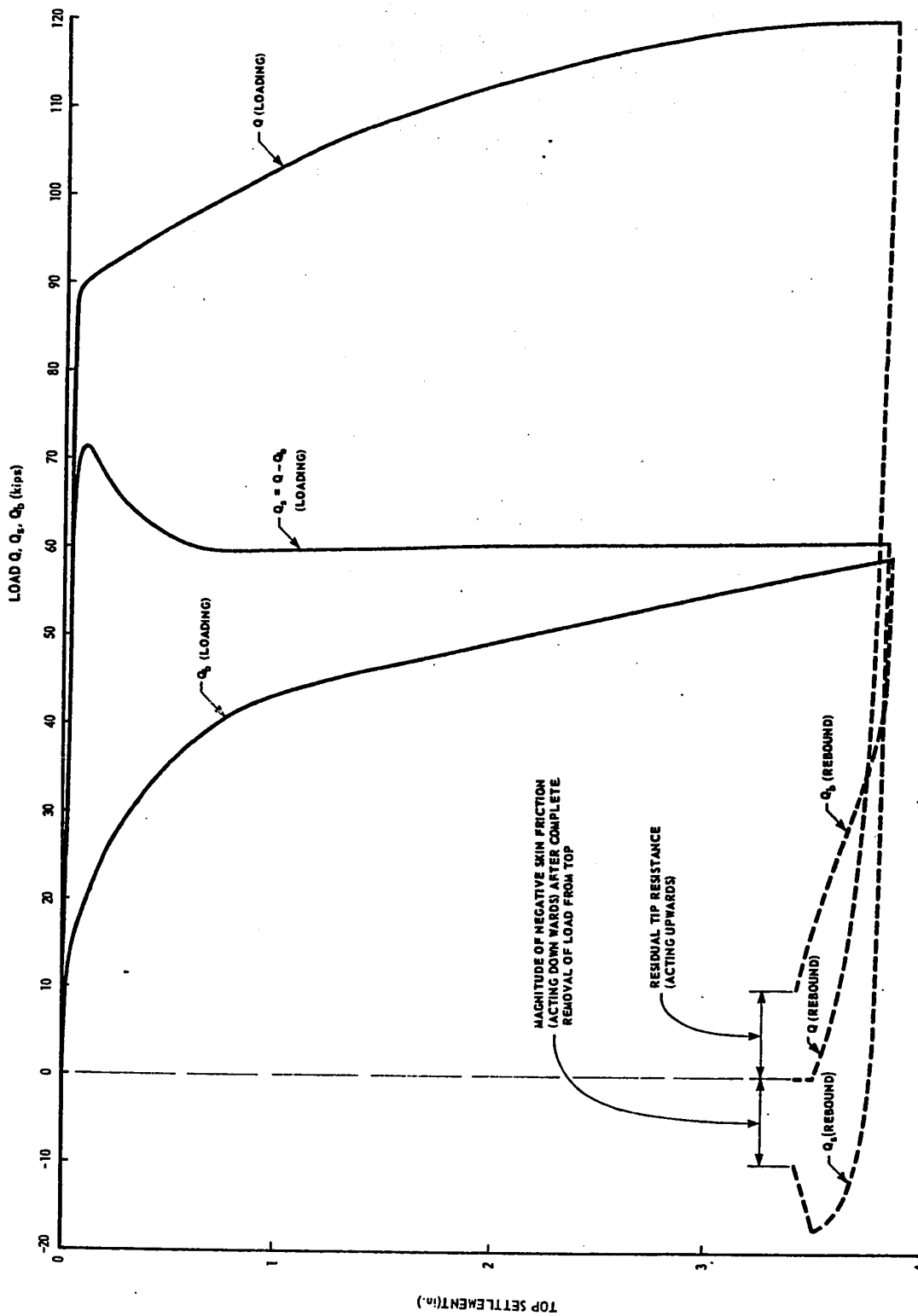


FIGURE: 6.5 PLOTS FOR BASE RESISTANCE Q_b , SHAFT RESISTANCE Q_s AND TOTAL LOAD Q vs. TOP SETTLEMENT (16 INCH PILE IN CLAY)

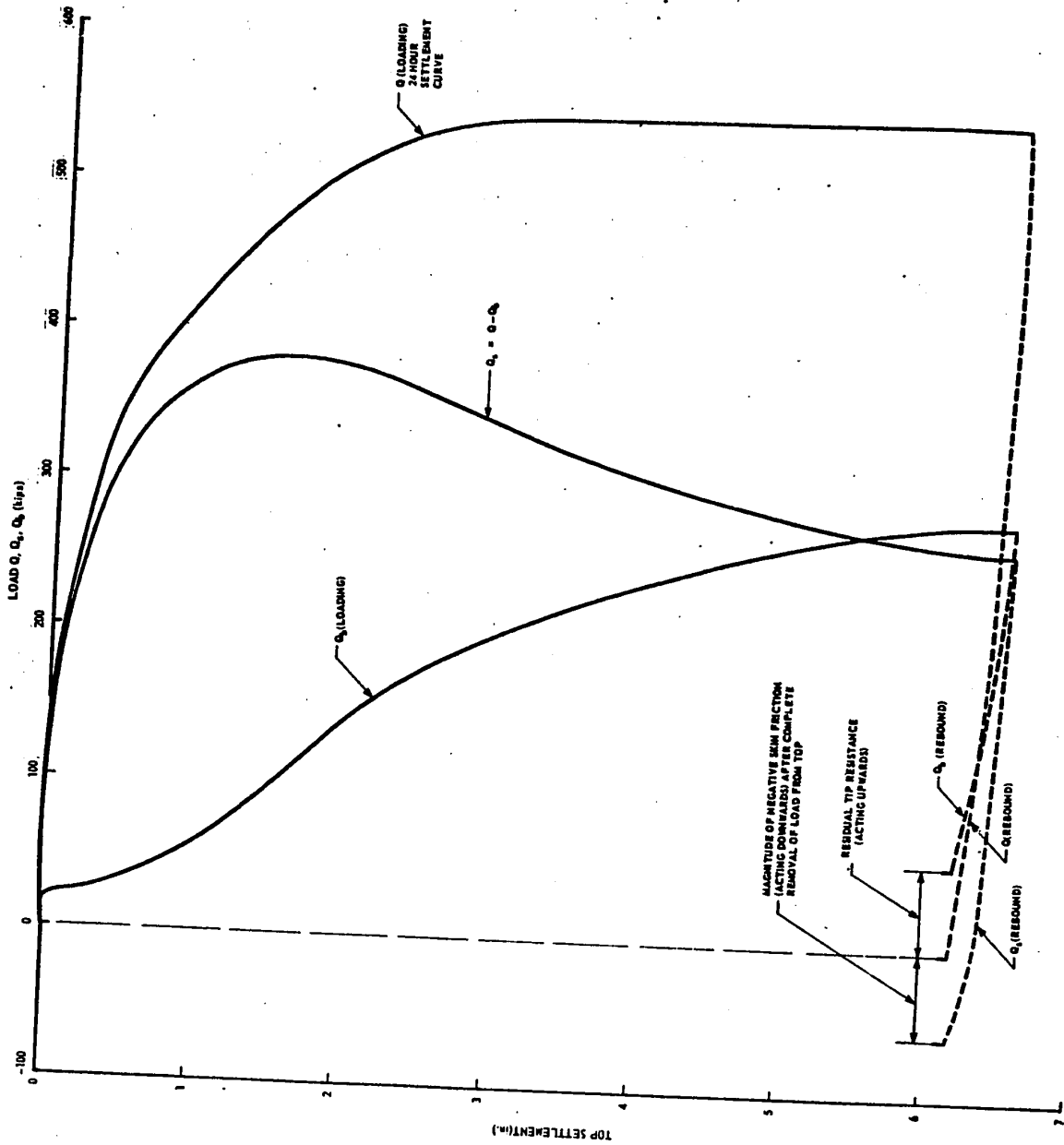


FIGURE 6.6 PLOTS FOR BASE RESISTANCE Q_b , SHAFT RESISTANCE Q_s AND TOTAL LOAD Q vs. TOP SETTLEMENT: (20 INCH PILE IN TILL).

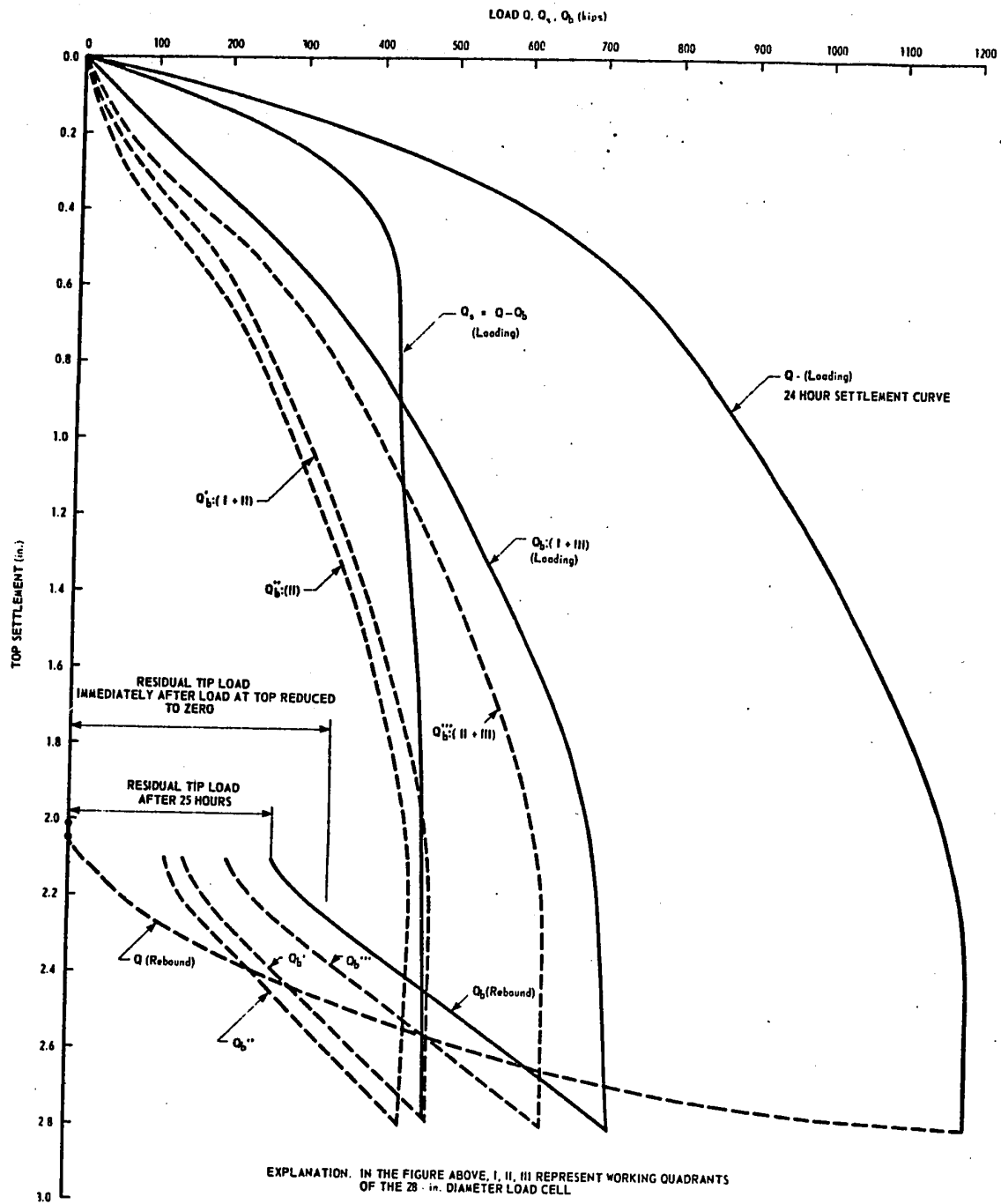


FIGURE: 6.7 PLOTS FOR BASE RESISTANCE Q_b , SHAFT RESISTANCE Q_s AND TOTAL LOAD Q vs. TOP SETTLEMENT; (28 in. PILE IN TILL).

a considerable magnitude of additional load was transferred to the base of the 16-in. diameter pile in clay (FIGURE 6.5). Whereas the shaft resistance curve flattened out after the peak, indicating nearly a constant value of Q_s , the base resistance continued mounting with further penetration of the pile. Up to a settlement of about 3.8 inches of the pile head, the base resistance value had not yet reached its peak value though from the shape of the lower end of the Q-curve, it can be easily made out that it was very close to that. Removal of load from pile top left some Residual Load at the tip (acting upwards) and an equal amount of Negative Skin Resistance (acting downwards) to balance it. The magnitudes are shown in the figure.

Embedded length appears to be a dominant factor governing the behaviour of piles in till. Whereas base-resistance build-up is slow for both the piles (FIGURES 6.6 and 6.7), the difference is characterized by the curves for Shaft Resistance in the two cases. Skin friction is mobilized fully corresponding to top settlement of 1.6 in. for short pile but appears to be still building at the maximum settlement of 2.8 in. reached by the long pile. Base Resistance curve Q_b for the 28 in. pile (FIGURE 6.7) drawn for the working quadrants (I and III) is the one adopted for analysis. The other three curves for tip resistance, shown dotted in the figure, have been drawn on the basis of other combinations of working quadrants, for comparison only. Both the skin friction and the base resistance curves in the case of these two piles appear to be levelling off at maximum settlements, indicating load transfer to the base of the order of about 60 per cent of the total load, for both piles. Rebound on unloading is of the order of 6 per cent of the total top settlement for the 20 in. pile and 27 percent of the total top settlement for the 28 in.

pile. This probably is indicative of the fact that complete shear failure of the shaft soil had occurred for the 20-in. pile having penetrated about 6.5 in. whereas the same did not happen for the 28-in. pile having penetrated only about 2.8 in.

6.4 Behaviour of Piles under Sustained Loads

Settlement behaviour of piles as a function of time at various stages of loading has been shown in FIGURES 6.8 and 6.9. This has been further amplified in FIGURE 6.10, illustrating the sustained effect of a single increment of load maintained for a long time. For all loads less than failure load settlement increases at a fast rate for the first two to three hours and then slowly levels off, showing no appreciable increase after about 8 hours. The rate of settlement-increase goes on mounting with each new increment of load added to the applied load, till the total load approaches the failure load and the settlement behaviour with respect to time registers a change, the pile then settling rapidly. These facts are amply illustrated by FIGURE 6.10, as also by the preceding two figures. Time settlement behaviour of piles in clay and till can, however, not be equated since their load-settlement characteristics are basically different from each other, as seen in FIGURES 6.1 to 6.4. Whereas settlement curves for piles in till are constantly drooping, those in clay show little if any settlement up to failure load. The rate of settlement as a function of time is therefore, in general, greater for piles in till than for piles in clay for comparable loads applied at top.

Settlement Recovery on complete removal of load from pile top, appears to be dependent primarily upon four factors, viz., the number of

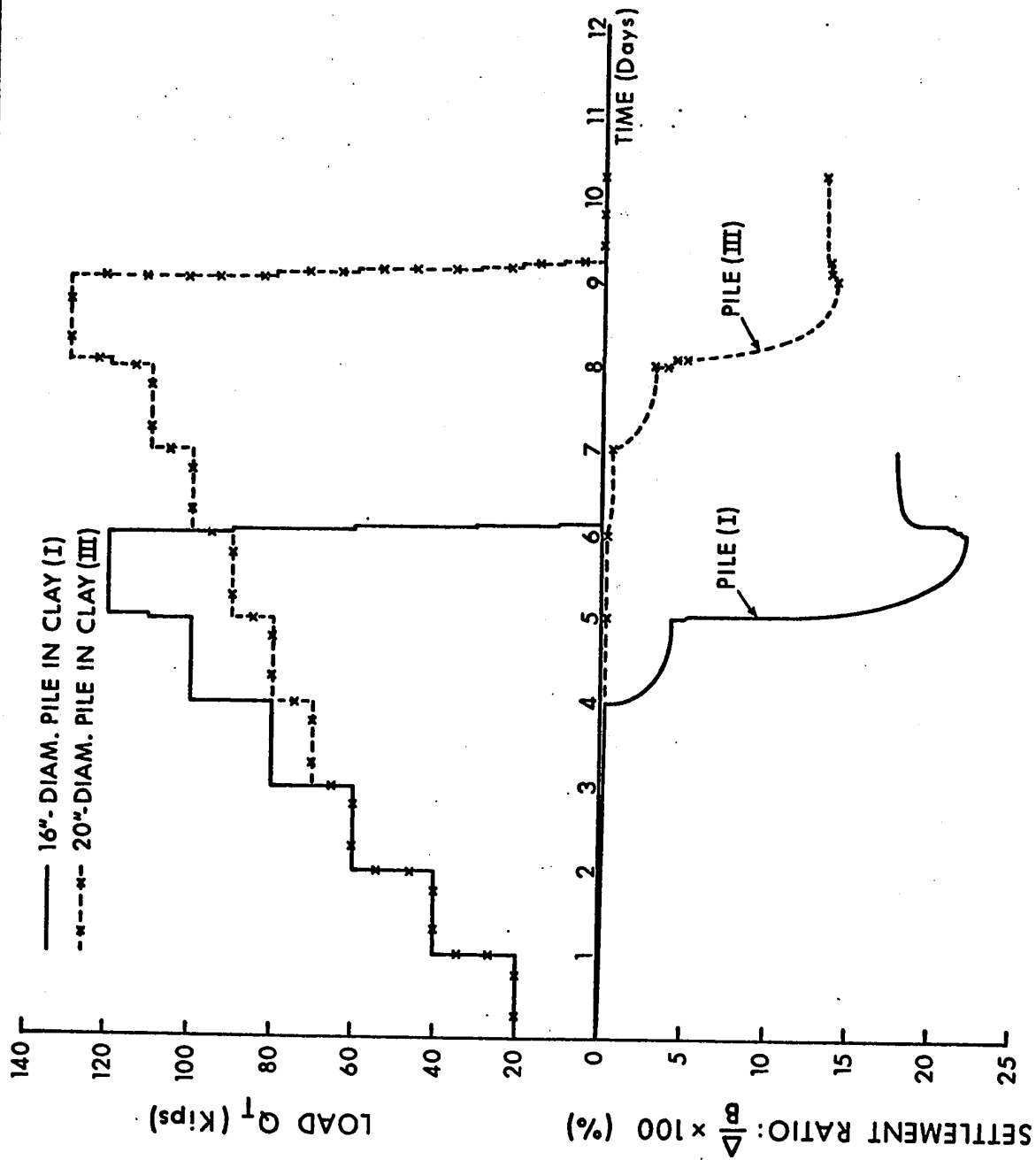
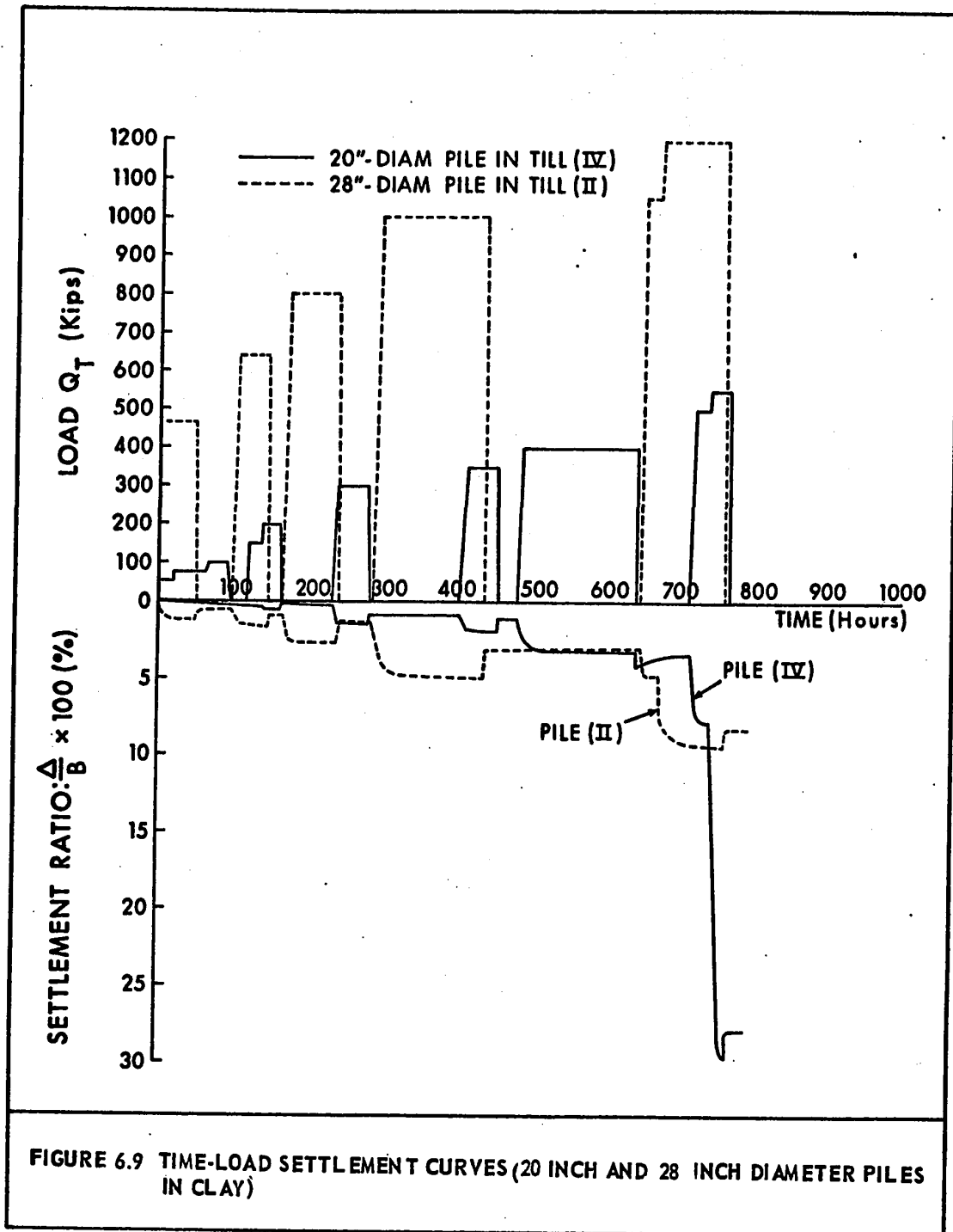


FIGURE: 6.8 TIME-LOAD-SETTLEMENT CURVES (16 INCH AND 20 INCH DIAMETER PILES IN CLAY)



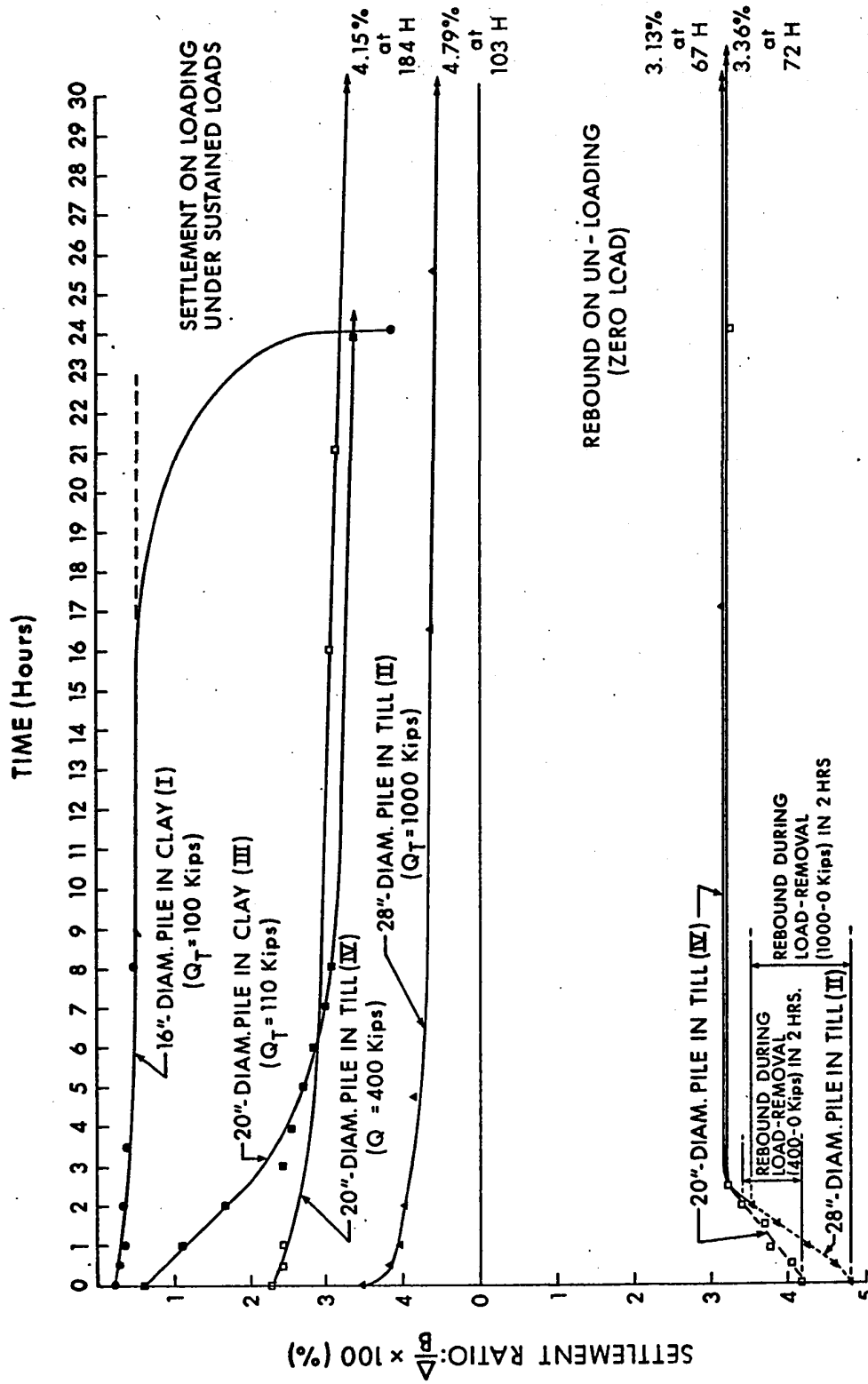


FIGURE: 6.10 TYPICAL TIME-SETTLEMENT CURVES, UNDER SUSTAINED LOADS.

loading and reloading cycles applied up to the maximum test load, compressibility characteristics of soil, modulus of elasticity of the material of the pile and finally the condition as to whether complete shear failure of the soil around the shaft had been approached or not. The rebound decreases with the increase in the number of repetitions and also if complete shear failure has occurred in the shaft soil. Rapid sinking of the pile at any stage of loading and the appearance of a pronounced peak in the Shaft Resistance curve perhaps indicate total shear failure having taken place in the surrounding soil. Taking the same value of the elastic modulus for the material of the piles and assuming similar compressibility characteristics of till below the pile tips, the difference in the final rebound values for 20-in. and 28-in. piles in till, seen in FIGURES 6.6, 6.7 and 6.10, can thus be explained on the ground that complete shear failure of soil did take place in the former case whereas the maximum load on pile top was not adequate to induce a similar condition in the latter case. A major portion of rebound for all piles, however, is relatively instantaneous. Recovery with passage of time as shall be observed in FIGURE 6.10 is small.

FIGURES 6.5, 6.6 and 6.7 illustrate also the manner in which the base resistance falls when load at pile top is reduced to zero. Magnitudes of Residual Tip Load after allowing the pile to recover for 24 hours have been indicated in the figures. Negative values of Skin Resistance, being exactly equal in magnitude and opposite in sense to that of the Tip Resistance at zero load, have also been shown in FIGURES 6.5 and 6.6.

Effect of sustained loads on the values of base resistance has been illustrated in FIGURE 6.11. Behaviour of piles in clay appears to be

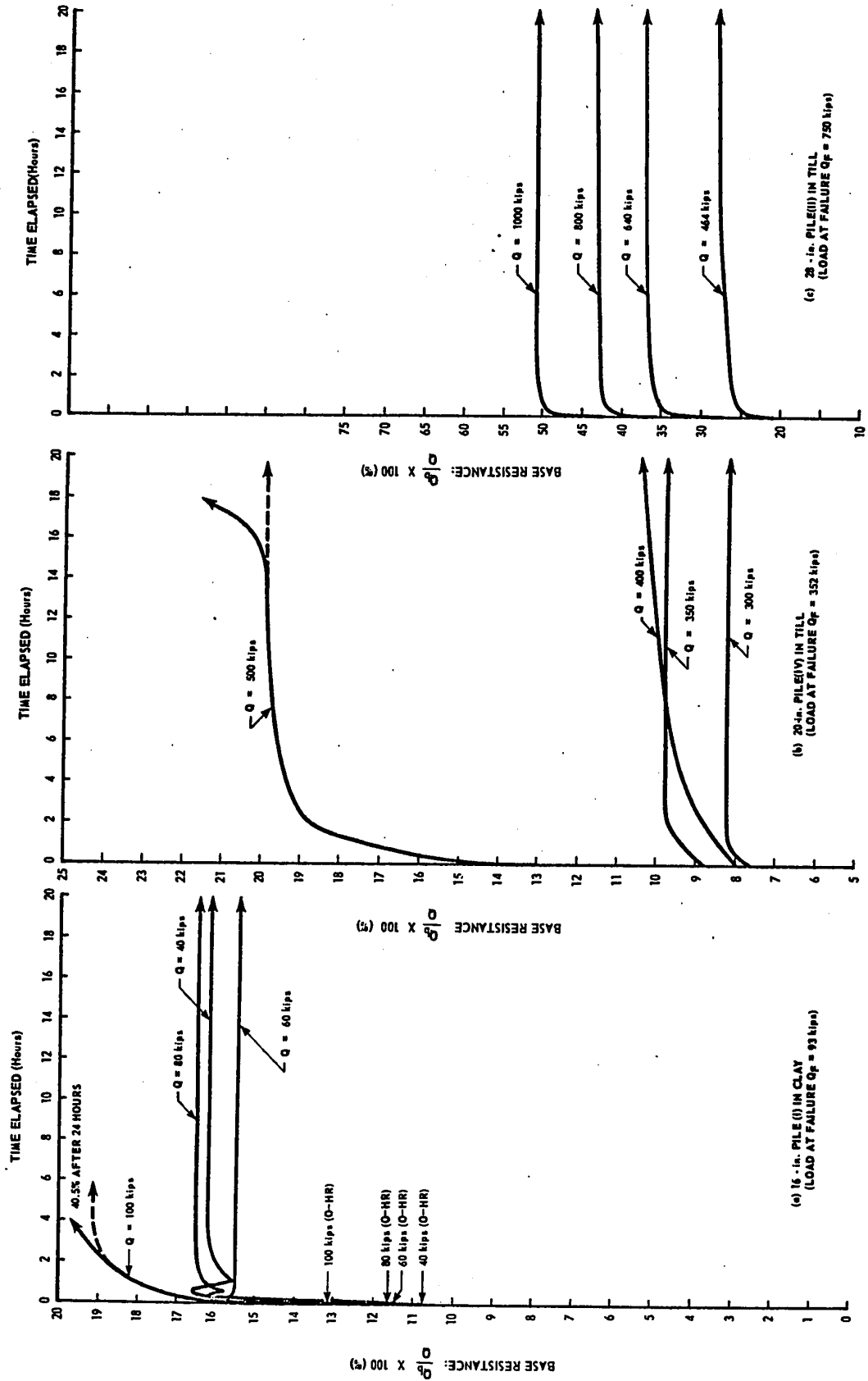


FIGURE: 6.11 TYPICAL PLOTS SHOWING VARIATION OF BASE RESISTANCE WITH TIME UNDER SUSTAINED LOADS.

slightly different from those in till. For loads less than the failure load, the base resistance for piles in clay builds up rapidly to a peak on the application of a new increment, then falls down to a certain extent, rebuilds slowly thereafter, and finally levels off. No peak is indicated when the load approaches the failure load for which settlement goes on increasing with the passage of time. For piles in till and for applied loads less than the failure load, the base resistance builds up in two to four hours, showing little increase thereafter without recording a peak anywhere. Mobilization of base resistance as a function of time at loads close to the failure load, appears to be similar to that of piles in clay. The difference in behaviour for the two soils indicates quick adjustment of particles along the shaft for piles in till but a temporary reversible straining of particles for piles in clay, dependent therefore on the shape and size of the particles.

Data concerning behaviour of piles under sustained loads appear in APPENDIX M.

6.5 Adjustment of Shaft Resistance and Base Resistance Values

Presence of concrete plugs forming the pile tips makes it necessary to adjust the measured values of Base Resistance as also the computed values of Shaft Resistance. Estimation of effective magnitudes for purposes of analysis, in the next chapter, has been based on the assumption that unit skin friction offered by the vertical peripheral surface of the plug in contact with the surrounding soil, is the same as the average skin friction along the shaft above the cell. The effective value Q_B of the base resistance at the bottom of the plug shall thus be given by:

$$Q_B = Q_b - \frac{H_1}{H} \cdot Q_s + W_p \quad \dots (6.1)$$

where Q_b is the value obtained from the strain indicator readings; Q_s is the difference ($Q - Q_b$); H the embedded length of the pile measured above the centre of the cell; H_1 the length of the plug from centre of the cell to tip of the pile; and W_p the weight of the concrete plug. Effective value of Shaft Resistance Q_s shall therefore be the difference ($Q - Q_b$).

CHAPTER VII

ANALYSES OF TEST DATA AND DISCUSSION

7.1 Introduction

In this chapter, the results of field tests presented in Chapter VI have been analysed and correlated with the strength characteristics of soil presented in Chapter V. An attempt has been made to evaluate the design parameters for bored-in piles installed in clay and till. Where field information is inadequate, use has been made of data from other sources.

In computing the Shaft Resistance by subtracting the measured Base Resistance from the total load at pile top, it has been assumed that the effect of interaction is insignificant and that the two components are independent and hence separable.

Essential pile data on which the computations in this chapter are based have been presented in TABLE VII-1.

7.2 Analysis of Base Resistance for Piles in Clay

Base Resistance Q_b as worked out from the strain indicator readings for 16-inch pile in clay has already been shown in FIGURE 6.5. Similar values for the 20-inch pile in clay for which the load cell did not function properly have been approximately estimated on the basis of measured shaft compression, on the assumption that both the piles in clay

TABLE VII-1
ESSENTIAL PILE DATA FOR COMPUTATIONS

Description	Pile Designation			
	I (16" IN CLAY)	II (28" IN TILL)	III (20" IN CLAY)	IV (20" IN TILL)
1. Nominal Diameter (in.)	16	28	20	20
2. Effective Diameter, B (in.)	17.25 (B ₁)	29.5 (B ₂)	22.0 (B ₃)	22.0 (B ₄)
3. Actual Base Bearing Area, A _b (in. ²)	233	683	381	381
4. Sectional Area of Steel effective as reinforcement (in. ²)	0.5% A _b	13.4	0.5% A _b	13.4
5. Equivalent [†] Sectional Area, A _e (in. ²)	241	295 (upper length) 777 (lower length)	394	295 (upper length) 475 (lower length)
6. Equivalent Modulus of Pile Material: composite section (computed value), E (psi.)	3.625 x 10 ⁶	4.6 x 10 ⁶	3.625 x 10 ⁶	4.6 x 10 ⁶
7. Effective Circumference (in.)	54.2	92.6	69.1	69.1
8. Total Depth of Installation* (ft.)	20	49.5	16	38
9. Free Standing Length (in.)*	41.25	346	42	344
10. Effective length of contact with soil from top up to mid-depth of cell,* H (in.)	177.88	241.25	130.63	116.63
11. Effective length of contact with soil from mid-depth of cell up to bottom of concrete plug,* H ₁ (in.)	33.63	28.75	29.38	21.38
12. Height of Load-Cell* (in.)	4.75	8.5	6.75	6.75
13. Thickness of concrete plug at bottom* (in.)	31.25	24.5	26	18
14. Shaft Contact Area for length H ₂ (in. ²)	9641	22340	9027	8059
15. Contact Area for length H ₁ (in.)	1823	2662	2030	1477

[†] For the transformed section, accounting for the sectional area of the steel pipe used in till, or nominal vertical reinforcement used for piles in clay (modular ratio: $E_{\text{steel}}/E_{\text{concrete}} = 8$).

* From Figure 4-14.

behaved in a similar manner.

For any shaft of length H and sectional area A , having an elastic modulus E for the material, the deformation ΔH under an axial load Q can be computed by using Hooke's law giving $\Delta H = QH/AE$. In the case of a pile, however, because of its embedment in soil, the stress due to the applied load Q at top goes on decreasing with depth. For small increments of load in the beginning of a pile test, the effect of the load does not reach the pile tip (D'APPOLONIA, 1963; TROW, 1967; BROMS, 1968). On the lines suggested by TROW (1967), it can be shown APPENDIX N) that for a pile of length H and diameter B , the critical load Q_c applied at top when its effect just reaches the tip, is given by:

$$Q_c = 1/2 \pi KBH^2 ; \quad \dots (7.1)$$

and the corresponding shaft compression is given by:

$$\Delta H = \frac{2}{3} Q_c \cdot \frac{H}{AE} \quad \dots (7.2)$$

where $K = k \gamma' \tan \phi_d$. In this equation k is the coefficient of lateral earth pressure, γ' the effective unit weight of soil and ϕ_d the mobilized angle of friction.

Based on the over-consolidation ratio ranging from about 6 at a depth of 3 feet below surface to about 2 at a depth of 20 feet and an average value of plasticity index of 40, the coefficient k_0 of earth pressure at rest, reflecting approximately the value of k for use in the above equation, as scaled from the plots by BROOKER and IRELAND (1965), ranges from 0.9 to 1.2, for the 16-in. diameter 20 feet long pile in clay. Using $\gamma = 116$ pcf. and $\phi' = 30$ degrees, the critical load Q_c from equation (7.1) above works

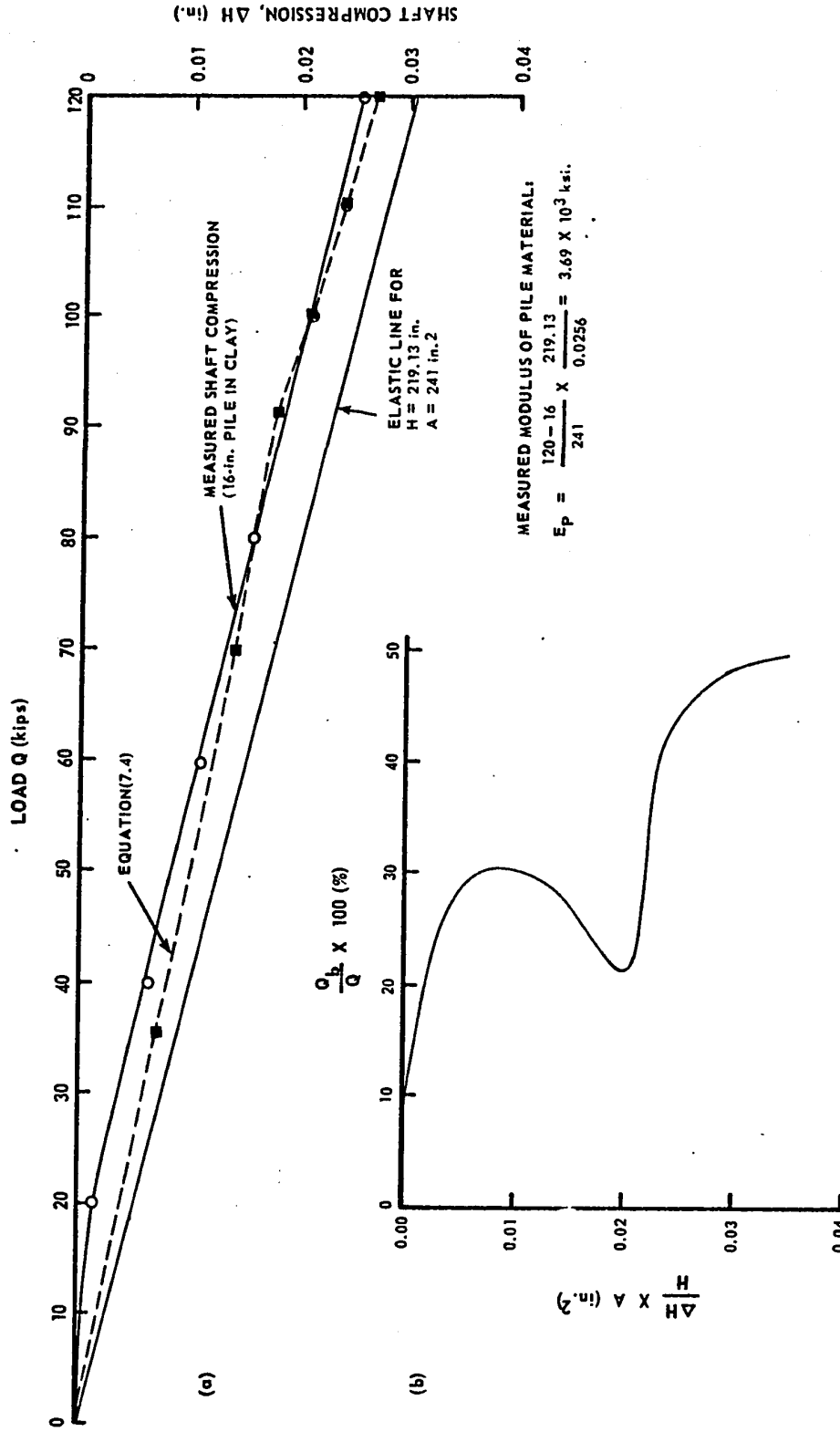
out to about 16 kips. The first increment of the applied load being 20 kips, it can be assumed that the tip started receiving its share of the load right from the beginning of the test. Thus when the applied load at top is Q and the corresponding measured tip resistance is Q_b , the approximate deformation of the pile is given by:

$$\Delta H = \frac{Q_b \cdot H}{AE} + \frac{2}{3} \cdot \frac{(Q - Q_b)}{AE} \cdot H \quad \dots (7.3)$$

Using the dimensions given in TABLE VII-1, and adopting E for composite section equal to 3.625×10^3 ksi. (based on the supplied value of concrete crushing strength), the above equation for the 16-inch pile (I) can be re-written as (APPENDIX N):

$$\Delta H_1 = Q \left(18.3 + 6.77 \frac{Q_b}{Q} \right) \times 10^{-5} \quad \dots (7.4)$$

wherein Q_b , Q are measured in kips and ΔH_1 in inches. Axial deformation represented by this equation has been plotted in FIGURE 7.1 (a) along with the measured shaft compression. The difference in the values indicated by the two lines is not too large. Elastic line for the unobstructed deformation of the pile is also shown in the plot. Modulus of deformation indicated by the actual shaft compression line is 3.69×10^3 ksi. whereas its average value computed from the plot of equation (7.4) is a little higher, being 4.3×10^3 ksi. Measured values of shaft compression as ratio of H/A have been plotted against the base resistance Q_b , taken as percentage of applied load Q at top, in FIGURE 7.1(b) for the 16-inch pile. Assuming that the relationship represented by this plot holds for the other pile also, Q_b/A values for 20-in. pile have been scaled off using values computed from the measured shaft compression ΔH ,



NOTE:

IN THE FIGURE ABOVE, ΔH REPRESENT RESPECTIVELY THE EQUIVALENT SECTIONAL CONCRETE AREA OF THE TRANSFORMED SECTION AND THE LENGTH OF THE PILE (16-INCH DIAMETER IN THIS CASE) MEASURED FROM PILE HEAD TO THE TOP OF LOAD CELL.

FIGURE 7.1 PLOTS FOR MEASURED SHAFT COMPRESSION vs. APPLIED TOTAL LOAD AND MEASURED TIP RESISTANCE FOR 16-INCH PILE (I) IN CLAY.

the length H and the equivalent sectional area A for the 20-inch pile. FIGURE 7.2(b) represents the plot for Q_b so determined. Equation for deformation of the 20-inch pile (III) for the dimensions given in TABLE VII-1, using E equal to 3.625×10^3 ksi., can be written as (APPENDIX N):

$$\Delta H_3 = Q(9.02 + 3.05 \frac{Q_b}{Q}) \times 10^{-5} \quad \dots (7.5)$$

This relationship as seen from FIGURE 7.2(a) indicates deformation values comparable to the measured shaft compression plotted in the figure, and thus confirms the authenticity of the method used for obtaining Q_b values for the 20-in. pile. The assumption that E for concrete remains unchanged and that soil under the pile tips at different depths offers comparable resistance to penetration, would introduce an error of the order ± 10 percent as observed from the data for the recorded settlements. For piles of nearly the same length or for tips resting on strata having nearly the same physical characteristics, this error would be considerably reduced. Nevertheless, the plot (FIGURE 7.1b) is not unique. Its use for other sites would involve the conditions in regard to the assumptions being satisfactorily met.

FIGURES 7.3 and 7.4 show the tip settlement of the piles obtained by subtracting the compressive deformation taken from FIGURES 7.1 and 7.2. The curves have been further adjusted by accounting for the contribution made by concrete plugs provided below the piles, using equation (6.1). Dimensionless parameters have been used for both the plots. Curves for Shaft Resistance have been obtained by subtracting Q_b from the corresponding Q -values.

From the shape of the curves for total capacity (FIGURES 6.1, 6.2, 7.3 and 7.4), it can be made out that settlement under the final

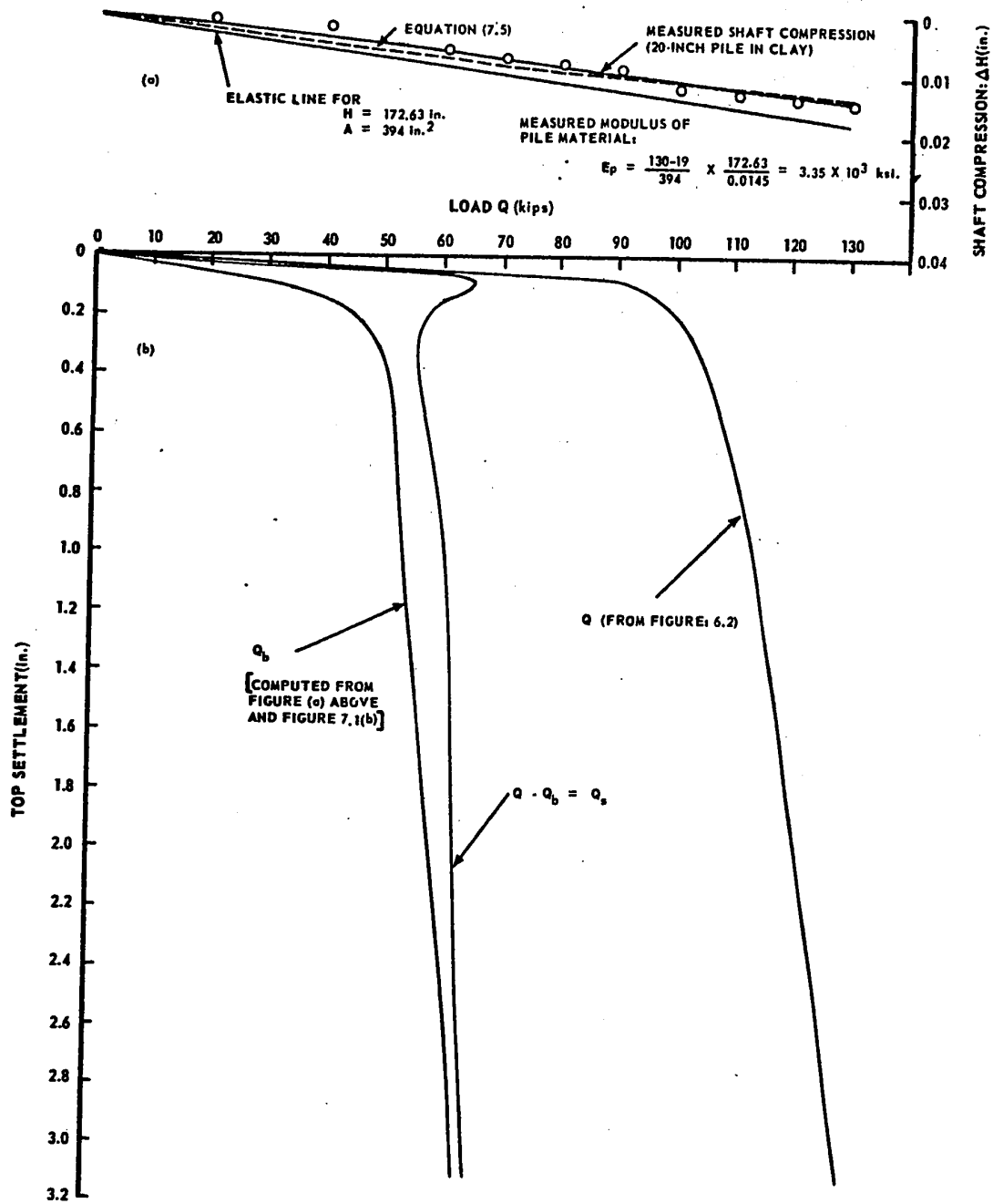


FIGURE: 7.2 PLOTS FOR MEASURED SHAFT COMPRESSION vs. APPLIED TOTAL LOAD AND TOP SETTLEMENT vs. COMPUTED BASE RESISTANCE FOR 20 INCH PILE (III) IN CLAY.

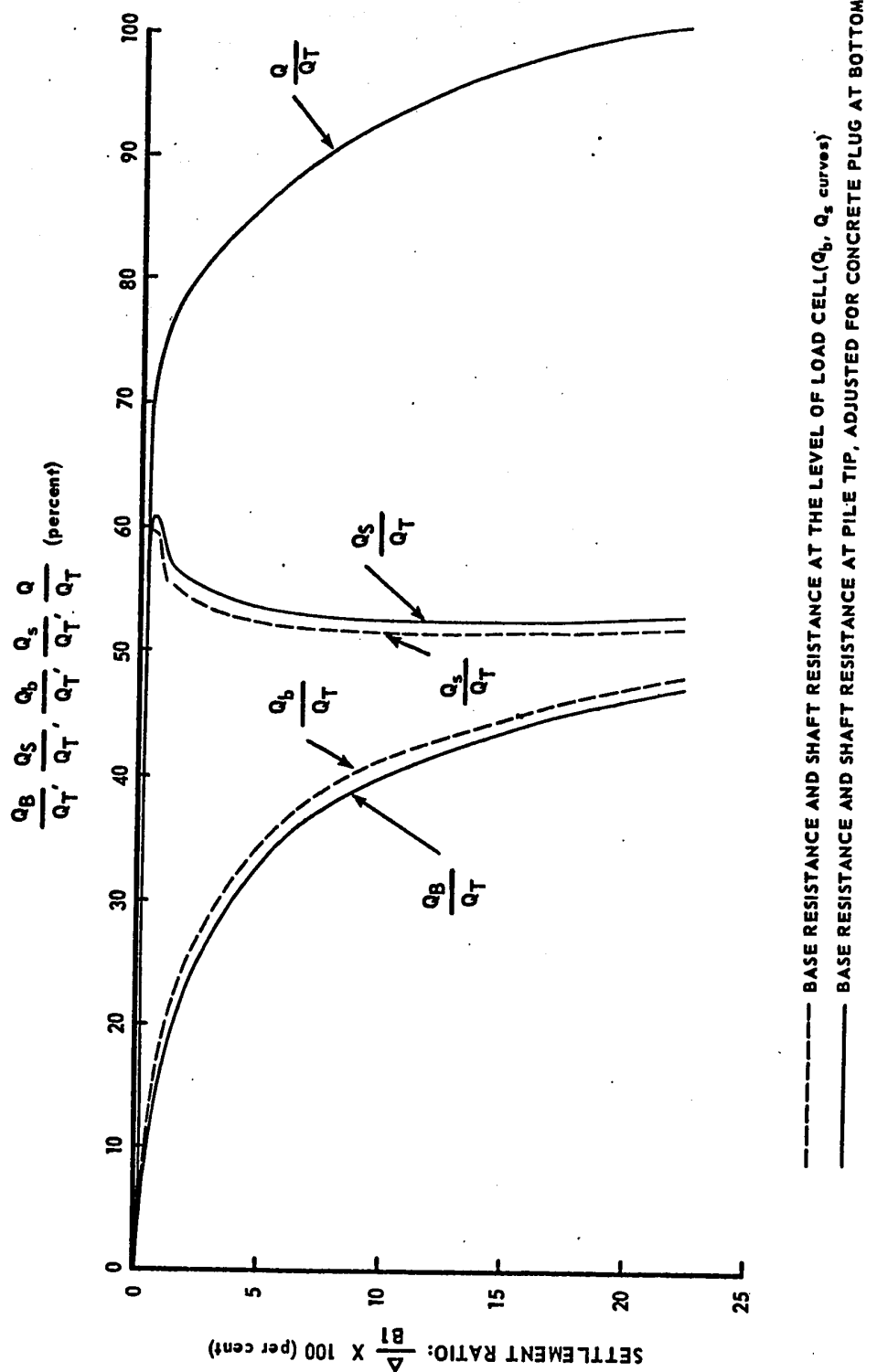


FIGURE 7.3 LOAD vs. TIP-SETTLEMENT CURVES, ADJUSTED FOR SHAFT COMPRESSION AND THE CONTRIBUTION OF CONCRETE PLUG BELOW LOAD CELL: 16 INCH PILE (I) IN CLAY.

increment would go on increasing with time. The indicated ultimate values of base resistance can safely be assumed to be the maximum for purposes of analysis. Ultimate bearing capacity computed on this basis works out to 165 psi. for 20-inch diameter 16 feet deep pile and 242 psi. for 16-inch diameter 20 feet deep pile. As shall be seen from FIGURE 5.1, the amount of clay present is of the order of 45 and 27 percent respectively at depths of 16 and 20 feet below ground surface, the rest being a mixture of silt and fine sand. Soil is nearly saturated (degree of saturation of the order of 92 percent) and is of medium dense consistency (average N-value: 23). Under the loaded pile tip, it is presumed, it would behave like a typical $c-\phi$ material. Immediate drainage under the pile-tip at 16 feet depth, where percentage of silt and montmorillonite clay is relatively high and soil is nearly saturated, cannot be expected. Similar conditions exist under the pile tip at 20 feet, though the composition of soil indicates a little higher percentage of fine sand. A very small amount of drainage if at all from the nearly saturated compact mixture of clay, silt and fine sand may take place in that case. For purposes of analysis, however, undrained conditions have been assumed. Undrained angle of shearing resistance as obtained from triaxial tests (TABLE V-1), has average values of 5.5 and 11.5 degrees, the undisturbed cohesion being 10.8 and 7.8 psi. respectively for the soil at 16 and 20 feet depth. Based on this information, the ultimate bearing capacity for the soil under the tips of the two piles has been computed both on the basis of Terzaghi's as well as Meyerhof's Theories:

(a) TERZAGHI (1943), Ultimate Bearing Capacity Theory (condition of general shear failure):

From equation (2.2) (Chapter II), using the parameters assumed in the above paragraph we have from Terzaghi's Chart:

$$N_c = 7.4, N_q = 1.8, N_\gamma = 0 \text{ for } \phi = 5.5^\circ, \text{ and}$$

$$N_c = 10.2, N_q = 3.2, N_\gamma = 1.0 \text{ for } \phi = 11.5^\circ.$$

Substitution in equation (2.2) gives $q_u = 130, 161$ psi. respectively for the 16 feet and 20 feet deep piles.

(b) MEYERHOF (1951), Ultimate Bearing Capacity Theory (condition of general shear failure):

Bearing Capacity factor from Meyerhof's charts are:

$$N_c = 14.0, N_q = 2.1, N_\gamma = 0.2 \text{ for } \phi = 5.5^\circ, \text{ and}$$

$$N_c = 20.5, N_q = 5.1, N_\gamma = 2.1 \text{ for } \phi = 11.5^\circ.$$

Using equation (2.3) we have $q_u = 179$ psi. and 247 psi. respectively for 16 feet and 20 feet deep piles.

Based on Terzaghi's Theory, a simpler approach by KRIZEK (1965) who dispenses with the use of charts for arriving at the values of bearing capacity factors and makes direct use of the friction angle, gives values of ultimate bearing capacity as 101 psi. and 136 psi. respectively for the two piles.

Under conditions of ultimate failure, computations based on Terzaghi's Theory, as observed from the results obtained in the above paragraphs, indicate rather conservative values of tip resistance. Meyerhof's theory on the other hand appears to give values slightly in excess of the measured ultimate capacity of the base. A look at the slow-rising lower ends of the mobilization curves for tip resistance clearly indicates

that the actual ultimate values at a little higher settlement would be slightly more than the final observed values. In other words, it can be safely presumed that actual values would agree favourably with the theoretical values if computed on the basis of Meyerhof's Theory. A greater emphasis on the determination of strength parameters of the soil is obviously necessary.

Depth of piles installed in the clay-silt-sand region can be expected to vary from 15 to 25 feet. Within this region values of the angle of the shearing resistance increase with depth as does the percentage of sand fraction and so also the N-values. The indicated base capacity can be expressed in terms of the product $N \times \text{depth below surface}$. But since there is no uniformity in the characteristics of the deposit at various depths, the importance of the depth factor is insignificant. Assuming that the N-values themselves include the effect due to depth, approximate correlation has been obtained in terms of N-values only. Indicated base bearing capacity equals roughly 9.2 and 9.6 times the respective N-values for 20-in. and 16-in. diameter piles respectively. A uniform value of 9 if adopted would give a conservative estimate for the entire depth region. Thus

$$q_u = 9 N \dots \text{psi.} \qquad \dots (7.6)$$

$$\text{or} \qquad q_u = 0.65 N \dots \text{tsf.} \qquad \dots (7.6a)$$

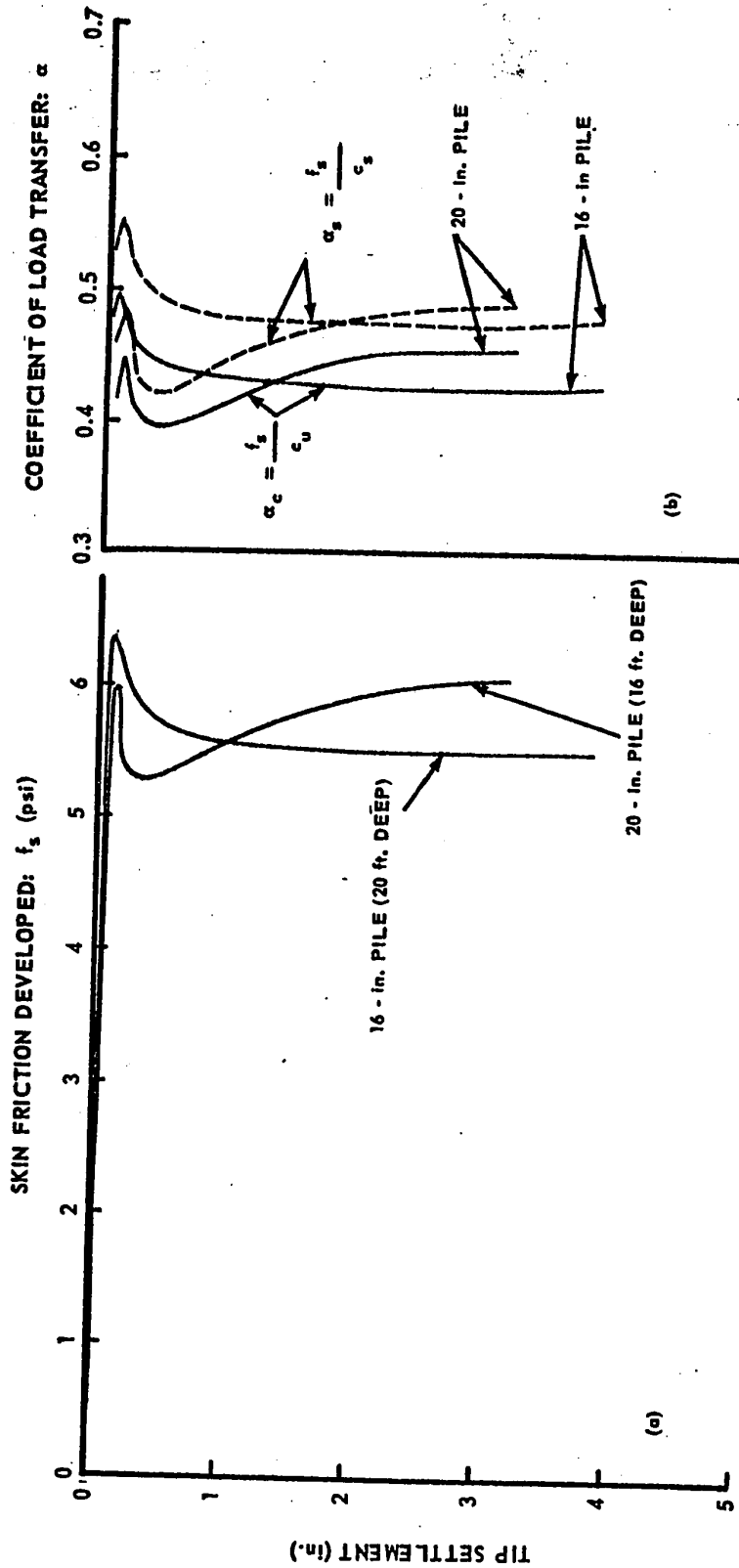
where N is obtained by averaging out the number of blows from various test holes at appropriate depths.

7.3 Analysis of Shaft Resistance for Piles in Clay

Values of Shaft Resistance, as described previously, have been obtained by subtracting Q_B from the corresponding Q -values. The plots after making necessary adjustments have been shown in FIGURES 7.3 and 7.4 for the two piles in clay. Maximum mobilization of skin friction, being about 50 to 60 per cent of the applied total load, occurs at a settlement ratio of nearly 0.6 per cent of the effective diameter of the pile. Shear failure in the soil along the shaft progresses slowly from top towards the tip of the pile as the load on pile-top increases. The effect of loading having produced ultimate shear failure of the shaft soil at the level of the tip manifests itself in the formation of a peak in the Q_s vs. settlement plot. Soil along the shaft at this instant is at various stages of failure offering maximum resistance corresponding to the peak of the stress-strain curve for soil close to the tip where relative movements are small and offering less resistance corresponding perhaps to the residual strength of soil near the surface where relative movements are large. This view draws sufficient indirect support from the shape of the curves representing the load carried by the pile section at various depths, as presented by SEED and REESE (1955), MOHAN et al. (1963), CAMBERFORT (1965) and TROW (1967). The slopes of the curves (representing coefficient of load-transfer), for the lower one-third length of the piles being larger than those for the upper two-thirds, indicates relatively large pick-up of load by the shaft soil close to the pile tip. With further penetration of pile, it appears, average value of residual shear strength might be effective. Mechanism of failure along the shaft, however, is not as simple as described above. It gets complicated by certain other factors which are simultaneously operating. Some comments in this connection have been offered in paragraph

7.10 of this chapter. The decision regarding the choice of suitable strength parameters for developing a correlation with field performance is, therefore, quite intriguing. Developed unit skin friction, f_s , computed from total Shaft Resistance Q_s , has been plotted against settlement of the tip in FIGURE 7.5(a). The difference in the absolute values of adhesion indicated by the two piles can be attributed to a number of cases, the most effective being their relative lengths of embedment. Shear strength of the soil at depths of 16 to 20 feet below surface is lower than the average shear strength in the upper 16 feet. In general, therefore, a lower average value should be expected for the 16-in. diameter 20 feet long pile. Actual behaviour as indicated by the plots is in agreement with this observation only for settlements beyond 1 inch. For the initial part, trend is just the opposite. A very important factor explaining this point is the sensitivity of Q_s values to the very drawing of the curves for total capacity Q and the base resistance Q_b . A slight change in the mode of joining various points for obtaining these plots is reflected very conspicuously in the difference plot, i.e., the plot for Q_s . One more factor which deserves mention in this connection is the use of arbitrary procedure based on relative values of shaft compression, for securing the Shaft Resistance values in the case of 20-in. diameter pile: the extrapolation, admittedly, is very large. In the light of the explanation offered above, the results obtained from the 16-inch diameter pile have been allowed to play a larger role in further analysis.

Plot for mean undisturbed shear strength (FIGURE 5.3) indicates unequal values at various depths. Assuming weighted average values of



EXPLANATION:

$\alpha_c = \frac{f_s}{c_u}$: COMPUTED FROM WEIGHTED AVERAGE OF MEAN
UNDRAINED OR UNCONFINED SHEAR STRENGTH.

$\alpha_s = \frac{f_s}{c_s}$: COMPUTED FROM WEIGHTED AVERAGE VALUE OF
UNDRAINED SOFTENED SHEAR STRENGTH.

FIGURE 7.5 DEVELOPED SKIN FRICTION AND COEFFICIENT OF LOAD TRANSFER PLOTTED AGAINST TIP SETTLEMENT (16 INCH, 20 INCH PILES IN CLAY).

the undisturbed, undrained shear strength c_u of 12.9 pounds per square inch for the 16-inch diameter pile and 13.4 pounds per square inch for the 20-inch diameter pile, curves for coefficient of load transfer α_c being the ratio of developed unit skin friction to the weighted average unit undrained shear strength have been plotted against tip settlement in FIGURE 7.5 (b). Obtained in a similar way, the plots for α_s being the ratio of the developed unit skin friction f_s to the undrained shear strength of the softened soil c_s have also been shown in the same figure. Peak value of α_c works out to be 0.495, the average for large settlements corresponding to maximum test loads on the piles, being 0.425 for 20-feet and 0.441 for 16-feet deep pile. Even the α_s values, shown by dotted lines in FIGURE 7.5 (b) are too low. The value of coefficient of load transfer computed on the basis of softened shear strength obtained from the laboratory test on the undisturbed samples soaked for four days or on the undisturbed samples removed after the conclusion of the load test from within one to two inches of the pile face, is thus far below unity. Development of a correlation on the basis of softened shear strength in this particular case is, therefore, not appropriate. It is quite evident from this discussion that some factor other than those considered above was responsible for lowering the value of α . Active in this case probably was the silt and sand content of soil which varied from 43 percent near the surface to about 90 percent at a depth of 30 feet (FIGURE 5.1). The process of drilling loosened the particles, remolded the soil considerably, destroying its original structure and making it lose a large part of its cohesion. Residual cohesion and the friction component of the silty sandy proportion was effective

thereafter. Considerable amount of caving observed during drilling would stand in testimony to this viewpoint. Low values of cohesion obtained from laboratory test results on remolded samples (TABLE V-1) would further support this explanation. Taking average of c_{ru} values from this table and assuming some contribution from the friction component, the value of α would work out to be close to unity. It therefore appears that the frictional capacity to the shaft is governed by the shear strength parameters for the remolded soil. Lack of adequate data on remolded soil, however, would not permit a satisfactory value of average cohesion or the active value of the friction angle at various depths to be worked out. No attempt has therefore been made to arrive at any correlation on this basis. Likewise, the same applied to the few residual strength values obtained at strains not too large. Analysis has therefore been made on the basis of undisturbed undrained or unconfined shear strength for which a large number of values are available. Due to heterogeneity of the soil, value of α would be expected to vary to a certain extent, but in the absence of additional information, a constant average of 0.43 applied to the weighted average value of undrained or unconfined shear strength \bar{c} of the undisturbed soil should give a fairly good approximation of unit skin friction. The following equation for unit skin friction can therefore be written:

$$f_s = 0.43 \bar{c} \quad \dots(7.7)$$

An approximate relationship for obtaining unit skin friction from penetration N-values, has also been attempted. N-values, as seen in FIGURE 5.3, vary with depth as does the shear strength. Weighted average for the entire depth of embedment has therefore been taken in this case too. Average values of skin friction in pounds per square inch work out to $0.244 \bar{N}$ for 16 feet long pile and $0.236 \bar{N}$ for 20 feet long pile. $0.24 \bar{N}$ would give a fair average. The relationship can therefore be written as:

$$f_s = 0.24 \bar{N} \dots \text{psi.} \dots (7.8)$$

$$\text{or} \quad f_s = \frac{\bar{N}}{58} \dots \text{tsf.} \dots (7.8a)$$

wherein f_s is the unit average skin friction developed along the shaft.

7.4 Analysis of Base Resistance and Shaft Capacity for 20-Inch Diameter Pile in Till

Reference here is made to the settlement plots shown in FIGURES 6.3, 6.6 and the test results given in APPENDIX L-3.

The curves have been replotted using dimensionless parameters in FIGURE 7.6. Adjustments have been made for the measured shaft compression and for the contribution of the concrete plug provided at bottom by making use of equation (6.1). Final curves corresponding to the settlement of the pile-tip have been shown by solid lines in the figure. Length of the plug in proportion to the embedded length of the pile being large, the resulting tip settlement curves have been bodily displaced to a considerable extent. Measured base resistance, as seen in the figure, is insignificant up to a settlement ratio of about 5 per cent. This is inconsistent with the

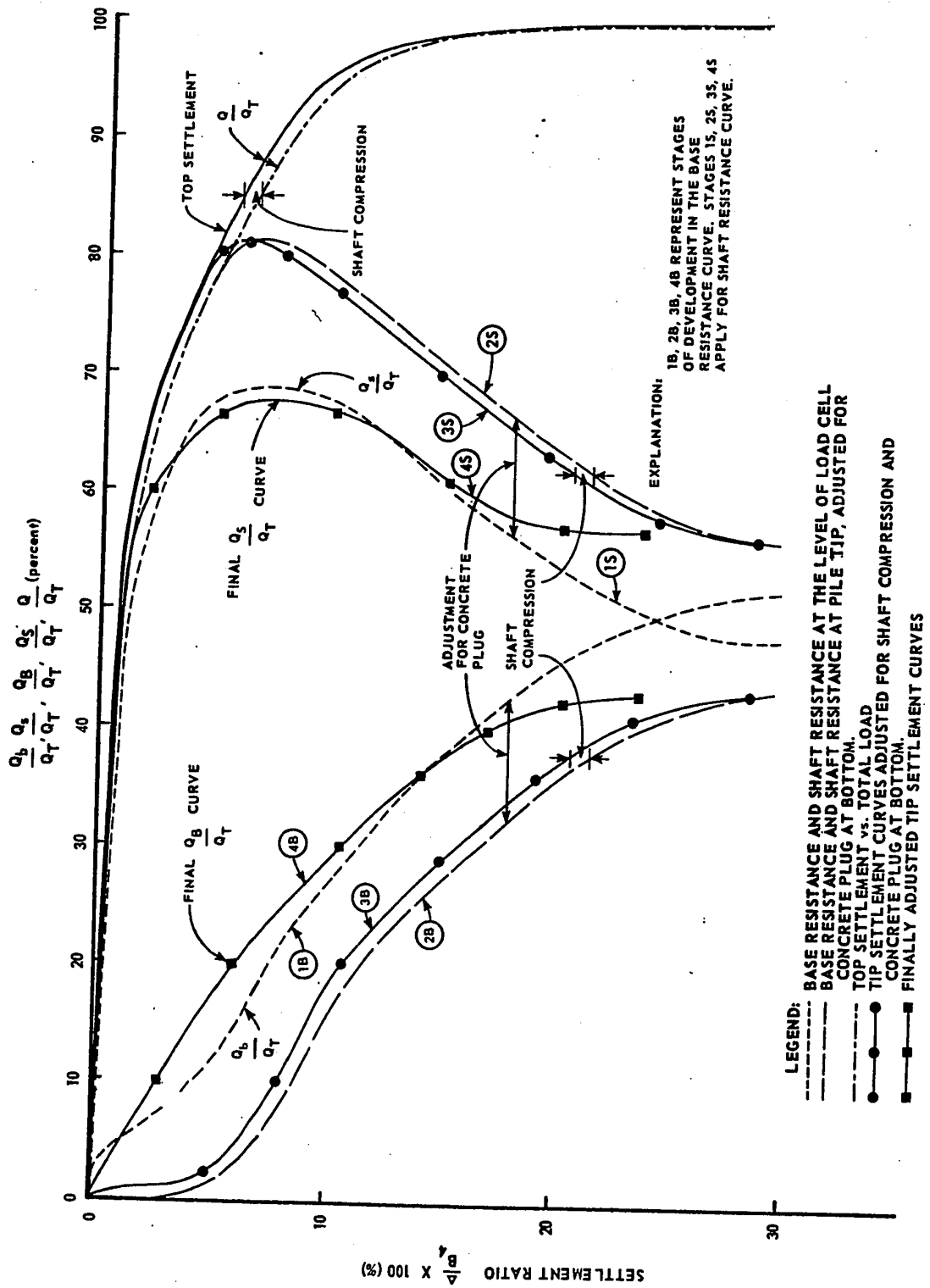


FIGURE: 7.6 LOAD vs. TIP-SETTLEMENT CURVES ADJUSTED FOR SHAFT COMPRESSION AND THE CONTRIBUTION OF CONCRETE PLUG BELOW LOAD CELL: 20 inch PILE (IV) IN TILL.

expected general performance of a short pile. A certain amount of caving in of the silty-sandy material from the upper strata at the time of lowering down of the cell is clearly indicated. The initial portion of the curve obviously corresponds to the behaviour of loose soil trapped between the bottom of the load cell and the top of the concrete plug. Ignoring the initial portion, the curve for base resistance has been re-drawn by shifting it bodily to the final position shown in the figure. Ultimate shear failure of the shaft soil (indicated by the peak in the plot for Q_s) took place corresponding to settlement ratio $\frac{\Delta}{B}$ of about 7.5 per cent. The difference in behaviour between piles in till and those in clay would be explained by the difference in the relative flexibilities of the pile material and the two soil types, being preconsolidated glacial till with a high unit weight in this case and a normal silty sandy clay deposit with relatively low unit weight in the former case. The shaft resistance falls off at a significant rate after attaining the peak and nearly levels off corresponding to a settlement of about 23.5 per cent of the effective base diameter. Base resistance on the other hand, builds up at a smaller rate and becomes constant beyond 23.5 per cent settlement. Analysis can now be made for the peak value of skin friction and the ultimate values (at large settlements) of both the base resistance and the shaft resistance indicated by the plots in FIGURE 7.6.

Ultimate unit Tip Resistance on the basis of value indicated in FIGURE 7.6 works out to 620 pounds per square inch of the bearing area of the pile. This depends to a very large extent on the characteristics of the soil immediately below the tip. Composition of soil at 38 feet depth, as seen in FIGURE 5.1, is: clay 24 per cent, silt 33 per cent and sand 43

per cent. Plasticity Index is very low and the degree of saturation is over 90 per cent. Available laboratory strength tests are too few to give a highly dependable average. The trend indicated by the undisturbed shear strength plot (FIGURE 5.3c) is, however, established by the N-value plot shown alongside. Under the loaded tip, it is extremely difficult to ascertain the actual drainage conditions. The one major difference between this dense glacial deposit (unit weight: about 140 pounds per cubic foot) and the overlying normal lake deposit (unit weight: about 118 pounds per cubic foot) is that in the present case silt and sand are also present in the form of frequent pockets. This would impart slightly better drainage characteristics to the soil. Laboratory values of the angle of shearing resistance obtained from undrained tests on remolded recompacted samples, though few, are not too low. Assuming the actual drainage conditions in the field to be somewhere between complete drainage and no drainage, the actual angle of shearing resistance would be higher than that indicated by the undrained tests. Development of any relationship on this basis, however, cannot be attempted since the shear strength parameters of intact soil are not available. Loss of cohesion on remolding is too drastic to be of any value. Average shear strength from unconfined compression tests is, however, available (FIGURE 5.3). A mean undisturbed shear strength of 45.5 pounds per square inch is indicated. Combined Bearing Capacity Factor thus works out to 13.6. And since it manifests in itself the contribution of both the cohesion and friction components, it may be represented by the dimensionless factor $N_{c\phi}$. Assuming Meyerhof's Theory to be applicable, the above-mentioned value of the bearing capacity factor would work out by using an angle of shearing resistance equal to

4.5 degrees. This, however, does not compare favourably with the laboratory value obtained from a few recompact samples. N_c value being very sensitive to ϕ -value, it is but necessary to average it on the basis of a large number of laboratory tests. Having obtained satisfactory value of shear strength parameters, the ultimate bearing capacity can be computed by making use of Meyerhof's Theory. The simplified relationship in this particular case, however, can be represented by the equation:

$$q_u = 13.6 c \quad \dots (7.9)$$

where c is the mean value of shear strength of the soil below the tip, obtained from unconfined compressive strength tests on undisturbed samples. Correlation with penetration N-values (FIGURE 5.3) gives the following equations:

$$q_u = 5 N \dots \text{psi.} \quad \dots (7.10)$$

$$\text{or} \quad q_u = 0.36 N \dots \text{tsf.} \quad \dots (7.10a)$$

Coming now to the computation of Shaft Resistance, the peak value of 68 per cent indicated in FIGURE 7.6 by Q_s curve represents an average skin friction of 39.2 pounds per square inch of the shaft area in contact with the soil. Weighted average value of shear strength obtained for the corresponding depth from the plot in FIGURE 5.3(c) works out to be 43.8 psi. In effect, as shall be observed from the extension of the upper bound curve towards right showing some values even beyond 80 psi., the actual average value of shear strength would be a lot higher than the indicated value of 43.8 psi. obtained from mean plot

drawn on the low side, in particular, in this high-strength region from 25 feet to about 40 feet below surface. Developed adhesion assuming shear strength value of 43.8 psi., works out to be about 89 per cent of the average shear strength along the pile face, i.e., the value of coefficient of peak adhesion α_{peak} is 0.89. This is in sharp contrast to the behaviour of piles in silty-sandy clay deposit wherein the normally laid soil particles first got remolded by drilling and then got softened after absorbing water from fresh concrete, thereby losing the natural cohesion to a large extent. Large scale laboratory and field testing of till in this region might place the mean shear strength at a value above 43.8 psi., in which case the value of α would drop down. Shaft friction appears to have settled down at tip settlement corresponding to about 23.5 per cent of base diameter (FIGURE 7.6). Adhesion indicated is 33.4 psi. giving α -value of 0.76. This appears to correspond closely to the only value of 35.6 psi. (APPENDIX K) being the residual strength of till obtained at not too large a strain. A more definite statement in this respect, however, cannot be made without large-scale testing of undisturbed samples carried to large strains in a shear box. For the time being, therefore, the shaft capacity shall be expressed as a function of average undrained shear strength \bar{c} in the following form:

$$f_s = 0.76 \bar{c} \quad \dots (7.11)$$

Using penetration N-values obtained from FIGURE 5.3, the following equation can be written:

$$f_s = 0.42 \bar{N} \dots \text{psi.} \dots (7.12)$$

$$\text{or } f_s = \frac{\bar{N}}{33} \dots \text{tsf.} \dots (7.12a)$$

where f_s is the ultimate unit skin friction and \bar{N} is the weighted average of N-values for the depth of embedment of the pile.

7.5 Analysis of Base Resistance and Shaft Capacity for 28-Inch Diameter Pile in Till

Based on the settlement curves shown in FIGURES 6.4 and 6.7, plots for the settlement of the tip adjusted for shaft compression and the contribution of the concrete plug at bottom have been redrawn in FIGURE 7.7 using dimensionless parameters. Summary of the corresponding test data appears in APPENDIX L-4.

The rate of build-up of shaft resistance is higher than that of tip resistance as in the case of other piles and the fall thereafter has been abrupt. Capacity of anchor piles supporting the loading beam having been reached, complete ultimate failure of this pile could not be achieved. Base and Shaft Resistance indicated by the appropriate curves in the figure, however, do appear to have nearly settled down to ultimate average values corresponding to a settlement ratio of about 7.7 per cent of base diameter. The shape of the shaft resistance curves clearly reflects the type of the strata through which the pile passes. For the upper half of the embedded length of the pile, soil is extremely stiff, plasticity index low, modulus of deformation very high, settlement of the pile very small and the Q_B versus settlement curve shows a quick, steep rise. For the lower half,

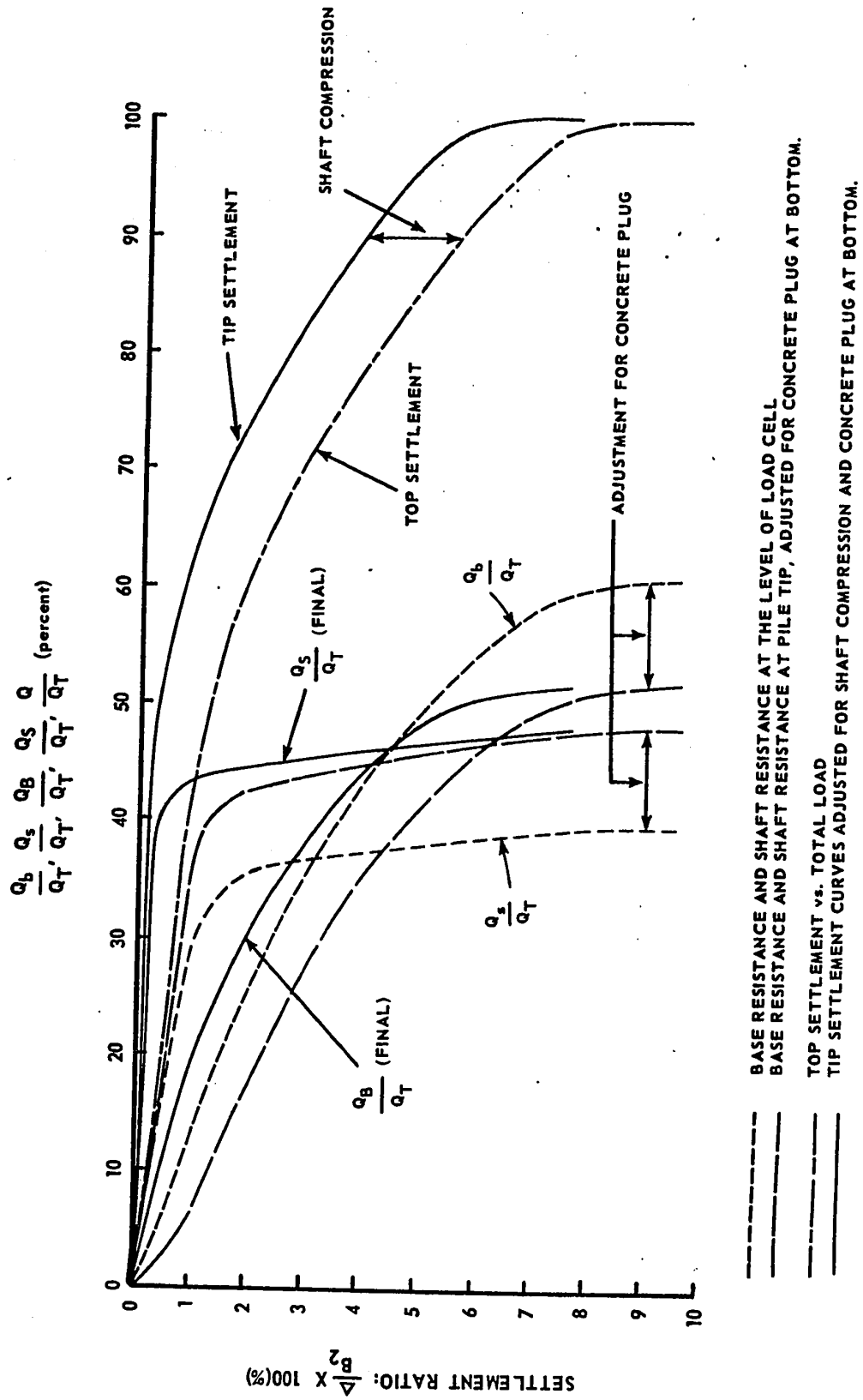


FIGURE 7.7 LOAD vs. TIP-SETTLEMENT CURVES ADJUSTED FOR SHAFT COMPRESSION AND THE CONTRIBUTION OF CONCRETE PLUG BELOW CELL: 28 INCH PILE (II) IN TILL.

however, conditions are exactly opposite and the curve flattens out showing a very small additional build-up for relatively large settlement. The pile tip, as shall be observed from the soil profile, rests on a layer constituting fine sand and some silt and clay below which some free water is also encountered. The drainage under the base can therefore be assumed as good and the tip bearing capacity can be computed accordingly. The soil at various depths is so heterogeneous in character that matching comparisons from existing information cannot be easily drawn. A couple of appropriate references bringing out the extent of variation in the behaviour of piles in till and the effect of pile length on the shape of the Shaft Resistance curve are, however, quoted here in this connection. PARSONS (1966) commenting on the variability of load-test results on two piles of equal diameter and approximately the same length with their tips embedded in glacial till at a certain test site reports an ultimate load of 110 tons corresponding to a gross settlement of 0.9 in. on one pile and a load of 150 tons corresponding to a settlement of only 0.7 in. on the other. Even when a soil can be assumed homogeneous, the variation introduced by different embedded lengths both in the shapes of the curves for shaft and base resistances as also in their ultimate magnitudes is tremendous. As the length increases, the curves flatten out and the peaks occur at larger settlements (MOHAN et al., 1963; COYLE and REESE, 1966; VESIC, 1967). Load-transfer in the case of short stiff piles is therefore relatively large.

Taking into consideration the observed characteristics of local till combined with the effect of difference in embedded length, the mobilization of base resistance and the shaft resistance for the two piles in till is quite commensurate with the environment.

Ultimate values of unit tip resistance and unit average shaft capacity computed on the basis of values indicated by the respective plots in FIGURE 7.7, work out to 907 psi. and 23.2 psi. respectively. Assuming cohesion to be small, an angle of shearing resistance of 20 degrees approximately is represented by the developed base bearing capacity. In the absence of adequate laboratory test information, both the base resistance and the shaft resistance can be expressed, as before, on the basis of unconfined compressive strength as also the penetration N-values obtained from FIGURE 5.3, by the following equations:

$$q_u = 25.5 c \quad \dots (7.13)$$

$$q_u = 8.4 N \dots \dots \text{psi.} \quad \dots (7.14)$$

$$\text{or} \quad q_u = 0.6 N \dots \dots \text{tsf.} \quad \dots (7.14a)$$

$$f_s = 0.55 \bar{c} \quad \dots (7.15)$$

$$f_s = 0.25 \bar{N} \dots \dots \text{psi.} \quad \dots (7.16)$$

$$\text{or} \quad f_s = \frac{\bar{N}}{55} \dots \dots \text{tsf.} \quad \dots (7.16a)$$

wherein the symbols q_u , c , \bar{c} , f_s , N , \bar{N} have the same meaning as given before in this chapter.

7.6 Further Comments on the Evaluation of Bearing Capacity of Piles in Till

It is possible to compute the base resistance of two piles from the measured values of shaft compression as in the case of piles in clay. This, however, has not been done since the major contribution to shaft

compression here is made by the free-standing length of the piles (about 27 feet) and the extrapolation based on the shortening of the relatively small embedded length would be too wild. Indirect verification has, however, been made by comparing the plots for measured shaft compression vs. total load, using known values of base resistance and the modulus of elasticity of the composite section. The curves obtained (not shown) are practically coincident, implying thereby that the base resistance can be computed from the measured shaft compression values provided the modulus of elasticity of composite section (concrete with steel used as reinforcement) is correctly known.

While developing the correlation between penetration N-values and base or shaft resistance, the depth variable has not been included since it is presumed that the effect of the overburden pressure is indirectly reflected in the N-value itself and since the penetration values, due to varying characteristics of the soil, do not indicate a consistent pattern (FIGURE 5.3) within the test depth.

Unit skin friction in tons per square foot for the two piles in silty-sandy clay, as indicated by equation (7.8a), is $\bar{N}/58$ and that for 28-in. pile in till (equation 7.16a) is $\bar{N}/55$. These values are comparable to those given by MEYERHOF (1956) and WOODWARD et al. (1961) for sands. A higher value equal to $\bar{N}/33$ (equation 7.12a) results in the case of short pile embedded entirely in very hard and stiff till. Absolute values of unit skin friction developed for short and long piles in till would work out to 4800 psf. and 3340 psf., the former representing the exceptionally stiff soil. MATICH (1967) gives an ultimate skin friction value of 3200 psf. obtained from load tests elsewhere in till possessing similar characteristics.

7.7 Some Remarks on the Residual Tip Resistance and Shaft Compression on the Removal of Load from Pile Top

After each loading cycle, the load at top is reduced to zero but some compression in the shaft is retained. The locked-in compression is a function of the mobilized skin friction acting downwards which exactly balances the residual tip resistance acting upwards. There appears to be existing some consistent relationship between the residual tip resistance or the equivalent balancing total skin friction (reflected by the residual shaft compression) and the maximum base resistance developed before the removal of any load. The pattern of the above-mentioned relationship changes relatively abruptly as the failure load is approached. The computed values being too few to define it clearly, attempts at making a quantitative evaluation have been abandoned.

7.8 Effect of Repeated Cycles of Loading and Unloading

As would be observed in FIGURES 6.3 and 6.4, the top settlement under any repeated load is approximately the same as the ultimate settlement under the previous increment for all loads up to failure load. Additional settlement caused by repetitions for loads beyond the failure load is noticeable, but does not appear to be very significant.

Effect of repetitions on the mobilization of base resistance and hence also the shaft resistance is also not appreciable. Difference in the measured values at a particular load under various cycles of loading, as seen from the actual readings (APPENDIX L-3) is quite insignificant.

From the data obtained in the present series of tests, it can therefore be concluded that the method of testing a pile by cyclic loading

neither produces any appreciable amount of additional settlement nor changes the proportions of base and shaft capacities, at least up to the failure load. And further, since it yields additional useful data and helps in the evaluation of net settlement in a better way, it may be worth while employing this procedure for any load test. Slight additional settlement, if any, obtained as a result of repeated loading, would only add to the available factor of safety.

7.9 Settlement Considerations

As pointed out in Chapter II, it is extremely difficult to ascertain settlement under a loaded pile. Apart from the physical characteristics of the soil below tip, it depends on the proportion of load transmitted immediately on loading as also on the gradual transfer of a part of shaft load to base with the passage of time. Extent of variability in the profile and the drainage conditions too play an important role in determining immediate as well as long-time consolidation settlement. Methods of computation outlined in Chapter II are very approximate and are suitable only when certain special conditions are met. 24-hour settlement curves drawn for various field piles in Chapter VI represent a condition somewhere in between the immediate and ultimate long-time settlements that the piles would experience. Equation (2.7) for immediate settlement would thus indicate settlement values less than those indicated by load-settlement plots. Consolidation settlement on the other hand, obtained by using the oedometer test results, would be higher. The soil behaves like a $c-\phi$ material and the condition " $\phi = 0$ " does not operate in any case. Evaluation of immediate settlement from the general equation (2.7) is complicated by the

choice of a suitable value for μ and the inadequacy of strain-data for undisturbed soil specimens of the silty sandy depth regions below the pile tips, needed for the computation of plane strain modulus of deformation $E/(1 - \mu^2)$.

In view of the facts stated above, it has been considered appropriate to make use of the actual field performance data for developing a suitable correlation so as to give a rough idea of the nature of settlements expected to take place under the service piles. Terzaghi's settlement formula (TERZAGHI, 1943) in the following form has been employed:

$$\frac{\Delta}{H_c} = C \cdot \log_e \frac{p_o + \sigma_z}{p_o} \quad \dots (7.17)$$

wherein Δ is the 24-hour settlement under any base load Q_B (obtained from FIGURES 7.3, 7.4, 7.6, or 7.7), σ_z the corresponding induced vertical stress at the centre of the compressible zone of depth H_c computed from the Q_B -values by using BOUSSINESQ's equation, p_o the initial effective overburden pressure and C the constant related to the compressibility of soil. It is difficult to establish the depth H_c of the compressible layer, since according to OHDE (1951) and MEYERHOF (1959), the centre of the zone of compression lies a little above the pile tip. It has been tentatively located at a height of 1 m. above tip by OHDE and can be worked out approximately from the zones of compression around the tip and the shaft drawn by MEYERHOF. In the present case, however, it has been assumed that the stresses under the loaded tip are effective up to a depth equal to twice the diameter of the tip. The above relationship can thus be re-written as:

$$\frac{\Delta}{2B} = C \cdot \log_e \left(\frac{p_o + \sigma_z}{p_o} \right) \quad \dots (7.18)$$

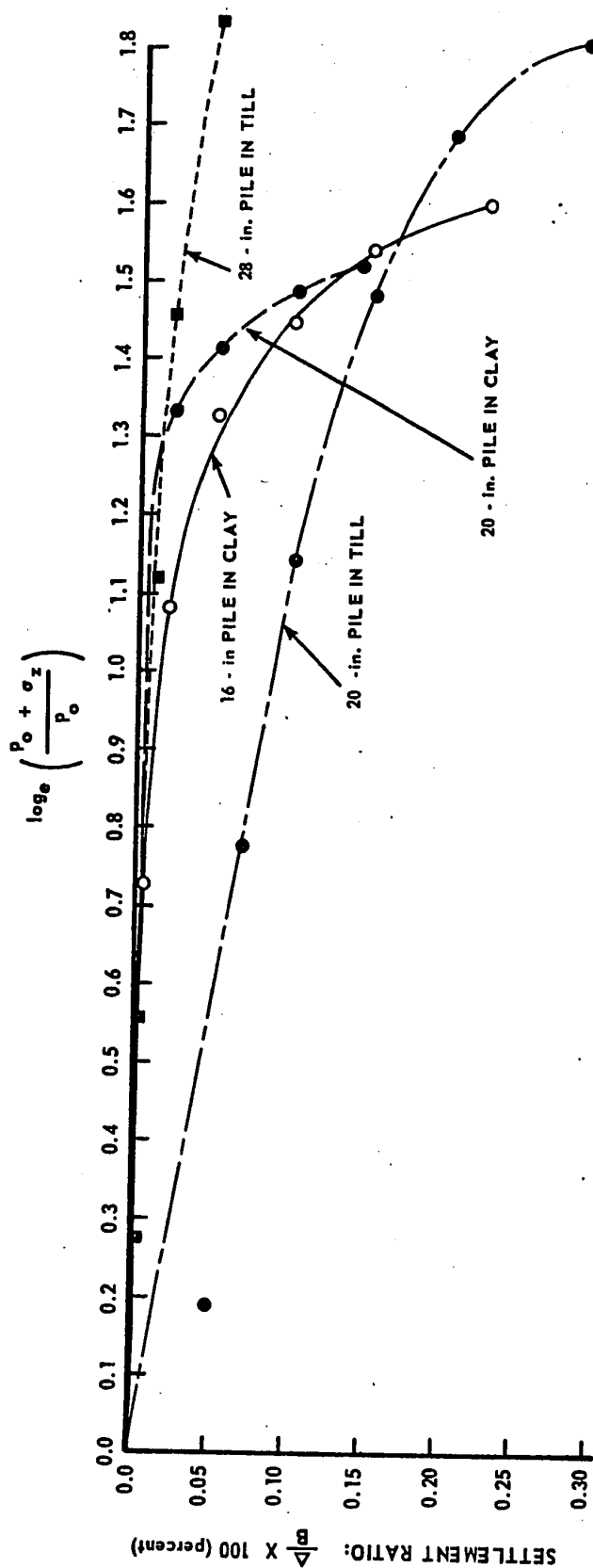
$$\text{or} \quad \frac{\Delta}{B} = 2C \cdot \log_e \left(\frac{p_o + \sigma_z}{p_o} \right) \quad \dots (7.18a)$$

$$\text{or} \quad \frac{\Delta}{B} = C_1 \cdot \log_e \left(\frac{p_o + \sigma_z}{p_o} \right) \quad \dots (7.18b)$$

$$\text{where} \quad C_1 = 2C \quad \dots (7.19)$$

If the relationship is linear, C_1 shall represent the slope of the plot between Δ/B and $\log_e [(p_o + \sigma_z)/p_o]$. The plots between these two quantities for all the four piles have been shown in FIGURE 7.8. They are approximately linear in the beginning but start drooping down showing excessive settlement for loads roughly in excess of the failure loads determined in Chapter VII. Magnitude of settlement after the sliding zones develop cannot perhaps be calculated by any known method. The correlation developed here is therefore related only to the initial straight line portions of the plots.

For the two piles in clay average C_1 -values of 1/150 and 1/180 for 16-in. and 20-in. diameter piles respectively are indicated. Computations if made on this basis, shall yield values of settlement slightly on the conservative side. It would be appropriate to rewrite the values of slope C_1 in terms of known values of field characteristics of soil, namely, the overburden pressure p_o at a depth equal to B below the tip and the average penetration N -value. Effective overburden pressure being 17.4 and 14.3 psi. in the two cases and the respective N -values from FIGURE 5.3 being 27 and 24, the values of C_1 work out to $\left(\frac{1}{193} \cdot \frac{N}{p_o} \right)$ for



EXPLANATION:

- A = SETTLEMENT OF TIP
- B = EFFECTIVE PILE DIAMETER
- p_o = EFFECTIVE OVER-BURDEN PRESSURE
- σ_z = VERTICAL STRESS INDUCED AT THE CENTRE OF THE LAYER (ASSUMED THICKNESS = 2B) BY LOAD CARRIED BY PILE TIP; COMPUTATIONS BY BOUSSINESQ'S EQUATION

FIGURE: 7.8 PLOTS FOR EVALUATING CONSTANT OF COMPRESSIBILITY OF SOIL.

16-in. diameter pile and $(\frac{1}{214} \cdot \frac{N}{p_o})$ for 20-in. diameter pile. An approximate value of $C_1 = \frac{1}{200} \cdot \frac{N}{p_o}$ would be suitable for application to both the piles. From equation (7.19), the value of C would then be $(\frac{1}{400} \cdot \frac{N}{p_o})$. The following equation for settlement can then be finally written:

$$\Delta = C \cdot H_c \cdot \log_e \left(\frac{p_o + \sigma_z}{p_o} \right) \quad \dots (7.17)$$

$$\text{where } C = \frac{1}{400} \cdot \frac{N}{p_o} \quad \dots \text{for piles in clay} \quad \dots (7.20)$$

Here both Δ and H_c are measured in inches. C is the constant of compressibility, the value of which is not dimensionally satisfied (p_o being taken in psi.). Proceeding in a similar way for the 28-in. pile in till which is considered to be more representative in behaviour than the other pile, the value of compressibility constant C for till works out to $(\frac{1}{300} \cdot \frac{N}{p_o})$, i.e.,

$$C = \frac{1}{300} \cdot \frac{N}{p_o} \quad \dots \text{for piles in till} \quad \dots (7.21)$$

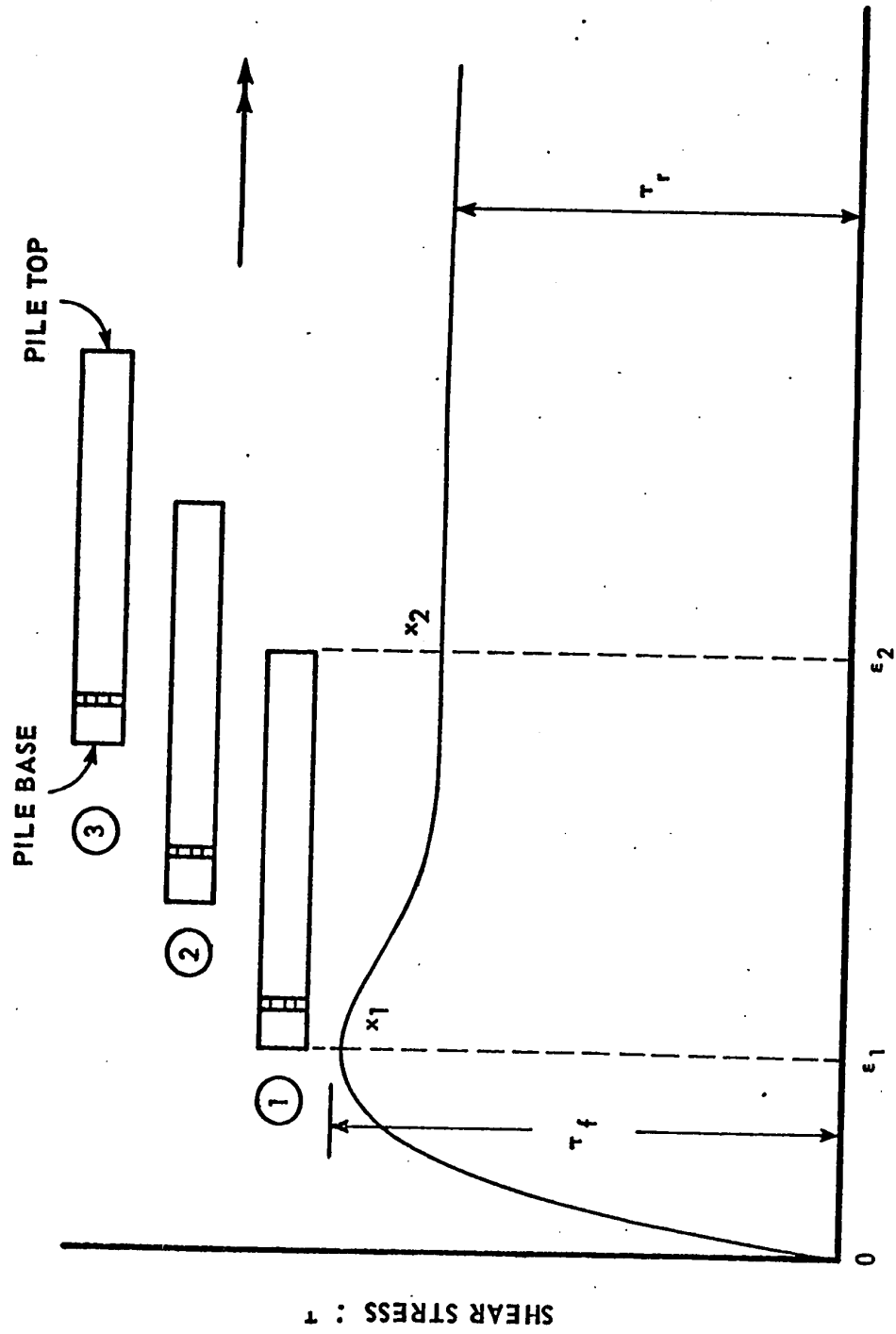
where p_o is measured in pounds per square inch.

The computation of σ_z for use in the above equations is required to be made from the values of base resistance developed under the pile tip and shall have to be approximately determined by subtracting the shaft resistance (computed on the basis of correlations developed earlier in this chapter) from the total load supposed to be applied at pile top. Due to a large number of assumptions involved, the computations on this basis shall give nothing more than a very crude approximation of settlement.

7.10 Relation of Load-Transfer to Soil Shear Strength and Mechanism of Pile Failure

The subject of load-transfer and mechanism of pile failure has been discussed in detail by D'APPOLONIA (1963) and COYLE and REESE (1966). A few comments made here as a consequence of analysis made in the foregoing paragraphs, pertain in particular to the behaviour of piles in local soil.

As the loads applied at top increase, failure of shaft soil in shear progresses gradually towards the tip of the pile, following the development of maximum shear strains. Complete failure along the shaft occurs when finally the soil near the base is strained beyond a certain stage and tip of the pile starts punching into the strata below. This stage is indicated by a steep rise in the base-resistance curve as reflected by the peak in the shaft resistance curve. Soil from top to bottom is then at various stages of shear failure. Referring to the stress-strain curve for the soil (FIGURE 7.9), the above-mentioned situation is represented by Stage 1 of the pile for which the resistance developed at tip has been shown to correspond to the strain ϵ_1 at peak value of shear strength τ_f . Imagining the pile to be moving from left to right relative to the strength plot with its centre line parallel to the strain-axis, the soil along shaft near the top must have been subjected to a strain equal to ϵ_2 having earlier passed through the peak value when the tip was somewhere to the left of the origin and had yet not experienced any strain. Stage 1 thus represents the beginning of the mobilization of base resistance at a high rate and the simultaneous development of peak in the shaft resistance curve. The skin friction offered at various points along the pile then varies in proportion to the shear strength represented by the plot between x_1 and x_2 .



STRAIN : ϵ

FIGURE 7.9 TYPICAL STRESS vs. STRAIN CURVE FOR AN UNDISTURBED SOIL SPECIMEN WITH SUPER IMPOSED PILE LENGTH AT VARIOUS STAGES OF FAILURE.

As the imagined movement of the pile continues towards right through Stages 2 and 3, which would correspond to applied loads at top being in excess of the failure load, the entire length of the pile would be ultimately thrown into the region of the plot representing residual shear strength τ_r . Resistance offered at each point along the shaft being the same, the settlement curve for total skin friction Q_s would tend to become parallel to the settlement-axis. The mobilization of skin resistance at various depths along the shaft is thus a function of the relative deformation of the pile with respect to the surrounding soil.

The development of the straight-line portion of load-settlement curves mentioned above is affected possibly by a number of factors giving rise to a slight upward trend to these curves at large settlements, as observed in some of the plots in the present case. At least one of these factors in the development of high pressures approaching passive pressures exerted by MEYERHOF's sliding surface impinging against the lower part of the shaft with increased penetration of the pile.

Referring again to FIGURE 7.9, it may be restated that the residual value of shear resistance shall be active at very large strains and would be applicable only for analysing the data from a field test where observations are made for loads beyond the failure load making the pile settle rapidly. In the case of service piles where allowable settlements are limited to small values, it is only the initial part of the stress-strain curves that would be really active. Further, the stress-strain curve shown in FIGURE 7.9

pertains to a typical undisturbed sample. The actual behaviour of the shaft soil may be quite different since it would depend upon the composition of soil, the degree of disturbance during drilling, the amount of excess water available from fresh concrete and the period elapsed between concreting the hole and test-loading the pile.

Taking for example the case of the two piles in silty clay, the soil on being disturbed at the time of drilling of holes got remolded and lost a major portion of its cohesion. The shaft resistance could better be related to the remolded than to the residual shear strength. Conditions were different for piles in stiff till. A high degree of adhesion was developed since there was apparently no loosening of particles. Actual degree of softening of the soil around the shaft can perhaps never be ascertained correctly at least for the type of soil encountered in the present case. Developing a correlation on the basis of four-day soaking of samples would therefore be a futile experiment. The best method of estimating the shaft resistance, in the opinion of the author, is to evaluate the undisturbed shear strength carefully from a very large number of samples and apply a reduction coefficient such as α to be established for field tests. Alternately, the correlation may be developed on the basis of measured cone resistance or penetration N-values.

CHAPTER VIII

SUMMARY STATEMENT OF THE FINDINGS

8.1 General

This chapter includes a summary of important results of laboratory tests on soil specimens, field test data and analysis, detailed discussion about which has been given in the three foregoing chapters, namely, Chapters V, VI and VII.

8.2 Strength and General Characteristics of Soil

The soil encountered was quite heterogeneous in character throughout the entire depth of exploration. Profiles shown in FIGURES 4.5 and 5.3 do not include details of varves of silt or thin layers of sand encountered off and on. The results of laboratory tests summarized below are therefore required to be viewed in the background of the aforesaid information.

1. The results of classification tests were presented in the form of plots in FIGURES 5.1 and 5.2. Composition and other physical characteristics of soil at various depths below surface indicated considerable amount of variation. Percentage of fine sand and silt (M.I.T. scale) vary within the limits of 45 percent near the surface and about 92 percent at a depth of 27.5 feet, the rest being the clay fraction. The soil is highly plastic in the upper fifteen feet, nearly non-plastic within the next 25 feet and possesses low to medium plasticity characteristics below 40 feet depth. Average value of moisture content within

the lake deposit is of the order of 30 to 35 percent and that within till is nearly uniform at 14 percent. Degree of saturation decreases from an average of 97 percent in the upper clay deposit to an average of 80 percent in the silty-sandy region. Saturation of 90 percent is maintained below 36 feet depth.

2. Both the lake deposits as well as the till deposits are over-consolidated, the former by dessication and the latter by the weight of the receding glacier. Preconsolidation pressures of the order of 1 to 2 tsf. are indicated by the samples removed from the upper layers and from 7 to 12 tsf. by those from till deposit. Laboratory oedometer tests show the lake deposits to be of a medium compressibility and till of relatively low compressibility.

3. Results of strength test have been plotted in FIGURES 5.3 and 5.4, and mean lines indicating average undisturbed undrained shear strength, softened shear strength and ultimate shear strength (used in preference to residual shear strength) at strains not too large have been drawn. Undrained shear strength gradually drops from a value of 20 psi at surface to 11 psi at a depth of 15 feet. High values up to 49 psi are indicated within the sandy silty and gravelly region between 20 and 35 feet below surface. Indicated average strength is of the order of 35 psi. for soil below this depth.

8.3 Summary of Pile Loading Test Results

Load-settlement plots have been shown in FIGURES 6.1, 6.2, 6.3, and 6.4 of Chapter VI. Increments of load applied at various stages for testing piles in till could not be maintained for the same duration of time, which in general was 24 hours or more. Settlements, it was recorded, were increasing even after 24 hours of sustained loading. Three sets of curves have been drawn in each case, that is, those representing immediate settlement, 24-hour settlement and the maximum recorded long-time settlement. Failure-loads have been arrived at on the basis of 24-hour settlement curves corresponding to the point of intersection of tangents drawn to the initial and final parts of these curves. These results together with the recorded rebound on the complete removal of load from the pile top have been summarized in TABLE VIII-1.

2. Modes of mobilization of Base Resistance Q_B and Shaft Resistance Q_S , obtained by subtracting the ordinates of Q_B from those of corresponding total load Q , vary depending upon the embedded length of the pile and the characteristics of the soil. Shaft Resistance curve indicates a pronounced peak for piles in clay and sustained peak for piles in till. Long piles tend to further flatten the development of peaks showing maximum values at different absolute settlements but nearly the same settlement ratios Δ/B as reported in the next paragraph. The rate of build-up of tip resistance is slow for small settlements but increases after the settlement corresponds to the peak in the Q_S curve.

3. Both the magnitude of Residual Tip Resistance and the elastic recovery of pile after removal of load from pile top appear to be related to the ultimate settlement of the pile tip. When complete shear failure of

TABLE VIII-1
SUMMARY OF PILE LOADING TEST RESULTS (FULL-LENGTH PILES)

Pile designation	Nominal Diameter and Description	Method of Testing	Maximum Applied Test Load (kips)	Yield Point Load corresponding to 24-hour Settlement (kips)	Top Settlement (in.)			Rebound as proportion of 24-hour settlement at maximum test load (per cent)	Remarks
					Immediate	24-hour	Maximum Recorded		
I	16-inch in clay	main-tained load test	120	93	0.03	0.23	-	10.7	On reloading, the gross settlement at top increased from 0.23 in. to a little over 0.6 in. at failure load.
II	20-inch in clay	main-tained load test	130	100	0.08	0.16	-	6.5	On reloading, the gross settlement at top increased from 0.16 in. to 0.19 in.
III	20-inch in till	cyclic loading procedure	550	352	0.38	0.46	0.48	5.5	
IV	28-inch in till	cyclic loading procedure	1200	750	0.54	0.63	0.65	28.0	Complete failure of pile not achieved--maximum recorded settlement at top being 2.78 inches.

shaft soil has taken place and the tip has started punching into the strata below, the magnitude may be relatively small compared to that when the extent of punching is small or nil.

4. For all sustained loads up to the failure load, settlement increases at a fast rate for the first two to three hours and then slowly levels off, showing no appreciable increase after about 8 hours. The rate of settlement increase goes on mounting with each new increment of load added to the applied load till the total load approaches the yield point. The pile at that stage starts sinking rapidly. In general, the rate of settlement-increase as a function of time is greater for piles in till than for piles in clay.

5. Settlement recovery as measured at pile top depends upon such factors as the number of loading and reloading cycles applied up to maximum test load, compressibility characteristics of soil and modulus of elasticity of the material of the pile in addition to the one already mentioned in sub-paragraph 3 above.

6. Rapid sinking of the pile at any stage of loading and the appearance of a pronounced peak are perhaps indicative of total shear failure having taken place in the soil surrounding the shaft.

7. A major portion of rebound is relatively instantaneous. Recovery with passage of time is small.

8. Effect of sustained loads on the mobilization of base resistance appears to be slightly different for piles in clay and till. Particles of till get adjusted quickly to the stress change as a result of addition of a new increment of load at pile top. No peak is therefore observed in the plots between Q_B and time. For piles in clay, a temporary reversible

straining of particles takes place under similar circumstances. Plots indicate a rapid build-up of base resistance to a peak immediately after the application of a new load increment. There is then a fall to a certain extent and relatively slow increase thereafter. All these changes take place in less than an hour when total applied load is less than the failure load. Q_B values finally level off about 2 hours after the application of any increment. At loads close to the failure load, the behaviour is similar for all piles when settlement goes on increasing with the passage of time.

8.4 Results of Analyses

Base Resistance values for the 20-inch pile in clay, owing to the malfunctioning of the load-cell, were not directly available. Approximate computations made from measured values of shaft compression on the assumption that behaviour of the two piles in clay is similar and that the value of E for concrete remains unchanged, give satisfactory values for further analysis, the error introduced in this case being of the order of ± 10 percent. The plot (FIGURE 7.1b) drawn in this connection is however not unique. Extrapolation to other sites would involve the conditions in regard to the assumptions being satisfactorily met.

2. Final tip settlement curves for Base Resistance and Shaft Resistance after necessary adjustments for shaft compression and the contribution of the concrete plug drawn by using dimensionless parameters indicate the maximum mobilization of skin resistance corresponding to a settlement ratio Δ/B of about 0.6 per cent for piles in clay (FIGURES 7.3 and 7.4) and about 7.5 per cent for piles in till, indicating a tremendous difference between the behaviour of piles in the two materials. The difference is explained on

the basis of relative flexibilities of the pile material and the two soil types, being the preconsolidated glacial till with a high unit weight in the latter case and a normal silty-sandy clay deposit with relatively low unit weight in the former case.

3. Soil under the pile tips behaves like a true $c - \phi$ material and the contribution of friction component to the ultimate bearing capacity is very significant. Soil being nearly saturated and clay being rich in montmorillonite, drainage under pile tips in clay has been assumed to be insignificant. For till, however, due to the presence of numerous pockets of sand and silt, the actual drainage would perhaps be better. The angle of shearing resistance in that case is somewhere in between the conditions of complete drainage and no drainage. Values of ultimate bearing capacity computed on the basis of Meyerhof's theory agree favourably with the measured values using angles of undrained shearing resistance as obtained from laboratory tests on undisturbed clay samples. Terzaghi's theory on the other hand gives very conservative values. The same, however, could not be verified completely for piles in till due to lack of laboratory information.

4. Peak value of developed skin friction for piles in clay is of the order of 6.4 psi. The ultimate value at large settlements ranges from about 5.5 to 6.0 psi. against weighted average soil shear strength of 12.9 to 13.4 psi. For piles in till mobilized ultimate skin friction values of 33.4 psi. and 23.2 are indicated, the higher values being applicable to the short pile. Weighted average undisturbed shear strength of soil in the two cases is 43.8 and 42.3 psi. respectively. The influence of the depth of embedment on the developed skin friction was found to be quite significant.

5. Both the magnitude of developed skin friction at peak and the corresponding settlement are sensitive to the very plotting of curves for total capacity Q and base resistance Q_B . A slight change in the mode of joining various points for obtaining these plots is reflected conspicuously in the difference plot, i.e., the curve for Q_S .

6. Total Ultimate Skin Resistance for all piles is of the order of 48 to 57 per cent of the maximum applied load causing rapid settlement. As a rough approximation the load at top at that stage may be assumed to be shared equally by the tip and the shaft of the pile. This proportion will, however, change when piles in till also embrace the lake deposits.

7. Peak value of the coefficient of load-transfer for piles in clay is 0.495, the average ultimate at large settlements being 0.43. This is in sharp contrast to the respective values of 0.89 and 0.655 (being the average of 0.76 and 0.55) for piles in till. It appears that the normally-laid soil particles in the former case first got remolded by drilling and then got softened after absorbing water from fresh concrete, thereby losing the natural cohesion to a large extent. This, however, did not happen in the case of piles in dense till wherein an intimate bond was established between relatively undisturbed soil and concrete. Ultimate unit shaft friction roughly corresponds to the remolded shear strength of the soil in the former and perhaps to the residual strength in the latter case.

8. Correlations for computing base capacity and shaft resistance have been developed by the usual method by using shear strength values from unconfined compression tests or undrained triaxial tests on undisturbed samples. Due to the difficulty in obtaining truly undisturbed samples of local soil especially those of till which contains numerous loose pockets of silt and sand, it was considered appropriate to depend more on

the penetration N-values which reflect the in-situ strength characteristics of the soil in a better way. The relationships developed in Chapter VII have been summarized in TABLE VIII-2.

9. There appears to be existing some consistent relationship between the residual tip resistance or the equivalent balancing total skin friction (reflected by the residual shaft compression) and the maximum base resistance developed before the removal of any load.

10. From the data obtained in the present test series, it can be concluded that the method of testing a pile by cyclic loading neither produces any appreciable amount of additional settlement nor changes the proportions of base and shaft capacities, at least up to the failure load.

11. A rough approximation of settlement under service piles can be made by using the following relationship due to TERZAGHI (1943):

$$\Delta H = C \cdot H_c \cdot \log_e \left(\frac{p_o + \sigma_z}{p_o} \right) \quad \dots (7.17)$$

wherein Δ is the 24-hour settlement in inches and C (dimensions: inch square per pound) is the Compressibility Constant, the value of which as obtained from field data, is given by:

$$C = \frac{1}{400} \cdot \frac{N}{p_o} \dots \dots \text{for piles in clay} \quad \dots (7.20)$$

$$\text{and} \quad C = \frac{1}{300} \cdot \frac{N}{p_o} \dots \dots \text{for piles in till} \quad \dots (7.21)$$

Here H_c in inches is the depth of the compressible layer below the pile tip assumed equal to twice the effective diameter of the pile base, p_o the overburden pressure in psi. at a depth equal to $\frac{1}{2}H_c$ below the tip;

TABLE VIII-2
SUMMARY OF CORRELATIONS DEVELOPED FOR COMPUTING BASE-CAPACITY
AND SHAFT RESISTANCE OF FULL-LENGTH PILES

PILES EMBEDDED WHOLLY IN	UNIT ULTIMATE BASE CAPACITY: q_u (tons per sq. ft. of base bearing area)		UNIT SHAFT RESISTANCE: f_s (tons per sq. ft. of shaft contact area)	
	based on mean undrained soil shear strength	based on average penetration N-values	based on weighted average shear strength along shaft	based on weighted average penetration N-values along shaft
CLAY	$cN_c + \gamma D_f N_q + \gamma N_{\gamma}$	0.65 N for 15 < h < 25 ft.	0.43 \bar{c}	$\frac{\bar{N}}{58}$
	13.6 c for short pile 25.5 c for long pile	0.36 N for short pile 0.6 N for long pile	0.76 \bar{c} for short pile 0.55 \bar{c} for long pile	$\frac{\bar{N}}{33}$ for short pile $\frac{\bar{N}}{55}$ for long pile
TILL				

Explanatory Notes: In the above table:

r = radius of pile base in feet,
 γ = moist unit weight of soil above water table or buoyant weight if below water table,
 N_c , N_q , N_{γ} = Meyerhof's dimensionless bearing capacity factors,
h = depth of pile tip below surface in feet,
c = mean shear strength of undisturbed soil below tip in tsf, (undisturbed cohesion)
 \bar{c} = weighted average shear strength of undisturbed soil along shaft in tsf,
N = mean penetration value (no. of blows) for soil under pile tip,
 \bar{N} = weighted average penetration value (no. of blows) for shaft soil.

N is the average penetration value and σ_z the vertical stress in psi. induced by the tip load Q_B at the centre of the layer.

For the computation of ΔH , the values of Q_B shall have to be initially estimated by subtracting the shaft resistance (computed on the basis of correlations developed for Q_S) from the expected total load Q at top.

12. The skin friction offered to the penetration of a pile is different at various depths along the shaft and depends upon the degree of straining of the soil particles as also on the fact as to whether ultimate shear failure at a particular depth has taken place or not. This, at any instant, can be related to the stress-strain curves for the soil.

13. It is only at very large settlements during a pile test carried to failure that the skin resistance offered would correspond to the residual shear strength of the soil. It could be the remolded shear strength if the soil constitutes a normally consolidated mixture of clay, silt and sand when the very process of drilling makes the soil lose a considerable part of cohesion. Different conditions may develop in other situations.

14. In service piles where allowable settlements are limited to small values, it is only the initial part of the stress-strain curve that is really active.

15. Actual behaviour of shaft soil depends upon the composition of soil, the degree of disturbance during drilling, the amount of excess water available from fresh concrete and the period elapsed between concreting the hole and test-loading the pile.

16. Softened shear strength obtained by testing of undisturbed samples

after soaking, does not represent the actual strength of shaft soil in all cases. The best method of estimating the shaft resistance is perhaps the application of reduction coefficient such as α to the undisturbed original shear strength obtained from a very large number of tests. This coefficient would then absorb the effect of all variations arising out of any of the factors responsible for affecting the soil shear strength in specific cases. Alternately, a correlation may be developed on the basis of measured cone-resistance or penetration N-values.

CHAPTER IX

RECOMMENDED PROCEDURE FOR DESIGN

9.1 Introduction

Results from the analyses of present series of tests are supposed to be helpful in evaluating the expected approximate pile bearing capacity of bored piles installed in Edmonton soil. As mentioned in Chapter V, the interface between the lake deposit and till below is bowl-shaped in which the thickness of lake sediments varies from 16 feet to nearly 36 feet (BAYROCK and HUGHES, 1962; BAYROCK and BERG, 1966). Deposition within the lake area having taken place under similar environments, the mechanical composition of soil at various locations and depths is comparable. Data published by various authorities including those mentioned above, confirms this. In the present series, till was encountered at a depth of about 25 feet below surface and the soil characteristics at test site, as mentioned in Chapter V, compare favourably with the average characteristics elsewhere. The site chosen was therefore quite representative.

Short bored piles are not justified unless they are resting on an extremely firm substratum (BUISSON, 1964). Ignoring the contribution of upper 4 feet depth which would be affected by seasonal changes, it perhaps shall not be appropriate to rest the pile tips at a depth less than 15 feet below surface. Investigation in Chapter VII has already been made for piles installed with their tips in the depth region 15 to 25 feet where

the depth 25 feet represents the interface between lake soil and till. For thickness of lake deposits greater than 25 feet, suitable modification where necessary has to be made.

Design recommendations made in this chapter have been based on test results of only two piles in clay and two in till. Extent of laboratory investigation on soil was too little compared to that warranted by the importance of the project required to lay down general design parameters. Extrapolation of the results to other sites, obviously, would need very careful consideration. Another prerequisite for application of results elsewhere would be the requirement of drilling and concreting procedure similar to the one used for the test piles (Chapter IV).

It must be stated here that the correlations developed and the procedure outlined below apply only to single piles or where they are isolated so as to ensure that the stressed zones of adjacent piles do not overlap. Further also, the nature of settlements under a single pile is very different from that of a group of piles for which additional investigation would be necessary. The approximate settlements computed for single piles therefore would not apply.

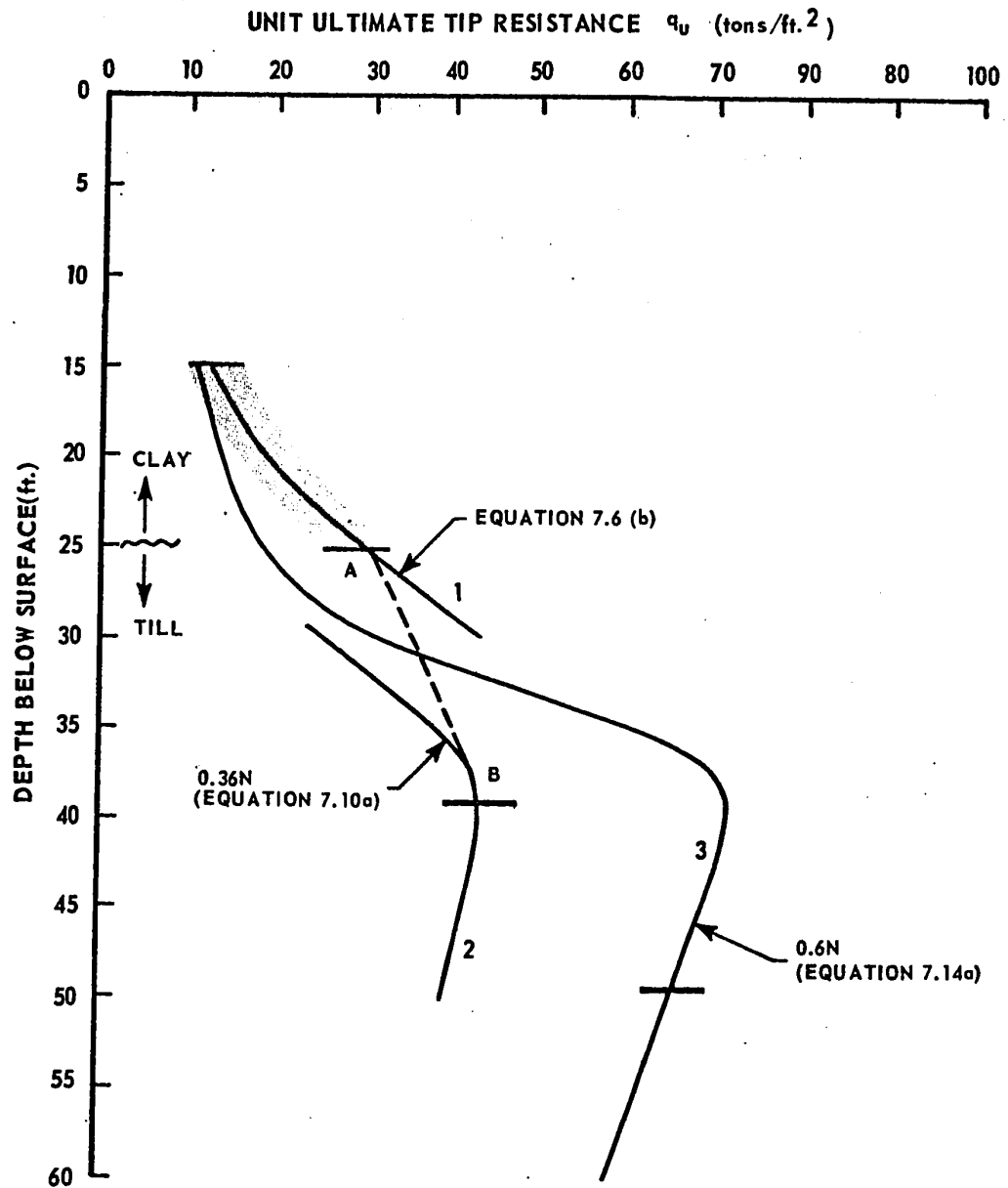
9.2 Computation of Ultimate Base Bearing Capacity

As has been shown in the previous chapters, the frictional component plays a very important role in the determination of ultimate base bearing capacity of all piles having depth of embedment greater than 15 feet. It would be extremely difficult if not impossible to procure truly intact samples for laboratory testing and if obtained would show considerable amount of scatter on the shear-strength plot. Evaluation of mean on the

basis of a few tests may often be misleading or in some cases even dangerous. Computation of tip bearing capacity in the absence of in-situ test values would always be a tricky affair inasmuch as local soil profile, in particular its portion in till, is concerned. Of the correlations developed in Chapter VII, it would always, therefore, be safer to make use of a relation involving the mean penetration N value obtained from tests in various bore-holes in preference to the one involving laboratory shear strength as the parameter.

Due to the heterogeneity of the strata it is impossible to lay down a single rule for computing ultimate bearing capacity Q_{BU} at all depths. It appears to be necessary to split the depth into three regions, viz., 15 to 25 feet, 25 to 40 feet, and over 40 feet. For pile-tips resting anywhere at depths from 15 to 25 feet, Meyerhof's general formula for ultimate bearing capacity (equation 2.3) is applicable, the values of the angle of shearing resistance to be used being those obtained from triaxial undrained tests. In the absence of such tests, equation (7.6) making use of field N -values may be employed.

Very high N -values approaching those for rock are reported for upper till for a depth of about 15 feet below the interface. Plot 1 in FIGURE 9.1 represents the equation (7.6b) and the shaded portion shown on it between 15 and 25 feet depth is the one recommended for use in the above paragraph. The remaining part in till would give very high values which, though nearly correct, would not be recommended for general use. Thick short horizontal lines shown on plots 2 and 3 represent the depth at which the tips of the two piles in till rest. These two plots have been drawn on the basis of correlation for q_u developed in Chapter VII. Test values



NOTE: THICK LINES AND SHADED BAND INDICATE THE DEPTH OR DEPTH REGION FOR WHICH THE DERIVED EQUATIONS HOLD EXACTLY.

FIGURE: 9.1 CURVES REPRESENTING TIP BEARING CAPACITY BY VARIOUS EQUATIONS AT VARIOUS DEPTHS.

of ultimate bearing capacity are represented by the points of intersection of these plots with the small horizontal lines. Exact variation in the depth region 25 to 40 feet which constitutes very hard silty-sandy-gravelly till is not known. It is definitely higher than the values indicated by the upper portion of plots 2 and 3 and would be close to those represented by plot 1. In the absence of additional information, a linear variation in q_u values following a similar variation in the N-values plot (FIGURE 5.3) may be adopted from 25 to 37.5 feet as shown by the dotted line AB in FIGURE 9.1. For the rest of the depth where conditions are similar, plot 2 should give satisfactory results. Very high value of q_u shown by the long pile in till appears to be an exceptional case where the tip incidentally was resting on a layer of sand which exhibited a value similar to that in the region immediately below 25 feet depth.

In summary, in the absence of dependable laboratory strength values, ultimate base bearing capacity under a pile at any depth in the local soil may be approximately predicted from the following relationships:

1. For piles wholly within the lake soil:

$$Q_{BU} = 0.65 N. A_b \dots \text{ton} \quad \dots (9.1)$$

where A_b is measured in square feet.

2. For piles with their tips resting within the upper 12.5 feet of till deposit:

$$Q_{BU} = (30 + 1.05 d) A_b \dots \text{ton} \quad \dots (9.2)$$

where d is the depth in feet within the till layer and varies from 0 to 12.5 feet. Values computed by this relationship are

likely to be on the conservative side.

3. For piles with their tips resting more than 12.5 feet below till interface:

$$Q_{BU} = 0.36 N \cdot A_b \dots \text{ton} \dots (9.3)$$

9.3 Computation of Shaft Resistance

Ultimate Total Capacity of Pile Shaft can be estimated from the following formulae:

$$Q_{SU} = \alpha \cdot \bar{c} \cdot A_s \dots \text{ton} \dots (9.4)$$

or
$$Q_{SU} = \beta \cdot \bar{N} \cdot A_s \dots \text{ton} \dots (9.5)$$

wherein α is the coefficient of skin friction being the ratio of ultimate average developed skin friction f_s to the weighted average undisturbed shear strength of the soil \bar{c} both measured in tons psf. Symbol β represents the coefficient of reduction to be applied to the weighted average value of penetration N (number of blows) for the embedded length of the shaft. A_s in the above equation is the contact area between shaft and soil measured in square feet. Computed values of α and β are recorded in TABLE VIII-2 of Chapter VIII. For the portion in lake soil, value of α has been obtained on the basis of a large number of undisturbed samples of soil whereas that for till depends upon relatively small number of tests on samples not entirely undisturbed in the true sense of the word. α -values for till recorded in the above-mentioned table shall therefore not be recommended for general use. Computation on the basis of N -values, however, it is believed, shall give a more dependable estimation. β -values of

1/58 and 1/55 which may be considered equal for all practical purposes are applicable for all piles in clay and for the long pile in till. Increase in its value to 1/33 for the short pile in till is due to the very hard strata of the upper till region. Assuming a uniform value of 1/58 for the entire profile, nominal increase in the value may be effected by introducing a suitable factor to account for variations in the length of embedment. Estimation of total Shaft Resistance may therefore be made by using the following general formulae:

1. For piles wholly within the lake soil, ultimate shaft capacity is represented by equations (9.4) and (9.5) where $\alpha = 0.43$ and $\beta = 1/58$.
2. For piles with their tips resting in till:

$$Q_{SU} = \beta (\bar{N}_1 \cdot A_{S1} + m \cdot \bar{N}_2 \cdot A_{S2}) \dots \text{ton} \dots (9.6)$$

wherein β equals 1/58, \bar{N}_1 and \bar{N}_2 represent the weighted average N-values for embedded depths in lake soil and those in till respectively, A_{S1} and A_{S2} are the corresponding shaft contract areas in square feet. Value of factor m varies from 1 to 1.6, the smaller being applicable for a total depth of about 50 feet and the larger for about 40 feet or less; values for intermediate depths to be interpolated suitably.

9.4 Factors of Safety and Evaluation of Working Load

It is essential to ensure that a certain minimum factor of safety is available both against bearing capacity failure as well as against excessive settlement at the pile tip. The two would assume varying

degree of importance in different cases. Taking for example the present series of tests, the short pile in till rests on stiff but excessively deformable strata and so is more vulnerable to failure by settlement than the long pile which is resting on a bed of sand in which case the settlement would be small and of immediate nature depending upon the proportion of load transferred to the tip. In general, if the soil is homogeneous, long piles would deform more and settle less compared to short ones showing the opposite effect, since a considerable portion of total load is prevented from reaching the bottom in the former case. In the present case, however, all piles resting anywhere between 25 and 35 feet would behave as short piles, but since their tips would be bearing on hard and relatively incompressible sandy-silty-gravelly strata, they would probably be safe both against bearing capacity failure and against excessive settlement. Structural capacity of the pile would then be the governing factor in design. Similar conditions are encountered at a depth of 50 feet below surface. Elsewhere in till (depth 35 to about 45 feet), settlements may be more critical. Both the conditions may be equally important for pile tips resting between 15 and 25 feet below surface. In each case, however, it would be necessary to ensure that the structural capacity of the pile, assumed to be behaving as a short column, is not reached.

For a normal pile test, a single factor of safety applied on the yield-point load may be employed to arrive at a suitable working load or alternately the working load be obtained on the basis of maximum allowable gross or net settlement. A different procedure shall, however, be necessary if the total capacity is computed by adding up the base capacity and shaft resistance by making use of the equations developed in paragraphs 9.2 and

and 9.3 above, since in that case the same factor of safety applied to the two components would not be compatible with the corresponding settlements. It can be observed from the settlement curves that shaft resistance builds up to the peak value very fast, i.e., for a small value of settlement corresponding to which the mobilized base resistance is relatively insignificant. A factor of safety if applied on Shaft Resistance shall result in only a minor change in the overall factor of safety available for the service pile. The Shaft Resistance component of Total Load Capacity is therefore of major importance.

FIGURE 9.2(a) shows plots for net settlement of the tip for the two piles in clay. Right up to the failure loads of 93 and 100 kips respectively for the 16-in. and 20-in. piles, the settlement indicated is insignificant. And further, since the curves correspond to ultimate settlements after 24 hours, it is reasonable to presume that primary consolidation of soil is nearly complete. Long-time transfer of load from shaft to the tip can be presumed to be small and hence also additional settlement. In this case, therefore, the smallest practical factor of safety can be applied on the yield-point load. Before suggesting a suitable value, it would be necessary to study the possible effect on shaft capacity as a result of any factor of safety F applied to total load capacity and vice-versa. Idealized plots for Q_B and Q_S calculated on the basis of approximate relationships given in paragraphs 9.3 and 9.4 have been shown in FIGURE 9.2(b). Base capacity is assumed to have reached its ultimate value at a tip settlement of 1.5 inches obtained by adopting the actual settlement at 75 per cent of ultimate base load, as shown. For drawing the initial portion of idealized shaft capacity curve, a settlement value

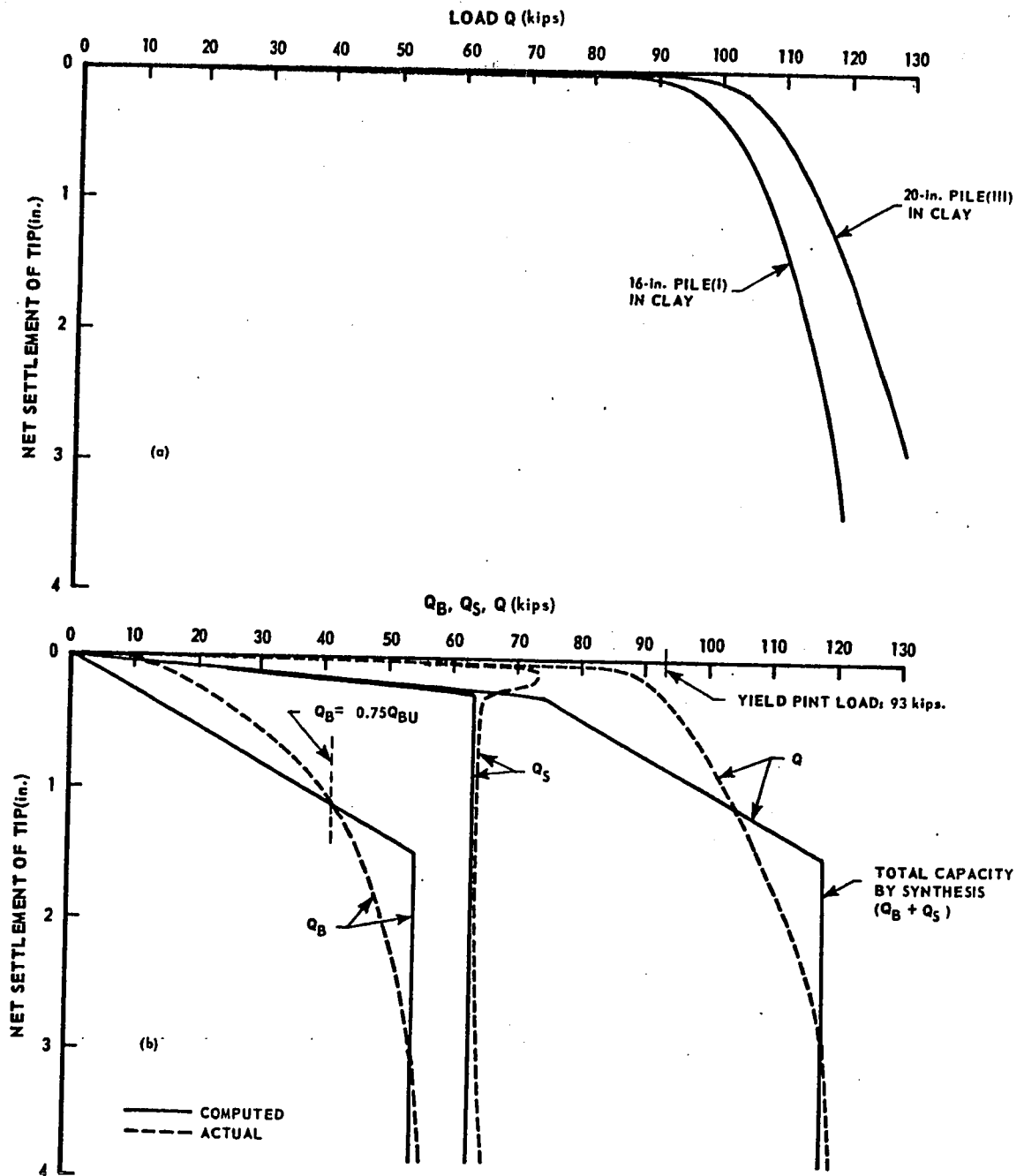


FIGURE 9.2 (a) PLOTS FOR NET SETTLEMENT CURVES FOR PILES IN CLAY
(b) IDEALIZED PLOTS FOR Q_B , Q_S AND FOR 16-INCH PILE (I) IN CLAY.

corresponding to Q_s value indicated by the lower end of the peak has been chosen. For overall factors of safety F varying from 3 down to 1.2 applied to the yield-point load of 93 kips, working values have been obtained from the idealized total capacity curve plotted by synthesizing the corresponding values of Q_s and Q_b (FIGURE 9.2). Values so obtained have been split up into the respective components Q_s and Q_b and the available safety factors F_s , F_b on these components obtained by using the ultimate values of shaft and base resistances. The plots shown in FIGURE 9.3 indicate the relationship between the applied overall factor of safety F and the derived safety factors F_s , F_b . A very high factor of safety is available on the base capacity corresponding to any value of F or F_s . Assuming primary consolidation to be nearly complete, there is no likelihood of any serious long-time settlement taking place. But still if a portion of shaft load is eventually transferred to the tip, sufficient margin of safety for base load would still be available. Both the share of shaft load as well as the ultimate shaft resistance values in that case would drop correspondingly. It is believed that the original factor of safety on shaft capacity would be nearly maintained. Appropriate factors of safety can thus be chosen from the F_s vs. F plot (FIGURE 9.3) ensuring compatibility between settlements at the values of shaft and total capacities. An overall factor of safety of 2 corresponds to F_s value of 1.61 and of 2.5 corresponds to F_s value of 1.84. Appropriate value, depending upon the degree of control of operations during drilling and concreting, can be chosen. For normal operations carried out by experienced foundation engineering firms, an overall factor of safety of 2 is suggested to be applied to the results of a load test wherein settlements were recorded for 24 hours.

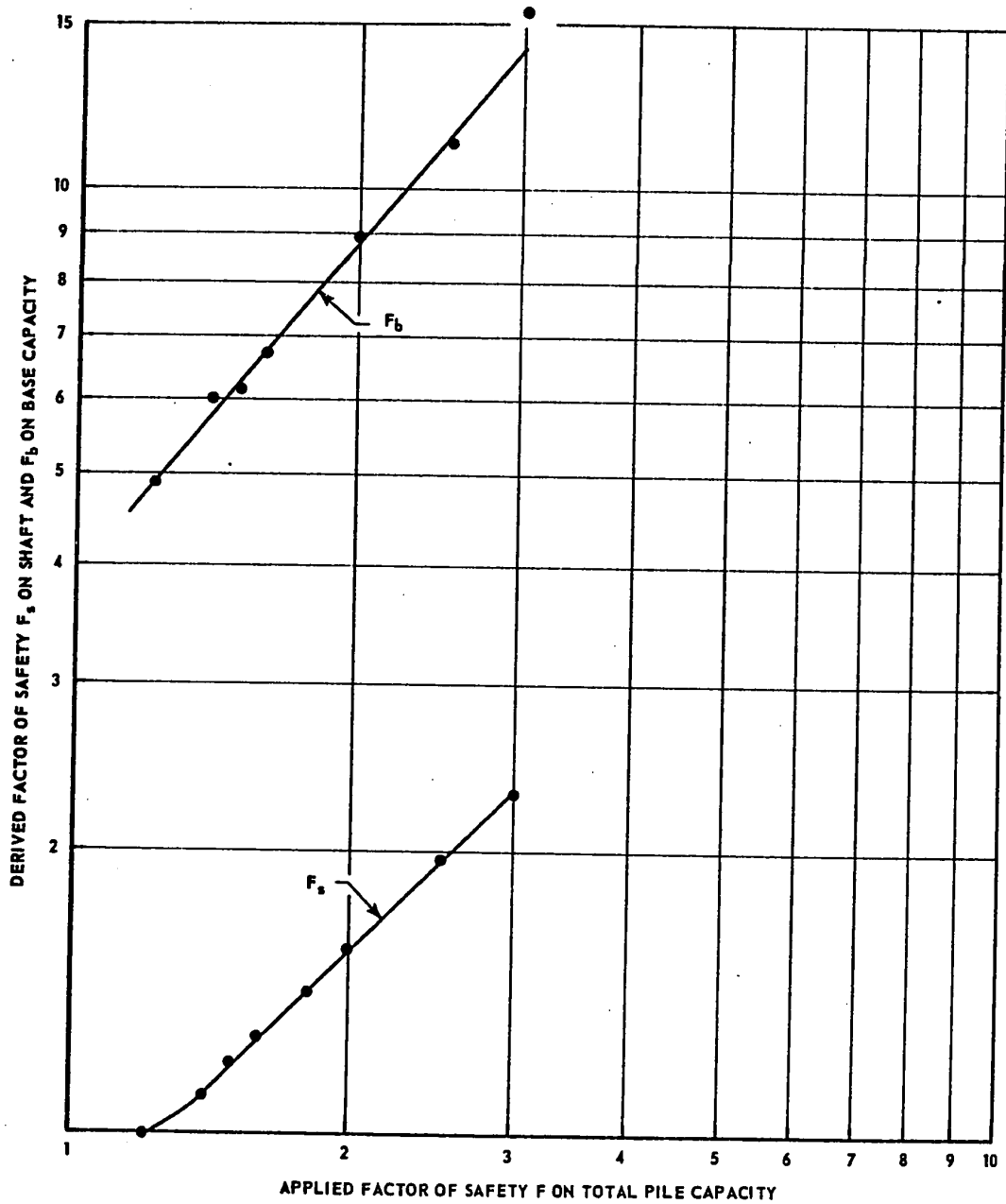


FIGURE: 9.3 RELATION BETWEEN OVERALL FACTOR OF SAFETY F AND DERIVED FACTORS OF SAFETY F_s AND F_b ON SHAFT AND BASE CAPACITIES.

Approximate value of working load in the absence of a load test can thus be computed from:

$$W.L. = \frac{Q_{SU}}{F_s} + \frac{Q_{BU}}{F_b} \quad \dots (9.7)$$

wherein Q_{SU} and Q_{BU} are the computed ultimate values obtained by using the correlations presented in paragraphs 9.2 and 9.3 and F_s , F_b can be chosen from FIGURE 9.3 corresponding to any desired overall factor of safety F .

The above relationship can be applied for computing working load for piles in till also, but F_s and F_b values shall be different. It is not possible to spell out these values in this case, since the piles are embedded solely in till passing clear through lake soil. Complete embedment would cause the shaft resistance and the base resistance curves to flatten out showing ultimate mobilization at relatively large settlements.

Having computed the working load by method of synthesis, approximate check for ultimate settlement both under the working load and under the would-be yield-point load may be made by using equation (7.17). Section of pile should finally be checked against structural failure due to crushing of concrete at pile head. An appropriate factor of safety should be provided.

CHAPTER X

CONCLUSIONS AND RECOMMENDATIONS

10.1 General

The investigation under report comprises two phases of load tests on piles. The first one summarized in Chapter III concerns tests on four scaled bored piles in uniformly graded plastic silt and the second one constitutes investigation of full length field tests also on bored piles, two installed in Edmonton lake deposit and two in dense till below. The scope of investigation has been quite limited in the former case where only a preliminary study of the general behaviour of loaded piles in silt was undertaken. Laboratory testing was mainly restricted to unconfined compression tests. The conclusions drawn below are quite limited in application to the actual field piles by direct extrapolation, since the effects of scaling down were not studied. Work on field piles, on the other hand, was of a more elaborate nature. Based on actual performance, some rules have been suggested to arrive at the working load for full-length piles. Extensive laboratory testing, particularly on samples of till, could not be carried out for want of time. The rules suggested herein shall therefore require confirmation before being used for predicting the working loads.

10.2 Conclusions and Recommendations Based on the Results of Load Tests on Scaled Piles in Silt

1. Load-settlement curves for total pile capacity, tip resistance

and shaft capacity are all similar in shape with the peak values occurring almost simultaneously at settlement ratios (Δ/B) ranging from 2.8 per cent to 4.2 per cent. Contribution of base resistance being less than 10 per cent, piles under similar conditions may be designed as friction piles.

2. Magnitude of shaft capacity developed is closely related to the shear strength of softened soil around. Coefficient of adhesion α_2 being the ratio of unit load transfer to unit shear strength of softened soil has a nearly constant value approaching unity. It is therefore the strength reduction coefficient α_1 , being the ratio of soil shear strength after and before concreting the hole, which is responsible for fall in the value of coefficient of load transfer $\alpha (= \alpha_1 \cdot \alpha_2)$, after concreting. Average value of α obtained from tests in silt works out to 0.83.

3. Additional load capacity obtained as a result of bellling the pile tip is relatively insignificant primarily due to low shear strength of soil at base. It can therefore be concluded that for deep piles in saturated silt where bearing area is small compared to total shaft area, enlargement of pile-base is neither economical nor useful.

4. The values of bearing capacity factor N_c are much lower (of the order of 6 to 6.25) for nearly saturated silt (degree of saturation about 90 per cent) than for clay under similar conditions, that is, on the assumption that " $\phi = 0$ " condition is applicable. Relatively slow rate of mobilization of base resistance is due to the compressibility of silt or the possible shifting of positions by the individual particles under the effect of load.

5. Reduction in shear strength of soil bears a linear relationship to water-cement ratio (measured here in terms of slump) of concrete after

mixing and with the increase in moisture content. Coefficient of skin friction α is also similarly related to increase in moisture content of the soil around the shaft.

6. Silt loses part of its apparent cohesion on coming in contact with water.

7. There is some evidence to show that during the process of drilling, water from surrounding soil migrates to the shear zones.

8. It appears that a more elaborate study is necessary to understand the exact behaviour of piles in this type of soil. Strict control during drilling and mixing of concrete must be exercised. Effect of free water from concrete on total pile capacity is very drastic. Water-cement ratio to be used should be standardized, since otherwise even an actual load test might be grossly misleading. This aspect would assume greater importance in view of the uncertainty of silt regaining strength with the passage of time. Instrumentation of the pile should preferably be done along the shaft in addition to providing a load-cell at bottom, so as to measure the load transferred at various sections of the pile. This would permit the use of the general equation (3.3) for computing shaft resistance. Appropriate instrumentation to study the effect of loading on the pore-water pressures developed is also highly desirable.

10.3 Conclusions Derived from Results of Tests on Full-Length Piles

Following conclusions appear to be justified in connection with load tests on field piles:

1. Compression of the shaft is a function not only of the applied load Q at top and modulus of elasticity E of the material but also that

of mobilized base resistance at any stage of loading. It is therefore possible to estimate roughly the values of base resistance from a knowledge of measured shaft compression. If actual operating value of E for the material is obtained from a load test on an instrumented pile, a correlation can be obtained between the measured values of shaft compression, the applied total load and the resulting base-resistance in terms of E and the pile-length H . This can then be employed for ascertaining Q_B -values elsewhere under similar assumed conditions. The method used in paragraph 7.2 shows good agreement between computed and measured values.

2. Effects of pile-length and soil type are clearly brought out by the results of tests on field piles. Shaft Resistance curves indicate pronounced peaks after a steep rise (i.e., corresponding to very small settlements) for piles in clay and sustained peaks for piles in till. Long piles tend to further flatten the development of peaks showing maximum values at different absolute settlements but nearly the same settlement ratio (Δ/B) of about 0.6 percent for piles in clay and 7.5 per cent for piles in till. This tremendous difference has been explained on the basis of relative flexibilities of the pile material and the two soil types being normally consolidated silty sandy clay deposit in the former case and dense glacial till in the latter case.

3. Both the magnitudes of Residual Tip Resistance and the elastic recovery of pile after removal of load from top, appear to be dependent upon ultimate settlement of pile tip. When complete shear failure of shaft soil has taken place and the tip has started punching into the strata below, these magnitudes are relatively small compared to those when the extent of punching is small or nil. Complete shear failure of shaft soil is indicated by

rapid settlement of pile during testing and the appearance of a peak in the Shaft Resistance curve.

4. The rate of settlement-increase as a function of time is greater for piles in till than for piles in clay.

5. Soil under pile tips behaves like a true $c - \phi$ material and the contribution of friction is very significant. Analysis of results concerning piles in clay shows that ultimate Bearing Capacity can be safely computed on the basis of Meyerhof's Theory. Terzaghi's Theory, on the other hand, gives conservative values. These statements, however, could not be confirmed for piles in till due to lack of laboratory data.

6. Both the magnitude of developed skin friction at peak and the corresponding settlement are sensitive to the very plotting of curves for total capacity Q and the base resistance Q_B .

7. Developed ultimate shaft resistance corresponds roughly to the remolded value of shear strength for piles in clay silty sandy lake deposit and probably to the residual value of shear strength for piles in till.

8. Correlations for computing ultimate capacity of pile based on field N-values, it is believed, better represent the in-situ strength, in particular of the local soil, and so are more dependable than those based on laboratory test results.

9. The developed skin resistance depends upon a number of factors. It may roughly correspond to softened shear strength, remolded shear strength, or residual shear strength in different situations. The best method of obtaining a correlation for it is to apply a reduction coefficient such as α to the undisturbed shear strength based on the results of a large number of tests. This coefficient α would then absorb the effect

of all the variations arising out of any of the factors responsible for affecting the soil shear strength in specific cases. A correlation based on N-values, or cone-resistance values is better suited for piles in cohesionless soils as well as in till.

10. From the data obtained in the present test series, it can be concluded that the method of testing a pile by Cyclic Loading neither produces any appreciable amount of additional settlement nor changes the proportions of base and shaft capacities, at least up to the failure load.

11. Characteristics of Edmonton soil vary constantly with depth and it is not possible to compute ultimate base bearing capacity Q_{BU} by making use of a single formula. Approximate predictions for various depth regions can, however, be made from the following relationships:

- a. For piles wholly within the lake soil:

$$Q_{BU} = 0.65 N \cdot A_b \dots \dots \text{tons} \dots (9.1)$$

- b. For piles with their tips resting within the upper 12.5 feet of till deposit:

$$Q_{BU} = (30 + 1.05 d) A_b \dots \dots \text{ton} \dots (9.2)$$

- c. For piles with their tips resting more than 12.5 feet below till interface:

$$Q_{BU} = 0.36 N \cdot A_b \dots \dots \text{ton} \dots (9.3)$$

A_b in the above relationships represents the bearing area of the pile in square feet, and d in feet is the depth of embedment within till.

12. Approximate estimation of Total Shaft Resistance may be made by using the following formulae:

a. For piles wholly within the lake soil:

$$Q_{SU} = \alpha \cdot \bar{c} \cdot A_s \dots \text{ton} \dots (9.4)$$

$$\text{or } Q_{SU} = \beta \cdot \bar{N} \cdot A_s \dots \text{ton} \dots (9.5)$$

wherein $\alpha = 0.43$ and $\beta = 1/58$.

b. For piles with their tips resting in till:

$$Q_{SU} = \beta (\bar{N}_1 \cdot A_{S1} + m \cdot \bar{N}_2 \cdot A_{S2}) \dots \text{ton} \dots (9.6)$$

wherein $\beta = 1/58$ and \bar{N}_1 and \bar{N}_2 represent the weighted average N-values for depths of embedment in lake soil and in till respectively, A_{S1} and A_{S2} being the corresponding shaft contact areas in square feet. The symbol \bar{c} in the above equation is the weighted average undisturbed shear strength of soil along the shaft. Value of factor m varies from 1.0 to 1.6, the smaller one applicable for a total pile depth of about 50 feet and the larger one for about 40 feet or less; intermediate values to be interpolated suitably.

13. Working Load can be obtained by applying a suitable overall factor of safety F to the yield-point load if a pile test has been carried out. If, however, total ultimate capacity has been worked out by synthesizing the base and shaft capacities by employing the relationships presented in paragraphs 12 and 13 above, compatibility between the corresponding settlements shall have to be ensured. In that case working load is given by:

$$W.L. = \frac{Q_{SU}}{F_s} + \frac{Q_{BU}}{F_b} \dots (9.6)$$

wherein values of F_s and F_b , being the factors of safety for shaft and base resistance respectively, can be obtained from FIGURE 9.3 for any desired overall factor of safety F for piles in clay.

14. Settlements are not critical for piles installed in Edmonton soil, in particular, for pile tips resting within 35 feet depth below surface. An approximate check on the computed values of working load may, however, be made by using equations (7.17), (7.20) and (7.21).

15. Piles resting on relatively unyielding strata can withstand high loads. Selection of the pile should therefore finally be checked against structural failure due to crushing of concrete at pile head. An appropriate margin of safety should be available.

16. The profile shows relatively low values of settlements and high bearing capacities in the depth region varying from about 15 feet below top surface extending up to about 10 feet below till interface. It is therefore suggested that design length of piles be determined accordingly on that basis.

17. Shaft Compression is small and so may be ignored for obtaining net settlements in the case of piles in clay. Its effect for longer piles installed in till is, however, significant and should be accounted for.

10.4 Recommendations for Further Study of Full Length Piles

Evolution of an appropriate design method suitable for general soil conditions within a certain area is a slow and a continuous process. With each and every test conducted in the future, there would be scope for considerable improvement. It is, however, not always necessary to test load the piles exclusively for this purpose, though the establishment of

some sort of liaison between the University and the various Foundation Engineering firms appears to be desirable, so that wherever they happen to conduct any test at a particular site, an observer from the University is present. Some of the recommendations based on the experience gained from the present series of tests are listed below:

1. With a view to avoiding caving and sloughing, it would be desirable to provide casing for the excavated hole within the lake deposit. While withdrawing the casing and concreting the hole, it must be ensured that concrete is in intimate contact with the wall. By whatever practical methods possible, care should be taken to see that particles of soil are prevented from mixing with concrete. Likewise, the bottom of the hole must be cleared of any loose particles of soil before concreting is commenced. A chute, it is recommended, should be used to deposit concrete in small batches without impact.

2. The larger the number of intact specimens of soils obtained and tested, the more realistic are the ultimate values of strength parameters obtained. It would be preferable to obtain continuous samples from few test holes rather than procuring the same number of samples from a large number of holes. Continuous sampling would, in addition, give better indication of variations in soil profile.

Laboratory testing on undisturbed samples should include both drained and undrained triaxial tests with pore-water pressure measurements, shear box tests carried to large strains and tests on remolded as well as softened soil specimens in addition to the usual unconfined compression tests. If instrumentation in the field has been done to record the actual developed pore-water pressures, suitable parameters can be selected and

actual behaviour analysed.

3. In preference to tests on undisturbed samples mentioned above, correlations developed on the basis of in-situ strength characteristics of soil would give more dependable results under local soil conditions. It is therefore recommended that N-values be measured at 5 foot intervals or else static cone resistances be obtained for the entire profile.

4. In order to do away with the avoidable variations, the method of drilling, the size and proportions of aggregates for concrete mix design, water-cement ratio and slump, maximum allowable period between drilling and concreting a hole, must be standardized.

5. Instrumentation for a field test pile may include arrangements for measuring load-transfer at various depths in addition to providing a load measuring device at the pile tip. Piezometers installed near the bottom and also elsewhere shall help obtain the actual variations of the developed pore-water pressures as a result of loading. Moisture-meters, if installed, would help measure the rate of diffusion of water from fresh concrete radially away from the pile as also migration of water at all stages of test.

6. In the case of bored piles, mutual migration of water between concrete and surrounding soil goes on taking place for a certain length of time. And since the capacity of the shaft is directly related to the shear strength of shaft soil at the time of testing, it would be necessary to specify the period to be allowed to elapse before commencing test-loading.

7. Instead of applying maximum test load equal to the usually recommended value of twice the expected working load, it appears appropriate to carry the loads up to ultimate failure when rapid settlement is recorded.

This would give a better idea of available margin of safety and may even be economical since it would be possible to reduce the pile section or the length of embedment.

8. Settlements at various stages of loading of a test pile may preferably be recorded up to 24 hours, so as to permit a major portion of primary consolidation to take place. This shall eventually ensure a greater degree of safety inasmuch as ultimate settlement is concerned.

9. During the process of testing, unexpected rapid settlement may start taking place when applied load approximates the failure load. And since it might have to be left overnight, automatic recording of all instruments is recommended.

10. Repeated loading, it has been observed, neither produces any appreciable amount of additional settlement nor changes the proportions of base and shaft capacities, at least up to the failure load. And since it yields useful data helpful in the evaluation of net settlement, it is recommended that the method be employed for test loading piles in the future.

LIST OF REFERENCES

- APPOLONIA, E. D', 1963, Load Transfer in End Bearing Steel H-Piles, Proceedings American Society of Civil Engineers, S.M.2, New York.
- ARTICOGLU, N. C., 1961, Determining Ultimate Bearing Capacity of Precast Reinforced Concrete Piles from Deep Sounding Tests in Alsancak Harbour, Proceedings, Fifth International Conference on Soil Mechanics and Foundation Engineering, Paris.
- ASTM, 1957, Tentative Method of Test for Load-Settlement Relationships for Individual Piles under Vertical Axial Loads, Book of ASTM Standards, 1957.
- BAYROCK, L. A. and BERG, T. E., 1966, Geology of the City of Edmonton (Part I), Research Council of Alberta, Edmonton, Alberta.
- BAYROCK, L. A. and HUGHES, G. M., 1962, Surficial Geology of the Edmonton District, Alberta, Research Council of Alberta, Edmonton, Alberta.
- BEREZANTZER, V. G., 1965, Design of Deep Foundations, Proceedings, Sixth International Conference on Soil Mechanics and Foundation Engineering, Montreal.
- B.L.H. ELECTRONICS, 1965, Wire Strain Gage Specifications, Bulletin 100-2, Massachusetts (U.S.A.).
- B.L.H. ELECTRONICS, 1965, Strain Gage Handbook, Bulletin 103, Massachusetts (U.S.A.).
- BOLOGNESI, M. A. J. L., 1961, General Discussion on Piled Foundations, Proceedings, Fifth International Conference on Soil Mechanics and Foundation Engineering, Volume III, Paris.
- BROMS, B. B., 1968, End Bearing and Skin Resistance of Piles, Proceedings, American Society of Civil Engineers, S.M.1, New York.
- BROOKER, E. W. and IRELAND, H. O., 1965, Earth Pressure at Rest Related to Stress History, Canadian Geotechnical Journal, Volume II, Toronto.
- BUDD INSTRUMENTS LIMITED, 1966, Accessory Catalogue 2400, Hickory, Ontario.

- BUISSON, M., 1966, Short Piles, Proceedings of a Symposium on Bearing Capacity of Piles, Central Building Research Institute, Roorkee, India.
- BURLAND, J. B., BUTLER, F. G. and DUNICAN, P., 1966, The Behaviour and Design of Large Diameter Bored Piles in Stiff Clay, Symposium on Large Bored Piles, London.
- BURMISTER, D. M., 1940, Stress Distribution for Pile Foundations, Proceedings, Purdue Conference on Soil Mechanics, Purdue (U.S.A.).
- CAMBERFORT, H., 1965, Pieux et Groupes de pieux en terrain homogène, Proceedings, Sixth International Conference on Soil Mechanics and Foundation Engineering, Montreal.
- CANADA CEMENT COMPANY, 1951, Concrete Piles, Portland Cement Association, Montreal.
- CANADA CEMENT COMPANY, 1966, Concrete Information, Portland Cement Association, Montreal.
- CHELLIS, R. D., 1961, Pile Foundations (Second Edition), McGraw-Hill Book Company, New York.
- COOKE, R. W. and WHITAKER, T., 1961, Experiments on Model Piles with Enlarged Bases, Geotechnique, Volume II, London.
- COOLING, L. F. and GOLDER, H. Q., 1940, Portable Apparatus for Compression Tests in Clay Soils, Engineering 1940 (149).
- COYLE, H. M. and REESE, L. C., 1966, Load Transfer for Axially-Loaded Piles in Clay, Journal of Soil Mechanics and Foundation Engineering Division, American Society of Civil Engineers, Volume 92, New York.
- CRANDALL, J. S., 1936, Opening Discussion on Bearing Capacity of Piles, Proceedings, First International Conference on Soil Mechanics and Foundation Engineering, Cambridge (U.S.A.).
- DEB, A. K. and CHANDRA, S., 1964, The Load Bearing Capacity of Short Bored Piles in Expansive Clays, Symposium on Bearing Capacity of Piles, C.B.R.I. Roorkee, India.
- DE BEER, E. and MARTENS, A., 1957, Method of Computation of an Upper Limit for the Influence of Heterogeneity of Sand Layers in the Settlement of Bridges, Proceedings, Fourth International Conference on Soil Mechanics and Foundation Engineering, Volume I, London.
- DRANNIKOV, A. M., 1967, Construction on Loess Soils of Small Thickness, Proceedings, Third Asian Regional Conference on Soil Mechanics and Foundation Engineering, Haifa, Israel.

- FLETCHER, G. A., 1962, Pile Load Tests and Their Evaluation, Field Testing of Soils, ASTM, S.T.P. 322.
- FOX, E. N., 1948, The Mean Elastic Settlement of a Uniformly Loaded Area at a Depth Below the Ground Surface, Proceedings, Second International Conference on Soil Mechanics and Foundation Engineering, Rotterdam.
- FRISCHMANN, W. W. and FLEMING, W. G. K., 1962, The Use and Behaviour of Large Diameter Piles in London Clays, The Structural Engineer, Volume 40.
- GOLDER, H. Q. and LEONARDS, M. W., 1954, Some Tests on Bored Piles in London Clay, Geotechnique, Volume IV, London.
- GOLDER, H. Q., 1957, A Note on Piles in Sensitive Clays, Geotechnique, Volume VIII, London.
- GRAVENOR, C. P. and BAYROCK, L. A., 1968, Glacial Deposits of Alberta, Soils in Canada, Ed. R. F. Legget, Royal Society of Canada, Special Publication Number 3, Toronto.
- HANDBOOK OF ALUMINIUM, 1961, Aluminium Company of Canada.
- HAEFELI, R. and BUCHER, H., 1961, New Methods for Determining Bearing Capacity and Settlement of Piles, Proceedings, Fifth International Conference on Soil Mechanics and Foundation Engineering, Volume II, 1961, Paris.
- HARRIS, C. H., 1964, Model Pile Behaviour in a Clay Soil, M.Sc. Thesis (Unpublished), University of Alberta, Edmonton.
- HOBBS, N. B., 1963, An Analytical Approach to the Bearing Capacity and Settlement of the Large Diameter Bored Piles, Proceedings of the Institute of Civil Engineers, Paper 6616, Volume 25, London.
- HORN, H. M. and DEERE, D. U., 1962, Frictional Characteristics of Minerals, Geotechnique, Volume XII, London.
- HUIZINGA, T. K., 1951, Application of Results of Deep Penetration Tests to Foundation Piles, Building Research Congress.
- JAKY, J., 1948, On the Bearing Capacity of Piles, Proceedings, Second International Conference on Soil Mechanics and Foundation Engineering, Volume I, Rotterdam.
- KEZDI, A., 1957, Bearing Capacity of Piles and Pile Groups, Proceedings, Fourth International Conference on Soil Mechanics and Foundation Engineering, Volume II, London.

- KEZDI, A., 1965, General Report on Deep Foundations, Proceedings, Sixth International Conference on Soil Mechanics and Foundation Engineering, Montreal.
- KISHIDA, H. and MEYERHOF, G. G., 1965, Bearing Capacity of Pile Groups under Eccentric Loads in Sand, Proceedings, Sixth International Conference on Soil Mechanics and Foundation Engineering, Montreal.
- KRIZEK, R. J., 1965, Approximation for Terzaghi's Bearing Capacity Factors, Proceedings, American Society of Civil Engineers, New York.
- LEONARDS, G. A. (ed.), 1962, Foundation Engineering, McGraw-Hill Book Company Incorporated, New York.
- LO, K. Y. and STERMAC, A. G., 1964, Some Pile Loading Tests in Stiff Clay, Canadian Geotechnical Journal, Volume I, Number 2, Toronto.
- LONDE and JAMES, 1961, Concrete Engineer's Handbook, McGraw-Hill, 1961.
- MANSUR, C. I. and FOCHT, J. A., Jr., 1956, Pile Loading Tests, Morganza Floodway Control Structure, Transactions, American Society of Civil Engineers, Volume 121, New York.
- MATICH, M. A. J., 1967, Some Load Tests on Drilled Cast-in-Place Concrete Caissons, Canadian Geotechnical Journal, Volume IV, Toronto.
- MEYERHOF, G. G., 1950, Discussion on the Use of Shear Strength Measurements in Practical Problems by H. Q. Golder and W. H. Ward, Geotechnique, Volume II, London.
- MEYERHOF, G. G., 1951, The Ultimate Bearing Capacity of Foundations, Geotechnique, Volume II, London.
- MEYERHOF, G. G., 1956, Penetration Tests and Bearing Capacity of Cohesionless Soils, Proceedings, American Society of Civil Engineers, S.M.1, New York.
- MEYERHOF, G. G., 1959, Compaction of Sands and Bearing Capacity of Piles, Proceedings, American Society of Civil Engineers, New York.
- MEYERHOF, G. G. and MURDOCK, L. J., 1953, An Investigation of the Bearing Capacity of Some Bored and Driven Piles in London Clay, Geotechnique, Volume III, London.
- MINDLIN, R. D., 1936, Force at a Point in the Interior of a Semi-Infinite Solid, Physics, Volume 7.
- MOGAMI, T. and KISHIDA, H., 1961, Some Piling Problems, Proceedings, Fifth International Conference on Soil Mechanics and Foundation Engineering, Paris.

- MOHAN, D. and CHANDRA, S., 1961, Frictional Resistance of Bored Piles in Expansive Clays, Geotechnique, Volume XI, London.
- MOHAN, D. and JAIN, G.S., 1961, Bearing Capacity of Bored Piles in Expansive Clays, Proceedings, Fifth International Conference on Soil Mechanics and Foundation Engineering, Paris.
- MOHAN, D., Jain, G.S. and KUMAR, V., 1963, Load Bearing Capacity of Piles, Geotechnique, Volume XIII, London.
- MURDOCK, L.J., 1948, Concrete Materials and Practice, Edward Arnold Company, London.
- OHDE, J., 1951, Zur Gestaltung und Berechnung von Pfahlrosten, Strassen- und Tiefbau, Strassenbau und Strassenbaustoffe, Heft 9, 11, 12, Heidelberg.
- ORCHARD, D. F., 1962, Concrete Technology, John Wiley and Sons, New York.
- PARSONS, J.D., 1966, Piling Difficulties in the New York Area, Proceedings, American Society of Civil Engineers, Volume 92(I), January 1966, New York.
- PECK, R.B., 1961, Records of Load Tests on Friction Piles, Special Report Number 67, HRB, National Research Council, Washington, D.C.
- PECK, R.B., 1958, A Study of the Comparative Behaviour of Frictional Piles, Highway Research Board, Special Report 38.
- POTYONDY, 1961, Skin Friction Between Soils and Construction Materials, Geotechnique, Volume XI, London.
- REESE, L.C., 1964, Load versus Settlement for an Axially Loaded Pile, Proceedings of the Roorkee Symposium on Bearing Capacity of Piles, Part 2, Cement and Concrete, New Delhi, India.
- RENNIE, R.J., 1966, Residual Strength of a Clay Till Applied to Little Smoky River Landslide, M.Sc. Thesis (Unpublished), University of Alberta.
- SALAS, J.A.J. and BELZUNCE, J.A., 1965, Resolution theorique de la distribution des forces dans des pieux, Proceedings, Sixth International Conference on Soil Mechanics and Foundation Engineering, Montreal.
- SCHMITTER, G., 1961, Neure Pfahlgrundungen, Swiss Civil Engineering Journal, Volume 79, Number 2, Zurich.
- SCOTT, R.F., 1962, Principles of Soil Mechanics, Addison Wesley Publishing Company Incorporated, Reading, Massachusetts (U.S.A.).

- SEED, H.B. and REESE, L.C., 1955, Pressure Distribution Along Friction Piles, ASTM Proceedings, Volume 55.
- SEED, H. B. and REESE, L. C., 1957, The Action of Soft Clay Along Friction Piles, Transactions, American Society of Civil Engineers, Volume 122, New York.
- SHIELDS, GRAY and EVANS, R. C., Piling, Concrete Publications, London.
- SKEMPTON, A. W., 1942, An Investigation of the Bearing Capacity of Soft Clay Soil, Journal of the Institution of Civil Engineers, Volume 18, Number 5, London.
- SKEMPTON, A. W., 1951, The Bearing Capacity of Clays, Building Research Conference, Proceedings, Volume 1.
- SKEMPTON, A. W., 1959, Cast-in-situ Bored Piles in London Clay, Geotechnique, Volume IX, London.
- SKEMPTON, A. W., 1964, The Long Term Stability of Clay Slopes in London Clay, Proceedings, Fourth International Conference on Soil Mechanics and Foundation Engineering, London.
- SKEMPTON, A. W., 1966, Summing Up Comments, Symposium on Large Bored Piles, Institution of Civil Engineers, London.
- SKEMPTON, A. W. and BJERRUM, L., 1957, A Contribution to the Settlement Analysis of Foundations on Clay, Geotechnique, Volume VII, London.
- SODERBERG, L. O., 1962, Consolidation Theory Applied to Foundation Pile Time Effects, Geotechnique, Volume XII, London.
- SOWERS, G. F., 1961, The Bearing Capacity of Friction Pile Groups in Homogeneous Clay from Model Studies, Proceedings, Fifth International Conference on Soil Mechanics and Foundation Engineering, Paris.
- SOWERS, G. F. and FAUSOLD, M., 1961, The Bearing Capacity of Friction Pile Groups in Homogeneous Clay from Model Studies, Proceedings, Fifth International Conference on Soil Mechanics and Foundation Engineering, Paris.
- TAYLOR, D. W., 1948, Fundamentals of Soil Mechanics, Asia Publishing House, Bombay.
- TENG, W. C., 1962, Foundation Design, Prentice-Hall, New Jersey.
- TERZAGHI, K., 1942, Discussions on Pile Driving Formulas, Proceedings, American Society of Civil Engineers, New York.
- TERZAGHI, K., 1943, Theoretical Soil Mechanics, John Wiley and Sons, New York.

- TERZAGHI, K. and PECK, R. B., 1967, Soil Mechanics in Engineering Practice, John Wiley and Sons, New York.
- THURMAN, A. G. and D'APPOLONIA, E., 1965, Computed Movement of Friction and End Bearing Piles Embedded in Uniform and End-Bearing Piles, 1965, Proceedings, Sixth International Conference on Soil Mechanics and Foundation Engineering, Montreal.
- TOMLINSON, M. J., 1957, The Adhesion of Piles Driven in Clay Soils, Proceedings, Fourth International Conference on Soil Mechanics and Foundation Engineering, Volume 2, London.
- TOMLINSON, M. J., 1963, Foundation Design and Construction, Pitman and Sons, London.
- TROW, W. A., 1967, Analysis of Pile Load Test Results, Proceedings, Canadian Good Roads Association, Forty-Eighth Annual Convention.
- TSCHEBOTARIOFF, G. P., 1951, Soil Mechanics, Foundations and Earth Structures, McGraw-Hill Book Company, New York (First Edition, 1951).
- VAN DER VEEN, C., 1953, The Bearing Capacity of a Pile, Proceedings, Third International Conference on Soil Mechanics and Foundation Engineering, Zurich.
- VAN WEELE, A. F., 1957, A Method of Separating the Bearing Capacity of a Test Pile into Skin Friction and Point Resistance, Proceedings, Fourth International Conference on Soil Mechanics, London.
- VESIC, A. S., 1967, Ultimate Loads and Settlements of Deep Foundations, Symposium on Bearing Capacity and Settlement of Foundations, Duke University, U.S.A.
- WARD, W. H., 1961, A Hardening Effect of Concrete on Clay, Geotechnique, Volume II, London.
- WATERWAYS EXPERIMENT STATION, 1950, Pile Loading Tests, Combined Morganza Floodway Control Structure, Technical Memorandum Number 3-308, Vicksburg.
- WENTWORTH, SHIELDS, GRAY and EVANS, 1960, Concrete Materials, Concrete Publications, London.
- WESTERN CAISSONS FOUNDATIONS LIMITED, 1966, General Report---Bulletin on Pile and Caisson Foundations, Saskatoon.
- WHITAKER, T., 1957, Experiments with Model Piles in Groups, Geotechnique, Volume VII, London.
- WHITAKER, T., 1962, One Hundred Ton Load Cell for Pile Loading Tests, Engineering, Number 194.

- WHITAKER, T. and COOKE, R. W., 1961, A New Approach to Pile Testing, Proceedings, Fifth International Conference on Soil Mechanics and Foundation Engineering, Volume II, Paris.
- WHITAKER, T. and COOKE, R. W., 1965, Bored Piles with Enlarged Bases in London Clay, Sixth International Conference on Soil Mechanics and Foundation Engineering, Montreal.
- WHITAKER, T. and COOKE, R. W., 1966, An Investigation of Shaft and Base Resistance of Large Bored Piles in London Clay, Symposium on Large Bored Piles, Institution of Civil Engineers, London.
- WILSON, G., 1941, The Calculation of Bearing Capacity of Footings on Clay, Journal of the Institute of Civil Engineers, Volume 17, London.
- WILSON, S. D., 1962, The Use of Slope Measuring Devices to Determine Movements in Earth Masses, Field Testing of Soils, ASTM S.T.P. 322.
- WOODWARD, R. J., LUNDGREN, R. and BOITANO, J. D., 1961, Pile Loading Tests in Stiff Clays, Proceedings, Fifth International Conference on Soil Mechanics and Foundation Engineering, Paris.
- WU, T. H., 1966, Soil Mechanics, Allyn and Bacon, Boston.

APPENDIX A

DESIGN OF THE LOAD CELL, PROPERTIES OF CELL MATERIAL,

GAGE CONNECTIONS AND CALIBRATION CURVES

(SCALED PILES IN SILT)

PROPERTIES[†] OF ALUMINUM ALLOY: 65 S-T6

(at 25° C)

- | | |
|--------------------------------------|---|
| 1. Ultimate tensile strength: | 46.5 x 10 ³ psi. |
| 2. Yield Strength: | 40.0 x 10 ³ psi. |
| 3. Modulus of Elasticity: | 10.0 x 10 ⁶ psi. |
| 4. Brinell Hardness Number: | 95 |
| 5. Ultimate Shear Strength: | 30 x 10 ³ psi. |
| 6. Compressive Yield Strength: | approximately the same
as for tension for short
cylinders (i.e., small
$\frac{l}{r}$ ratio). |
| 7. Coefficient of Thermal Expansion: | $\alpha = 0.0000238/^{\circ}\text{C}.$ |

- NOTES:
1. Yield strength taken at 0.2% of original gage length,
 2. Main alloying constituent: magnesium or magnesium silicate

[†]From Handbook of Aluminium, Aluminium Company of Canada, 1961.

LOAD-CELL DESIGN

Material: Aluminum Grade 65 S-T6.

Desired Sensitivity: 1 lb. load on the cell indicating a strain of
1 micro-inch/inch.

Try: 4 solid cylinders

Gage-length of the available strain-gage (in the Structures Lab) = $\frac{1}{2}$ inch.

Assuming one gage to be mounted on each cylinder, and with separate indicator reading for each gage (ignoring the effect of Poisson's ratio for rough calibrations), sectional area for each pillar needed,

$$A = \frac{PL}{E\epsilon} = \frac{1 \times \frac{1}{2}}{10 \times 10^6 \times 1 \times 10^{-6}}$$

$$= 0.05 \text{ in.}^2,$$

giving a diameter of 0.252 in.

Since the minimum trim width of the gage under consideration is $11/32$ in., it was feared that during mounting it might get stretched laterally and so get damaged. It was therefore decided to raise the diameter to the practical minimum of 0.3 in. ($A = 0.071 \text{ in.}^2$).

Total load expected to be transferred to the tip in the case of belled-out pile was estimated to be roughly of the order of 4000 lbs.

$$\begin{aligned}\text{Estimated maximum stress} &= \frac{4000}{0.284} \\ &= 14,100 \text{ lbs./in.}^2,\end{aligned}$$

which is well within the elastic range for the material.

Practical minimum length of the pillars from considerations of gage-installation is about 1.5 in. This gives length/diameter ratio of 5 which is quite satisfactory for a short cylinder under compressive loads.

$$\text{Strain for } \frac{1}{2}'' \text{ gage length} = \frac{14100}{10 \times 10^6} \times \frac{1}{2} = 705 \times 10^{-6} \text{ in.}$$

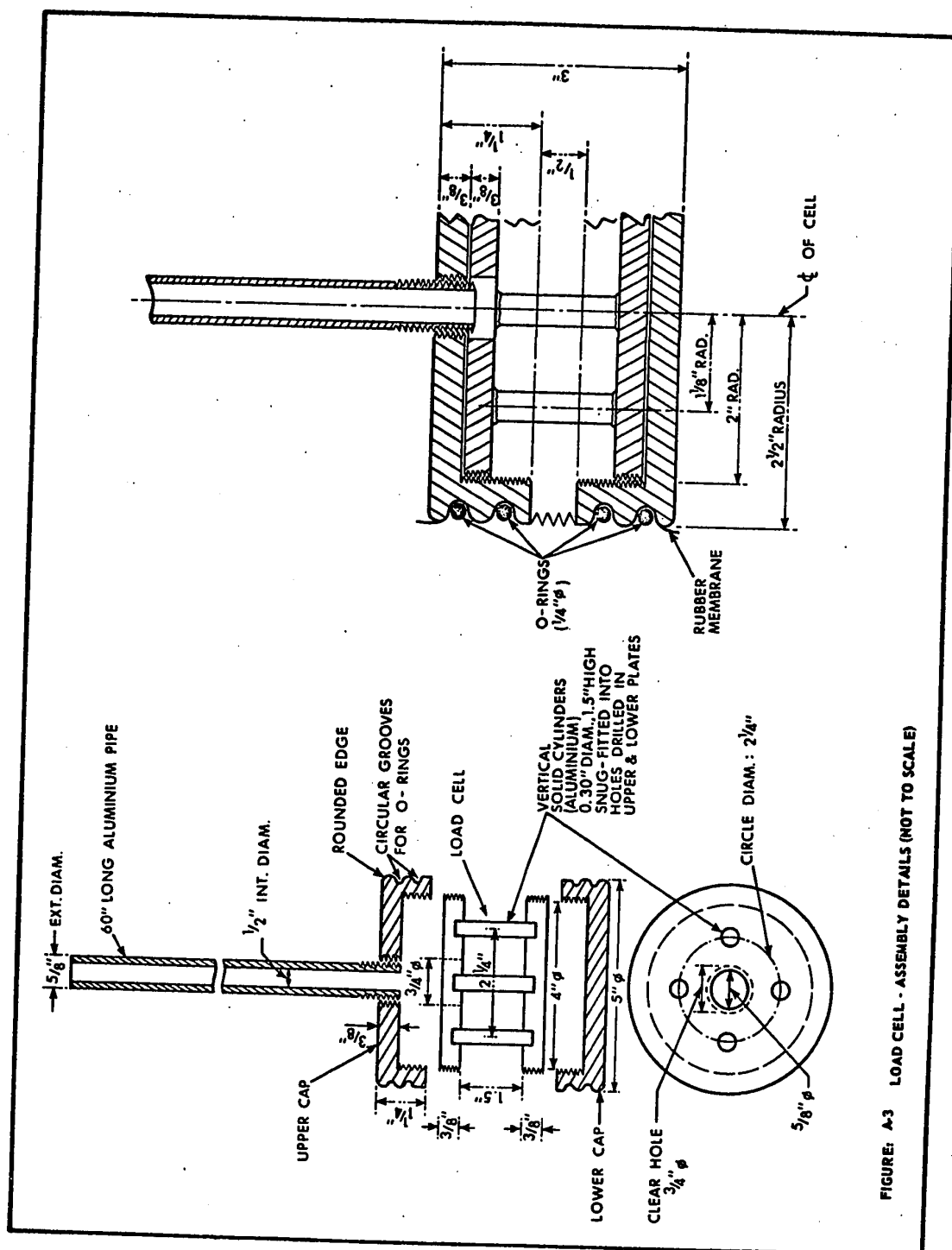
which is well within the recording range of the indicator..

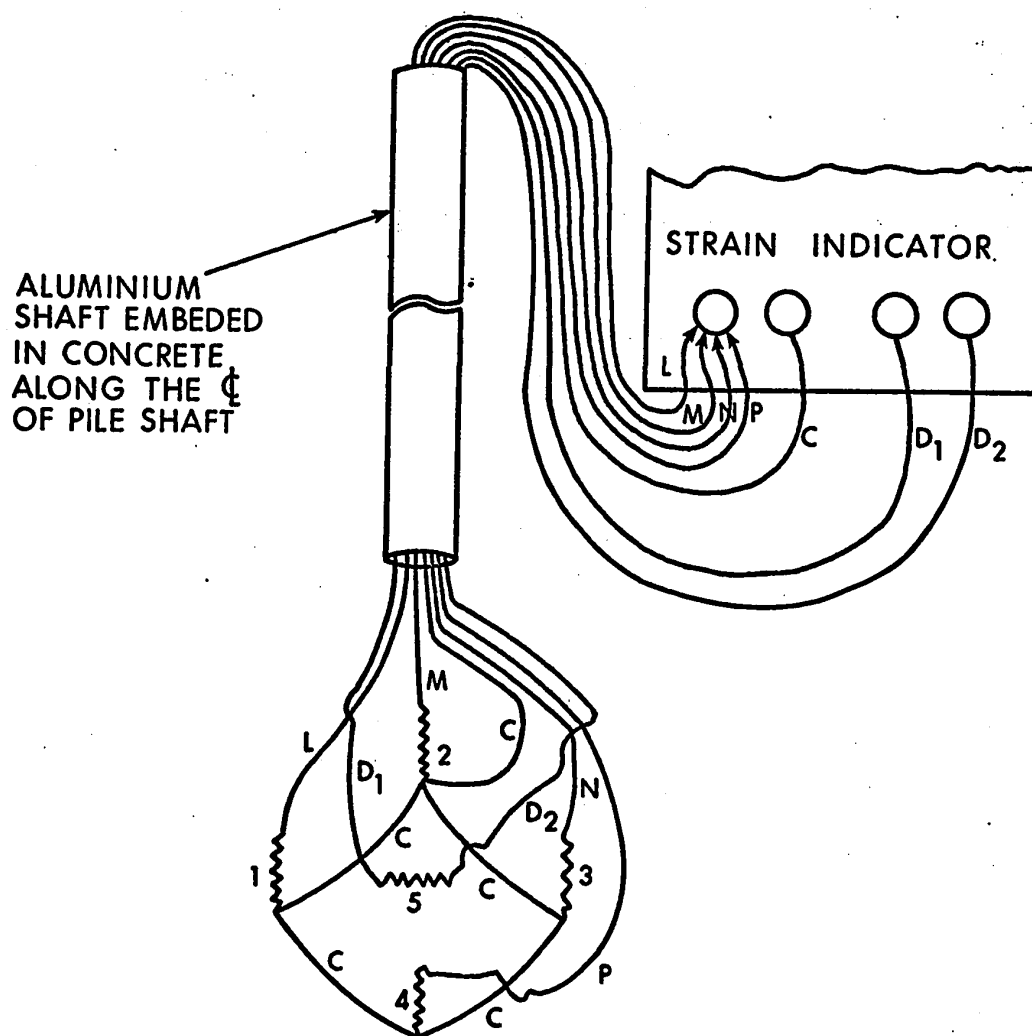
Total strain for one pound load at the top of cell, therefore, shall equal

$$\frac{705}{4000} \times 4, \text{ i.e., } 0.705 \mu\text{-in.}$$

∴ PROPOSED CELL:

- 4 solid aluminum 65 S-T6 cylinders, 0.30 in. diameter, 1.5 in. high snug-fitted into holes in the two parallel plates, each 3/8 in. thick;
- 4 strain gages (with one dummy-compensating gage) having a gage length of 1/2 inch (grid width: 9/64 in.).





LEGEND

- 1, 2, 3, 4. GAGES MOUNTED ON PILLARS.
- 5. DUMMY (TEMP. COMPENSATING) GAGE.
- C COMMON LEAD (ACTIVE).
- L, M, N, P INDIVIDUAL LEADS FROM GAGES (ACTIVE).
- D₁ D₂ LEADS FROM THE DUMMY GAGE,

FIGURE: A-4 GAGE CONNECTIONS WITHIN THE CELL (PILES IN PIT SILT)

CALIBRATION DATA FOR LOAD CELL I

Load in Lbs.	STRAIN GAGE NUMBER											
	1			2			3			4		
	Reading on the Indicator	Net Deflection (μ -in.)		Reading on the Indicator	Net Deflection (μ -in.)		Reading on the Indicator	Net Deflection (μ -in.)		Reading on the Indicator	Net Deflection (μ -in.)	
		Ini- tial	Ad- justed		Ini- tial	Ad- justed		Ini- tial	Ad- justed		Ini- tial	Ad- justed
0	12,320	0	0	12,800	0	0	11,045	0	0	12,200	0	0
500	11,685	635	629	12,540	260	255	11,200	-155	-152	12,080	120	114
1,000	11,325	995	983	12,315	485	475	11,090	-45	-40	11,890	310	298
1,500	10,995	1,325	1,307	12,090	710	695	10,930	115	107	11,720	480	462
2,000	10,700	1,620	1,596	11,900	900	880	10,770	275	271	11,535	665	641
2,500	10,415	1,905	1,875	11,740	1,060	1,035	10,595	450	436	11,335	865	835
3,000	10,130	2,190	2,154	11,565	1,235	1,204	10,410	635	418	11,110	1,090	1,054
3,500	9,880	2,440	2,398	11,420	1,380	1,343	10,250	795	776	10,910	1,290	1,248
4,000	9,590	2,730	2,682	11,250	1,550	1,507	10,070	975	954	10,665	1,535	1,487
4,500	9,350	2,970	2,916	11,130	1,670	1,621	9,945	1,100	1,077	10,490	1,710	1,656
5,000	9,150	3,170	3,110	10,990	1,810	1,755	9,790	1,225	1,230	10,315	1,885	1,825
0	12,380			12,855			11,070			12,260		

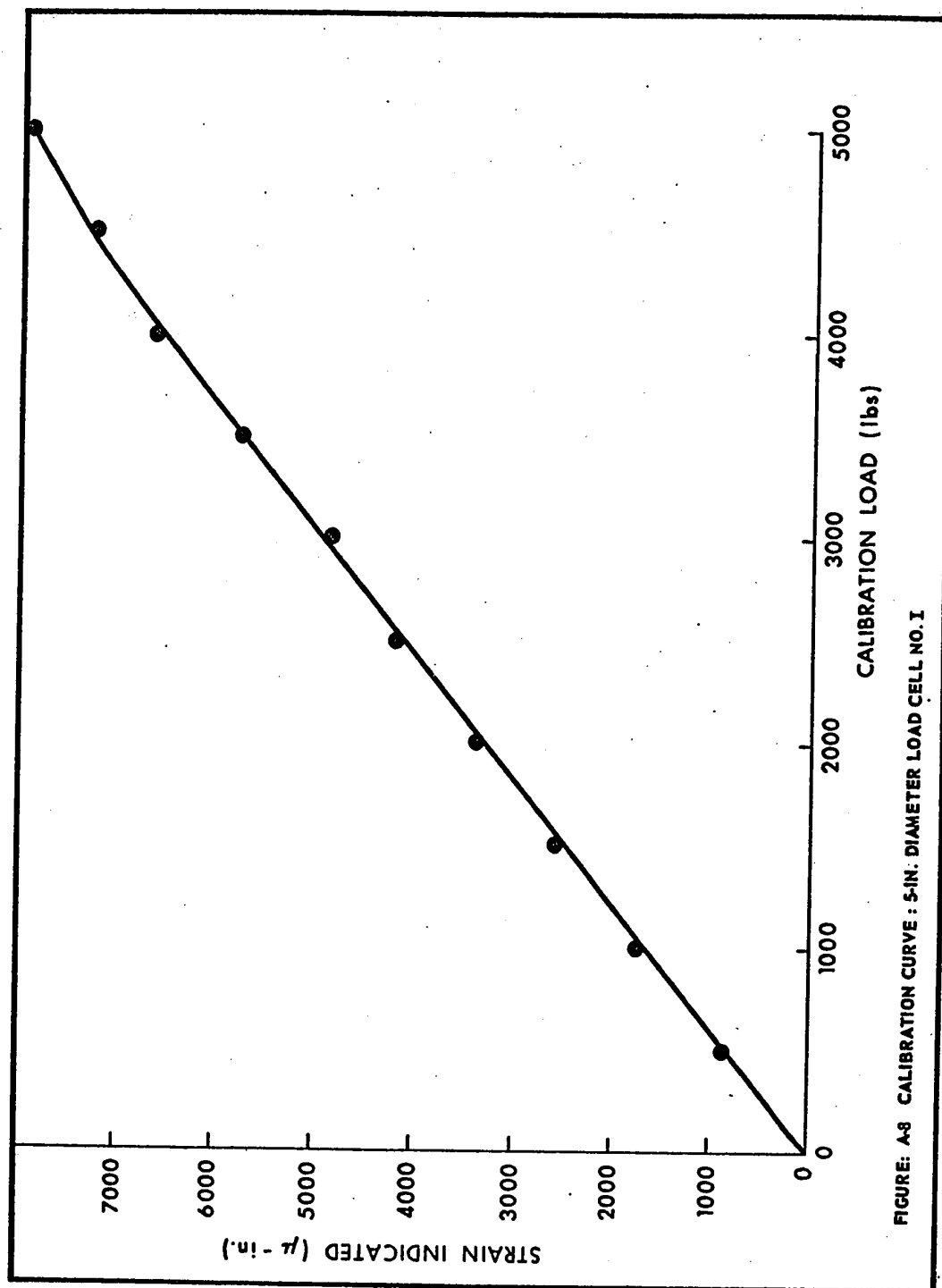
CALIBRATION DATA FOR LOAD CELL II

Load in Lbs.	STRAIN GAGE NUMBER											
	5				6				7			
	Reading on the Indicator	Net Deflection (-in.)		Reading on the Indicator	Net Deflection (-in.)		Reading on the Indicator	Net Deflection (-in.)		Reading on the Indicator	Net Deflection (-in.)	
		Ini- tial	Ad- justed		Ini- tial	Ad- justed		Ini- tial	Ad- justed		Ini- tial	Ad- justed
0	12,935	0	0	12,445	0	0	12,365	0	0	12,700	0	0
500	12,540	395	395	12,360	85	84	11,850	515	514	12,670	30	29
1,000	12,265	670	670	12,180	265	263	11,500	865	863	12,635	65	63
1,500	12,030	905	905	12,010	435	432	11,230	1,135	1,132	12,590	110	107
2,000	11,765	1,170	1,170	11,810	635	631	11,010	1,355	1,351	12,500	200	196
2,500	11,550	1,385	1,385	11,650	795	790	10,830	1,535	1,530	12,410	290	285
3,000	11,325	1,610	1,610	11,500	945	940	10,670	1,695	1,690	12,330	370	364
3,500	11,150	1,785	1,785	11,335	1,110	1,105	10,510	1,855	1,850	12,260	440	433
4,000	10,980	1,955	1,955	11,200	1,245	1,240	10,405	1,960	1,955	12,180	520	512
4,500	10,800	2,135	2,135	11,050	1,395	1,390	10,280	2,085	2,080	12,100	600	591
5,000	10,615	2,320	2,320	10,890	1,555	1,550	10,145	2,220	2,215	12,020	680	670
0	12,935			12,440			12,360			12,690		

DATA FOR PLOTTING CALIBRATION CURVES

(Cells: I and II)

LOAD in lbs.	NET TOTAL STRAIN (micro-inches)	
	<u>CELL I</u>	<u>CELL II</u>
0	0	0
500	846	1,022
1,000	1,710	1,859
1,500	2,571	2,576
2,000	3,388	3,348
2,500	4,181	3,990
3,000	4,830	4,604
3,500	5,765	5,173
4,000	6,630	5,662
4,500	7,270	6,196
5,000	7,920	6,755



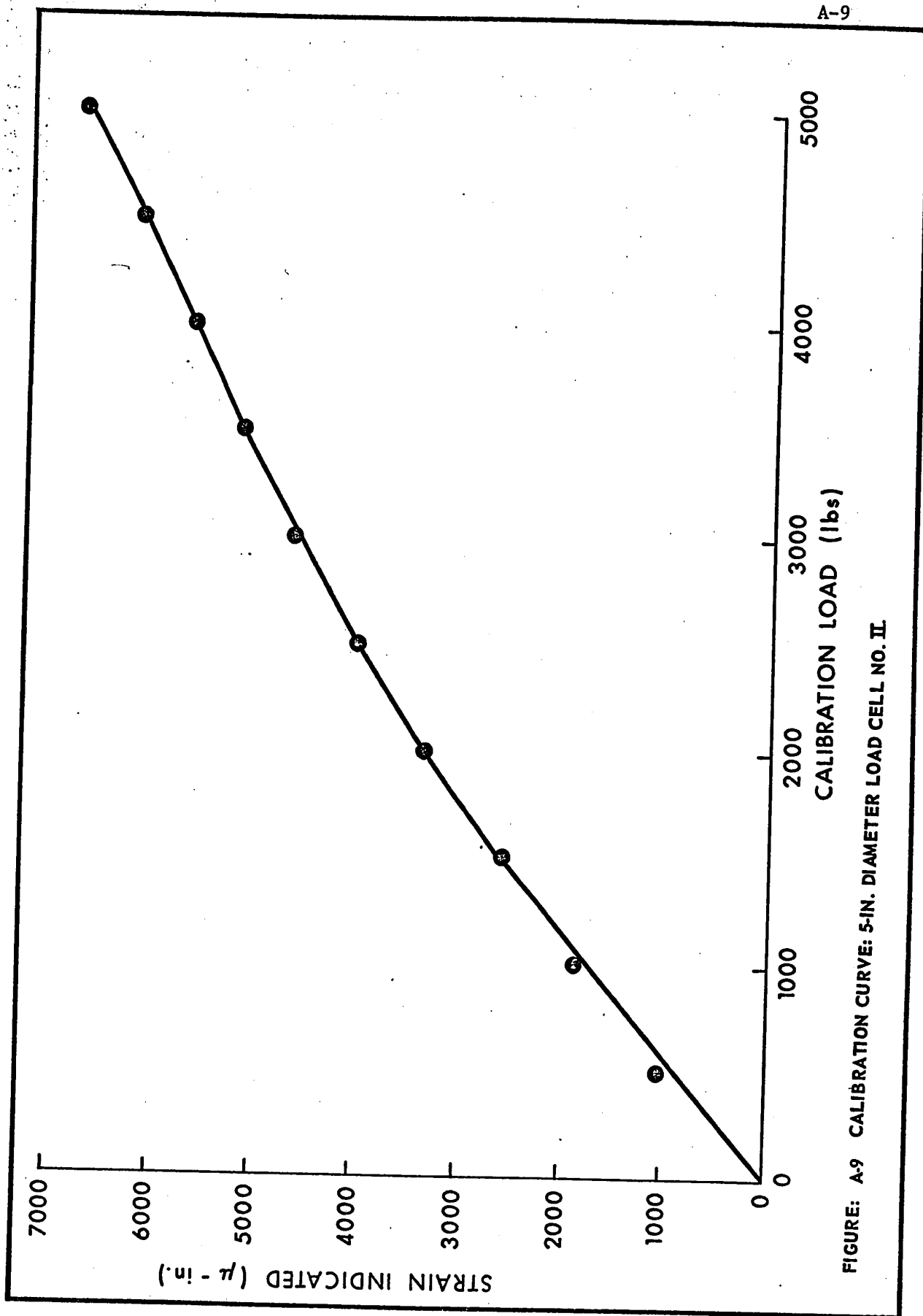


FIGURE: A-9 CALIBRATION CURVE: 5-IN. DIAMETER LOAD CELL NO. II

APPENDIX B

CONCRETE MATERIALS, MIX-DESIGN, CYLINDER STRENGTH

(PILES IN SILT)

COARSE AGGREGATE ANALYSIS

(Concrete Mix)

<u>Sieve Size</u>	<u>Weight Retained (lbs.)</u>	<u>% Retained</u>	<u>Cumulative % Retained</u>
1"	0	0	0
3/4"	0.30	1.1	1.1
3/8"	15.63	58.4	59.5
#4	10.03	37.5	97.0
Pan	0.80	3.0	100.0
Total	26.76	100.0	

FINE AGGREGATE ANALYSIS

(Concrete Mix)

Wt. sample unwashed: 580.8 gm. : (100.0)
 Wt. sample washed: 566.4 gm. : (97.5)
 Wt. passing - 200 ASTM sieve: 14.4 gm. : (2.5)

Sieve No.	Wt. Retd. (gm.)	Percentage Wt. Retd.	Cumulative % Retd.
3/8"	0.0	0.0	0.0
4	17.5	3.0	3.0
8	85.2	14.7	17.7
16	54.6	9.5	27.7
30	60.0	10.3	37.5
50	208.4	35.8	73.3
100	122.9	21.1	94.4
Pan	17.8	3.1	97.5
Silt	14.4	2.5	100.0
Total	580.8	100.0	253.1

Fineness Modulus (F.M.) = 2.53.

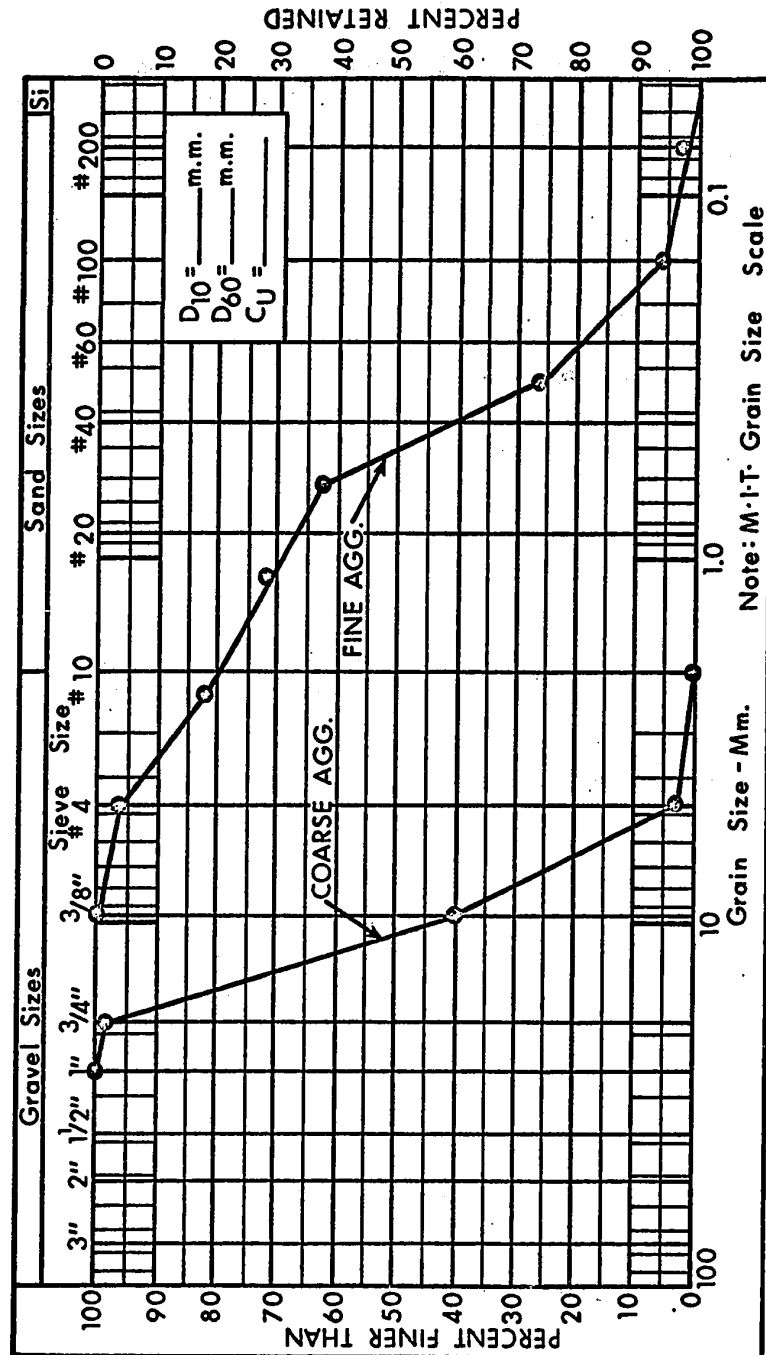


FIGURE: B-3 GRADATION CURVES FOR COARSE AND FINE AGG. (CONCRETE MIX)

CONCRETE MIX DESIGN

Quantity of Concrete Needed:

$$\frac{\pi (5)^2}{4} \times 50 \times \frac{1}{(12^3)} = 0.67 \text{ cft. per pile}$$

General Requirements:

Small Slump--water/cement ratio to be just adequate for complete hydration of cement--water proportion to be such that vapour-pressure gradients set up between concrete and the surrounding mix are the minimum.

Strength Requirements:

Maximum Load Expected: 5 tons

Sectional Area of the Pile: 19.7 in.^2

Intensity of Loading: $5 \times 2240/19.7$
 $= 565 \text{ lbs./in.}^2 \text{ (maximum)}$

Crushing Strength Requirement: 3×565
 or (say) 1700 lbs./in.^2

Early development of strength necessary.

28-Day Strength Requirement: 3000 lbs./in.^2 (giving approximately $2/3$ rd. strength, i.e., about 2000 lbs./in.^2 after 7 days).

Quantity of Water Needed (Canada Cement)

$= 6\frac{1}{2} \text{ imp. gallons per bag of cement used.}$

Quantities of Materials (3/4-in. maximum size for coarse aggregate and F.M. of 2.50 for fine aggregate):

water:	37 gallons per cu. yd. of concrete,
cement:	5.9 bags per cu. yd. of concrete,
fine aggregate:	1490 lbs. per cu. yd. of concrete,
coarse aggregate:	1460 lbs. per cu. yd. of concrete.

--Properties to be adjusted to give a slump of 3" to 4", duly taking into account the initial moisture content of the aggregates.

COMPRESSIVE STRENGTH OF CONCRETE

(at seven days)

Concrete for Pile	Slump (in.)	Ultimate (Crushing) Strength (lbs.)	Unit Ultimate Strength (lbs./in. ²)
A	3	58,500	2,070
B	4	55,500	1,970
C	2 3/4	79,500	2,820
D	3 1/2	65,600	2,320
E	4	64,000	2,260

APPENDIX C

ENGINEERING PROPERTIES OF PIT SOIL AND

TYPICAL STRENGTH PLOTS

ENGINEERING PROPERTIES OF PIT SOIL

1. Particle-Size Distribution (M.I.T. Scale):

Sand size particles (> 0.06 mm.): 7%,
 Silt size particles (0.06 to 0.002 mm.): 86%,
 Clay size particles (< 0.002 mm.): 7%.

$$D_{10} = 0.0036 \text{ mm.}$$

$$D_{60} = 0.029 \text{ mm.}$$

$$c_u = \frac{D_{60}}{D_{10}} = 12.4$$

2. Specific Gravity: 2.70.

3. Atterberg Limits:

Liquid limit (W_L): 34.2%,
 Plastic Limit (W_P): 21.9%,
 Shrinkage Limit (W_S): 19.0%,
 Plasticity Index (I_P): 12.3.

4. Compaction:

	<u>o.m.c.</u>	<u>Maximum Dry Density</u>
Standard Proctor:	21.5%	100.7 lbs./ft. ³
Modified AASHO:	15.3%	113.0 lbs./ft. ³

5. Unconfined Compressive Strength (for soil remolded at Standard Proctor conditions):

$$\text{average: } 6.4 \text{ lbs./in.}^2$$

6. Compressibility Characteristics (for soil remolded at Standard Proctor conditions):

Compression Index: $C_c = 0.143,$
 $C_s = 0.019.$

UNCONFINED COMPRESSION TEST

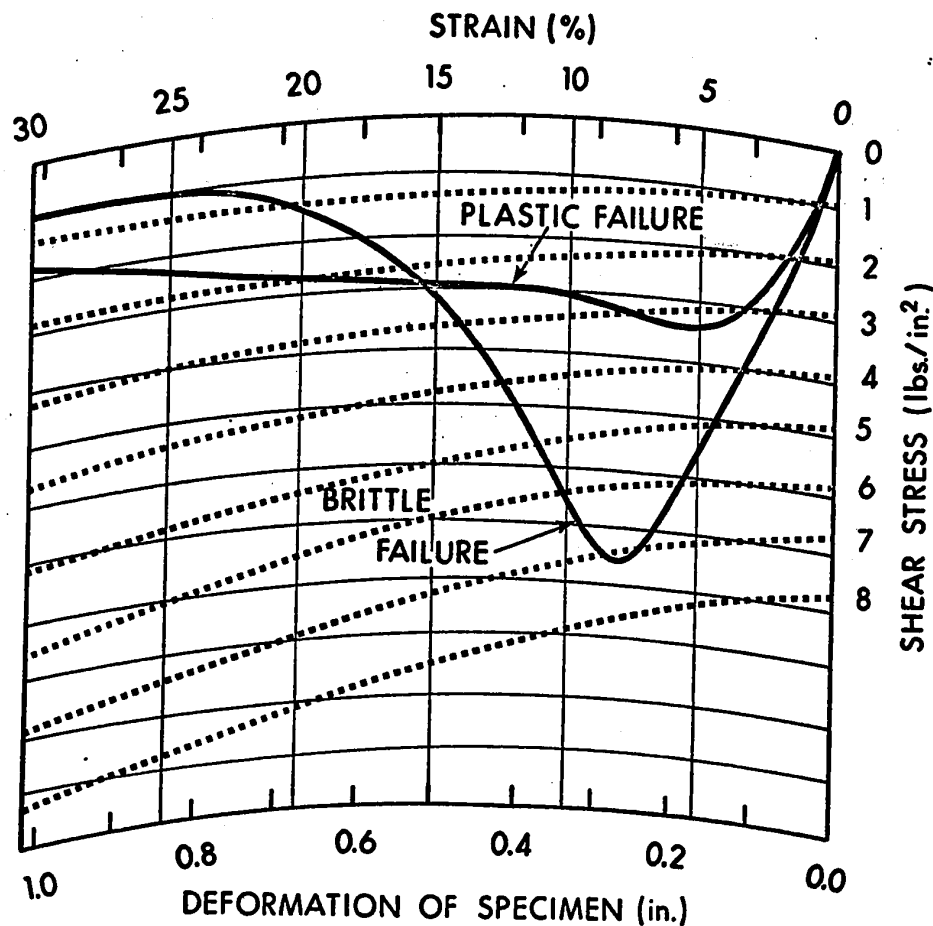
DATE:

SOIL TYPE: PLASTIC SILT

SPRING No. A-12

STIFFNESS 14.7 lbs./in.²

SAMPLE No.:



MOISTURE CONTENT CONTAINER No.:

MAXM. COMP

MOISTURE CONTENT % DRY DENSITY lbs./ft.³

STRESS:

3.5 lbs./in.²

(DOTTED LINES REPRESENT SUPERIMPOSED MASK.)

FIGURE: C-2 TYPICAL RESULTS ON THE BRITISH PORTABLE COMPRESSION TESTING MACHINE.

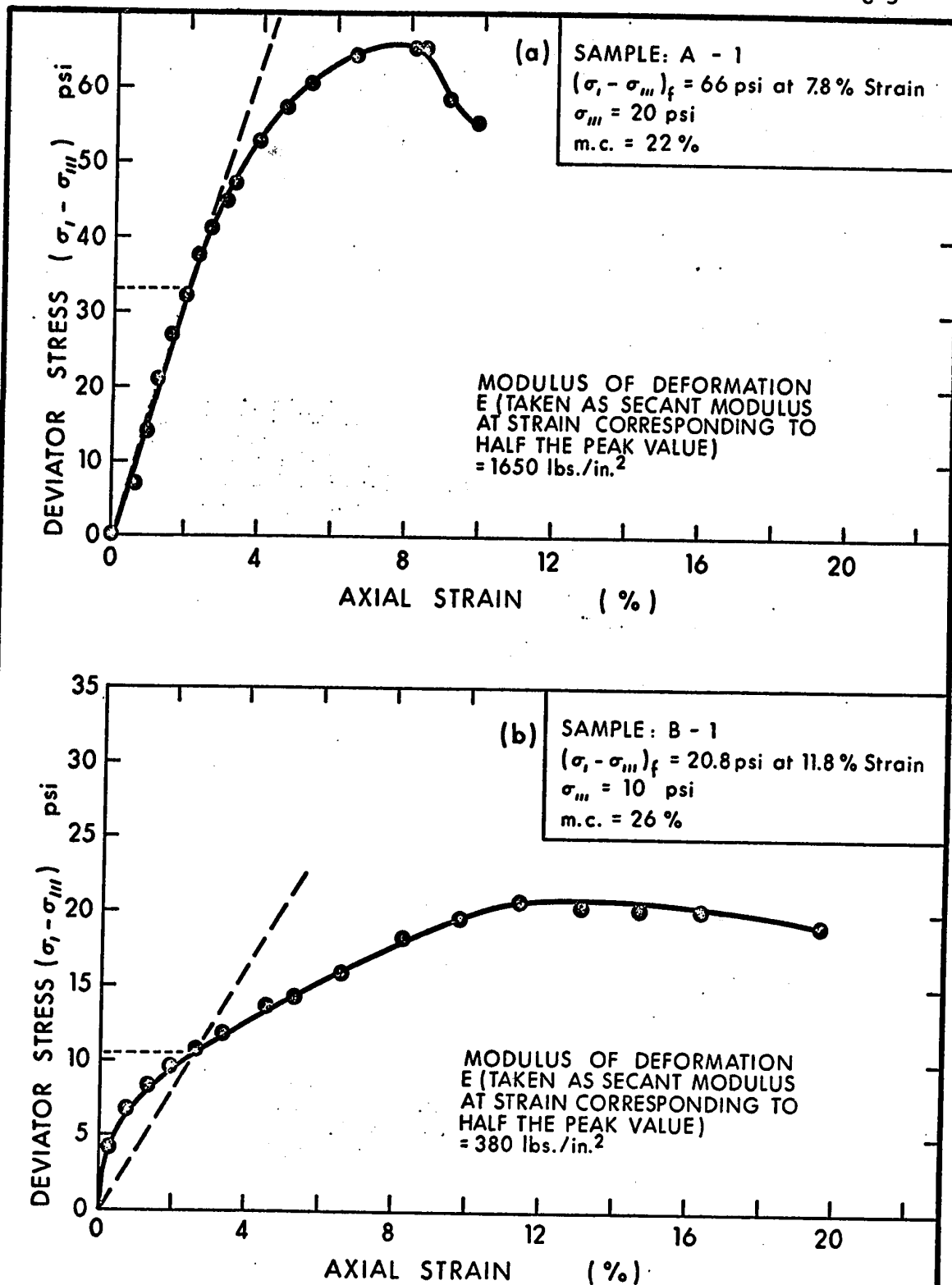


FIGURE: C-3 TYPICAL STRESS-STRAIN CURVES FOR PIT SILT.

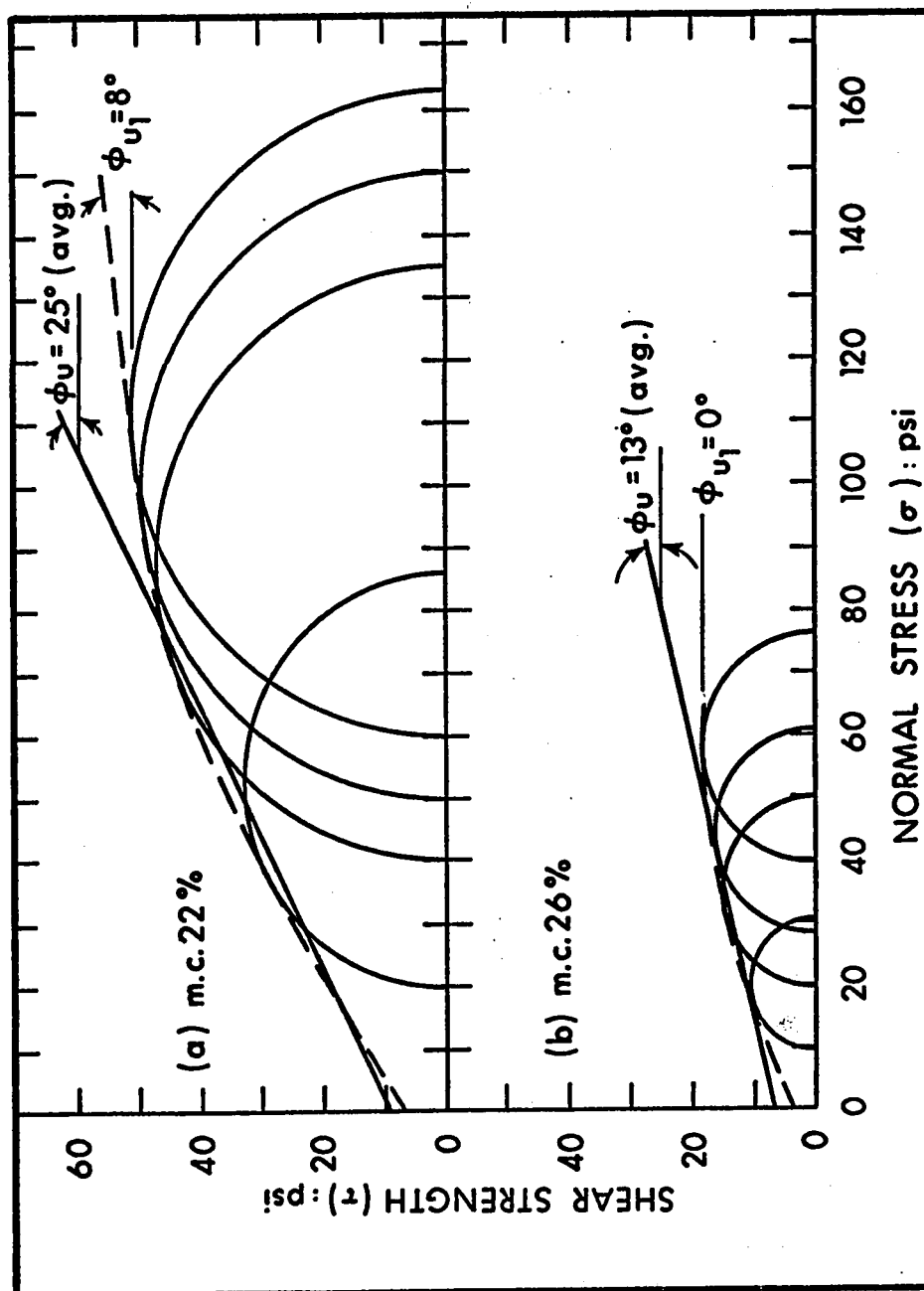


FIGURE C-4 MOHR'S ENVELOPES FOR TOTAL STRESSES - RESULTS OF UNDRAINED TRIAXIAL TESTS ON LAB - COMPACTED SAMPLES.

APPENDIX D

CALIBRATION CURVE AND DATA FOR 25-TON HYDRAULIC JACK

(SCALED PILES IN SILT)

DATA FOR HYDRAULIC JACK CALIBRATION

(1000 psi. gage)

Load on the Ram (lbs.)	Pressure Indicated (psi.)
-	-
500	90
1,000	132
2,000	230
3,000	321
4,000	420
5,000	510
6,000	602
7,000	698
8,000	792
9,000	888
10,000	982

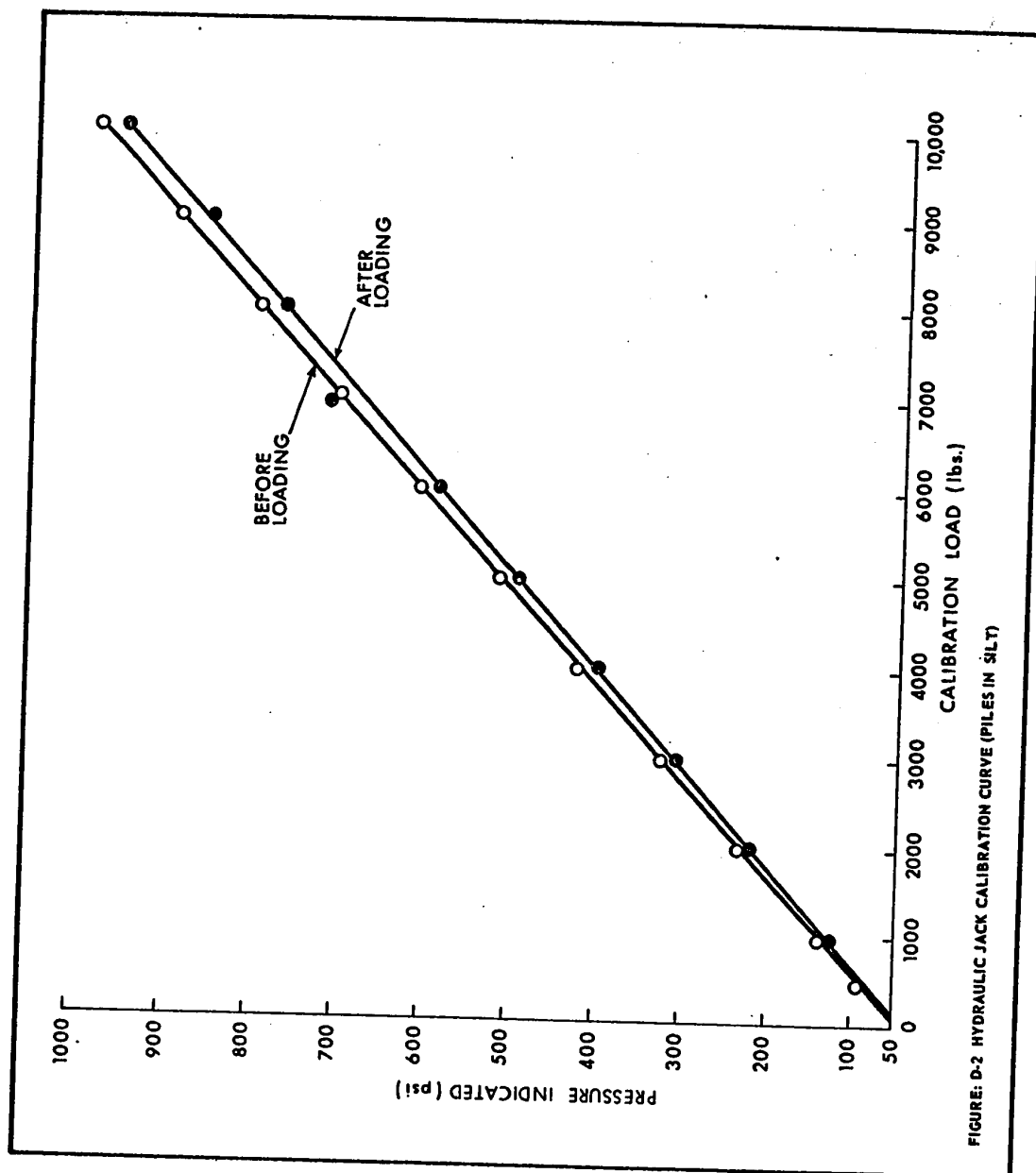


FIGURE D-2 HYDRAULIC JACK CALIBRATION CURVE (PILES IN SILTY)

APPENDIX E

LOAD TEST DATA

(SCALED PILES IN SILT)

LOAD TEST DATA FOR PILE B

Weight of hydraulic ram and other weights on pile: 150 lbs.

Initial Reading (before concreting)		Reading on the Indicator (Cell No. I)				Dial Gage Read- ing x 10 ³ in.
		Strain Gage Number				
		1	2	3	4	
Initial Reading (after concreting)		12,370	12,820	11,110	12,225	
		12,325	12,775	11,070	12,205	
LOADING						
Load (lbs.)	Reading on Pr. Gage (psi.)					
0		12,020	12,555	10,840	11,910	0.0
1,000	182	11,990	12,530	10,785	11,890	8.9
		11,990	12,530	10,785	11,890	9.1
		11,990	12,530	10,780	11,890	10.1
		11,990	12,530	10,785	11,890	11.0
		11,990	12,530	10,785	11,890	11.0
2,000	274	11,980	12,505	10,750	11,870	17.4
		11,980	12,505	10,745	11,870	21.0
		11,980	12,505	10,745	11,870	21.3
		11,980	12,505	10,745	11,870	21.9
		11,980	12,505	10,745	11,870	22.0
3,000	367	11,975	12,495	10,690	11,845	30.0
		11,970	12,490	10,680	11,845	35.0
		11,970	12,490	10,680	11,845	37.5
		11,970	12,490	10,680	11,845	38.0
		11,970	12,490	10,680	11,845	38.2
4,000	462	11,960	12,470	10,615	11,830	50.0
		11,955	12,455	10,590	11,840	60.0
		11,955	12,445	10,585	11,840	64.5
		11,955	12,445	10,580	11,840	67.5
		11,950	12,440	10,575	11,840	70.5
①	②	③	④	⑤	⑥	⑦

LOAD TEST DATA FOR PILE B (continued)

①	②	③	④	⑤	⑥	⑦
5,000	555	11,870	12,405	10,505	11,830	90
		11,855	12,365	10,495	11,810	131
		11,850	12,370	10,485	11,800	147
		11,860	12,379	10,488	11,800	159
		11,855	12,379	10,488	11,800	170
6,000	650	11,835	12,270	10,415	11,760	230
		11,840	12,305	10,440	11,740	352
		11,850	12,338	10,440	11,735	425
		11,850	12,340	10,450	11,735	490
		11,850	12,349	10,450	11,730	555
7,000	745	11,740	12,300	10,400	11,700	650
		11,745	12,300	10,400	11,700	860
		11,745	12,300			919
		11,745	12,295	10,900	11,700	935
		11,745	12,294	10,395	11,700	986
5,000†	555					956
3,000	367					945
0	90					964

†Unloading each increment at $\frac{1}{2}$ hour intervals.

LOAD TEST DATA FOR PILE C

Weight of hydraulic ram and other weights on the pile: 150 lbs.

Initial Reading (before concreting) Initial Reading (after concreting)		Reading on the Indicator (Cell No. II) Strain Gage Number				Dial Gage Reading $\times 10^3$ in.
		5	6	7	8	
		13,000	12,410	12,380	12,700	
		12,980	12,390	12,365	12,675	
LOADING						
Load (lbs.)	Reading on Pr. Gage (psi.)					
0	90	12,670	12,290	12,185	12,545	0.0
400	128	12,650	12,280	12,155	12,515	4.5
		12,640	12,270	12,150	12,525	5.0
		12,635	12,270	12,145	12,525	5.5
		12,630	12,270	12,145	12,525	6.0
		12,630	12,275	12,140	12,525	6.0
1,000	182	12,605	12,245	12,055	12,515	8.0
		12,615	12,255	12,065	12,515	9.0
		12,615	12,250	12,070	12,515	9.5
		12,615	12,245	12,075	12,510	10.0
		12,610	12,240	12,070	12,510	10.0
2,000	274	12,530	12,210	12,015	12,500	16.0
		12,540	12,220	12,025	12,510	17.5
		12,535	12,215	12,025	12,505	18.5
		12,555	12,229	12,030	12,510	19.0
		12,555	12,230	12,030	12,515	19.5
3,000	367	12,470	12,195	11,970	12,500	26.5
		12,480	12,195	11,980	12,500	28.5
		12,485	12,195	11,985	12,505	29.0
		12,485	12,195	11,985	12,505	29.0
		12,490	12,200	11,995	12,510	29.0
①	②	③	④	⑤	⑥	⑦

LOAD TEST DATA FOR PILE C (continued)

①	②	③	④	⑤	⑥	⑦
4,000	462	12,345	12,161	11,940	12,495	41.0
		12,390	12,160	11,940	12,495	46.0
		12,395	12,160	11,945	12,495	47.5
		12,390	12,155	11,945	12,495	48.5
		12,390	12,160	11,945	12,500	49.0
5,000	555	12,300	12,125	11,900	12,490	57.0
		12,300	12,120	11,890	12,485	65.0
		12,285	12,110	11,890	12,485	68.0
		12,290	12,115	11,890	12,490	70.0
		12,280	12,115	11,890	12,490	71.0
6,000	650	12,160	12,055	11,820	12,470	82.0
		12,130	12,035	11,795	12,460	107.0
		12,120	12,030	11,785	12,465	122
		12,130	12,030	11,780	12,455	130
		12,120	12,030	11,785	12,565	137
6,500	692	12,065	12,010	11,750	12,450	147
		12,050	12,005	11,745	12,450	189
		12,045	12,030	11,740	12,445	228
		12,070	12,035	11,735	12,445	247
		12,065	12,050	11,730	12,445	261
7,000	745	12,020	12,050	11,710	12,420	280
		12,040	12,080	11,710	12,410	360
		12,035	12,090	11,715	12,410	393
		12,030	12,100	11,715	12,410	415
		12,035	12,105	11,720	12,405	427
7,500	797	11,950	12,100	11,700	12,375	462
		11,945	12,120	11,700	12,365	540
		11,925	12,125	11,700	12,355	620
		11,925	12,135	11,710	12,360	681
		11,915	12,130	11,705	12,350	712
8,000	840	11,885	12,120	11,705	12,340	760
		11,860	12,140	11,710	12,330	845
		11,840	12,140	11,700	12,330	895
		11,830	12,140	11,700	12,330	935
		11,825	12,140	11,695	12,325	960
6,000	650					943
3,000	367					933
0	90					820

NET TOTAL STRAIN INDICATED FOR VARIOUS INCREMENTS OF LOADING

(Cell I under Pile B)

Total Load on Pile (lbs.)	Strain Recorded by Indicator (μ -in.)				
	Gage 1	Gage 2	Gage 3	Gage 4	Total
					Increase Cumulative
150	-	-	-	-	-
1,150	30	25	65	20	140
2,150	10	25	40	20	235
3,150	10	15	65	25	350
4,150	20	50	105	5	540
5,150	95	61	87	40	823
6,150	5	30	38	70	966
7,150	75	55	55	30	1,181

DATA FOR INCREMENT LOADING (TOTAL LOAD ON PILE) AND LOAD TRANSFERRED THROUGH CELL I (PILE B)

Average diameter of pile B = 5.15 in.

Pressure Indicated on Hyd. Jack Gage (psi.)	Total† Load (lbs.)	Net Total Strain Recorded on Indicator (μ-in.)	Load Transferred Through Load-Cell No. I (lbs.)	Settlement at the end of the loading increment	
				$\Delta \times 10^3$ (in.)	$\frac{\Delta}{B} \times 10^3$ (in.)
90	150	0	0	0	0
182	1,150	140	85	11	2.14
274	2,150	235	143	22	4.27
367	3,150	350	213	38.2	7.42
462	4,150	540	328	70.5	13.7
555	5,150	823	501	170	33.0
650	6,150	966	586	555	108
745	7,150	1,181	720	986	192
555	5,150	-	-	956	186
367	3,150	-	-	945	184
90	0 + 50	-	-	864	168

† Total load includes the weight of the hydraulic ram and any other weight placed at the top of the pile.

NET TOTAL STRAIN INDICATED FOR VARIOUS INCREMENTS OF LOADING

(Cell II under Pile C)

Total Load on Pile (lbs.)	Strain Recorded by Indicator (μ -in.)					
	Gage 3	Gage 4	Gage 5	Gage 6	Total	
					Increase	Cumulative
150	-	-	-	-	-	-
950	40	35	70	15	160	160
1,700	20	15	45	20	100	260
2,700	65	10	40	- 5	110	370
3,800	65	30	35	5	135	505
4,750	100	40	50	10	200	705
5,700	90	45	55	10	200	905
6,750	160	85	105	25	375	1,280
7,250	55	- 20	55	20	110	1,390
7,750	30	- 55	10	30	15	1,405
8,300	120	- 25	15	55	160	1,565
8,800	90	- 10	10	25	115	1,680

DATA FOR INCREMENT LOADING (TOTAL LOAD ON PILE) AND LOAD TRANSFERRED THROUGH CELL II (PILE C)

Average diameter of pile B = 5.31 in.

Pressure Indicated on Hyd. Jack Gage (psi.)	Total† Load (lbs.)	Net Total Strain Recorded on Indicator (μ-in.)	Load Transferred Through Load-Cell No. II (lbs.)	Settlement at the end of the loading increment	
				$\Delta \times 10^3$ (in.)	$\frac{\Delta}{B} \times 10^3$
-	150	-	0	-	-
128	950	160	50	6	1.15
182	1,700	260	80	10	1.92
276	2,700	370	120	19.5	3.74
367	3,800	505	180	29	5.55
462	4,750	705	280	49	9.40
555	5,700	905	410	71	13.6
650	6,750	1,280	670	137	26.3
692	7,250	1,390	730	261	50.1
745	7,750	1,405	750	427	81.9
797	8,300	1,565	840	712	137
840	8,800	1,680	930	960	186
650	6,750	-	-	943	184
367	3,800	-	-	933	182
90	0 + 150	-	-	820	160

†Total load includes the weight of the hydraulic ram and any other weight placed at the top of the pile.

DATA FOR LOAD TEST (PILE D)

Average diameter of pile, B = 5.25 in.

Pressure Indicated (psi.)	Total [†] Load (lbs.)	Settlement Dial Readings (in. x 10 ³)					$\frac{\Delta}{B} \times 10^3$
		Initial	After			Final	
		0 min.	7½ min.	15 min.	22½ min.	30 min. (Δ)	
90	50	-	-	-	-	-	-
128	1,050	5.1	6.0	6.2	6.3	6.4	1.22
182	1,550	7.6	8.9	9.3	9.8	10.3	1.96
274	2,550	17.4	21.1	21.2	21.3	21.4	4.08
367	3,650	26.0	31.1	33.0	33.8	34.5	6.57
462	4,650	39.0	45	47.5	48.5	50.5	9.61
555	5,550	68.0	75	79	81.5	82	15.6
602	6,050	90.0	120	130	140	150	28.6
650	6,600	165	220	260	290	310	58
697	7,050	330	390	440	475	510	97
745	7,600	520	635	670	705	733	140
555	5,550	-	-	-	-	725	138
367	3,650	-	-	-	-	709	135
90	0 + 50	-	-	-	-	604	115

[†]Total load includes the weight of the hydraulic ram supported at the top of pile.

٦

Average diameter of pile, B = 5.18 in.

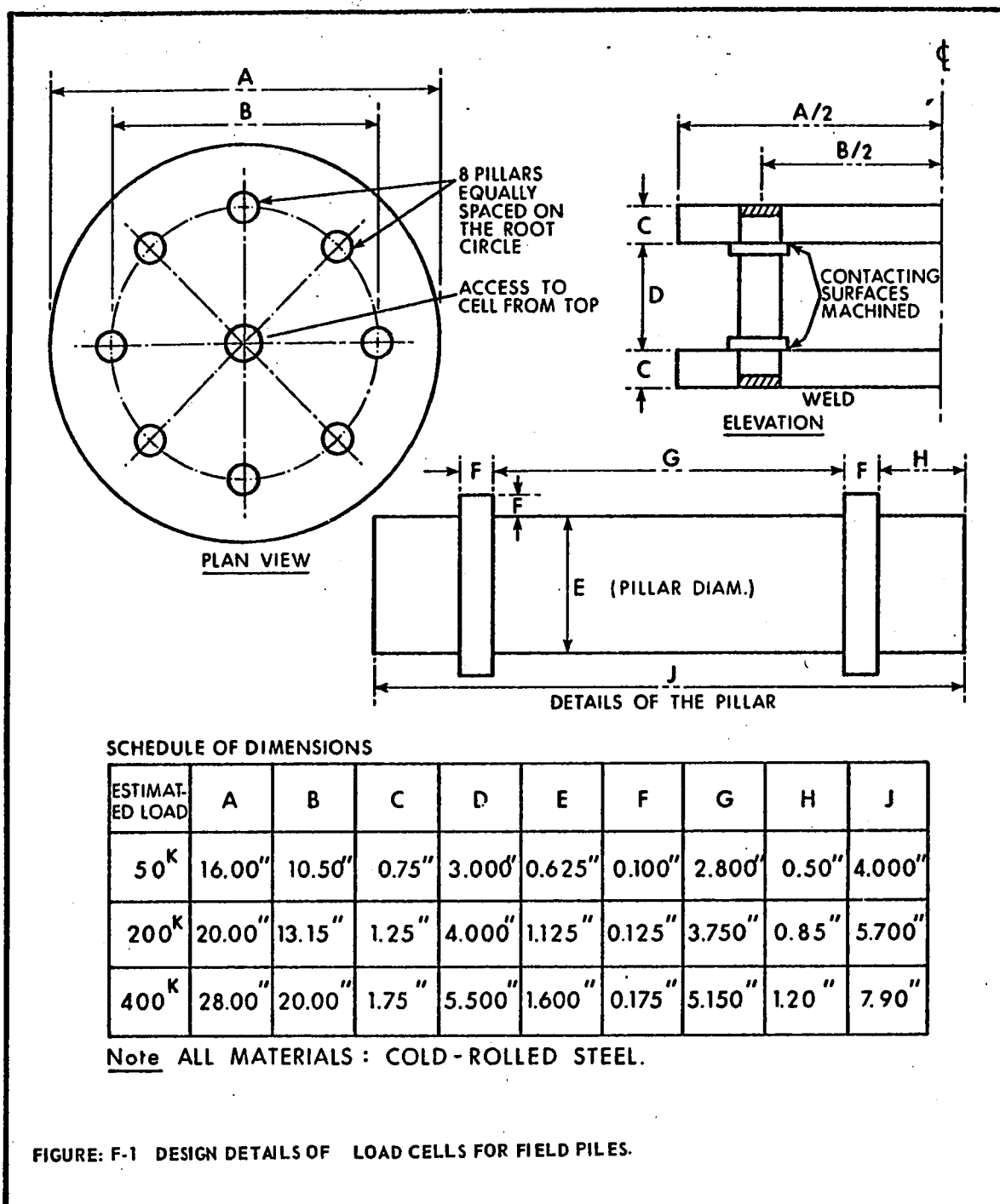
Pressure Indicated (psi.)	Total† Load (lbs.)	Settlement Dial Readings (in. x 10 ⁻³)					$\frac{\Delta}{B} \times 10^3$
		Initial 0 min.	After			Final 30 min. (Δ)	
			7½ min.	15 min.	22½ min.		
0	150	-	-	-	-	-	-
120	1,050	4.5	5.0	5.0	5.5	5.5	1.06
155	1,400	6.5	7.0	7.5	8.0	8.0	1.55
230	2,250	12.5	17	17.5	17.5	17.5	3.38
310	3,100	22	28	29	30	31.0	5.98
387	3,900	39	50	52	54	54.5	10.5
464	4,750	61	111	181	209	217.5	41.9
500	5,150	240	330	360	378	385	74.3
536	5,500	395	470	485	512	545	105
573	5,900	560	676	721	756	787	152
611	6,250	807	943	981	1,023	1,052	203
387	3,900	-	-	-	-	1,049	202
230	2,250	-	-	-	-	1,038	200
90	0 + 150	-	-	-	-	985	190

[†]Total load indicates the weight of hydraulic ram and other loads supported at the top of pile.

APPENDIX F

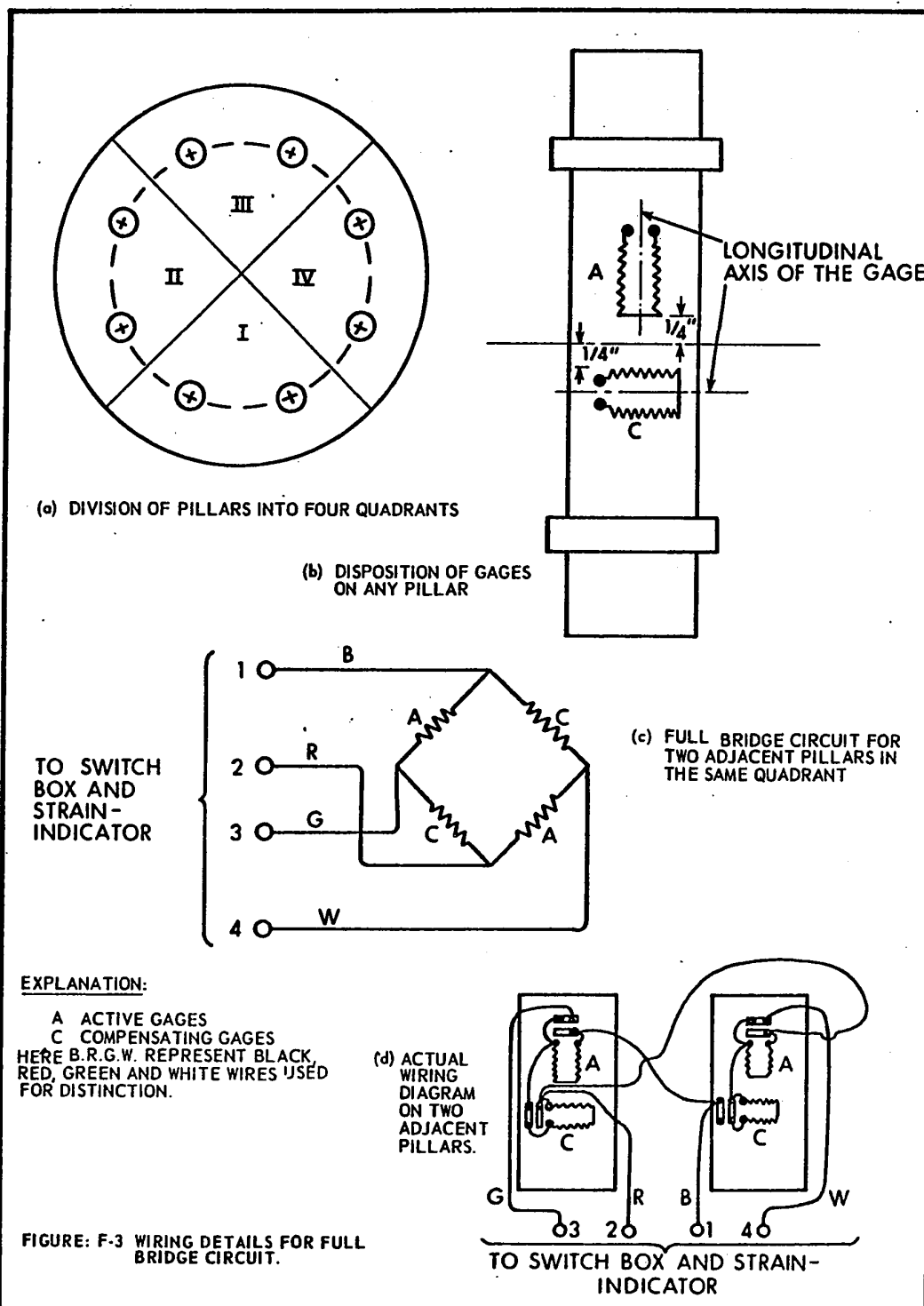
DESIGN AND FABRICATION DETAILS OF LOAD CELLS

FOR FIELD PILES



FINISHED DIMENSIONS OF LOAD CELLS

Nominal Diameter	Actual Overall Diameter	Actual Depth
(in.)	(in.)	(in.)
16	16.5	4.75
20 (A-1)	21.25	6.75
20 (A-2)	20.75	6.75
28	28.5	8.50



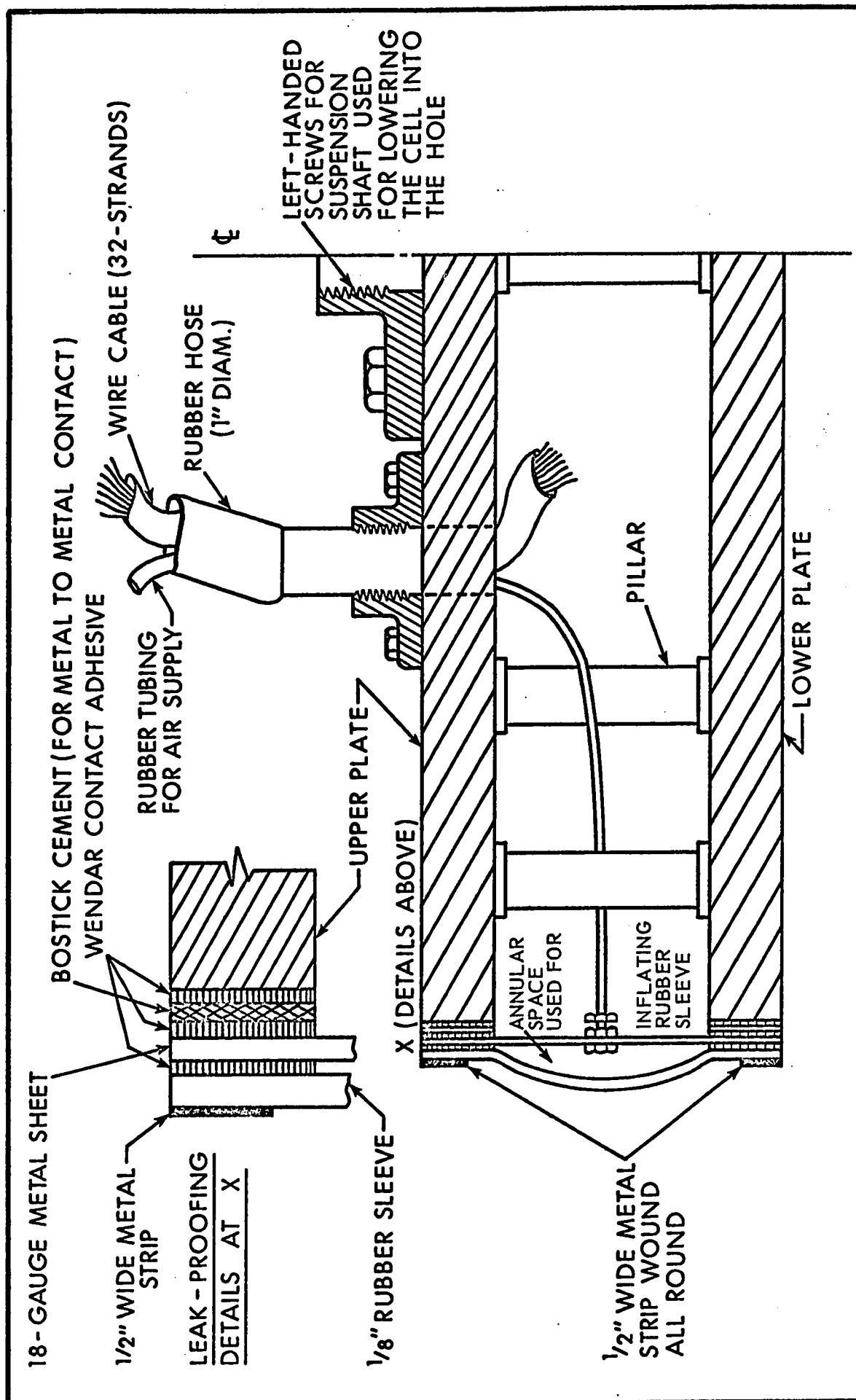


FIGURE: F-4 HALF SECTION THROUGH ASSEMBLED LOAD CELL (NOT TO SCALE).

APPENDIX G

CALIBRATION CURVES AND DATA FOR LOAD CELLS

(FULL-SCALE PILES)

CALIBRATION DATA FOR 16"-DIAMETER LOAD CELL IN CLAY

Calibrating Load (kips)	Cumulative Differences (Indicator Reading x 10 ⁶ in.)						
	I	II	III	IV	I + III	II + IV	I+II+III+IV
0	0	0	0	0	0	0	0
2.5	85	82	89	78	174	160	334
5	177	152	178	152	355	304	659
10	342	275	356	230	698	505	1,203
15	506	394	528	304	1,034	698	1,732
20	670	505	690	389	1,360	894	2,254
30	1,028	716	1,054	592	2,082	1,308	3,390
40	1,332	1,006	1,413	882	2,745	1,888	4,633
50	1,622	1,312	1,775	1,217	3,397	2,529	5,926

NOTE: I, II, III, IV above indicate the working quadrants of the cell.

CALIBRATION DATA FOR 20" DIAMETER LOAD CELL (A-2) IN CLAY

Calibrating Load (kips)	Cumulative Differences (Indicator Reading x 10 ⁶ in.)					
	I	III	IV	I + III	I + IV	III + IV
0	0	0	0	0	0	0
5	71	74	76	145	147	150
10	150	158	163	308	313	321
20	240	268	248	508	488	516
40	446	474	459	920	905	933
60	659	674	669	1,333	1,328	1,343
80	867	871	869	1,738	1,736	1,740
100	1,071	1,063	1,064	2,134	2,135	2,127
120	1,267	1,278	1,254	2,515	2,521	2,502
140	1,455	1,439	1,449	2,894	2,904	2,888
160	1,645	1,630	1,647	3,275	3,292	3,277

NOTE: I, III, IV above indicate the working quadrants of the cell.

CALIBRATION DATA FOR 28"-DIAMETER LOAD CELL IN TILL

Calibrating Load (kips)	Cumulative Differences (Indicator Reading $\times 10^6$ in.)					
	I	II	III	I + II	I + III	II + III
0	0	0	0	0	0	0
12.5	20	119	- 9	139	11	110
25	49	274	13	323	62	287
37.5	76	430	41	506	117	471
50	107	590	67	697	174	657
75	196	858	126	1,054	322	984
100	290	1,097	197	1,387	487	1,294
125	393	1,294	279	1,687	672	1,573
150	504	1,467	365	1,971	869	1,832
200	723	1,794	529	2,517	1,252	2,323
250	951	2,106	699	3,056	1,650	2,805
300	1,172	2,396	881	3,568	2,053	3,277
350	1,379	2,686	1,035	4,065	2,414	3,721

NOTE: I, II, III above indicate the working quadrants of the cell.

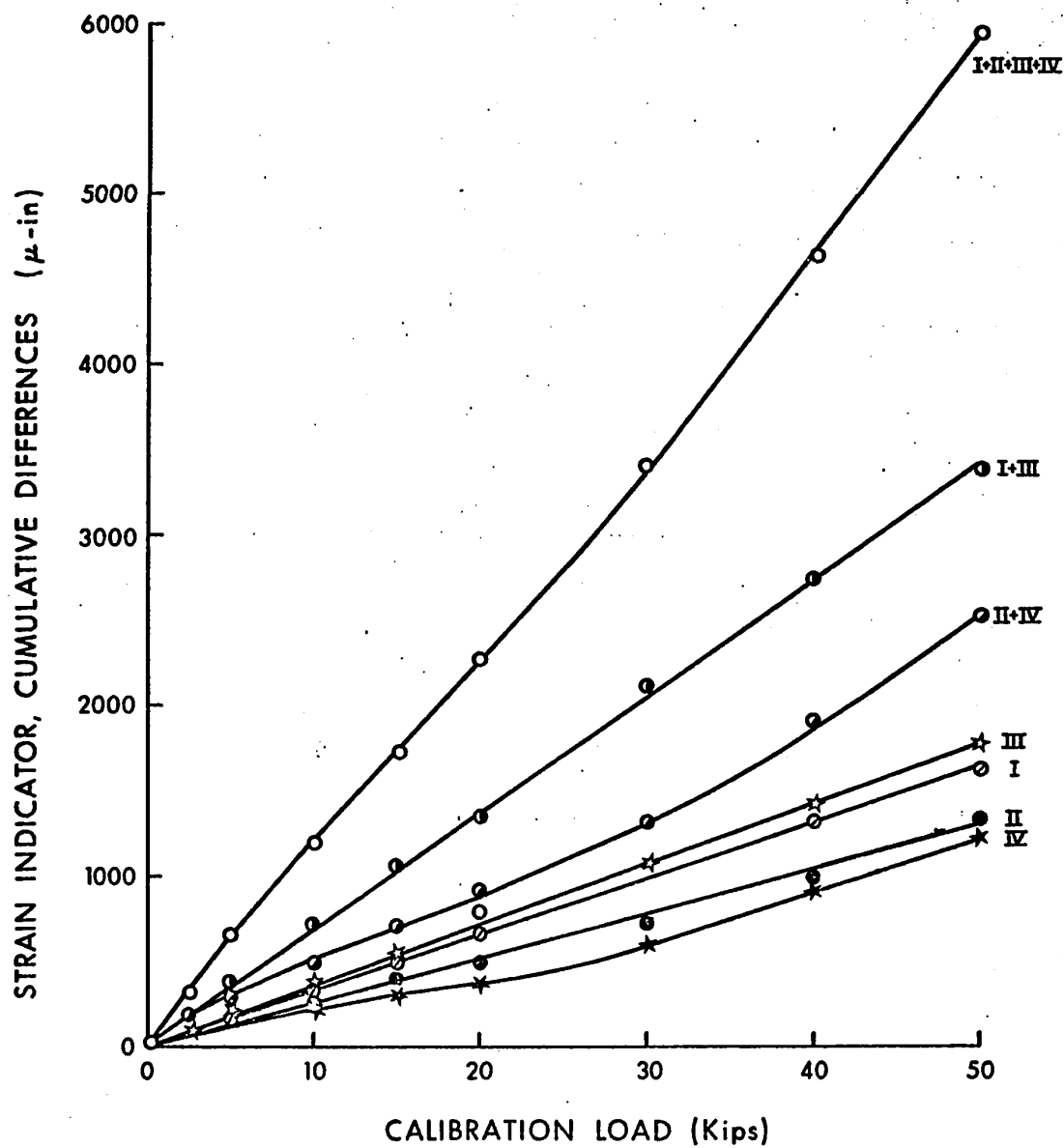


FIGURE: G-5 CALIBRATION CURVES FOR 16 INCH DIAMETER LOAD CELL
(I, II, III, IV: WORKING QUADS)

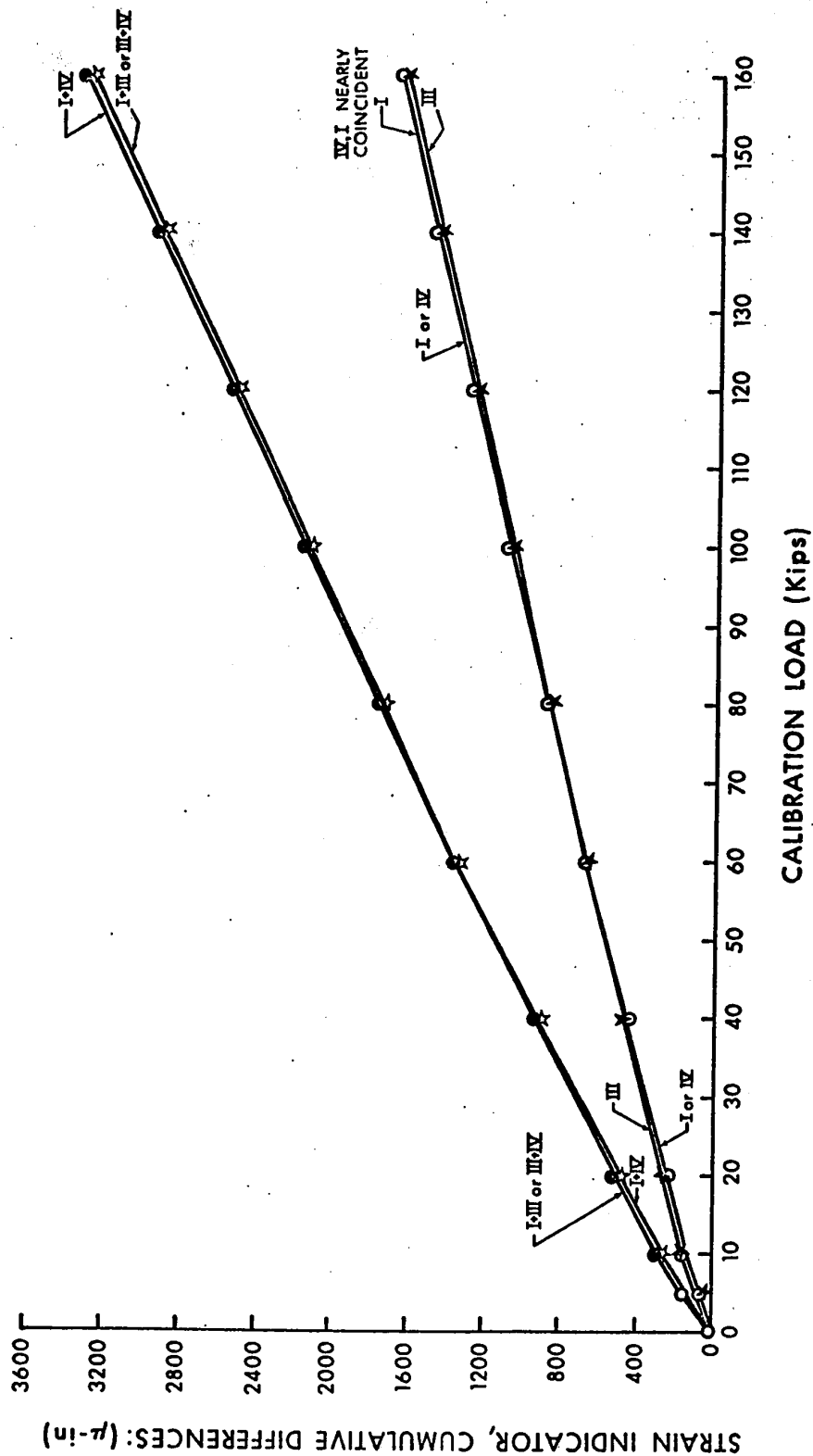


FIGURE G-6 CALIBRATION CURVES FOR 20 INCH DIAMETER LOAD CELL A-2 IN CLAY
(I, II, III, IV: WORKING QUADS)

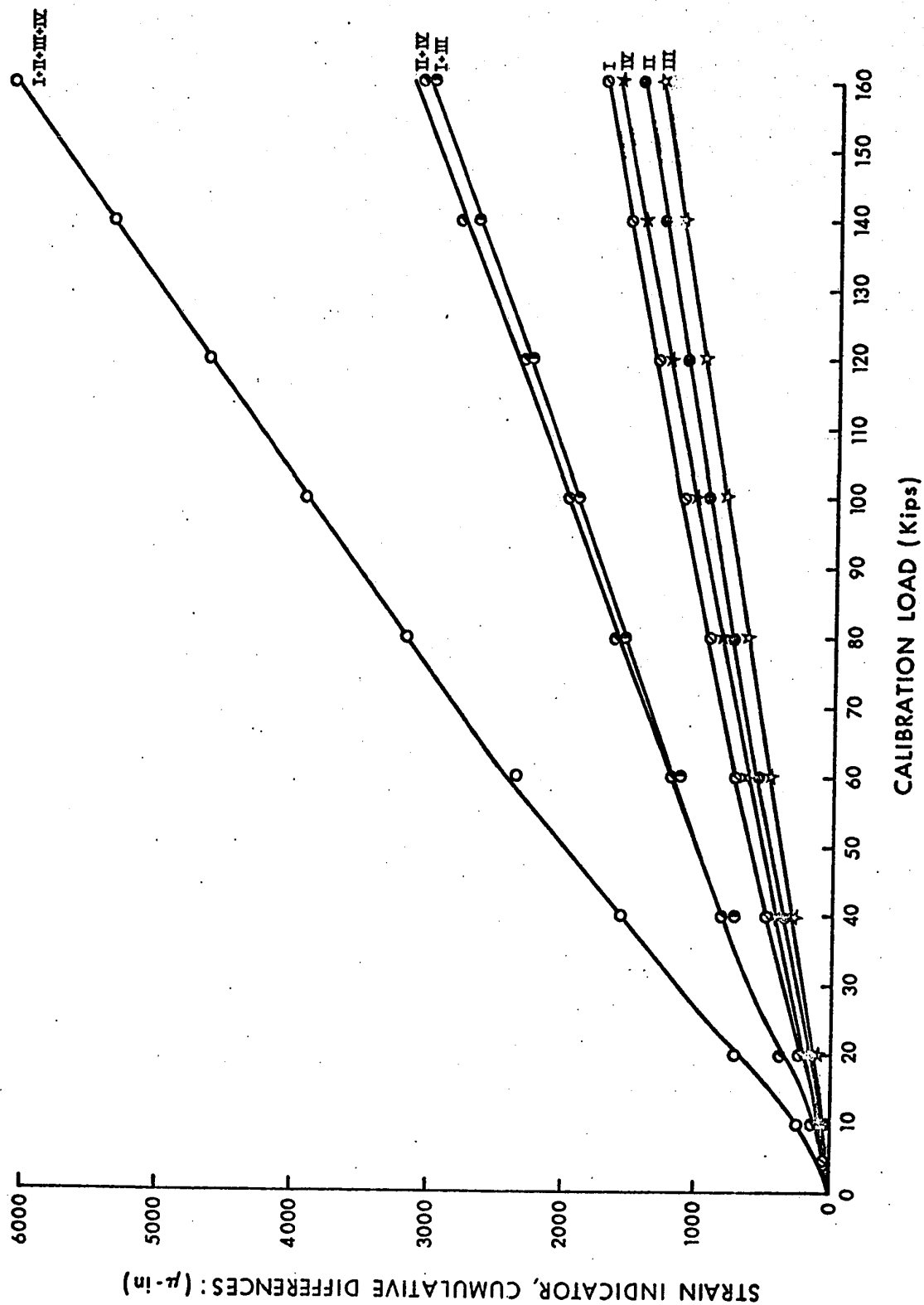


FIGURE: G-7 CALIBRATION CURVES FOR 20 INCH DIAMETER LOAD CELL A-1 IN TILL (I,II,III,IV: WORKING QUADS)

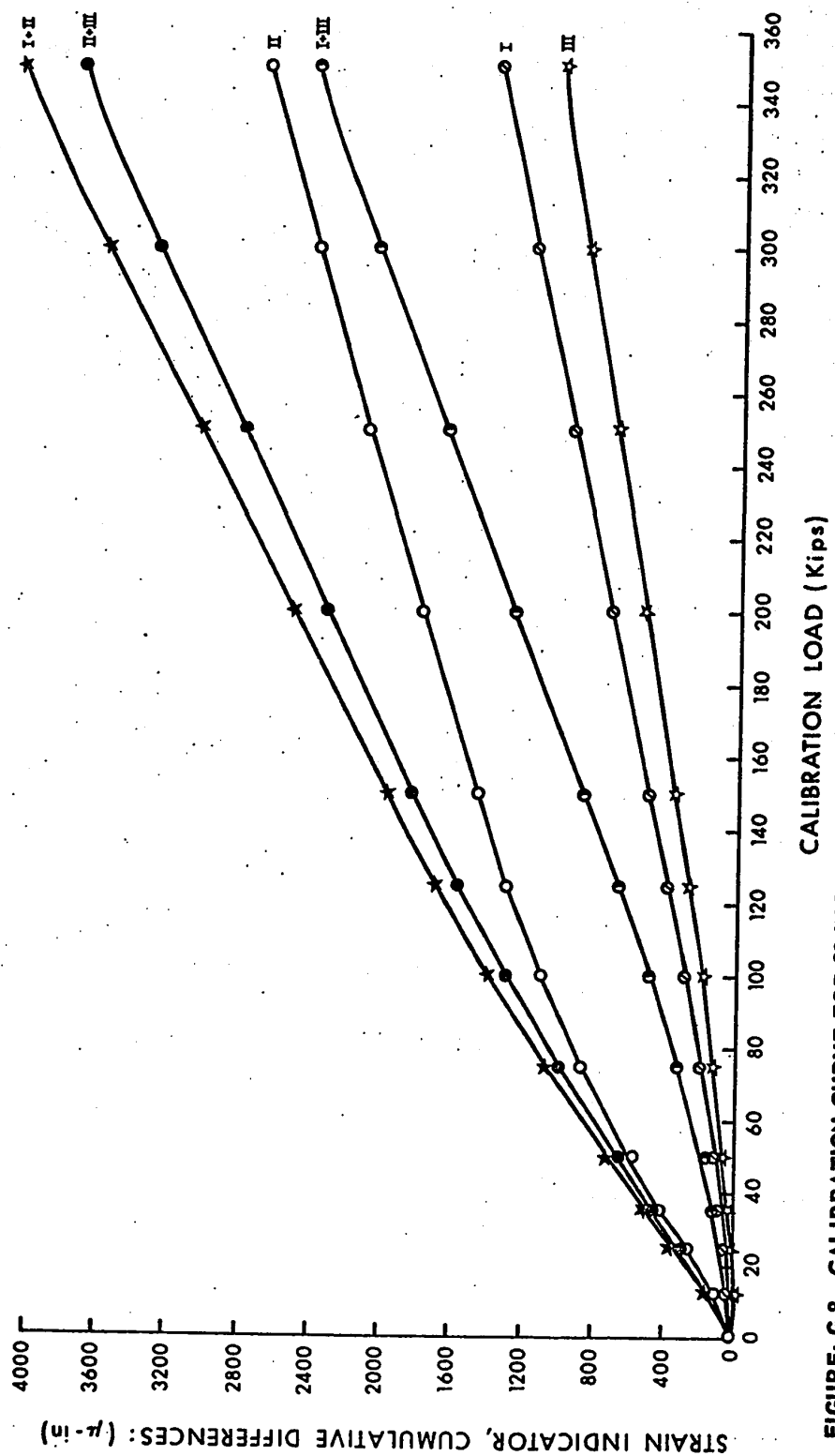


FIGURE: G-8 CALIBRATION CURVE FOR 28 INCH DIAMETER LOAD CELL (I,II,III: WORKING QUADS).

APPENDIX H

CALIBRATION CURVES AND DATA FOR HYDRAULIC JACKS
AND DETAILS OF THE LOAD MAINTENANCE SCHEME
USED FOR FIELD PILES

CALIBRATION DATA FOR HYDRAULIC JACK NUMBER I

Calibrating Load (kips)	Gage Pressure (psi.)	Gage Pressure (psi.)
0	10	20
25	200	205
50	395	400
75	570	580
100	740	750
125	930	950
150	1,140	1,150
175	1,305	1,330
200	1,505	1,520
225	1,710	1,720
250	1,900	1,905
275	2,090	2,080
300	2,295	2,290
325	2,470	2,470
350	2,640	2,650
375	2,830	2,840
400	3,000	3,000

CALIBRATION DATA FOR HYDRAULIC JACK NUMBER II

Calibrating Load (kips)	Gage Pressure (psi.)	Gage Pressure (psi.)
0	10	10
25	210	210
50	405	400
75	580	570
100	760	750
125	950	950
150	1,140	1,150
175	1,330	1,330
200	1,530	1,520
225	1,730	1,720
250	1,900	1,900
275	2,070	2,080
300	2,280	2,290
325	2,460	2,460
350	2,650	2,640
375	2,810	2,830
400	3,000	3,000

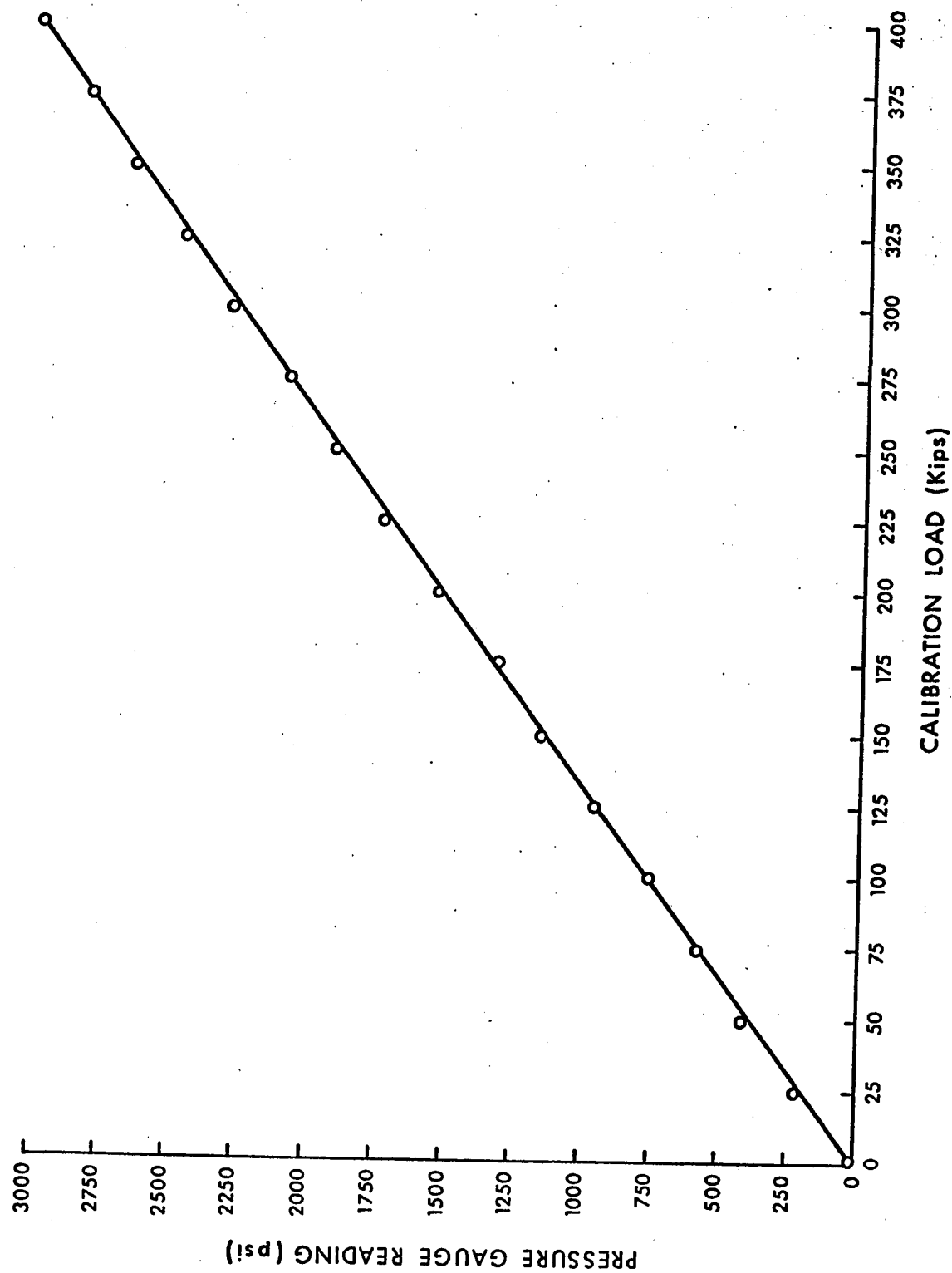


FIGURE: H-3 CALIBRATION CURVE FOR HYDRAULIC JACK NO. 1

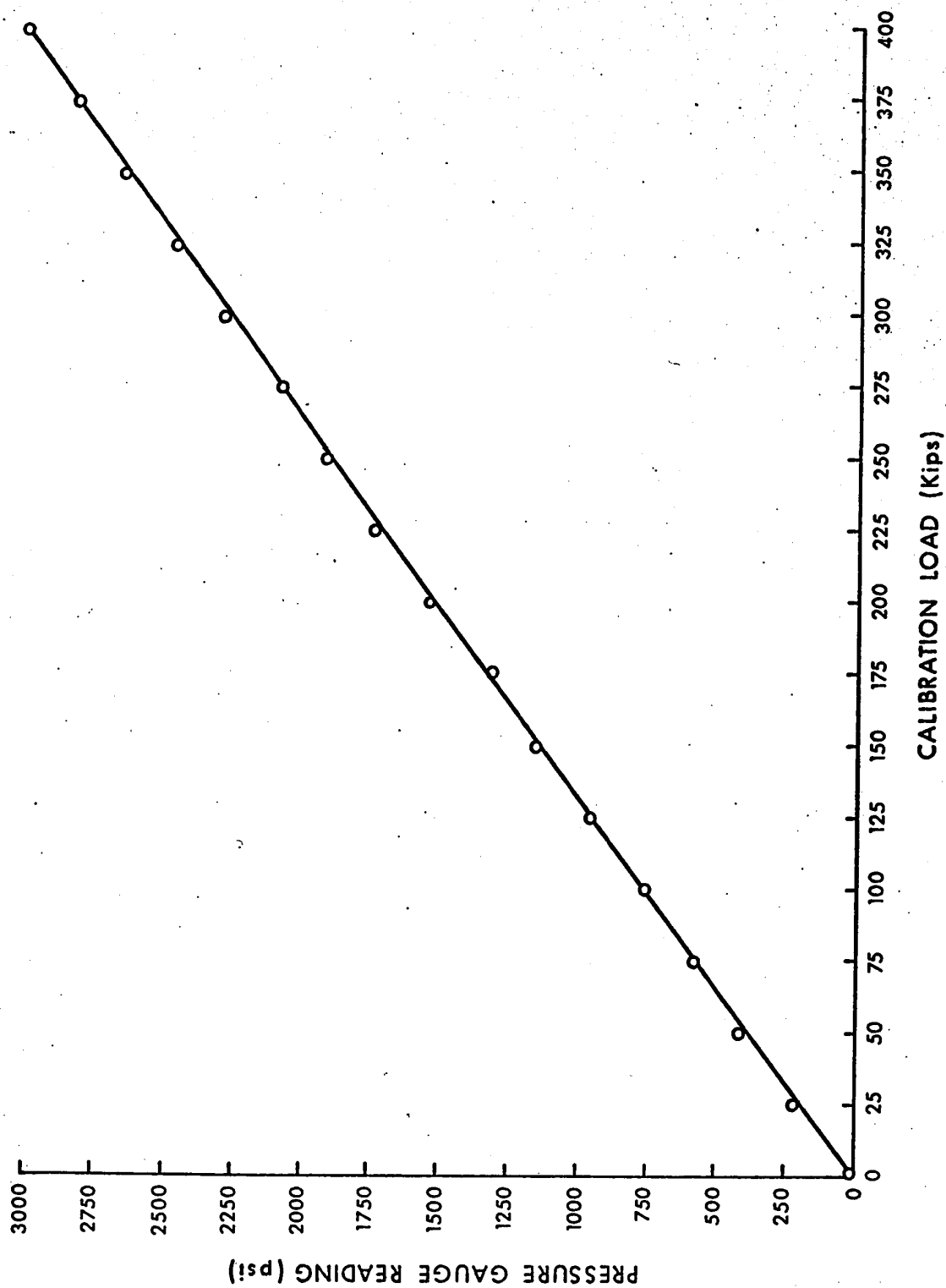


FIGURE: H-4 CALIBRATION CURVE FOR HYDRAULIC JACK NO. 2 CALIBRATION LOAD (kips)

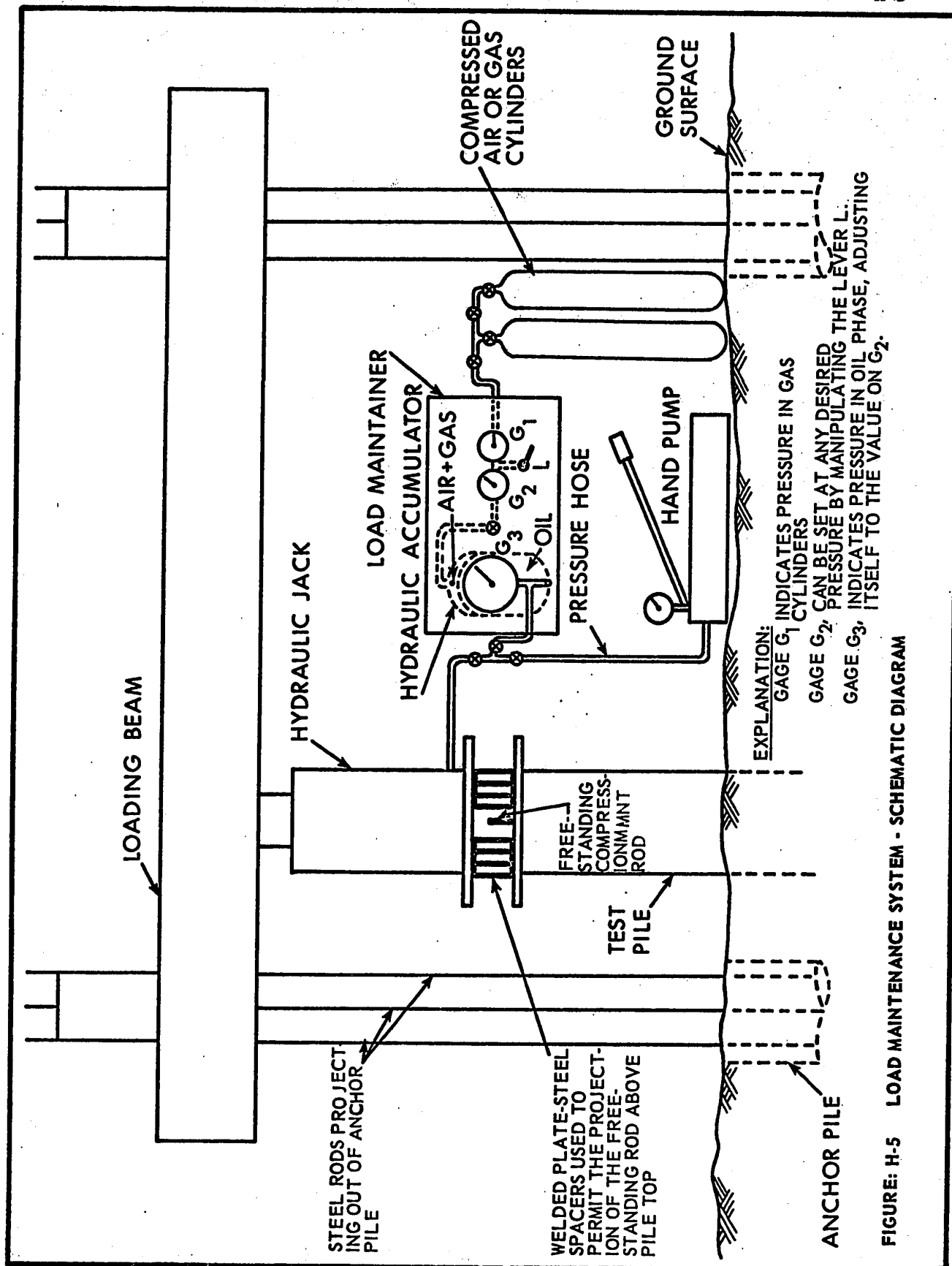
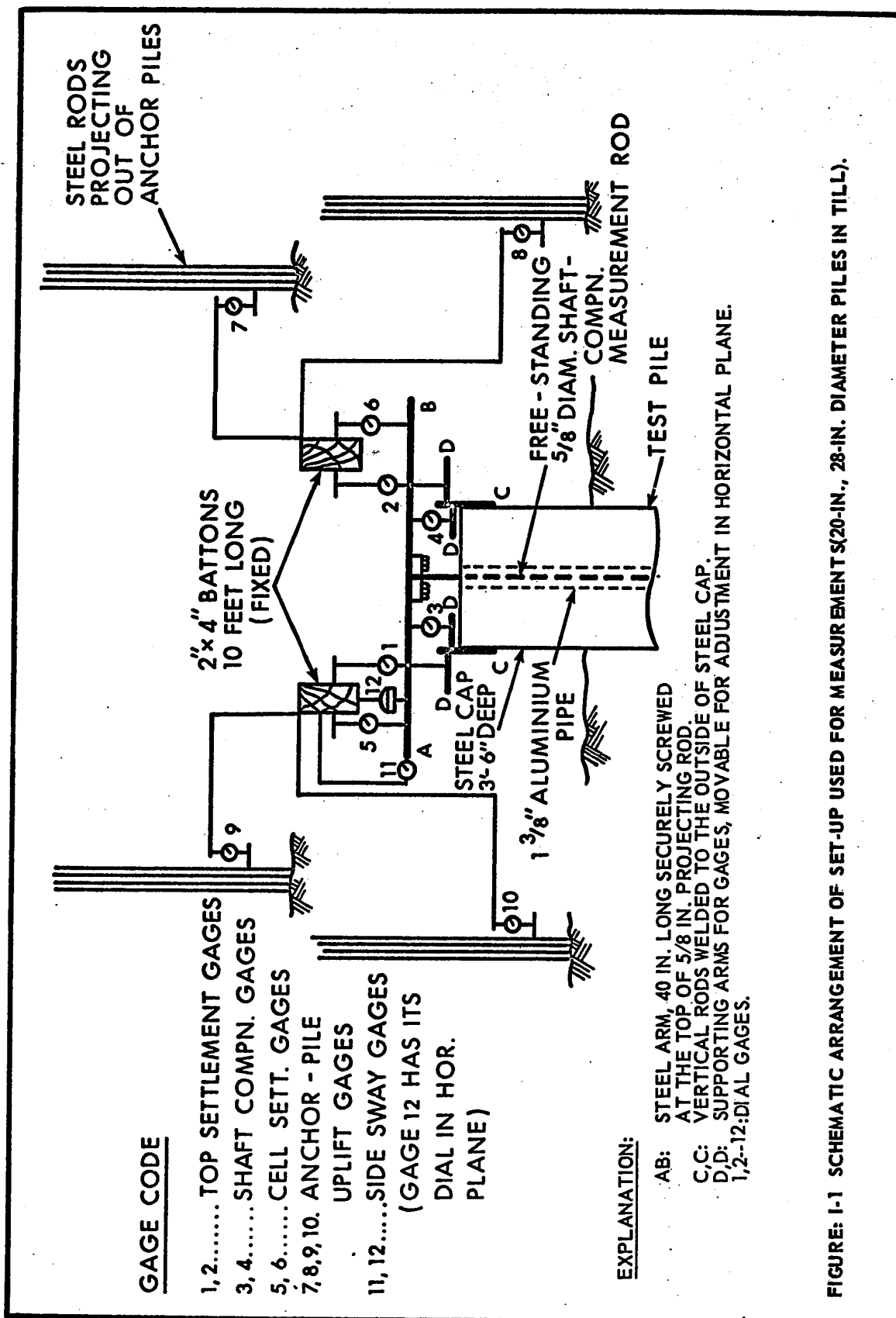


FIGURE: H-5 LOAD MAINTENANCE SYSTEM - SCHEMATIC DIAGRAM

APPENDIX I

SCHEMATIC ARRANGEMENT OF SET-UP USED FOR
MEASUREMENTS FOR PILES IN TILL



APPENDIX J

RESULTANT SIDE-SWAY AT TOP OF 28-INCH DIAMETER

PILE UNDER A LOAD OF 1200 KIPS

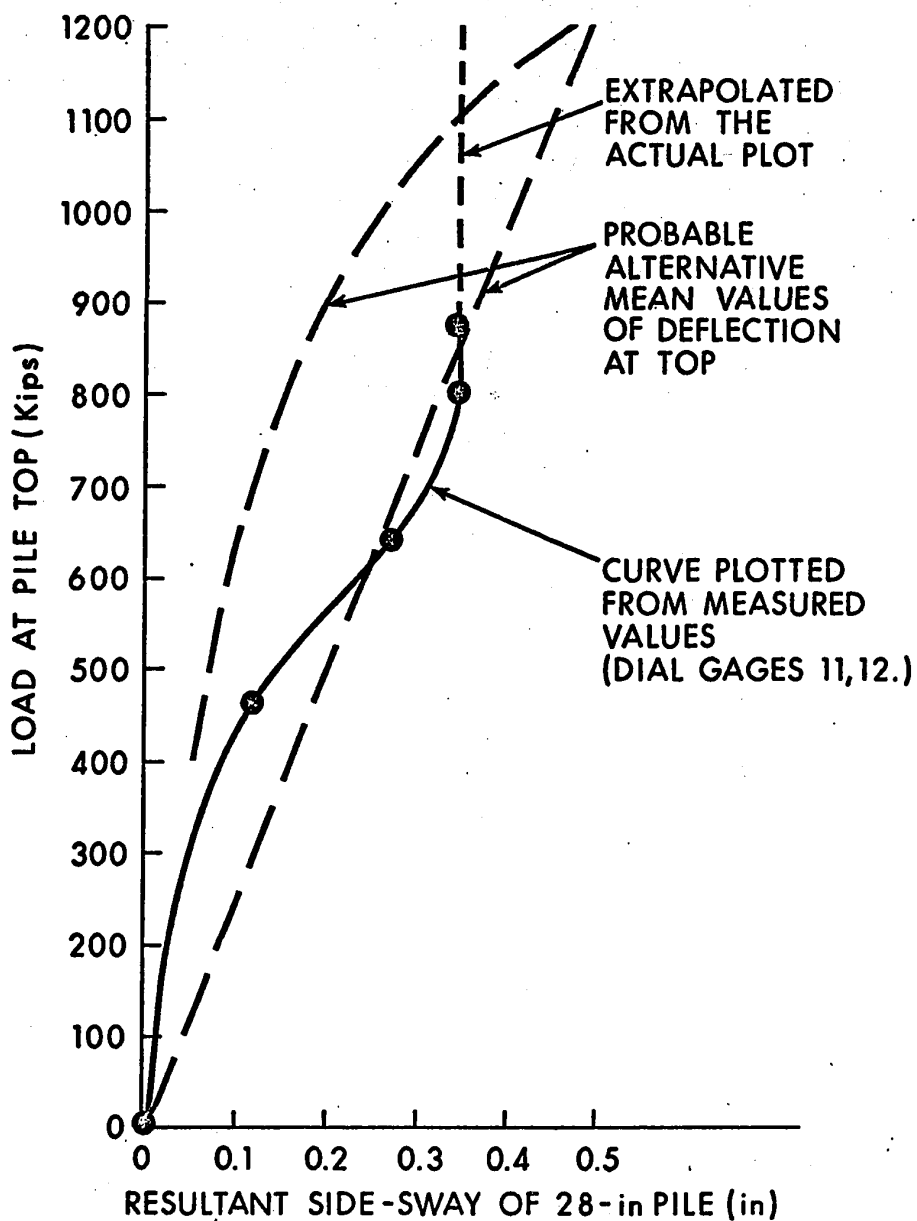


FIGURE: J-1 RESULTANT SIDE-SWAY AT TOP OF 28-IN. DIAMETER PILE UNDER A LOAD OF 1200 KIPS.

APPENDIX K

PARTIAL DATA FOR SHEAR STRENGTH

OF FIELD SOIL

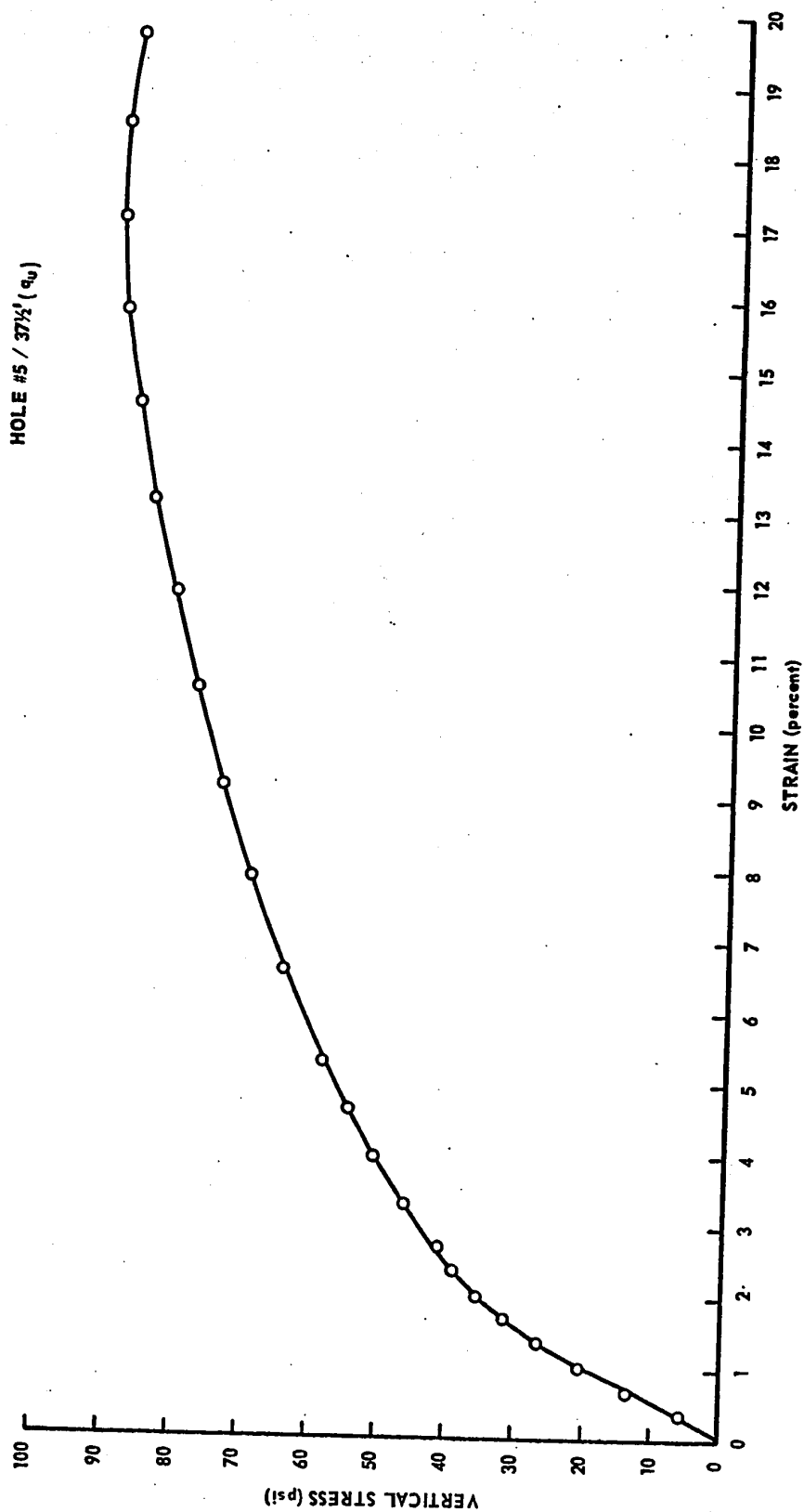


FIGURE K-1 TYPICAL STRESS-STRAIN CURVE FOR UNCONFINED COMPRESSION TEST ON TILL.

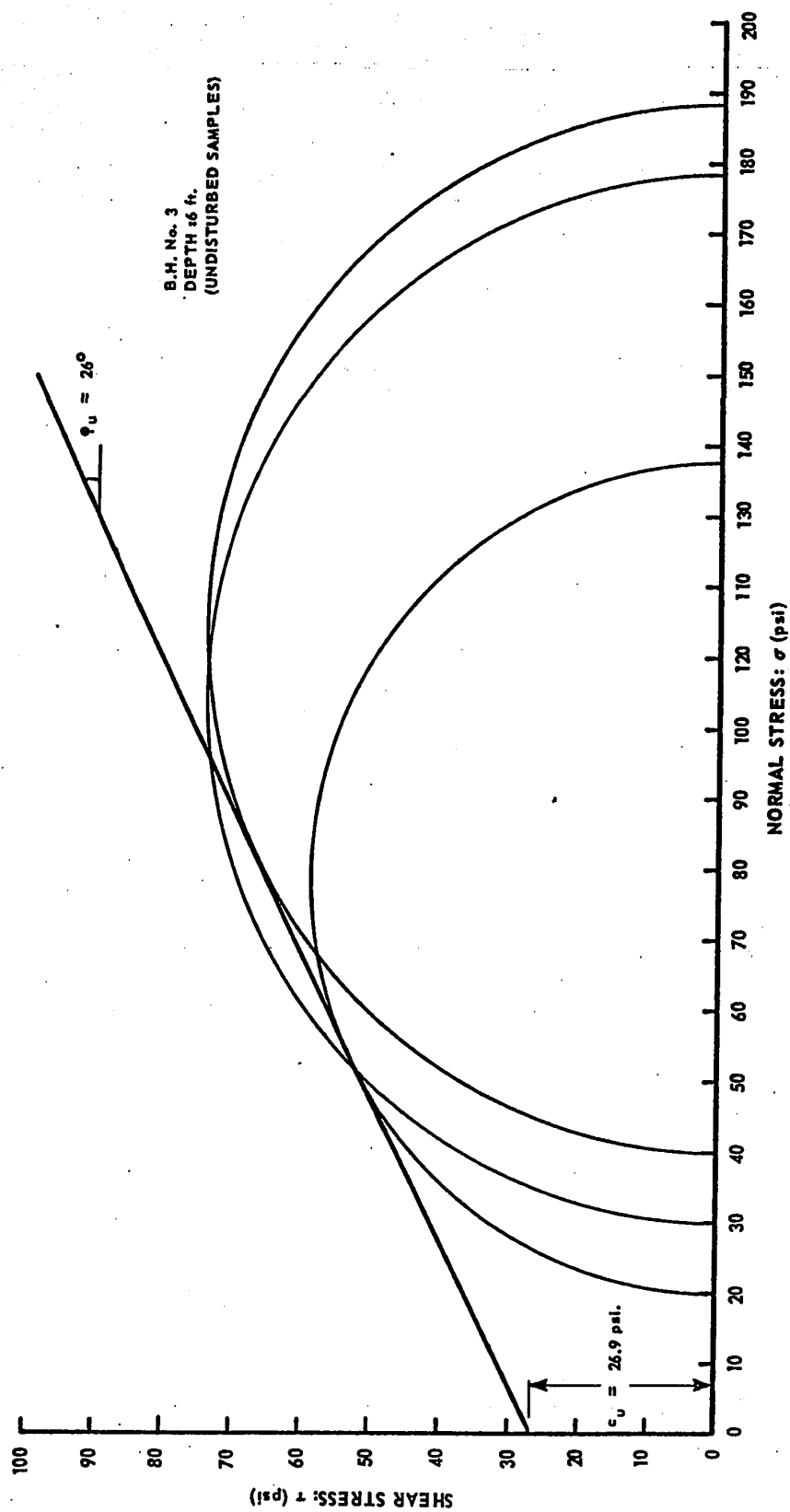


FIGURE: K-2 MOHR'S ENVELOPE FOR TOTAL STRESSES.

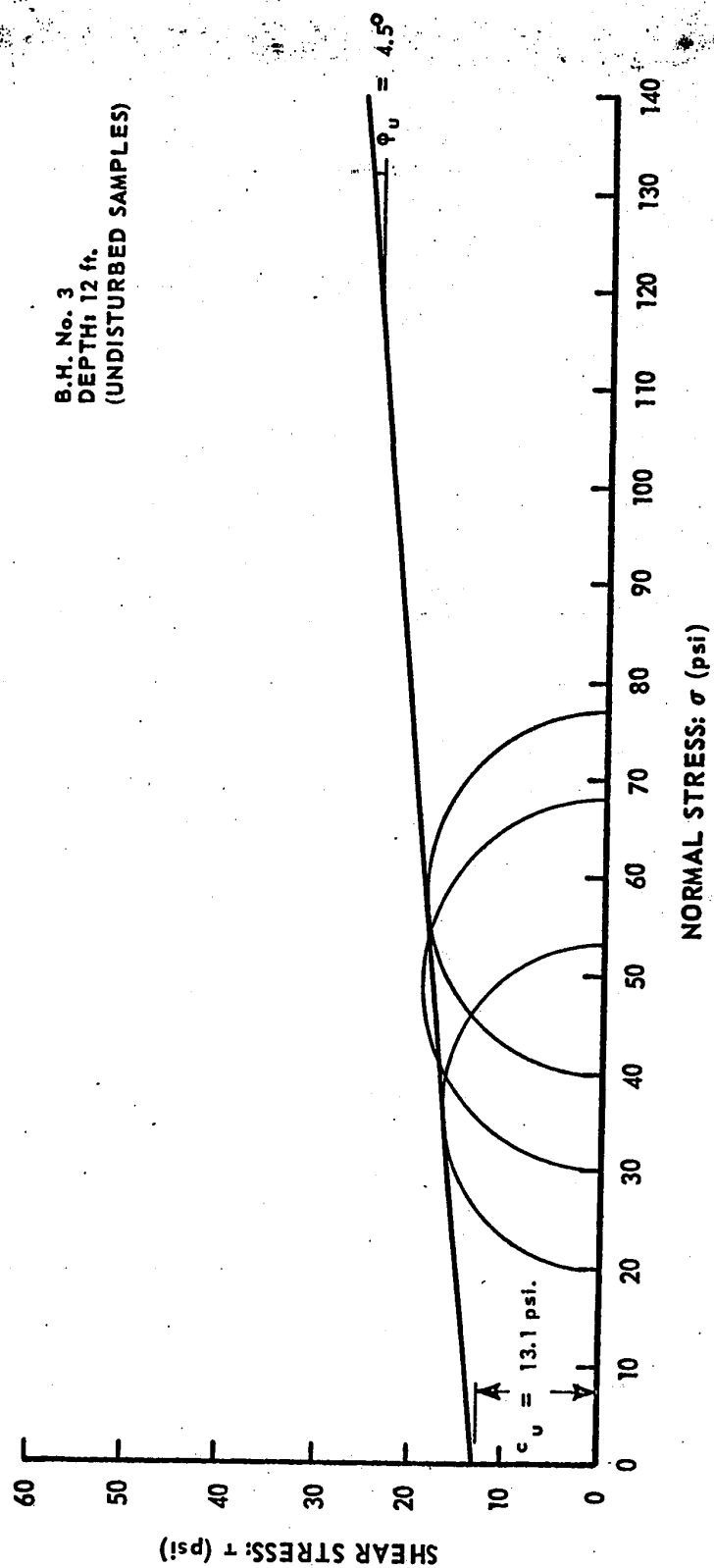


FIGURE K-3 MOHR'S ENVELOPE FOR TOTAL STRESSES.

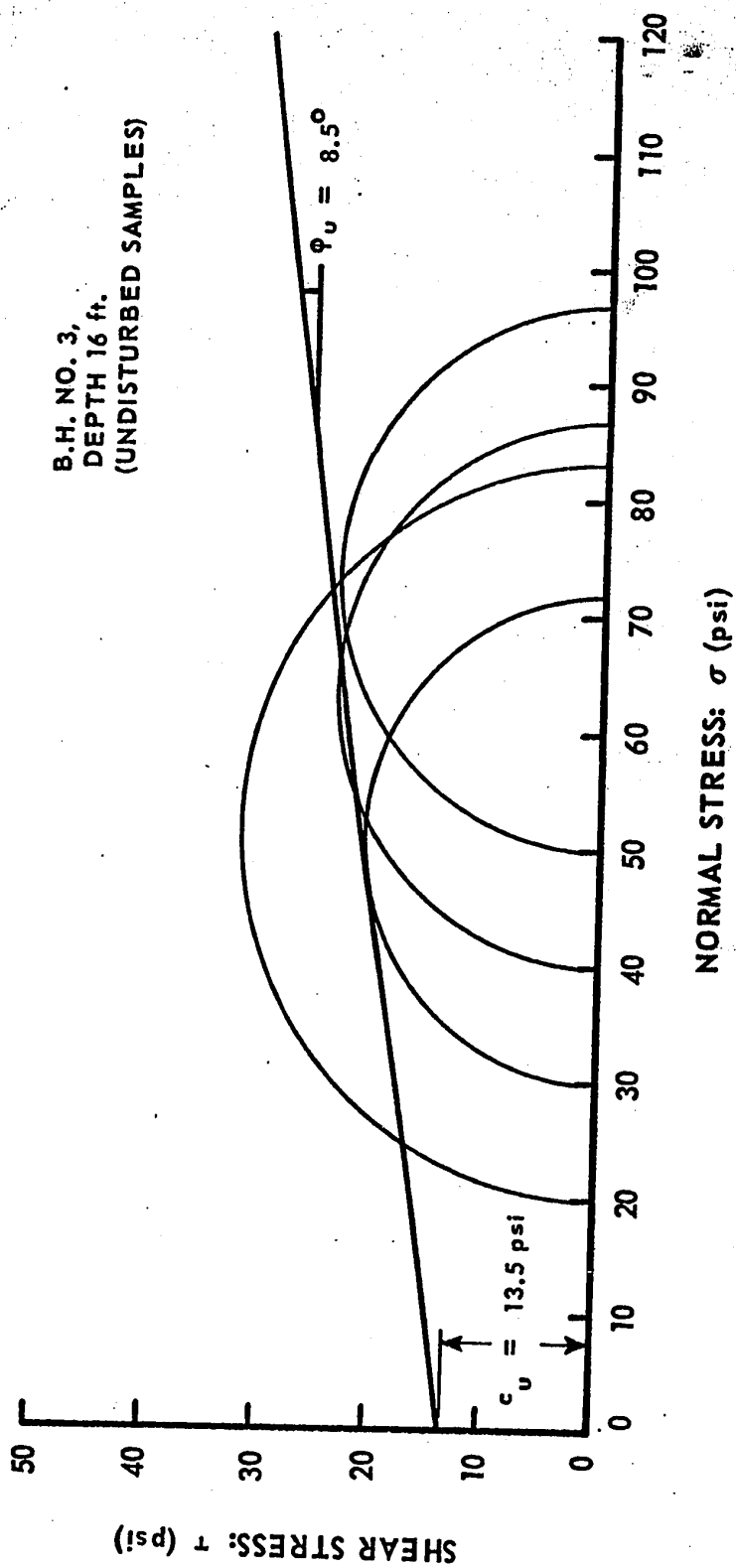


FIGURE K-4 MOHR'S ENVELOPE FOR TOTAL STRESSES.

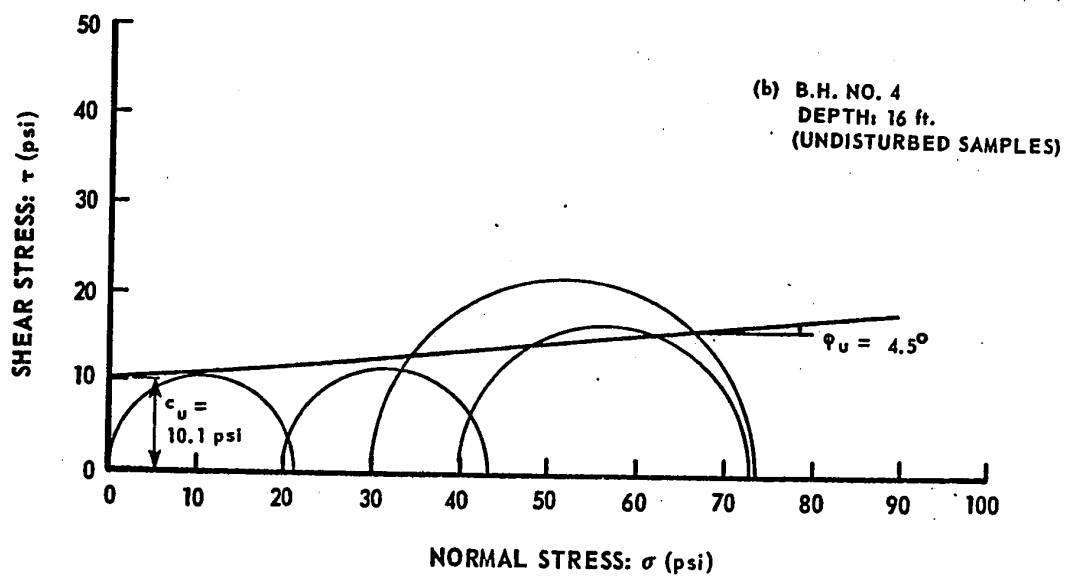
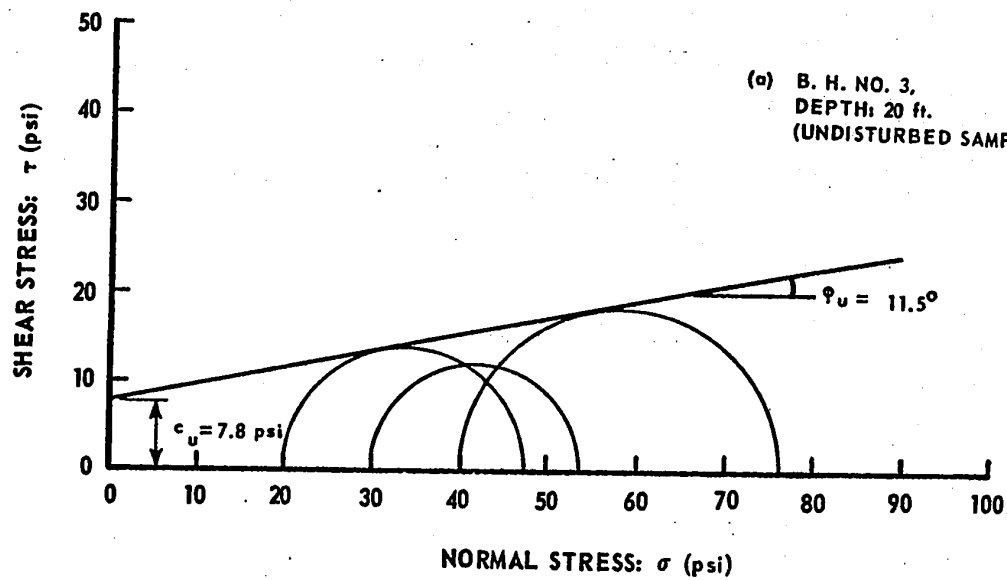


FIGURE: K-5 (a,b) MOHR'S ENVELOPE FOR TOTAL STRESSES.

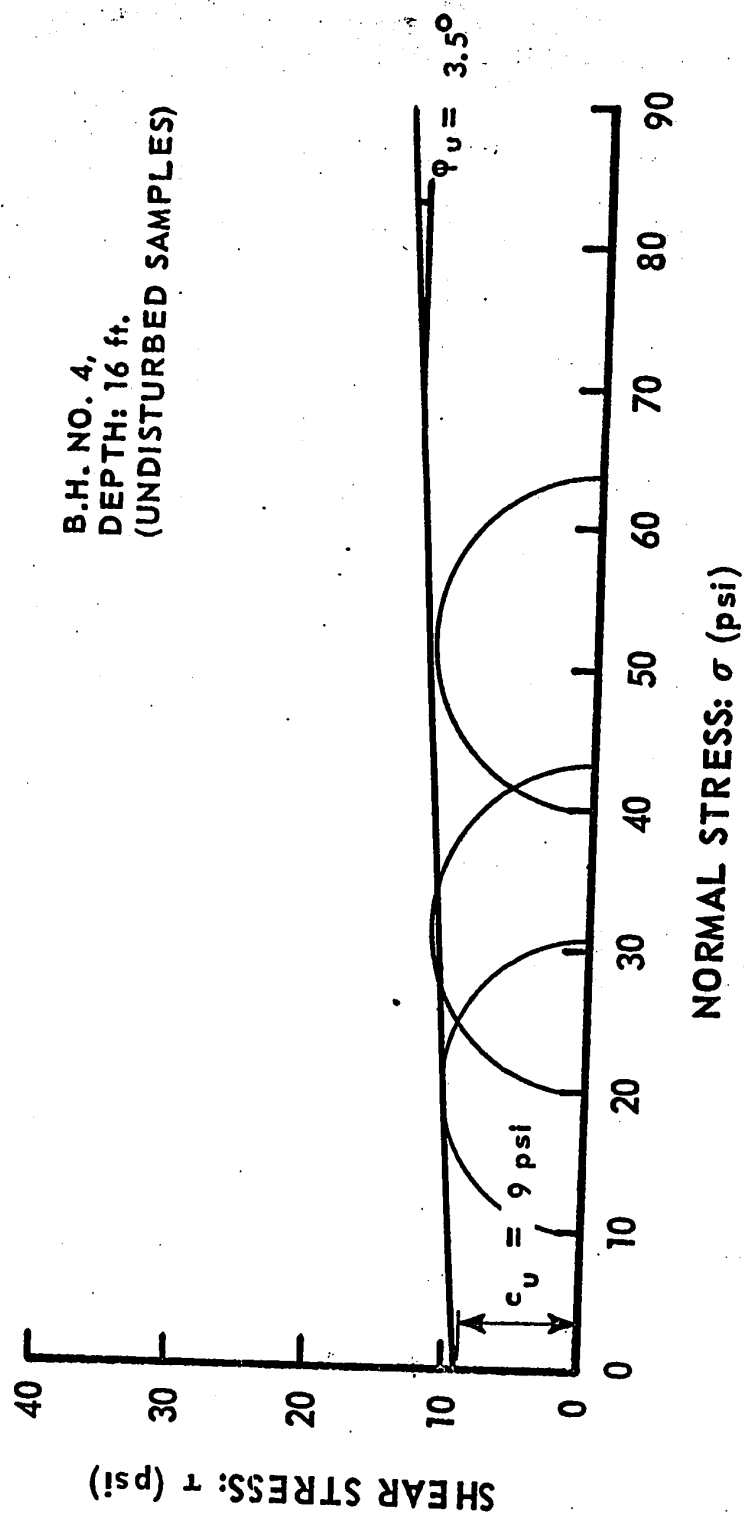


FIGURE: K-6 MOHR'S ENVELOPE FOR TOTAL STRESSES.

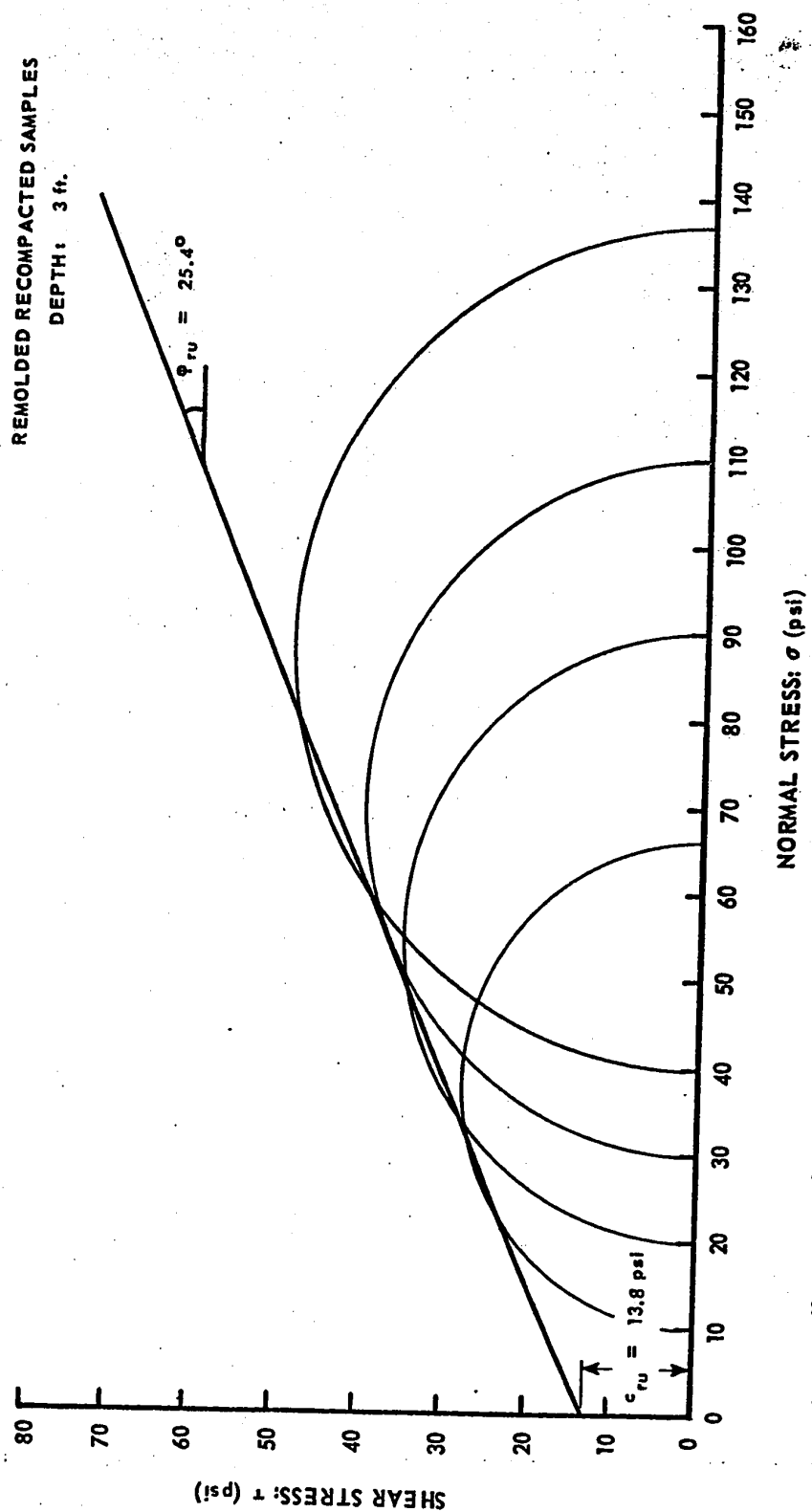


FIGURE K-7 MOHR'S ENVELOPE FOR TOTAL STRESSES.

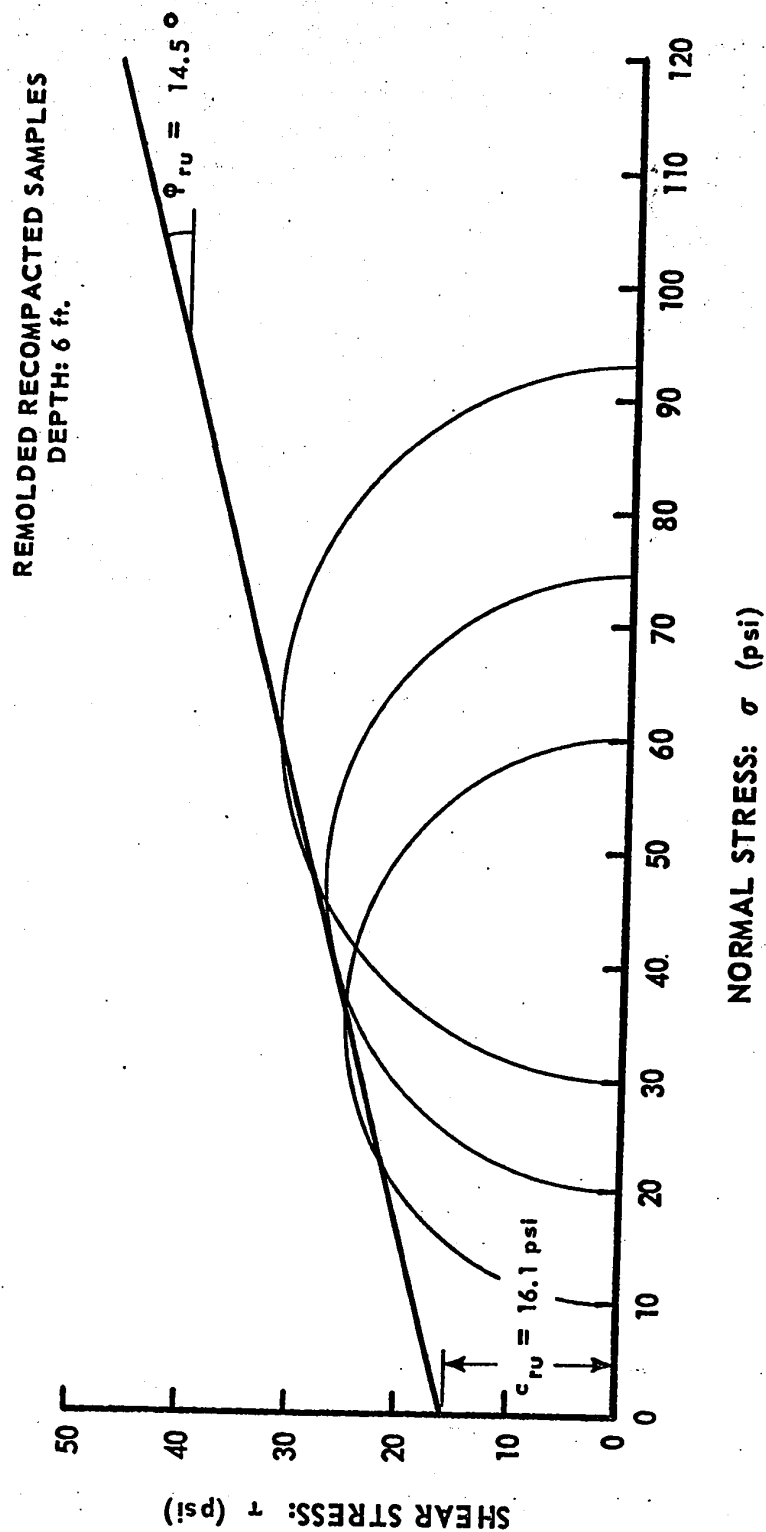


FIGURE: K-8 MOHR'S ENVELOPE FOR TOTAL STRESS.

REMOLDED RECOMPACTED SAMPLES
DEPTH: 9 ft.

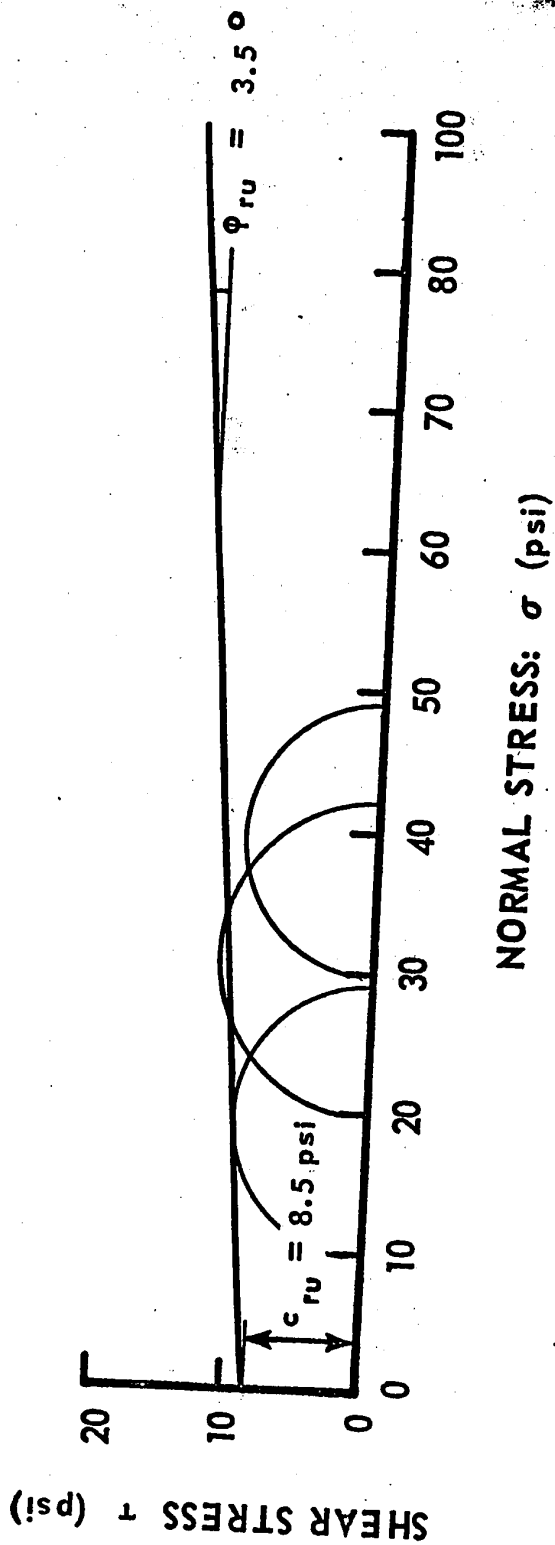


FIGURE: K-9. MOHR'S ENVELOPE FOR TOTAL STRESS.

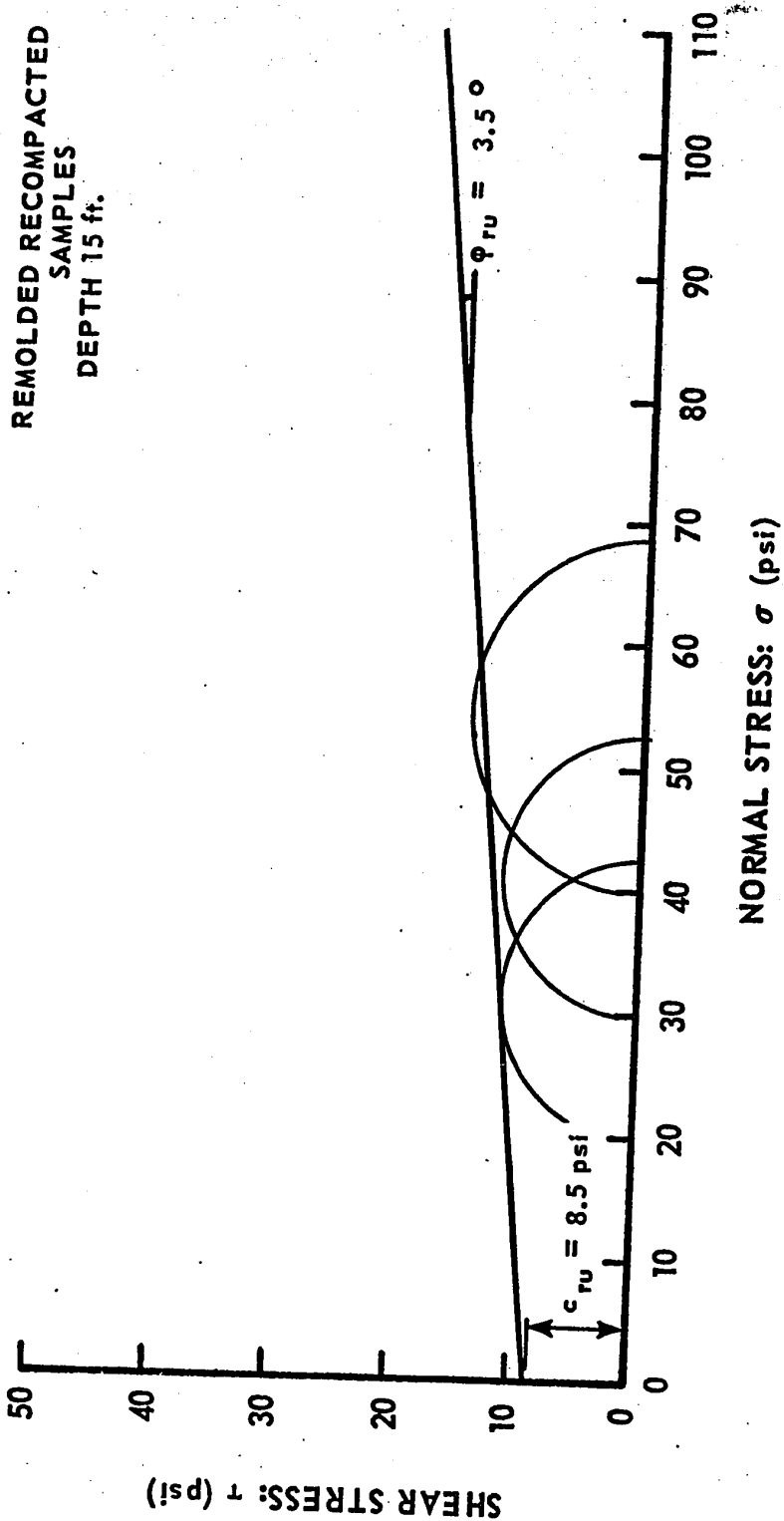


FIGURE: K-10 MOHR'S ENVELOPE FOR TOTAL STRESSES.

REMOLDED RECOMPACTED SAMPLES
DEPTH: 24 ft.

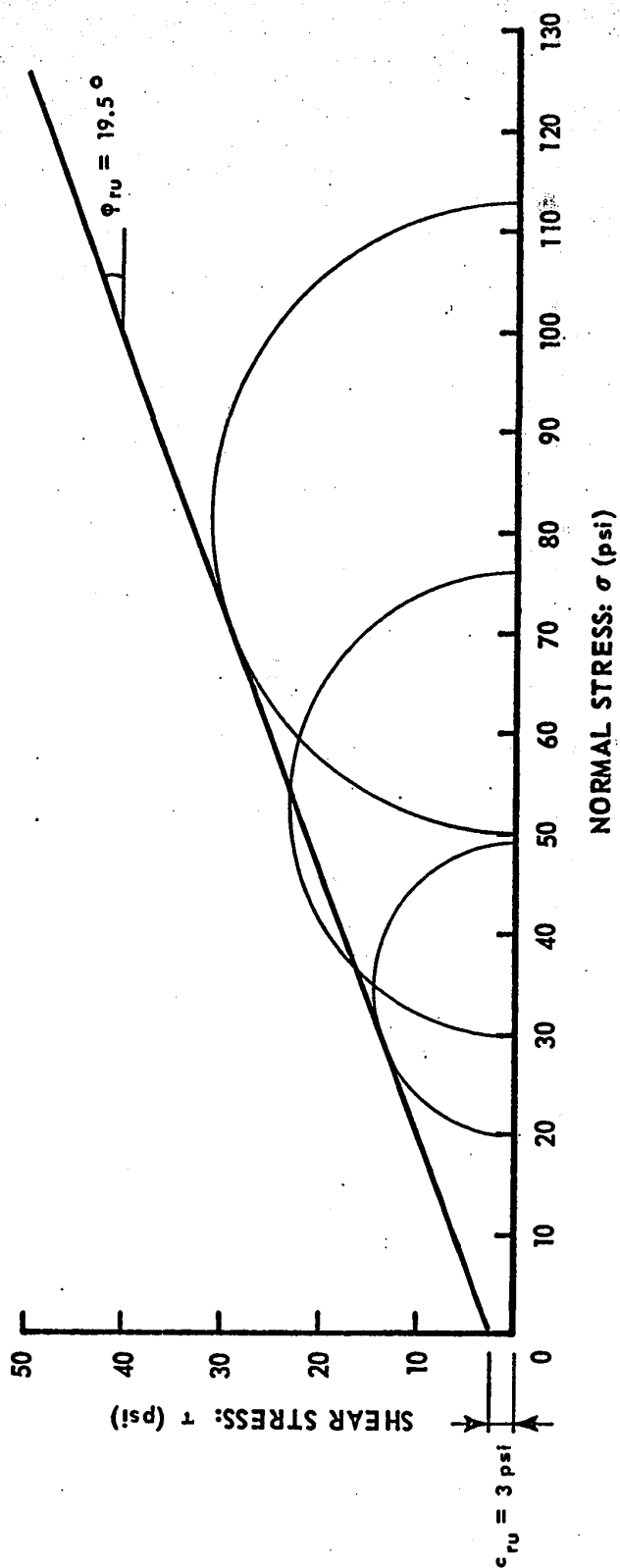


FIGURE: K-11 MOHR'S ENVELOPES FOR TOTAL STRESS.

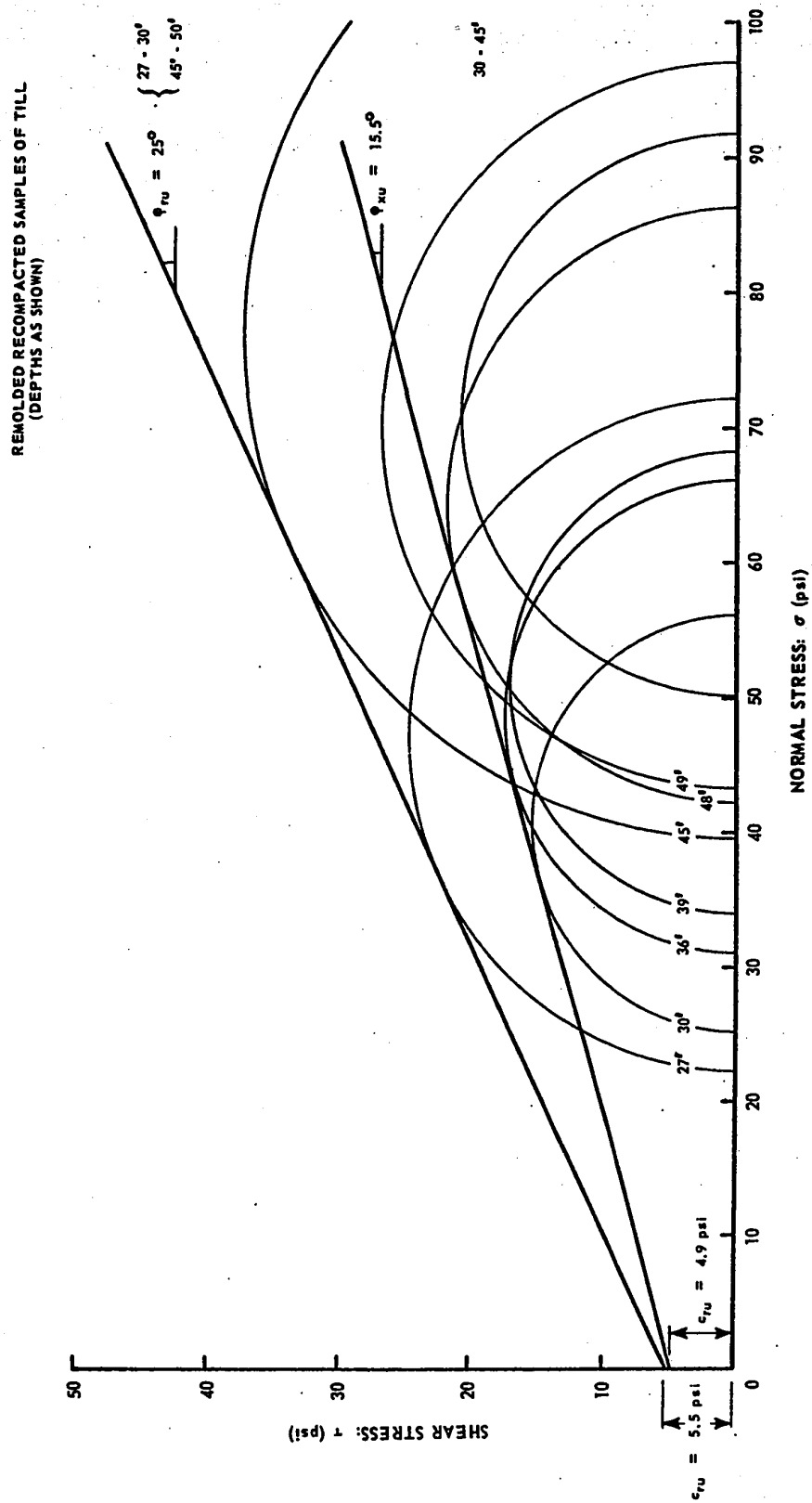


FIGURE: K-12 MOHR'S ENVELOPE FOR TOTAL STRESS

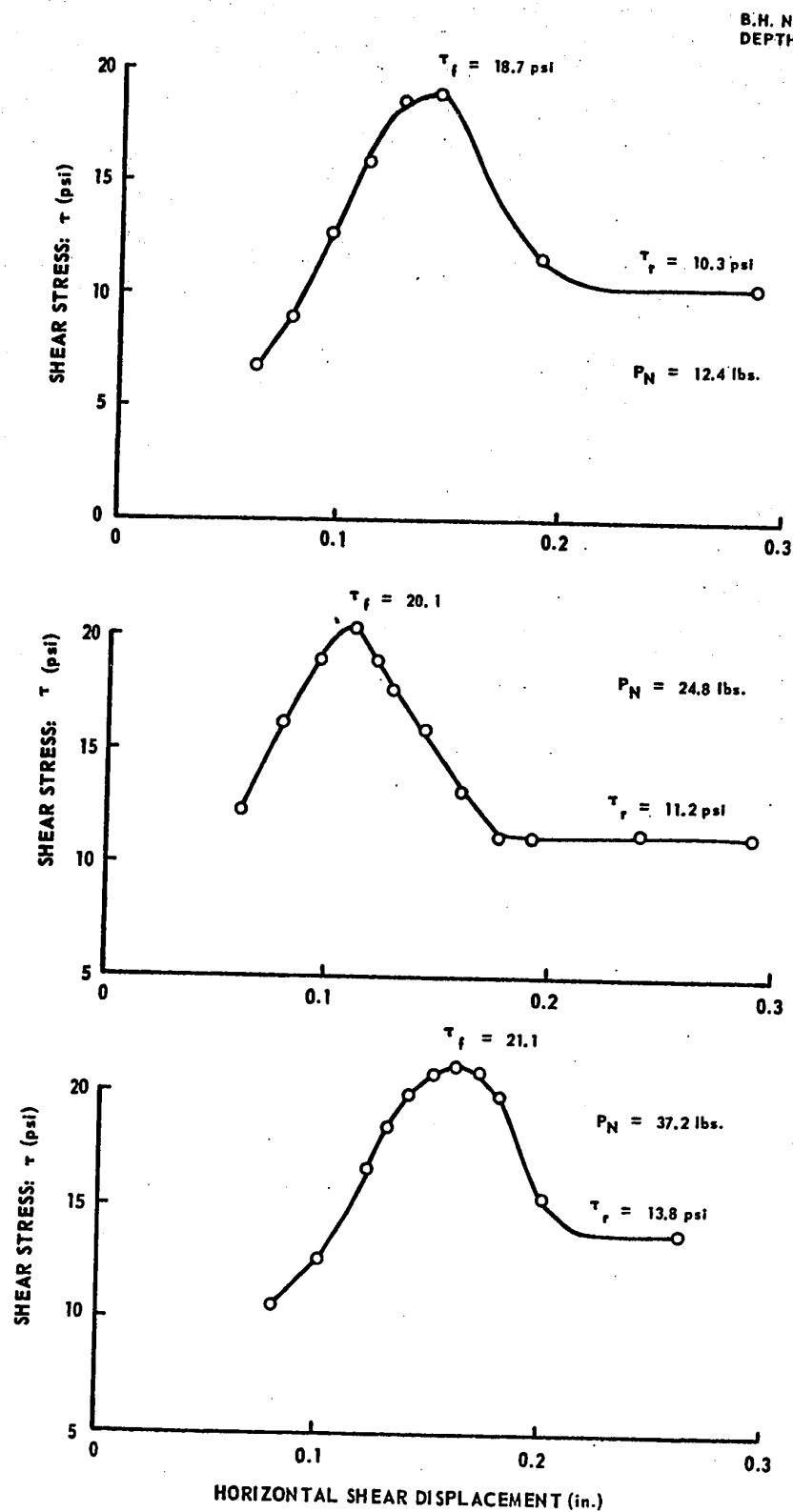


FIGURE: K-13 STRESS DEFORMATION PLOTS FOR BOX SHEAR TESTS.

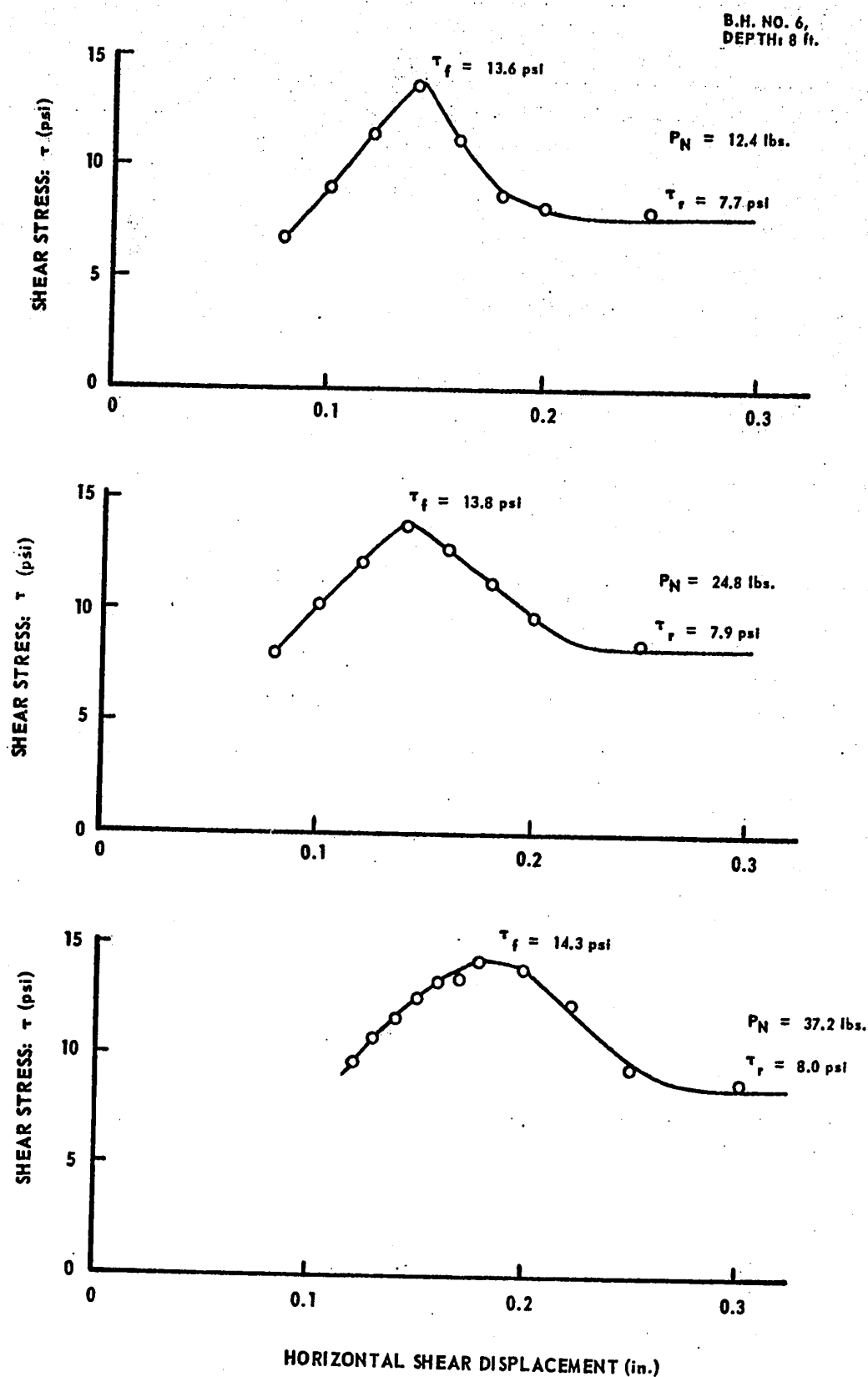


FIGURE: K-14 HORIZONTAL SHEAR DISPLACEMENT (in.) STRESS DEFORMATION PLOTS FOR BOX SHEAR TESTS.

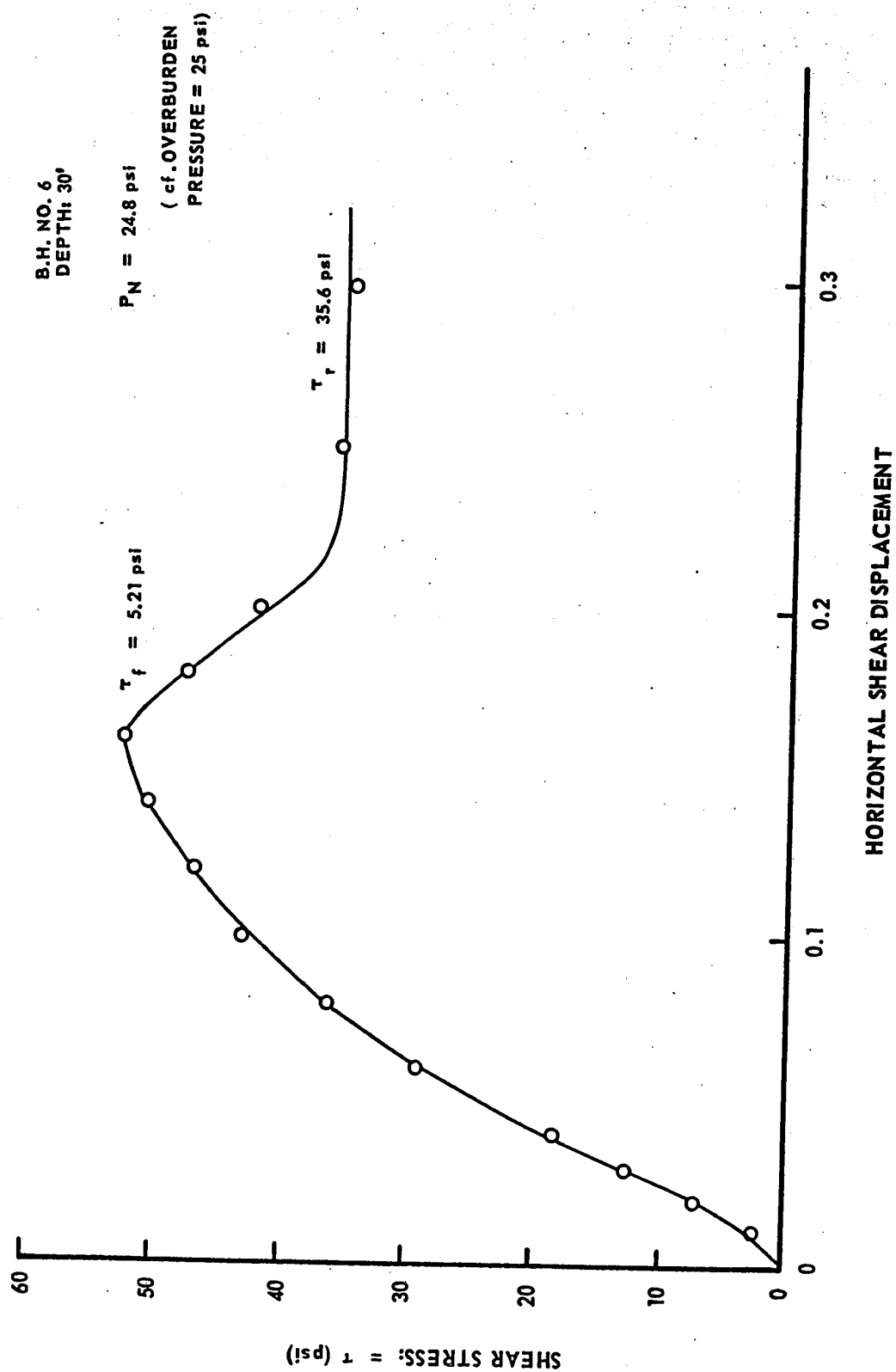


FIGURE K-15 STRESS DEFORMATION PLOT FOR BOX SHEAR TEST.

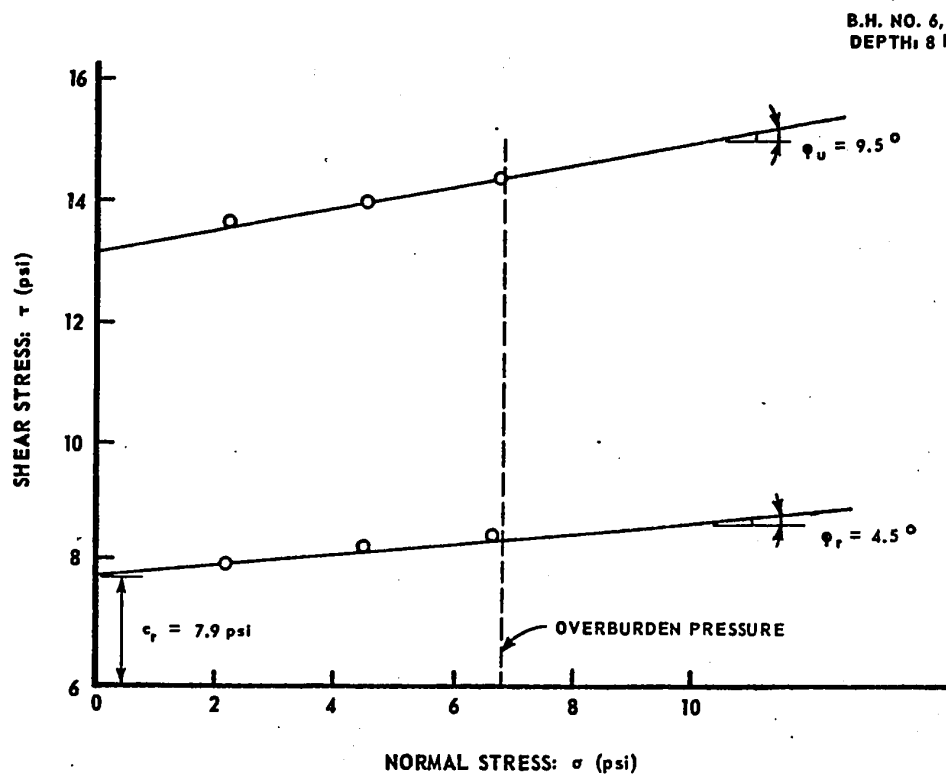
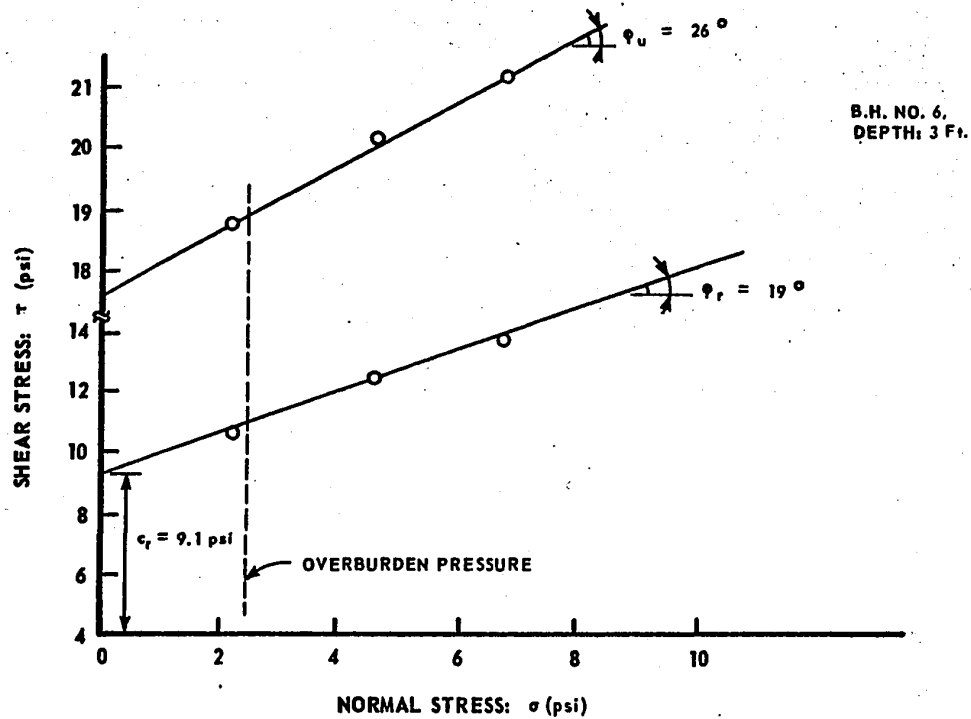


FIGURE: K-16 UNDISTURBED AND RESIDUAL STRENGTH PARAMETERS FROM BOX SHEAR TESTS.

APPENDIX L

SUMMARIES OF LOAD TEST DATA AND COMPUTATIONS

(FULL-LENGTH FIELD PILES)

SUMMARY OF FIELD TEST RESULTS AND COMPUTATIONS

(16-in. Pile in Clay)

Load (kips)	Top Settlement, Δ (in.)	$\frac{\Delta}{B_1} \times 100$ (%)	Shaft Compn. (in.)	Total Change in the Instrument Reading, Qds. I+II+III+IV (micro-inches)	Base Resistance from Calibration Curve (kips)
0	0	0	0	0	0
20 (0) (24H)	0.008 0.009	0.05 0.05	0.0013	466	3.2
40 (0) (24)	0.009 0.009	0.05 0.05	0.0061	879	6.0
60 (0) (24)	0.010 0.012	0.06 0.07	0.0101	1,144	10.5
80 (0) (24)	0.027 0.038	0.16 0.22	0.0157	1,537	14.0
100 (0) (24)	0.045 0.753	0.26 4.36	0.0211	1,974 4,715	17.0 40.5
110 (0) (1/2)	0.835 0.920	4.84 5.33	0.0235	4,960	42.5
120 (0) (24)	1.930 3.820	11.88 22.14	0.0256	5,231 5,620	44.5 59.9

B_1 = Effective Diameter of Pile I = 17.25 in.

SUMMARY OF FIELD TEST-RESULTS AND COMPUTATIONS (continued)

Load (kips)	Top Settlement, Δ (in.)	$\frac{\Delta}{B_1} \times 100$ (%)	Shaft Compn. (in.)	Total Change in the Instrument Reading, Qds. I+II+III+IV (micro-inches)	Base Resistance from Calibration Curve (kips)
90 (0) (1/2)	3.80	22.02	0.0254	} 4,835	41.4
60 (0) (1/2)	3.77	21.8	0.0246	} 4,646	39.9
30 (0) (1/2)	3.68	21.3	0.0239	} 3,565	32.0
20 (0) (1/2)	3.67	21.3	0.0231	} 3,264	29.1
10 (0) (1/2)	3.61	20.9	0.0223	} 3,186	28.5
0 (0) (1/2) (24)	3.49 3.41	20.3 19.7	0.0201	1,995 1,812 1,188	17.4 15.7 9.7
50 (0) (1/2)	3.451	18.3	0.0218	1,561	16.8
90 (0) (1/2)	3.74	21.7	0.0227	4,837	41.4
120 (0) (23m)	8.41 10.16	48.7 58.8	0.0238	5,335 5,506	45.3 47.3

L-1

SUMMARY OF FIELD TEST RESULTS AND COMPUTATIONS

(20-in. Pile in Clay)

Load (kips)	Top Settlement, Δ (in.)	$\frac{\Delta}{B_3} \times 100$ (%)	Shaft Compn. (in.)	Total Change in the Instrument Readings, Qds. I + III (micro-inches)	Base Resistance from Calibration Curve (kips)
0	0	0	0	0	0
20 (0)	0.005	0.02		54	1.6
(1/2)	0.006			48	1.5
(24)	0.007	0.03	0.0003	32	0.1
40 (0)	0.014	0.06		62	0.19
(1/2)	0.015			59	0.18
(24)	0.017	0.08	0.0015	45	0.14
60 (0)	0.025	0.11		92	0.28
(1/2)	0.029			82	0.25
(24)	0.039	0.18	0.0051	81	0.24
70 (0)	0.044	0.20		112	0.34
(1/2)	0.046			104	0.31
(24)	0.051	0.23	0.0063	103	0.30
80 (0)	0.056	0.25		123	0.37
(1/2)	0.058			123	0.37
(24)	0.069	0.31	0.0079	127	0.38
90 (0)	0.072	0.33		153	0.46
(1/2)	0.072			143	0.43
(24)	0.087	0.39	0.0089	139	0.42

I-2

B_3 = Effective Diameter of Pile III = 22.0 in.

SUMMARY OF FIELD TEST RESULTS AND COMPUTATIONS (continued)

Load (kips)	Top Settlement, Δ (in.)	$\frac{\Delta}{B_3} \times 100$ (%)	Shaft Compn. (in.)	Total Change in the Instrument Reading, Qds. I + III (micro-inches)	Base Resistance from Calibration Curve (kips)
100 (0) (1/2) (24)	0.092 0.101 0.124	0.42 0.56		171 165 173	0.51 0.49 0.52
110 (0) (1/2) (24)	0.132 0.182 0.746	0.60 3.39	0.0114 0.0129	209 261 434	0.63 0.78 1.30
120 (0) (1/2) (1 1/2)	0.836 0.862 0.969	3.80 4.40		487 480 480	1.46 1.44 1.44
130 (0) (1/2) (24)	1.031 1.210 3.109	4.68 14.1		607 533 295	1.82 1.60 0.88
80 (0) (1/2)	3.101 3.099	14.1 14.1	0.0145	282 275	0.85 0.82
60 (0) (1/2)	3.091 3.083	14.0 14.0	0.0136	203 203	0.61 0.61
30 (0) (1/2)	3.069 3.059	13.9 13.9	0.0126	99 97	0.30 0.29

L-2

SUMMARY OF FIELD TEST RESULTS AND COMPUTATIONS (continued)

Load (kips)	Top Settlement, Δ (in.)	$\frac{\Delta}{B_3} \times 100$ (%)	Shaft Compn. (in.)	Total Change in the Instrument Reading, Qds. I + III (micro-inches)	Base Resistance from Calibration Curve (kips)
20 (0) (1/2)	3.053 3.046	13.9 13.8	0.0121	60 58	0.18 0.17
10 (0) (1/2)	3.037 3.027	13.8 13.8	0.0113	24 21	0.07 0.63
0 (0) (1/2) (24)	3.019 2.987 2.957	13.7 13.4	0.0096	- 5 -17 -33	- - -
50	3.000	13.6	0.0119	-	
100	3.043	13.8	0.0127	164	0.49
130 (0) (1/2) (3.49)	3.415 7.102 9.400	15.5 32.3 42.7	0.0134	189 124 101	0.56 0.37 0.30

L-2

SUMMARY OF FIELD TEST RESULTS AND COMPUTATIONS

(20-in. Pile in Till)

Load-Cycle (K)	Load (K)	Top Settlement Δ (in.)	$\frac{\Delta}{B_4} \times 100$ (%)	Shaft Compn. (in.)	Cell Settlement (in.)	Total Change in the Instrument Reading, Qds. I+II+III+IV (in.)	Base* Resistance (using Calib. Curve) (kips)
0-100	0 [†]	0.000		0.000	0.000	0	0
	12.5	- 0.0025		0.00125	- 0.0035	42	2.5
	25	- 0.0030		0.0080	- 0.006	91	5.0
	37.5	- 0.0305		0.0133	- 0.375	222	9.5
	50	- 0.028		0.01615	- 0.035	281	11.5
	62.5	- 0.0245		0.01925	- 0.035	343	13.0
	75	- 0.0195		0.02175	- 0.315	443	15.5
	87.5	- 0.0125		0.0254	- 0.0245		
	100 (1/2H)	- 0.005	- 0.02	0.0273	- 0.0055	589	18.5
	(24)	- 0.002	- 0.01	0.0277	- 0.0025	572	18.3
	75	- 0.007		0.0268		508	17.0
	50	- 0.016		0.0256		392	14.0
	25	- 0.027		0.0228		227	9.7
	0 (1/2H)	- 0.039	0.18	0.0156		142	7.0
	(17 1/2H)	- 0.041	0.19	0.0135		37	2.2
	(24H)	- 0.041	0.19	0.0126		51	3.2

[†] All values of Δ after 1/2H except when stated otherwise.

*Values obtained from the calibration curves for I + III or II + IV Quadrant readings are approximately equal. Best approximation of the base resistance has therefore been made from the calibration curve for all the four quadrant readings combined.

NOTE: B_4 = Effective Diameter of Pile IV = 22.0; H = Hours; K = Kips.

SUMMARY OF FIELD TEST RESULTS AND COMPUTATIONS (continued)

Load-Cycle (K)	Load (K)	Top Settlement Δ (in.)	$\frac{\Delta}{B_4} \times 100$ (%)	Shaft Compn. (in.)	Cell Settlement (in.)	Total Change in the Instrument Reading, Qds. I+II+III+IV (μ -in.)	Base Resistance (using Calib. Curve) (kips)
0-200	0	-0.00.0		0.0285	-0.0295	620	19.2
	112.5	-0.0075		0.03225	-0.0240	662	20.0
	125	+0.155		0.0346	-0.0205	683	20.5
	137.5	0.0395		0.0376	-0.0005	693	20.7
	150	0.0445		0.0400	+0.0025	679	20.4
	162.5	0.0590		0.0428	0.0110	736	21.5
	175	0.0725		0.0473	0.0195	749	21.7
	187.5	0.085		0.0505	+0.028	757	22.0
	200 (1/2H) (26H)	0.104	0.39	0.0515	+0.0440	757	22.0
	150	0.093		0.0497		601	18.9
	100	0.068	0.31	0.0452		330	12.5
	50	0.045		0.0325		63	3.5
	20	0.030		0.0246		- 80	- 4.5
	0 (1/2H) (45H)	0.016	0.07	0.0112		-102	- 5.5
		0.027	0.12	0.0048		- 95	- 5.0
0-300	0				+0.0690	752	21.0
	212.5	0.1360	0.62	0.0556	0.0820	772	21.3
	225	0.1535		0.0600	0.0915	772	21.3
	237.5	0.1660		0.0636	0.1005	795	22.8
	250	0.1760	0.80	0.0670	0.1175	802	23.0
	262.5	0.1955		0.0698	0.1370	814	23.2
	275	0.2190		0.0746	0.1530	828	23.4
	287.5	0.2390		0.0782	0.1760	850	23.9
	300 (1/2H) (40H)	0.290	1.32	0.0824		893	24.8
		0.320	1.45	0.0894	+0.2240		

SUMMARY OF FIELD TEST RESULTS AND COMPUTATIONS (continued)

Load-Cycle (K)	Load (K)	Top Settlement Δ (in.)	$\frac{\Delta}{B_4} \times 100$ (%)	Shaft Compn. (in.)	Cell Settlement (in.)	Total Change in the Instrument Readings, Qds. I+II+III+IV (μ -in.)	Base Resistance (using Calib. Curve) (kips)	
0-300 (con- tinued)	225	0.298	1.24	0.0850		674	22.5	
	150	0.272		0.0645		453	15.7	
	75	0.227		0.0407		- 82	- 4.5	
	30	0.208		0.0379		-100	- 5.3	
	0 (1/2H) (22H)	0.174		0.0271		-106	- 5.5	
0-350		0.174	0.79	0.0274	0.165 0.178 0.192 0.201 0.214 0.240 0.250 0.270 0.280 0.301 0.342 1,086 738 305 - 26 - 91 -102 - 99	- 99	- 5.2	
	0		0.78					
	50	0.172		0.0281		-109	- 5.6	
	100	0.194		0.0313		- 71	- 4.0	
	150	0.222		0.0495		- 31	- 2.1	
	200	0.242		0.0601		154	7.3	
	250	0.270		0.0727		671	20.1	
	300	0.312		0.0873		903	25.0	
	312.5	0.322		0.0900		926	25.5	
	325	0.348		0.0933		963	26.2	
	337.5	0.364		0.0974		979	26.6	
	350 (1/2H) (39H)	0.386	1.75	0.1002				
	262.5	0.422	1.92	0.1030				
	175	0.405	0.0970			29.0		
	87.5	0.369	1.67	0.0746			21.5	
	35	0.321		0.0449			12.0	
	0 (1/2H) (24H)	0.284	1.16	0.0354			- 2.1	
		0.256	1.12	0.0298			- 4.8	
		0.246		0.0295			- 5.3	
						0.240	- 5.1	

F-3

SUMMARY OF FIELD TEST RESULTS AND COMPUTATIONS (continued)

Load-Cycle (K)	Load (K)	Top Settlement Δ (in.)	$\frac{\Delta}{B_4} \times 100$ (%)	Shaft Compn. (in.)	Cell Settlement (in.)	Total Change in the Instrument Reading, Qds. I+II+III+IV (μ -in.)	Base Resistance (using Calif. Curve) (kips)
0-400	0						
	50	0.259	1.17	0.0302		314	10.9
	100	0.282		0.0385		620	19.2
	150	0.310		0.0520		920	25.2
	200	0.332	1.51	0.0652		1,067	28.5
	250	0.367		0.0792		1,142	30.0
	300	0.394		0.0911		1,179	31.0
	350	0.423		0.1021		1,214	31.7
	362.5	0.454		0.1056		1,274	33.2
	375	0.478		0.1084		1,651	41.9
	387.5	0.502	2.48	0.1115		1,977	49.2
	400 (1/2H)	0.546		0.1146	0.443	1,588	40.3
	(21H)	0.685	4.15	0.1193	0.642	866	24.1
	(184H)	0.912		0.1231	0.789	267	10.9
	300	0.890	3.78	0.1188		4	0.2
	200	0.832		0.0900		- 105	- 5.3
	100	0.793		0.0602		- 107	- 5.3
	40	0.753		0.0423		- 125	- 6.1
	0 (1/2H)	0.704	3.20	0.0259	0.676		
	(22H)	0.707		0.0197			
	(70H)	0.738	3.35	0.0192			

SUMMARY OF FIELD TEST RESULTS AND COMPUTATIONS (continued)

Load-Cycle Cycle (K)	Load (K)	Top Settlement Δ (in.)	$\frac{\Delta}{B_4} \times 100$ (%)	Shaft Compn. (in.)	Cell Settlement (in.)	Total Change in the Instrument Reading, Qds. I+II+III+IV (μ -in.)	Base Resistance (using Calib. Curve) (kips)
0-550	400	0.998	4.54	0.1222	0.891		49.5
	423 (1/2H) (4H)	1.050	4.77	0.1306	1.036		63.4
	446 (1/2H)	1.102	5.00	0.1326		2,542	62.5
	(1 H)	1.209	5.48	0.1411	1.147		72.0
	500 (1/2H)	1.217	5.53	0.1411	1.159		70.4
	(17H)	1.507	6.83			2,829	90.8
	525 (1/2H)	1.607	7.30			3,579	104.5
	(4 1/2H)	1.714	7.79			4,080	115.8
	550 (1/2H)	1.821	8.28			4,494	123.0
	(20H)	1.930	8.77			4,752	135.6
	(24H)	5.872	26.69	0.1913		5,219	258
	500	6.513	29.60	0.1992		9,678	285
	450	6.513	29.60	0.1973		10,636	272
	400	6.507	29.58	0.1930		10,191	264
	350	6.482	29.46	0.1725		9,901	245
	300	6.450	29.32	0.1538		9,188	220
	250	6.431	29.23	0.1430		8,297	205
	200	6.400	29.09	0.1262		7,744	184
	150	6.371	28.96	9.1114		7,003	164
	100	-0.338	28.81	0.0954		6,241	144
	50	6.291	28.59	0.0770		5,536	117
	0 (1/2H)	6.241	28.37	0.0590		4,547	92
	(24H)	6.152	27.96	0.0380		3,604	57.3
		6.127	27.85	0.0314		2,332	58.2
						2,366	

L-4

SUMMARY OF FIELD TEST RESULTS
AND COMPUTATIONS

SUMMARY OF FIELD TEST RESULTS AND COMPUTATIONS

(28-in. Pile in Till)

Load-Cycle (K)	Load (K)	Top Settlement Δ (in.)	$\frac{\Delta}{B_2} \times 100$ (%)	Shaft Compn. (in.)	Cell Settlement Δ_1 (in.)	Shaft Compn. (Computed) $\Delta - \Delta_1$ (in.)
0-464	0	0.000		0.0000	0.0000	
	58	0.016		0.0080	0.009	0.007
	116	0.037		0.0240	0.015	0.022
	174	0.062		0.0413	0.032	0.030
	232	0.092		0.060	0.033	0.059
	290	0.118		0.0788	0.047	0.071
	348	0.156		0.0972	0.062	0.094
	406	0.192		0.1156	0.083	0.109
	464 (1/2)	0.234	0.79	0.1355	0.107	0.127
	(42)	0.263	0.89	0.1432	0.124	0.139
	348	0.239	0.81	0.1281	0.114	
	232	0.195		0.0925	0.105	
	116	0.143		0.0534	0.092	
	46.4	0.110		0.0298	0.082	
	0 (1/2)	0.084	0.28	0.0137	0.072	
	(46 1/2)	0.075	0.25	0.0093	0.0655	

 B_2 = Effective Diameter of Pile II = 29.5 in.

CONTINUED FROM PAGE 319 (facing)

Change in the Instrument Reading (μ -in.)			Base Resistance from Calibrn. Curves (in kips)			
Quadrant I δ_1	Quadrant II δ_2	Quadrant III δ_3	$\delta_1 + \delta_3$	$\delta_1 + \delta_2$	$\delta_2 + \delta_3$	I + III I + II II + III II
0	0	0	0	0	0	0 0 0 0
8	16	8	16	24	24	10 2 2 2
24	43	21	45	67	64	18 6 6 5
54	99	50	104	153	149	32 13 13 10
100	173	92	192	273	265	50 22 21 17
141	239	142	283	380	381	68 29 30 22
186	304	182	368	490	486	82 37 37 27
241	392	234	475	633	626	93 45 47 32
305	502	312	617	807	814	118 58 61 41
343	599	381	724	942	980	132 67 74 50
						• a A x
302	538	332	634	840	870	120 60 66 44
223	414	224	447	637	638	95 46 48 35
130	261	109	239	391	370	59 29 29 23
73	163	53	126	236	216	38 19 18 16
30	78	20	50	108	98	24 10 9 8
31	77	17	48	108	94	24 10 8 8

L-4

SUMMARY OF FIELD TEST RESULTS

AND COMPUTATIONS

(continued)

SUMMARY OF FIELD TEST RESULTS AND COMPUTATIONS (continued)

Load-Cycle (K)	Load (K)	Top Settlement Δ (in.)	$\frac{\Delta}{B_2} \times 100$ (%)	Shaft Compn. (in.)	Cell Settlement Δ_L (in.)	Shaft Compn. (Computed) $\Delta - \Delta_L$ (in.)
0-640	80	0.101		0.0302	0.074	
	160	0.128		0.0509	0.084	
	240	0.159		0.0746	0.092	
	320	0.193		0.0994	0.102	
	400	0.227		0.1231	0.112	
	480	0.264		0.1470	0.127	
	560	0.321		0.1741	0.157	
	640	0.414	1.40	0.2092	0.218	0.194
	(37)	0.462	1.57	0.2190	0.258	
	480	0.426		0.1919	0.246	
	320	0.361		0.1411	-0.233	
	160	0.286	0.97	0.0803	0.213	
	64	0.236		0.0493	0.197	
	0	0.196	0.66	0.0241	0.179	
	(1/2)	0.185	0.63	0.0141	0.173	
	(19)					

CONTINUED FROM PAGE 321 (facing)

Change in the Instrument Reading (μ -in.)				Base Resistance from Calibrn. Curves (in kips)			
Quadrant I δ_1	Quadrant II δ_2	Quadrant III δ_3	$\delta_1 + \delta_3$	$\delta_1 + \delta_2$	$\delta_2 + \delta_3$	I + III	I + II II + III II
86	93	56	142	179	149	41	15 13 10
136	256	106	242	392	362	60	29 28 23
191	345	169	360	536	514	81	39 39 29
246	433	240	486	678	673	101	49 51 36
300	521	316	616	821	837	118	59 63 43
361	635	412	773	996	1,047	139	84 79 53
459	803	567	1,026	1,262	1,370	169	89 106 58
616	1,169	852	1,468	1,785	2,021	226	132 169 107
660	1,255	940	1,600	1,915	2,195	243	144 187 119
584	1,160	842	1,426	1,744	2,002	220	128 167 106
458	982	666	1,124	1,440	1,648	183	103 132 87
313	750	456	769	1,063	1,206	137	75 92 64
217	579	311	528	796	890	107	57 67 48
140	433	203	343	573	636	78	41 48 36
142	427	192	334	569	619	77	40 46 35

L-4

SUMMARY OF FIELD TEST RESULTS

AND COMPUTATIONS

(continued)

SUMMARY OF FIELD TEST RESULTS AND COMPUTATIONS (continued)

Load-Cycle (K)	Load (K)	Top Settlement Δ (in.)	$\frac{\Delta}{B_2} \times 100$ (%)	Shaft Compn. (in.)	Cell Settlement Δ_1 (in.)	Shaft Compn. (Computed) $\Delta - \Delta_1$ (in.)
0-800	100	0.233	0.79	0.0559	0.190	0.250
	200	0.256		0.0713	0.195	
	300	0.299		0.0882	0.208	
	400	0.342		0.1343	0.220	
	500	0.382	1.16	0.1650	0.233	
	600	0.438		0.2018	0.251	
	700	0.510		0.2328	0.293	
	800 (1/2)	0.640		0.2706	0.390	
	(66)	0.755	2.39	0.2891	0.488	
	600	0.704		0.2521	0.473	
	400	0.623		0.1910	0.454	
	200	0.530		0.1224	0.429	
	80	0.459	1.80	0.0747	0.404	
	0 (1/2)	0.402		0.0418	0.372	
	(32 1/2)	0.386		0.0340	0.370	

CONTINUED FROM PAGE 323 (facing)

Change in the Instrument Reading (μ -in.)				Base Resistance from Calibrn. Curves (in kips)					
Quadrant I	Quadrant II	Quadrant III							
δ_1	δ_2	δ_3	$\delta_1 + \delta_3$	$\delta_1 + \delta_2$	$\delta_2 + \delta_3$	I + III	I + II	II + III	II
212	531	273	485	743	804	101	53	60	42
293	661	376	669	954	1,037	125	68	78	57
380	798	489	869	1,178	1,287	150	83	100	68
462	933	617	1,079	1,395	1,550	177	99	123	81
541	1,059	738	1,279	1,600	1,797	201	116	146	95
634	1,217	898	1,532	1,851	2,115	234	138	179	113
763	1,461	1,109	1,872	2,224	2,570	277	173	225	149
954	1,749	1,389	2,343	2,703	3,138	338	218	284	196
1,020	1,807	1,445	2,465	2,827	3,252	352	228	296	204
914		1,322	2,236			322			
744		1,113	1,857			275			
546		856	1,402			217			
401		640	1,041			172			
292		476	768			137			
296		468	764			137			

L-4

SUMMARY OF FIELD TEST RESULTS
AND COMPUTATIONS

(continued)

SUMMARY OF FIELD TEST RESULTS AND COMPUTATIONS (continued)

Load-Cycle (K)	Load (K)	Top Settlement Δ (in.)	$\frac{\Delta}{B_2} \times 100$ (%)	Shaft Compn. (in.)	Cell Settlement Δ_1 (in.)	Shaft Compn. (Computed) $\Delta - \Delta_1$ (in.)
0-1000	125	0.427	1.45	0.0610	0.388	0.334
	250	0.481		0.1019	0.402	
	375	0.538		0.1421	0.420	
	500	0.596	2.02	0.1830	0.438	
	625	0.663		0.2283	0.451	
	750	0.728		0.2689	0.487	
	875	0.868		0.3116	0.584	
	1,000 (1/2)	1.137	3.85	0.3615	0.803	
	(103)	1.412	4.78	0.3862	1.056	
	750	1.355	4.59	0.3448	1.040	
	500	1.255		0.2689	1.013	
	250	1.130	3.83	0.1801	0.975	
	100	1.031		0.1152	0.940	
	0 (1/2)	0.952	3.23	0.0694	0.858	
	(69H)	0.924	3.13	0.0567	0.841	

CONTINUED FROM PAGE 325 (facing)

Change in the Instrument Reading (μ -in.)				Base Resistance from Calibr. Curves (in kips)			
Quadrant I	Quadrant II	Quadrant III		$\delta_1 + \delta_3$	$\delta_1 + \delta_2$	$\delta_2 + \delta_3$	
δ_1	δ_2	δ_3					I + III I + II II + III II
386	913	582		968	1,299	1,495	162 92 118 79
512	1,089	738		1,250	1,601	1,827	198 116 149 98
638	1,272	908		1,546	1,910	2,180	236 144 186 121
758	1,445	1,083		1,841	2,203	2,528	273 171 221 146
886	1,621	1,256		2,142	2,507	2,877	311 200 257 175
1,003	1,784	1,418		2,421	2,787	3,202	347 223 291 200
1,202	2,115	1,737		2,939	3,317	3,852	412 277 369 252
1,463	2,509	2,164		3,627	3,972	4,673	500 337 443 320
1,556	2,466	2,186		3,742	4,022	4,652	515 341 441 312
1,436	2,304	2,032		3,468	3,740	4,336	480 315 408 284
1,202	1,997	1,733		2,935	3,199	3,730	412 264 346 234
900	1,631	1,354		2,254	2,531	2,985	325 200 269 187
664	1,337	1,048		1,712	3,001	2,385	256 246 207 130
486	1,085	790		1,276	1,571	1,875	201 113 154 98
506	1,107	790		1,296	1,613	1,897	204 117 157 101

L-4

SUMMARY OF FIELD TEST RESULTS

AND COMPUTATIONS

(continued)

SUMMARY OF FIELD TEST RESULTS AND COMPUTATIONS (continued)

Load-Cycle (K)	Load (K)	Top Settlement Δ (in.)	$\frac{\Delta}{B_2} \times 100$ (%)	Shaft Compn. (in.)	Cell Settlement Δ_1 (in.)	Shaft Compn. (Computed) $\Delta - \Delta_1$ (in.)
0-1200-0	150	0.967	3.28	0.0815	0.858	
	300	1.031		0.1347	0.861	
	450	1.103		0.1852	0.948	
	600	1.186	4.02	0.2407	0.977	
	750	1.262		0.2900	1.002	
	900	1.342		0.3402	1.029	
	1,050	1.565	4.97	0.3958	1.238	
	1,100	1.756		0.4241	1.370	
	1,150	1.871		0.4421	1.468	
	1,200 (1/2)	2.163	7.33	0.4781	1.760	0.403
	(119 3/4)	2.783		0.5688	2.252	0.531
	900	2.740	9.29	0.5253	2.243	0.497
	600	2.576		0.4111	2.200	0.376
	300	2.410		0.2911	2.147	0.263
	100	2.252	7.29	0.1892	2.095	0.157
	0 (1/2)	2.151		0.1304	2.051	0.100
	(25)	2.116		0.1144	2.028	0.088

CONTINUED FROM PAGE 327 (facing)

Change in the Instrument Reading (μ -in.)				Base Resistance from Calibn. Curves (in kips)					
Quadrant I δ_1	Quadrant II δ_2	Quadrant III δ_3	$\delta_1 + \delta_3$	$\delta_1 + \delta_2$	$\delta_2 + \delta_3$	I + III	I + II	II + III	II
617	1,255	938	1,555	1,872	2,193	237	140	187	108
782	1,470	1,154	1,936	2,252	2,624	287	177	231	151
974	1,681	1,390	2,364	2,655	3,071	341	213	277	184
1,182	1,947	1,643	2,825	3,129	3,590	398	216	331	226
1,346	2,154	1,857	3,203	3,500	4,011	446	292	368	259
1,522	2,397	2,090	3,612	3,919	4,487	498	332	424	300
1,783	2,833	2,592	4,375	4,616	5,425	595	396	521	369
1,946	2,995	2,742	4,688	4,941	5,737	635	427	553	395
2,048	3,195	2,962	5,010	5,243	6,157	676	456	597	411
2,130	3,377	3,140	5,270	5,507	6,517	708	480	633	457
2,213	3,308	3,210	5,423	5,521	6,518	727	481	633	445
2,104	3,145	3,036	5,140	5,249	6,181	691	456	599	419
1,756	2,613	2,495	4,251	4,369	5,108	579	374	488	334
1,366	2,077	1,956	3,322	3,443	4,033	461	287	377	252
962	1,611	1,453	2,415	2,573	3,064	346	203	277	173
717	1,345	1,116	1,833	2,062	2,461	272	157	215	131
						-	-	-	-

APPENDIX M

DATA FOR TIME vs. SETTLEMENT AND TIME vs. BASE-RESISTANCE

PLOTS UNDER SUSTAINED LOADS

(FULL-LENGTH PILES)

DATA FOR TIME vs. SETTLEMENT PLOTS UNDER SUSTAINED LOADS

(16" Diameter Pile in Clay)

LOAD AT TOP, Q = 100 KIPS (LOADING CYCLE):

Time Elapsed (hrs.)	Top Settlement Δ (in.)	Settlement Ratio $\frac{\Delta}{B_1} \times 100$ (%)
0	0	0.22
0.5	0.045	0.26
1	0.056	0.32
2	0.057	0.33
3.5	0.069	0.40
8	0.084	0.49
24	0.753	4.36

$B_1 = 17.25$ in. (Effective Diameter of Pile I)

DATA FOR TIME vs. SETTLEMENT PLOTS UNDER SUSTAINED LOADS

(20"-Diameter Pile in Clay)

LOAD AT TOP, Q = 110 KIPS (LOADING CYCLE)

Time Elapsed (hrs.)	Top Settlement Δ (in.)	Settlement Ratio $\frac{\Delta}{B_3} \times 100$ (%)
0	0.132	0.60
0.5	0.182	0.83
1	0.244	1.11
2	0.366	1.66
3	0.523	2.42
4	0.559	2.54
5	0.594	2.70
6	0.627	2.85
7	0.651	2.96
8	0.674	3.06
24	0.746	3.39

$B_3 = 22.0$ in. (Effective Diameter of Pile III)

DATA FOR TIME vs. SETTLEMENT PLOTS UNDER SUSTAINED LOADS

(20"-Diameter Pile in Till)

LOAD AT TOP, Q = 400 KIPS (LOADING CYCLE)

Time Elapsed (hrs.)	Top Settlement Δ (in.)	Settlement Ratio $\frac{\Delta}{B_4} \times 100$ (%)
0	0.502	2.28
0.5	0.530	2.41
1	0.538	2.45
16	0.676	3.07
21	0.685	3.11
30	0.753	3.42

184	0.912	4.15

UNLOADING FROM 400 to 0 KIPS IN 2 HOURS

Load 400K	0	0.912	4.15
↓	0.5	0.890	4.05
	1	0.832	3.78
	1.5	0.793	3.60
0	2	0.753	3.42
	2.5	0.704	3.20
	24	0.707	3.21
	72	0.739	3.36

$B_4 = 22.0$ in. (Effective Diameter of Pile IV)

DATA FOR TIME vs. SETTLEMENT PLOTS UNDER SUSTAINED LOADS

(28"-Diameter Pile in Till)

LOAD AT TOP, Q = 1000 KIPS (LOADING CYCLE)

Time Elapsed (hrs.)	Top Settlement Δ (in.)	Settlement Ratio $\frac{\Delta}{B_2} \times 100$ (%)
0	1.023	3.47
0.5	1.137	3.85
1	1.166	3.95
2	1.194	4.05
4.75	1.224	4.15
16.5	1.292	4.38
25.5	1.319	4.47
--		
103	1.412	4.79

UNLOADING FROM 1000 to 0 KIPS IN 2 HOURS

LOAD	0	1.412	4.79
1000K	0.5	1.355	4.59
	1	1.255	4.25
↓	1.5	1.130	3.83
0	2	1.031	3.49
	2.5	0.952	3.23
	17	0.932	3.16
	67	0.924	3.13

$B_2 = 29.5$ in. (Effective Diameter of Pile II).

DATA FOR TIME vs. BASE-RESISTANCE CURVES UNDER SUSTAINED LOADS
(16"-Diameter Pile in Clay)

Time Elapsed (hrs.)	TOP LOAD							
	Q = 40 kips		Q = 60 kips		Q = 80 kips		Q = 100 kips	
	Q_B (kips)	$\frac{Q_B}{Q} \times 100$ (%)	Q_B	$\frac{Q_B}{Q} \times 100$ (%)	Q_B	$\frac{Q_B}{Q} \times 100$ (%)	Q_B	$\frac{Q_B}{Q} \times 100$ (%)
0	4.3, 6.3	10.8, 15.8	6.9, 9.4	11.5, 15.7	9.3, 13.0	11.6, 16.2	13.1, 17.0	13.1, 17.0
0.5	6.4	16.0	9.3	15.5	12.6	15.8	17.4	17.4
1	6.2	15.5	9.3	15.5	13.0	16.3	18.0	18.0
2	6.4	16.0	9.3	15.5	13.0	16.3	18.6	18.6
4	6.5	16.2	9.3	15.5	13.2	16.5	19.7 [†]	19.7 [†]
8	6.4	16.0			13.3	16.6	32.8	32.8
24	6.9	17.2	9.3	15.5	13.1	16.4	40.5	40.5

[†]At 3.5 hrs.

DATA FOR TIME vs. BASE-RESISTANCE CURVES UNDER SUSTAINED LOADS

(20"-Diameter Pile in Till)

TOP LOAD, Q = 300 KIPS				TOP LOAD, Q = 350 KIPS			
Time Elapsed (hrs.)	Q _B (kips)	$\frac{Q_B}{Q} \times 100$ (%)		Time Elapsed (hrs.)	Q _B (kips)	$\frac{Q_B}{Q} \times 100$ (%)	
0	23.3	7.77		0	26.5	8.83	
0.5	23.7	7.90		0.5	27.2	9.07	
1				1	29.5	9.83	
---				23	29.4	9.80	
40	24.7	8.23		39	29.8	9.93	
TOP LOAD, Q = 400 KIPS				TOP LOAD, Q = 500 KIPS			
Time Elapsed (hrs.)	Q _B (kips)	$\frac{Q_B}{Q} \times 100$ (%)		Time Elapsed (hrs.)	Q _B (kips)	$\frac{Q_B}{Q} \times 100$ (%)	
0	31.6	7.90		0	70.5	14.10	
0.5	33.2	8.30		2	93.6	18.72	
1	33.3	8.32		16.5	100.6	20.12	
16	41.2	10.30		17	104.3	20.86	
21	41.9	10.48					
30	43.8	10.95					

184	49.2	12.30					

M-6

DATA FOR TIME vs. BASE-RESISTANCE CURVES UNDER SUSTAINED LOADS
(28"-Diameter Pile in Till)

TOP LOAD, Q = 464 KIPS				TOP LOAD, Q = 640 KIPS			
Time Elapsed (hrs.)	Q _B (kips)	$\frac{Q_B}{Q} \times 100$ (%)	Time Elapsed (hrs.)	Q _B (kips)	$\frac{Q_B}{Q} \times 100$ (%)	Time Elapsed (hrs.)	Q _B (kips)
0	100.1	21.6	0	178.0	27.1	0	178.0
0.5	118.8	25.6	0.5	225.5	35.2	0.5	225.5
1	120.0	25.9	1	228.7	35.7	1	228.7
1.5	121.0	26.1	1.5	228.9	35.8	1.5	228.9
2	121.7	26.2	2	229.1	35.9	2	229.1
6	123.7	26.7	4	232.7	36.4	4	232.7
16	130.0	28.0	12	238.8	37.3	12	238.8
24	132.0	28.4	37	242.4	37.9	37	242.4
TOP LOAD, Q = 800 KIPS				TOP LOAD, Q = 1000 KIPS			
Time Elapsed (hrs.)	Q _B (kips)	$\frac{Q_B}{Q} \times 100$ (%)	Time Elapsed (hrs.)	Q _B (kips)	$\frac{Q_B}{Q} \times 100$ (%)	Time Elapsed (hrs.)	Q _B (kips)
0	184.3	23.0	0	423	42.3	0	423
0.5	336.5	42.1	0.5	500	50.0	0.5	500
1	338.8	42.4	1	503	50.3	1	503
1.5	339.7	42.5	2	505	50.5	2	505
2	340.7	42.6	4.75	510	51.0	4.75	510
5	342.1	42.8	16.5	509	50.9	16.5	509
10	346.1	43.3	25.5	509	50.9	25.5	509
18	347.6	43.5	--			--	
30	350.3	43.8	103	515	51.5	103	515

APPENDIX N

DETERMINATION OF CRITICAL LOAD Q_c ON THE PILE TOP

WHEN ITS EFFECT JUST REACHES THE PILE TIP

AND

COMPUTATION OF SHAFT COMPRESSION FROM KNOWN

AVERAGE VALUE OF ELASTIC MODULUS

AND MEASURED DIMENSIONS

OF PILES

DETERMINATION OF CRITICAL LOAD Q_c APPLIED AT PILE TOP

WHEN ITS EFFECT JUST REACHES THE TIP

(AFTER TROW, 1967)

1. The resistance offered by soil increases with the depth of the pile and at any depth x below surface, its value is given by:

$$\begin{aligned} R_x &= \int_0^x k\gamma'x \tan \phi_d \cdot \pi B \cdot dx \\ &= k\gamma' \tan \phi_d \cdot \pi B \cdot \frac{x^2}{2} \\ &= K \cdot \pi B \cdot \frac{x^2}{2} \end{aligned} \quad \dots (1)$$

where $K = k\gamma' \tan \phi_d$,
 k = coefficient of lateral earth pressure,
 B = diameter of the pile,
 ϕ_d = mobilized angle of friction,
 γ' = effective unit weight of soil around pile.

The Net Axial Load on the pile at depth x is then equal to $(Q-R)$, where Q is the applied load at top. When the effect of load just reaches the tip, $Q = R$,

$$\text{or the Critical Load, } Q_c = K\pi B \cdot \frac{H^2}{2} \quad \dots (11)$$

where H is the length of the pile.

2. The total axial compression ΔH is given by:

$$\Delta H = \int_0^H \frac{Q_x \cdot dx}{AE}$$

where Q_x is the net axial load on the pile at any depth x , and A the sectional area of pile.

$$= \frac{1}{AE} \int_0^H (Q_c - K \cdot \pi B \cdot \frac{x^2}{2}) dx$$

$$= \frac{Q_c \cdot H}{AE} - \frac{K\pi B}{AE} \cdot \frac{H^3}{6}$$

But from relation (ii) above,

$$H^2 = \frac{2Q_c}{K\pi B}$$

$$\therefore \Delta H = \frac{Q_c H}{AE} - \frac{2Q_c \cdot H}{6} = \frac{2}{3} \frac{Q_c \cdot H}{AE} \quad \dots (iii)$$

COMPUTATION OF SHAFT COMPRESSION FROM KNOWN AVERAGE VALUE
OF ELASTIC MODULUS AND MEASURED DIMENSIONS OF PILES

(a) Using equation (7.3) and data from TABLE VII-1, the shaft compression ΔH , for 16-inch diameter pile (I) in clay is given by:

$$\Delta H_1 = Q \cdot \frac{41.25}{A_e \cdot E} + Q_B \cdot \frac{177.85}{A_e \cdot E} + (Q - Q_B) \cdot \frac{177.88}{A_e \cdot E} \cdot \frac{2}{3}$$

where ΔH_1 is measured in inches, Q and Q_B in kips, A_e in square inches and E in kips per square inch.

Simplifying, we have:

$$\Delta H_1 = \frac{1}{A_e \cdot E} (159.83 Q + 59.29 Q_B).$$

For the 16-inch pile, $A_e = 241 \text{ in.}^2$ and $E = 3.625 \text{ ksi}$.

$$\therefore \Delta H_1 = Q (18.3 + 6.77 \frac{Q_B}{Q}) \times 10^{-5} \quad \dots (7.4)$$

(b) For 20-inch pile (III) in clay,

$$\begin{aligned} \Delta H_3 &= Q \cdot \frac{42}{A_e \cdot E} + Q_B \cdot \frac{130.63}{A_e \cdot E} + (Q - Q_B) \cdot \frac{130.63}{A_e \cdot E} \cdot \frac{2}{3} \\ &= \frac{1}{A_e \cdot E} (129.09 Q + 43.54 Q_B) \end{aligned}$$

Here $A_e = 394 \text{ in.}^2$ and $E = 3.625 \times 10^3 \text{ ksi.}$

$$\therefore \Delta H_3 = Q \left(9.02 + 3.05 \frac{Q_B}{Q} \right) \times 10^{-5} \quad (7.5)$$

APPENDIX O

LIST OF SYMBOLS USED IN THE TEXT

LIST OF SYMBOLS

A, A_s	Sectional area of pile shaft
A_b	Sectional area of pile base (pile bearing area)
A_e	Equivalent sectional area of pile (inclusive of transformed area of reinforcement)
A_s	Contact area between shaft and soil
A_{s1}, A_{s2}	Shaft contact areas for portions of embedded length within lake soil and till respectively
B	Breadth of foundation (diameter of pile)
C	Constant of Compressibility
C_c	Compression Index
C_s	Swelling Index
C_{kd}	Static cone resistance in kg./cm.^2 or tons/ft.^2
c	Unit apparent cohesion of soil
c_a	Average unit adhesion between soil and shaft
c_b	Average soil shear strength below base
c_s	Softened shear strength of soil (mean)
c_u	Undrained shear strength of soil (mean)
\bar{c}	Mean undisturbed shear strength of soil along shaft
c_r	Residual unit cohesion of soil (undisturbed soil)
c_{ru}	Undrained cohesion (remolded soil)
D, D_f	Depth of foundation to the bottom of the footing, depth of pile
d	Depth of pile embedment below clay-till interface

E	Modulus of elasticity of the material or equivalent modulus of pile material (composite section)
E_p	Measured modulus of pile material
F	Desired (overall) factor of safety
F_b	Factor of safety on Ultimate Base Capacity
F_s	Factor of safety on Ultimate Shaft Resistance
f_d	Depth factor for correcting the value of consolidation settlement
f_s	Average unit skin friction developed over the shaft
H	Length of the pile or effective length of contact between pile shaft and soil from top up to mid-depth of load-cell
H_1	Effective length of contact between pile shaft and soil from mid-depth of cell up to bottom of concrete plug
H_c	Maximum depth of compressible layer
I	Influence factor the value of which depends upon shape and rigidity of the foundation
K	A dimensionless number related to stress-strain properties and the strength characteristics of the soil, used in computing immediately settlement. Also $K = k \cdot \gamma' \tan \phi_d$
k	Coefficient of lateral earth pressure of soil against pile shaft
k_o	Coefficient of earth pressure at rest
L	Length of foundation
m	A factor (value varying from 1 to 1.6) used for computing Shaft Capacity
m_v	coefficient of volume compressibility
N	standard penetration values (below counts) for 12-inch penetration
\bar{N}	weighted average value of N taken for the entire depth in question
N_c, N_q, N_γ	General bearing capacity factors (dimensionless)

P_s	Swelling pressure
P	Total overburden pressure at foundation level
P_o	Effective overburden pressure at foundation level
Q	Applied load at any stage
Q_c	Critical load applied at pile top when its effect just reaches the tip
Q_F	Failure load on pile (yield-point load)
Q_T	Maximum test load on pile
Q_b	Base resistance component of Q at the level of load-cell
Q_B	Base resistance component of Q at pile tip
Q_{BU}	Ultimate base capacity
Q_s	Shaft resistance component of Q corresponding to Q_b
Q_S	Shaft resistance component of Q corresponding to Q_B
Q_{SU}	Ultimate shaft resistance
Q_{Bmax}	Maximum value of Q_B
Q_{Smax}	Maximum value of Q_S
q	loading pressure on pile shaft
q_a	Allowable unit bearing capacity
q_{ult}	Ultimate value of q
q_n	Net ultimate unit bearing capacity
q_u	Ultimate unit bearing capacity, or unconfined compressive strength as detailed in the text
R	total resistance offered by soil to the penetration of pile shaft
W_p	Weight of concrete plug below the load-cell
z	Any depth below foundation

α	Coefficient of load transfer
α_1	Coefficient of reduction being the ratio of soil shear strength after and before concreting used for piles in silt
α_2	Coefficient of adhesion, i.e., the ratio of unit load-transfer to unit shear strength of softened soil used for piles in silt
α_c	Coefficient of load transfer computed from weighted average of mean undrained or unconfined shear strength = f_s/c_u
α_s	Coefficient of load transfer computed from weighted average of mean undrained softened shear strength = f_s/c_s
β	Coefficient of reduction to be applied to weighted average value of penetration N (number of blows) for computing shaft capacity
γ	Moist unit weight of soil above water table or buoyant if below water table.
γ'	Effective unit weight of soil
$\bar{\gamma}$	Average density of soil within depth D of pile
γ_1	Increased unit weight of soil produced to counteract the shear stress developed over the surface of Terzaghi's outer failure cylinder and skin friction developed over pile shaft
Δ	Total settlement of foundation ($\Delta_1 + \Delta_c$) or settlement of pile tip or 24-hour settlement as described in the body of thesis
Δ_1	Settlement of load-cell
Δ_{lab}	Consolidation settlement from laboratory oedometer test
Δ_i	Immediate settlement under the foundation
Δ_c	Long-time consolidation settlement under the foundation
ΔH	Axial compression in shaft
$\delta_1, \delta_2, \delta_3$	Change in strain indicator reading (micro-inches)
ϵ	Axial strain in a triaxial undrained test

μ	Poisson's ratio for the material
μ_c	Reduction coefficient to be applied to laboratory settlement value
τ	Shear stress on the plane of failure
τ_f, τ_r	Maximum value of τ at failure and the residual value of shear stress
σ	Unit normal stress
$(\sigma_1 - \sigma_3)$	Deviator stress in a triaxial test
σ_z	Normal stress at a depth z below the loaded tip
ϕ	Angle of shearing resistance
ϕ'	Effective angle of shearing resistance
ϕ_d	Mobilized angle of friction
ϕ_u	Undrained angle of shearing resistance (undisturbed soil)
ϕ_r	Residual angle of shearing resistance
ϕ_{ru}	Undrained angle of shearing resistance (remolded soil)
ω	A factor accounting for the variation in the values of shear strength due to physical and environmental characteristics of soil